Bioprocess design considerations for the manufacture of pluripotent stem cell derived retinal pigment epithelium for the treatment of age-related macular degeneration

Thesis submitted for the degree of

Doctor of Engineering In
Biochemical Engineering

Amelia Ronnaug Rose Lane

The Advanced Centre for Biochemical Engineering

Department of Biochemical Engineering

University College London

Declaration

I, Amelia Ronnaug Rose Lane, confirm that the work presented in this thesis is my own. Where information has been derived from other sources, I confirm that this has been indicated in the thesis.

Acknowledgements

Thank you to my supervisors, Professor Chris Mason for recruiting me to this exciting project and for his enthusiasm and advice, and Professor Pete Coffey for his knowledge, wisdom and support throughout.

Thanks to everyone at the London project - your knowledge, dedication, hard work and enthusiasm for the project has been inspiring. Particularly Mayaan, Shazeen, LiLi,, Amanda, Matt, Ant, Carlos and Jean for patiently teaching me new techniques and for all the interesting conversations and insights both in and out of the Eagle.

In the UCL RegenMed lab I sincerely thank Ludmilla Ruban for training me in HESC culture and for looking out for me. To Dae, for unselfishly sharing his knowledge and for being an inspiringly hard worker and truly excellent friend. To Diana again for sharing her knowledge and insight at the most critical moments. Thank you to Kate for being such a kind and supportive friend as we went through the good and bad times together. Thanks to Iwan for all your optimism and help at the end with thesis reading. And to TPM, Guillia, Vishal, Owen, Shaz, Nat, John and Yemisi for being the finest office buddies, friends and colleagues. I am also very grateful for the help of Martin Town in the biochemical engineering for designing and making our imaging system. Thank you also to my masters student Lissa Philip.

Thank you to my very good friends and flat mates Sioned and Sarah for their proof reading help, LYMTLI and my sis Freya for listening to me moan and always coming up with constructive solutions. Thank you to the Meek-O'connor family for very kindly having me to stay with them many times during the completion of this thesis, for many delicious meals and interesting conversations. Thank you to the wonderful Elbaz family and my amazing grandmother Bestemor for having me to stay for the last months of writing up, it has been such a pleasure to sit round your table, thank you for your kindness. Thank you to my parents and brother Oliver, for your proof reading, financial and emotional support from across the world. Your wise words helped me to maintain perspective and I will always be grateful. Lastly to Innes, thank you for supporting me and encouraging me always - your patience, kindness and optimism make everything possible.

Finally I want to thank my sponsors the Rosetrees trust and the engineering and physical sciences research council for their support.

Abstract

Human embryonic stem cells (HESC) are a promising source of retinal pigment epithelium (RPE) for the treatment of common and incurable forms of blindness such as age-related macular degeneration (AMD). Whilst most HESC lines will produce some pigmented RPE cells when allowed to overgrow and spontaneously differentiate for 30-60 days, the efficiency of this process is highly variable and the critical factors which determine target cell yield remain largely uncharacterised. This will prove problematic in the large-scale production of RPE cells needed for cell therapy. In this project the aim was to identify and minimise sources of variability during differentiation and to develop an efficient and scalable HESC-RPE differentiation protocol.

Using a novel imaging platform in combination with quantitative gene expression analysis and immunocytochemistry, the relative differentiation efficiency in two new cell lines, Shef6 and Shef3 was characterised. It was found that the age of the starting HESC population, the cell seeding density and the passaging method used have a strong influence on RPE yields. It was also demonstrated that RPE can be generated from HESC following single cell dissociation and in the absence of feeder cells, thereby significantly simplifying cell culture logistics and reducing variability. In addition it was shown that the lower yielding cell line, Shef3, has a reduced innate propensity for neuroectoderm conversion and that by directing this process with a small molecule, dorsomorphin, efficiency can be significantly improved. Overall this novel protocol increased RPE foci yields per cm^2 by 5 fold in Shef6 and 4 fold in Shef3 compared to traditional mouse embryonic fibroblast (MEFs) co-culture systems. Since HESC-derived RPE are now entering clinical trials, it has become increasingly important to optimise manufacturing; this study identifies several critical parameters that could help develop a robust, scalable and cost-effective strategy for HESC-RPE manufacturing.

Table of Contents

List of Figures

Chapter 1

Chapter 2

Chapter 3

Chapter 4

Chapter 5

List of Tables

List of Abbreviations

AMD Age-related macular degeneration
ANOVA Analysis of variance
BNDF Brain derived neurotrohpic factor
BMHSC Bone marrow derived haematopoietic stem cells
BMMSC Bone marrow derived mesenchymal stem cells
cDNA Complementary deoxyribose nucleic acid
CM Feeder conditioned media
CRALBP Cellular retinaldehyde binding protien
DAPI Diamidino-2-phenylindole (nuclear stain)
DMSO Dimethyl sulfoxide
EB Embryoid body
EFTF Eye field transcription factors
FACs Fluorescence activated cell sorting
FBS Foetal bovine serum
FGF Basic fibroblast growth factor
GMP Good manufacturing practice
GNB Guanine nucleotide binding protein beta peptide 2
HESC Human embryonic stem cells
IGF Insulin growth factor
IGFBP Insulin like growth factor binding protien
IPSC Induced pluripotent stem cells
IRBP Insulin receptor binding protien
IQ Installation qualification
IV Intravenous
IVF In vitro fertilisation
LRAT Lecithin retinol acyltransferase
MAN Mannosidase alpha class 1B member 1
MEFs Mouse embryonic fibroblasts
MitF Microopthalimia asscociated factor
NEAA Non essential amino acids
NRT No reverse transcriptase control
NTC No template control (contains no cDNA)
OQ Operational qualification
PAX6 Paired box protein 6 gene
PBS Phosphate buffered saline
PFA Paraformaldehyde
POL Polymerase (RNA) II (DNA directed) polypeptide A
PQ Performance qualification
QPCR Quantitative, real-time PCR
QNR71 Quail neuroretina protein 71
RCS Royal college of surgeons (rat)
RDH5 Retinal dehydrogenase 5 (11 cis/9 cis)
RNA Ribonucleic acid
RPE Retinal pigment epithelium

RPE65 Retinal epithelium specific protein (65KDa)
RT-PCR Reverse transcription PCR (semi-quantitative)
Rx Retinal homeobox gene
SEM Standard error of the mean
SFEB Serum free embryoid body
TBP Tata binding protien
TGFβ transforming growth facotr β
TRP1/2 Tryosinase related protien 1/2
VEGF Vascular endothelial growth factor

Chapter 1: Literature review

1.1 Introduction

Human embryonic stem cells (HESC) have enormous potential as a limitless source of human cells that could be used in the treatment of degenerative diseases where replacement of aged or defective cells could restore function to damaged tissues. Age-related macular degeneration is an incurable form of blindness that is estimated to affect over two million people in the USA and UK alone, with incidence predicted to double over the next decade (Owen et al., 2012, Friedman et al., 2004). The disease is caused by the degeneration of a specific cell type found in the retina, the retinal pigment epithelium, which can be derived from HESC (Young et al., 1987, Vugler et al., 2007). Autologous RPE transplants in humans have shown that replacement of the defective retinal pigment epithelium can lead to re-establishment of the critical photoreceptor–RPE interaction and at least partial restoration of visual function (Da cruz et al., 2007). The eye is believed to be a highly suitable target organ for transplantation therapies due to its accessibility, immunologically privileged status and the ease with which grafts can be viewed (Da Cruz et al., 2007). Multicentre clinical trials using HESC derived RPE to treat dry AMD and Stargardt disease (so called 'juvenile macular degeneration') are currently underway (Schwartz et al., 2012).

HESC are derived from the inner cell masses of human blastocyst stage embryos (Thomson et al., 1998). Despite an increasing understanding of the mechanisms that control pluripotency, maintaining undifferentiated HESC in culture continues to be laborious and unpredictable, often generating heterogeneous cultures with variable growth rates and differentiation capacity (Akopian et al., 2010, Adewumi et al., 2007). Never the less, differentiation of HESC into putative RPE cells occurs robustly in many HESC and induced pluripotent stem cell (IPSC) lines. Pigmented cells expressing the characteristic gene and protein expression, pigmentation, and morphology of adult retinal pigment epithelium (RPE) cells have been reported by several groups (Rowland et al., 2012). Why this phenomenon occurs so readily in many HESC lines is not completely understood, though it has been suggested that standard culture conditions including components of the growth media and secretions from the inactivated mouse feeder layer contribute significantly, perhaps by

mimicking aspects of the highly conserved retinal development pathway (Vugler et al., 2008, Shi et al., 2008, Hongisto et al., 2012).

Reviewing the published accounts of HESC-RPE differentiation reveals significant variability in the reported timing and yields of RPE cells following HESC differentiation (table 1.1). This suggests that there are process critical variables which have not yet been identified, or are not routinely controlled, which have a profound impact of the productivity of HESC-RPE differentiation. Directed differentiation protocols based on our knowledge of in-vivo eye development have been used to generate photoreceoptor progentiors and RPE, in many of these protocols however it is not convincingly demonstrated that directed strategies are superior to so called 'spontaneous' methods in terms of overall cells in vs. cells out yield or in terms of reproducibility. Identification and optimisation of the variables that control the differentiation efficiency will be critical to overall process efficiencies and may ultimately determine the economic feasibility of HESC-RPE to treat AMD.

1.2 The Retina and Macular Degeneration

1.2.1 Anatomy and Physiology of the RPE

Light enters the eye through the window of the pupil and is focused by the lens onto a region of the retina known as the macula. The macula is an area around 3mm in radius centred around the fovea; it confers the greatest visual acuity and has a particularly high concentration of cone type photoreceptors (Curico et al., 1990). The retina consists of four physiologically distinct layers (Fig. 1.1): the photoreceptors, the retinal pigment epithelium (RPE), the Bruch's membrane and the choroid blood supply.

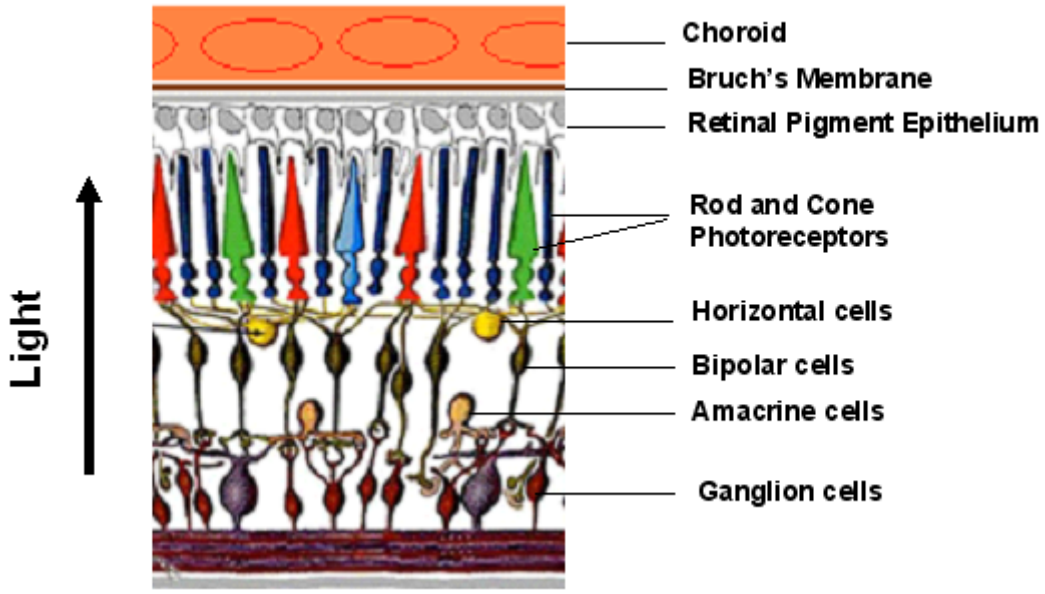

Figure 1.1 Schematic of the human retina. The retina consists of physiologically distinct layers. The basolateral side of the RPE forms part of the Bruch's membrane that separates the retina from the choroid blood supply. The RPE and photoreceptors are intimately connected via long microvilli

extending from the RPE around the photoreceptor outer segments. Diagram adapted from Kolb et al., 1995.

The first of these layers to be reached by incoming light contains the photoreceptors. Incident photons react with the light sensitive opsins which are abundant in the membranous stacks of the photoreceptor outer segments (Hall et al., 1973). Photoreceptors are constantly exposed to, and damaged by light. In order to preserve function, each photoreceptor undergoes a process of continual destruction and renewal of the light-processing outer segment. Stacks of visual pigment containing molecules in the outer segments are added at the base of the outer segment whilst old stacks are pinched off the other end and phagocytosed by the adjacent retinal pigment epithelium (Young et al., 1969).

The RPE cells lie directly behind the photoreceptors. Approximately twenty-three photoreceptors are supplied by one RPE in the fovea (Gao, 1992). The RPE possess long microvilli on their apical side which surround the rod and cone outer segments and engulf the shed outer segment discs. There is a burst of outer segment shedding and phagocytosis by the RPE at first light in the morning (Young et al., 1971). The basolateral side of the RPE forms part of the Bruch's membrane that lies between the fenestrated capillaries of the choroid and the retina. The cells have many important functions in the nourishment and maintenance of the photoreceptors. A critical role of the RPE, which is used to demonstrate the functionality of cells grown in culture, is in the phagocytosis of shed photoreceptor's outer segments (Carr et al., 2009). Shed segments bind to the RPE surface and are internalised a process in which the MerTK receptor is implicated (D'cruz et al., 2000). In the macular there are more photoreceptors per RPE cell and the RPE here are adapted to a higher turnover rate of shed outer segments (Weiter et al., 1986).

The RPE are highly susceptible to photo-oxidative damage; the environment of high intensity light exposure, rich oxygen supply and the abundance of polyunsaturated fatty acids together with continuous phagocytic activities lead to the generation of significant amounts of potentially toxic reactive oxygen intermediates (ROI) (Weiter et al., 1987). The RPE cells employ various protective strategies to minimise the toxicity of their environment (Straus et al., 2005). A large number of melanin

containing melanosomes which absorb light and reduce the photodynamic production of potentially toxic ROI are found in the RPE (Beatty et al., 2000). In addition the RPE accumulate anti-oxidative substances that sequester damaging free radicals (Boulton et al, 2001), including the antioxidant enzymes superoxide dismutase, catalase and peroxidase (which have micronutrient components of zinc, selenium and copper) antioxidant nutrients vitamin C (ascorbate), E (α-tocopherol), β-carotene and the caretenoides lutein and zeaxanthin (Micele et al., 1994).

The polarised RPE monolayer forms the retinal-blood barrier with tight junctions across the epithelium separating the subretinal space from the choriocapillaris and controlling the trans-epithelial transport of nutrients and waste products (Hughes et al., 1998). A large amount of water is produced in the retina and the RPE is responsible for removing it from the sub-retinal space and transporting it to the choriocapillaris. The apical side of the RPE membrane contain Na+ / K+ ATPases (Marmorstein et al., 2001) which supply the energy required for transepithelial transport and are important in setting up the ion gradients that enable the transport of chloride ions and water, the removal of photoreceptor metabolic end products, such as lactic acid and in maintaining pH (Strauss et al., 2005). These transport mechanisms are critical to homeostasis of the extra-photoreceptor matrix (Wimmers et al. 2007). Transport of glucose and supplementary Vitamin A (for use in the retinal cycle) from the choroid to the photoreceptors is also achieved by the RPE via specialised, receptor mediated processes (Pfeffer et al., 1986).

The RPE also has important functions in the retinoid cycle, the process by which 11-*cis*-retinal is regenerated from all-*trans*-retinol following light induced photoisomerization. The photoreceptors themselves lack the cis-trans isomerase enzyme required for this conversion. The transportation of the reduced form of all-*trans*-retinal (all–*trans*-retinol) from the intradiscal space of the photoreceptors, to the RPE is achieved in a process involving transporter protein ABCA4 and carrier protein IRBP. The regeneration of 11-*trans*-retinol is then carried out by enzymes (LRAT, RPE65,CRALBP,RDH5,) residing in the RPE cells as they recycle parts of the phagocytosed photoreceptor outer segments, before transporting the regenerated molecules back to the photoreceptors (Purves et al., 2001, Strauss et al., 2005).

Mutations in ABCA4 have been associated with Stargardt disease and age-related macular degeneration (Allikmets et al., 2000).

RPE exhibit polarised secretion of growth factors. In healthy eyes PEDF in secreted from the apical side of the epithelium, this growth factor has anti-angiogenic and neuroprotectant properties and reduces hypoxia induced apoptosis (Dawson et al., 1999). On the basal side of the RPE, small quantities of VEGF are secreted. This growth factor helps to prevent endothelial cell apoptosis and maintains the fenestrations in the choriocapillaris (Roberts et al., 1995). In response to injury the RPE have been shown to upregulate the secretion of additional neurotrophic factors bFGF and CNTF (Wen et al., 1995). In the diseased retina inappropriate secretions of these growth factors contributes to aberrant neovascularisation, as seen in 'Wet' AMD (Wada et al., 1999, Ishibashi et al., 1997).

In summary the high metabolic activity of the photoreceptors coupled with the intensity of incoming light is conducive to cellular damage in the adult human retina. The RPE are specially adapted to minimise this damage and protect the photoreceptors via a variety of mechanisms. In addition the RPE carry out vital functions in the digestion of photoreceptor outer segments, regeneration of molecules critical to the visual cycle, transportation of nutrients and waste products across the retinal blood barrier and the secretion of growth factors critical to retina and choroid health and function.

1.2.2 Embryonic development of the retina

The stages that mark the transformation from pluripotent inner cell mass to the formation of a differentiated, multilayered retina have been studied extensively in animal models including amphibians, chick, mouse and fish. The eye develops from multiple embryonic tissue layers, whilst the neuroectoderm forms the RPE and neural retina, the mesoderm contributes to the cornea and choroid layer, neural crest cells contribute to the cornea, cilary muscles, sclera and choroid layer and the ectoderm forms part of the lens and cornea (Schoenwolf et al., 2009). This section

focuses on embryonic development of the retina from the neuroectoderm. The process of retinal development is categorised into the following stages: neural induction and specification of the anterior neural plate, establishment of the eye field and optic vesicles and formation of the optic cup.

Neural Induction and specification of the anterior neural plate: Neural induction is triggered by the inhibition of BMP signalling by Chordin, Noggin and Follistatin which are released from the Spemann's organizer (Kessler et al., 1994, Wilson et al., 2004). Anteriorisation of the neural plate and formation of the forebrain is the default fate for neural induced tissue and at this stage FGFs, Retinoic acid and canonical Wnt signalling suppress anteriorization and induce posteriorization of the neural plate (Niehrs et al., 2004, Villanueva et al., 2002). The secreted proteins IGF and Cerberus specifically induce the expression of anterior neural plate transcription factor Otx2 (Pera et al., 2001).

Establishment of the eye field: The eye field forms in a region of the anterior neural plate surrounded by telencephalic precursors and cells that go on to form the hypothalamus (Esteve et al., 2006). Otx2 expression in the prospective forebrain region of the anterior neural plate primes this area for eye field formation, inducing the expression of a network of self-regulating eye field transcription factors (EFTFs) including Pax6, Six3, Lhx2 Rx1 and Six6 (Zuber et al., 2003). The EFTFs work together and in some cases mutually induce the expression of one another (Zuber et al., 2003). Rx is essential to optic vesicle invagination and its overexpression leads to excessive proliferation of both the RPE and neural retina (Bailey et al., 2004). Pax6 is also critical to optic cup formation, null mutants do not develop an optic cup and its ectopic expression has been shown to induce eye formation in Xenopus (Chow et al., 1999).

The optic vesicles are first morphologically distinguishable as lateral bulges evaginating from the forebrain region of the neural tube towards the surface ectoderm. Shh signalling suppresses the expression of eye field transcription factors down the midline of the neural tube thereby producing two distinct eye fields (Yang et al., 2004). As the vesicles grow outwards they become surrounded by mesenchyme derived from neural crest cells and head mesenchyme. This extraocular

mesenchyme starts to form on post-ovulatory day 24 and surrounds the entire vesicle by day 26 (Schoenwolf et al., 2009). Initially all regions of the optic cup are tri-potent and can form neural retina, RPE or optic stalk; the patterning and subsequent differentiation is induced by surrounding tissues (Slack et al., 2006). Signalling from the adjacent surface ectoderm, mediated by FGFs, induces neural retina via the homeobox transcription factor Chx10 (Zhao et al., 2001), whereas BMP or activin like signalling originating in the extraocular mesenchyme induces expression of the basic helix loop helix (bHLH) transcription factor, MitF, which specifies RPE and induces pigmentation as well as suppressing Chx10 (Fuhrmann et al. 2000, Nguyen et al., 2000). The combined expression of Otx2 and Wnt/βcatenin has been shown to induce MitF expression and drive the conversion of retinal progenitor cells into presumptive RPE in chick optic explants (Westenskow et al., 2010). The presumptive neural retina and the RPE express FGFs and BMPs respectively which help to consolidate their respective identities and define the boundary between these phenotypically distinct retinal layers (Vogel-Hopker et al., 2000, Zhao et al., 2001). As the optic vesicle continues to expand the distal portion comes into contact with the overlying surface ectoderm causing the optic vesicle and the ectoderm to invaginate in a process that requires the transcription factors Pax6, Lhx2 and Hes1 (Canto-Soler et al., 2006, Chow et al., 2001), (Fig.1.2).

Optic cup formation: Pigmentation (the production of melanin) in the presumptive RPE first occurs midway through the fifth post-ovulatory week, whereas neural retinal differentiation begins at the end of the sixth week (Schoenwolf et al., 2009). Oxt2 and MitF activate melanin synthesis genes Tyrosinase, Trp1, Trp2 and QNR71 (Martinez-Morales et al., 2003), at this stage Shh and Wnt play key roles in RPE maintenance (Shi et al., 2008). The basal lamina of the RPE goes on to form the Bruch's membrane shortly after pigmentation begins. By the sixth week the neural retina is patterned into an outer and inner neuroblastic cell layer. Subsequently, six classes of neurons and one glial cell type are formed in an evolutionarily conserved order; ganglion cells, cone photoreceptors, horizontal cells then amacrine and rod photoreceptors followed by biopolar cells and muller glia (Slack et al., 2006) (Fig. 1.1).

Figure 1.2 Schematic of human eye development. (A) The optic vesicles are first morphologically distinguishable as lateral bulges evaginating from the forebrain towards the surface ectoderm. Otx2 drives the expression of a network of eye field transcription factors Six3, Lhx2, Rx, Pax6 and Six6. (B) Extraocular tissues pattern the optic vesicle. Adjacent surface ectoderm secretes FGFs which induce Chx10 expression and formation of presumptive neural retina and BMP or activin like signals from the extraocular mesenchyme drive MitF expression and presumptive RPE. (C) The optic vesicle and thickened surface ectoderm invaginate to form a bilayered optic cup in which the outer layer becomes the pigmented RPE. Drawings adapted from Adler et al., 2007.

In summary understanding the developmental cues that lead to the specification of RPE cell fate in vivo is an important starting point in deciphering how RPE might be derived in HESC culture, although it is feasible that the in vitro derivation routes may differ in some details. Understanding of in vivo eye development is also critical in facilitating the characterisation of the stages of HESC differentiation enabling more targeted manipulation of differentiating cells in culture.

1.2.3 Pathophysiology of dry age-related macular degeneration

Age-related macula degeneration (AMD) is currently the leading cause of blindness in the western world (Chopdar et al., 2008). Incidence is strongly correlated with

age: pooled data from 15000 individuals across 3 continents found the incidence of AMD (all types) to be 0.2% in people aged 55-64 years old, rising to 13% of the population over 85 years (Smith et al. 1999). Continuing advances in technology and medicine are resulting in an ever increasing elderly population; this will lead to an inevitable increase in the incidence of age related illnesses such as AMD.

Patients afflicted with AMD suffer from a gradually diminished ability to carry out essential daily activities like driving, reading and recognizing faces often leading to complete loss of central vision. Impaired vision is a consequence of degeneration of the retinal pigment epithelium and Bruch's membrane specifically in the macula. With advancing age the RPE become less efficient at carrying out the essential functions outlined in section 1.2.1, partially due to what is now recognised as chronic, low grade inflammation in the central outer retina (Jager et al., 2008). Damaged RPE develop imperfections in their digestive functions leading to the gradual accumulation of toxic metabolic waste products such as lipofuscin which increasingly interfere with other cell functions (Young et al., 1987) and may induce apoptosis in the RPE (Strauss et al., 2004). The homeostatic environment of the retina thus becomes disturbed and undigested waste material termed 'drusen' begins to accumulate between the RPE and Bruch's membrane. Apoptosing or poorly functioning RPE cannot support the overlying photoreceptors leading to the photoreceptor cell death and loss of vision (Young et al., 1987).

The Bruch's membrane also undergoes significant changes with age, particularly in the submacular region. These changes include the deposition of extracellular matrix, lipids, collagen and advanced glycation end products (Gullapalli et al., 2005). The hydraulic conductance of the membrane also decreases with age, leading to the accumulation of fluid in the subretinal space (Bird et al., 1986). If the integrity of the Bruch's membrane is broken, new blood vessels may begin to form and invade the sub-retinal space. This is known as 'wet' or exudative AMD. These blood vessels are often leaky and result is a dense fibrovascular scar that may cover the whole macula area. Visual acuity usually declines more rapidly in Wet AMD (Chopdar et al., 2009).

1.2.4 Animal models of AMD

AMD is a complex and heterogeneous disease and no one animal model recapitulates all of its features. Rodent models with defects in the complement factor pathway, glucose and lipid metabolism, oxidative stress, inflammation responses and accelerated ageing have all been useful in elucidating the causative role of these various factors in disease pathology (reviewed in Pennesi et al., 2012). A major draw back of these rodent models is the absence of a cone-rich macular in the rodent retina. Rodents do display a higher concentration of photoreceptors in their central retina's relative to the periphery however, and the major anatomy (RPE, Burch's membrane, Choroid), is preserved across species (Zeiss et al., 2010).

The Royal College of Surgeons (RCS) rat is frequently used to investigate changes in the retina and the efficacy of potential treatments. The RCS rat possesses a recessively inherited retinal degeneration caused by an inability of the RPE to phagocytose photoreceptor outer segments. This is attributed to a deletion in a gene encoding the receptor tyrosine kinase (MerTK), which is involved in phagocytosis of shed outer segments (D'Cruz et al., 2000). In the RCS rat, shed outer segments build up in the sub-retinal space over time leading to the degeneration of the outer nuclear layer of the photoreceptors and blindness over the course of three months (Coffey et al., 2001). The RCS rat is particularly useful for investigating the possibility of photoreceptor rescue. The RCS rat has limitations as a model of AMD however as their Bruch's membranes do not deteriorate as seen in AMD, making the rats a poor model for graft integration (D'Cruz et al., 2000).

Polymorphisms in the gene encoding complement factor H (CFH) are implicated in being at risk for AMD (Edwards et al., 2005). With at least 50% of AMD cases associated with Y402H polymorphisms in the CFH gene, this is the single largest genetic risk factor. Genetically engineered CFH-/- double knock out mice display some retinal abnormalities similar to those seen in AMD (Coffey et al., 2007). These include accumulation of drusen like material, a re-organisation of organelles within the retinal pigment epithelium, disorganisation of the photoreceptor outer segments and thinning of the Bruch's membrane (Coffey et al., 2007). Thinning of the Bruch's

membrane is unique among AMD animal models, and this is thought to result from increased phagocytic activity as a result of the deregulated complement pathway.

The ELOVL4 transgenic mouse is used as a model for Stargardt macular degeneration, a form of early onset AMD characterised by photoreceptor degeneration and atrophy of the retinal pigment epithelium (RPE) in the central retina (Karan et al., 2005). ELOVL4 mice have a mutated form of a protein involved in long chain fatty acid synthesis in photoreceptor outer segments. This leads to the accumulation of improperly digested outer segments in the RPE, lipofuscin and phagosomes and subsequent RPE degeneration, primarily in the central retina.

Visual acuity in rodent models can be assessed using head-tracking experiments where animals are placed in the centre of a revolving drum lined with wave gratings of a particular width (Coffey et al., 2002) or in optomotry testing apparatus comprising four computer screens projecting a 3D rotating cyclinder (Lu et al., 2009). Rodents are unable to resolve the lines past a certain age as their vision deteriorates and therefore do not move their heads to track the lines. Optokinetic head-tracking has been shown to correlate well with photoreceptor preservation and is a sensitive method for assessing visual function (Haruta et al., 2004, Coffey et al., 2002, Lawrence et al., 2000).

1.2.5 Risk Factors and Treatment

AMD is caused by chronic, low grade inflammation in the central retina, the causes of which are multifactorial (Jager et al., 2008). Age dependent reduction in pigmentation of the RPE cells and in their secretion of an important antioxidant α-tocopherol (vitamin E) has been reported in AMD (Friedrichson 1995) and insufficient dietary intake of antioxidant rich foods may have a role to play (Evans et al., 2001), smoking also results in an increased risk of AMD. Other studies have linked hypertension, cardiovascular disease, alcohol consumption, oestrogen replacement and diet to AMD incidence, though this evidence is less consistent (Evans et al., 2001). Age and genetic makeup are currently the most important

known risk factors. Linkage analysis has revealed a particular area of chromosome 1 as a susceptibility locus for AMD (Hageman et al., 2005) this region harbours the complement factor H gene (Alternative pathway regulator factor H). Further studies have found that individuals who are homozygous for this 'at risk allele' are 7.4 times more likely to develop AMD (Klien et al., 2005). Individuals with the at-risk allele have a reduced capacity to down-regulate inflammation in response to infection or injury which fits with the theory of an inflammatory event being the initial cause of RPE deterioration in AMD (Hagemen et al 2005). In addition a smaller fraction of AMD cases have been linked to mutations in the gene encoding a ABCA4 transporter protein (see section 1.2.1) and Fibulin-5 which encodes a protein found on the Bruch's membrane (Allikmets et al., 2000, Stone et al., 2004, Tuo et al., 2004).

Therapies that target aberrant neovascularisation in the sub-retinal space have proven effective in the treatment of wet AMD. Photodynamic therapy involves a combination of drugs and laser treatment and can induce the destruction of new blood vessels (Bressler et al., 2000). Injection of VEGF-inhibitor based drugs Lucentis or Avastin (Genentech, CA, USA) are also routinely used to target new blood vessel formation (Csaky et al., 2003). None of these therapies are targeted at repairing the damaged RPE or photoreceptors and thus have a limited capacity to improve vision and are not applicable to patients with dry AMD. The cost of these treatments is significant: the dosing regime for Lucentis involves monthly intravitreal injections costing 2000 USD each, whereas photodynamic therapy is reported to cost 1800 USD per treatment (Meads et al. 2003).

Patients suffering from dry AMD do not have many treatment options. Randomised controlled trials have been undertaken to investigate the effects of antioxidant supplementation on AMD. These have included vitamins C, E, Zinc Sulphate, β-carotene and Lutein (Evans et. al., 2001). So far a positive effect has been seen in the case of lutein supplementation especially in combination with other antioxidants (Richer et al. 2002). In addition studies into the supplementation with Zinc oxide (Newsome et al. 1988) and a combination of Vitamin C, E, β-Carotene, Zinc and copper have been suggestive of a reduced risk of disease progression (Bartlett 2003).

1.3 Cell Therapy in the Treatment of AMD

Whilst the events occurring within the retina that lead to deteriorating vision in dry AMD are well documented, there is as yet no pharmaceutical means by which to halt the process. The retinal pigment epithelium has a pivotal role in the functioning of the photoreceptors and in maintaining homeostasis in the retinal environment. If follows that one approach to halting the deterioration has been to transplant healthy RPE cells into the subretinal space in an attempt to halt the disease progression. The potential benefit of RPE cell replacement has been investigated extensively in animals and more recently in humans (Reviewed in Da cruz et al., 2007).

1.3.1 Autologous RPE Grafts

RPE degeneration in AMD occurs specifically in the macula and the RPE, the choroid and Bruch's membrane in the periphery remain largely healthy. Thus the peripheral retina is an autologous source of RPE cells. Macular translocation surgery involves the surgical separation of the neural retina in the macular region and its subsequent rotation by 45 degrees and reattachment to a healthy region of RPE-choroid (Da Cruz et al., 2007). This technique has been used to treat patients with wet and dry AMD who do not respond to photodynamic therapy or anti VEGF drugs (Treumer et al., 2006, Joussen et al., 2006). An average follow up of three years on 40 patients receiving macular translocation surgery revealed a sustained improvement in visual acuity with 25% of patients maintaining a 3 line gain in best corrected visual acuity (Chen et al., 2010). In another variation, full thickness RPE - choroid patches are excised from the peripheral retina using a specially developed knife (Treumer et al. 2006, Joussen et al. 2006). The neurosensory retina in the macular region is first detached by the infusion of liquid into the subretinal space. The contiguous patch graft is then transferred to the sub-macular location using subretinal forceps where it is flattened and held in place by the injection of heavy silicon oil. This approach has been successful in improving visual function, and

adherence and vascularisation of the graft has been reported up to two years post transplant (Stagna et al., 2002, Joussen et al., 2006).

Retinal patch-graft and macular translocation surgeries are very complex and require great technical expertise. Thus far there has been a high rate of surgical complications including retinal detachment and macular oedema (Da Cruz et al., 2007, Gelisken et al., 2007, Maclaren et al., 2007). Despite their clinical benefit, the prolonged surgical time, significant trauma to the eye and difficulty in placing the graft in the correct location reduces the feasibility of these surgeries becoming a routine clinical procedure for AMD. In addition a number of AMD cases experience peripheral reticular degeneration (Lewis et al., 1985, Sunness et al., 1999) making translocation/harvesting of cells from the periphery potentially futile.

1.3.2 RPE sources for Allogeneic Transplant

Using healthy RPE from an external source reduces the surgery time and complexity as well as inflicting minimal trauma to the afflicted eye. Implanted cells or grafts made from outside sources have the additional advantage that they can be pre-made and standardized in terms of quality control, safety and efficacy. For these reasons an allogeneic cell graft is a more feasible option for large scale and routine clinical application.

Human RPE cells derived from donor eyes are in limited supply and harvested cells can only be kept in culture for a restricted number of passages making availability a problem for wide scale clinical use (Engelhardt et al., 2005). The difficulty in expanding the cells means that the capacity to do extensive safety and quality testing is also severely restricted.

Investigations into the therapeutic value of a spontaneously immortalised human RPE cell line ARPE19 and a genetically engineered human RPE line H1RPE7 have been performed in RCS rats (Coffey et al. 2002, Lund et al 2001). The cells in suspension were injected into the sub-retinal space of immunosuppressed rats. In both cases the injected cells preserved photoreceptors, visual responses and cortically

mediated vision compared to sham injected controls. These immortalised cell lines lose critical functionality after repeated passaging in culture however (Alge et al., 2003) and their therapeutic value is thought to come from their ability to deliver growth factors as appose to carrying out the full range of normal RPE functions (Wang et al. 2005).

The potential of human foetal derived RPE to replace diseased RPE in humans with AMD has also been investigated in a small scale clinical study (Algvere et al.,1994). The retina containing posterior segment of the eye was isolated from 15-17 week old foetuses and the choroid dissected away leaving the RPE cell sheets to grow on a culture dish. When patients were ready for surgery, an optimal patch was selected, the outer edge (where 'new growth' could be seen) was cut away and a specialised cannula-pipette device was used to pick up the patch and place it in the sub-foveal location. Only five subjects were trialled in this study. Whilst the RPE cells grew and integrated effectively into the space, the new RPE supported visual function for only a month. After this an accumulation of fluid in the sub-retinal space began to impair vision. It has been hypothesized that this is a slow form of a-cellular host-graft rejection (Algvere et al., 1999). These studies indicate potential for foetal stem cells and especially the advantages of transplanting the cells as patches. However it is unlikely to provide sufficient material for wide scale clinical use; foetal human RPE begin to show morphological abnormalities after 5-6 passages and are therefore not suitable as a universal donor source (Gullapalli et al., 2008). Creating the grafts relies on a supply of developing eyes from aborted foetuses which has both ethical and logistical problems.

In addition to RPE transplantation, clinical trials using non-differentiated stem cells derived from umbilical chords are being conducted in patients with dry AMD (http://clinicaltrials.gov, number NCT01226628). The undifferentiated cells were shown to improve visual parameters when injected subretinally into RCS rats, probably via the secretion of neural survival promoting growth factor such as brain derived neurotrophic factor (Lund et al., 2007, Ramsden et al., 2013). Similarly bone marrow derived mesenchymal stem cells (BMMSCs) have been shown to reverse the decline in visual parameters when injected into RCS rats (Lu et al., 2010), and bone marrow derived haematopoietic stem cells (BMHSCs) have been shown to migrate to

site of a damaged retina and express RPE65 in mice. No improvements in visual parameters were seen when these cells were injected into three patients with retinitis pigmentosa (Siqueira et al., 2011, Ramsden et al., 2013).

The main drawback of allogeneic transplants is their potential to illicit adverse immune responses. The ocular environment has been described as immunosuppressive and anti-inflammatory or 'immunologically privileged' (Niederkorn et al., 1990), however an AMD afflicted eye with a deteriorated Bruch's and reduced numbers of immunosuppressive RPE may no longer be such a benign environment for transplantation. After several studies of foetal RPE grafts in humans, it was concluded that rejection is common but not inevitable and risk factors include transplanting the graft close to the area of retinotomy, near to the fovea or transplanting large number of cells (Da Cruz et al. 2007). In the case of allogenic bone marrow derived mesenchymal stem cells, immunosuppression may not be as important, but early studies in rats indicated that their functionality is inferior to that of differentiation RPE cells (Ramsden et al., 2013).

In summary it is desirable to identify a source of RPE suitable for wide scale clinical use. The cells would ideally be fast to expand from an unlimited/abundant source, stable over indefinite passages and easy to assemble into a form that can be implanted in a simple and fast procedure. In addition the cells for therapy must be amenable in all aspects to the various regulatory authorities. A number of RPE cell sources have been trialled for their therapeutic value in the treatment of AMD in both RCS rats, and humans (Ramsden et al., 2013). In most cases some level of improved visual acuity or attenuation of deterioration was observed. The spontaneously immortalised ARPE19 cell line provides an abundant source of material but the cells do not possess all the key attributes of native RPE, foetal RPE on the other hand may function well but are scarcely available and thus not suitable for wide scale clinical application.

1.4 Pluripotent stem cells as a source of RPE

Pluripotent stem cells (human embryonic stem cells (HESC) and induced pluripotent stem cells (IPSC)) have the potential to differentiate into all cell types in the body, including RPE. The spontaneous formation of RPE was first described in primate embryonic stem cells in 2002 (Kawasaki et al., 2002). Pigmented areas appeared in primate ESC colonies after three weeks of co-culture with PA6 stromal cells. The phenomenon was subsequently reported two years later, this time using several human embryonic stem cell (HESC) lines including H1, H7 and H9 (Klimanskaya et al. 2004). The pigmented 'HESC-RPE' cells were at this time characterised using transcriptomics and found to compare favourably with primary RPE tissue. Following the discovery in 2007 of effective methods to reprogram adult somatic cells into a pluripotent state (Takahashi et al., 2007, Yu et al., 2007), so called induced pluripotent stem cells (IPSC) derived RPE have been produced from several lines and shown to have similar characteristics to HESC-RPE and foetal RPE (Buchholz et al., 2009, Carr et al., 2009, Kokkinaki et al., 2011). Since the start of this project in 2008 there have been over thirty independent accounts of deriving RPE cells from HESC and IPSC. The cell lines, techniques, timings and RPE yields (when known) from these various studies are summarised in at the end of this chapter in table 1.1.

The advantages of using HESC or IPSC as a source of RPE are multiple; their ability to self-renew indefinitely in culture makes for a theoretically unlimited source of clinical material and extensive characterisation has revealed their superior functionality relative to adult RPE lines (Klimanskaya et al., 2004, Vugler et al., 2008). Pluripotent stem cells are amongst the most biologically complex materials ever to be proposed for clinical use however and the mechanisms by which they differentiate into RPE are challenging to pick apart and control. In this section the origins and characteristics of HESC and IPSC are reviewed as are the methods for generating HESC-RPE.

1.4.1 Origins and characteristics of human embryonic stem cells

The isolation and establishment of human embryonic stem cell (HESC) lines was first described in 1998 (Thomson et al., 1998). The essential characteristics of human embryonic stem cells were defined in that report as follows: 1.derivation from the pre-implantation or peri-implantation embryo, 2. stable developmental potential to form derivatives of all three embryonic germ layers even after prolonged culture (pluripotency) and 3. prolonged undifferentiated proliferation (Thomson et al., 1998).

Derivation: Fertilised embryos donated by couples undergoing IVF are cultured to the blastocyst stage (6 days). The inner cell mass (ICM) is then isolated by immunosurgery before culturing in medium containing bovine serum albumin (BSA) on mitomycin C inactivated mouse embryonic fibroblasts (MEFs) (Thomson et al., 1998, Reubinoff et al., 2000). The BSA containing media and MEFs are materials originally developed in 1954 for the cultivation of HeLa cells (Puck et al., 1954). A number of improvements to the derivation methods have been made since the original study including the generation of HESC lines without destruction of the embryo (Chung et al., 2008) and the derivation of clinical-grade cGMP cell lines (Crook et al., 2007). These lines were derived on FDA approved clinical grade human foreskin fibroblasts, in cGMP manufactured BSA-based serum replacement medium. Isolation of the ICM was carried out manually to avoid the requirement for cGMP grade antibodies. These developments significantly reduced the obstacles in establishing HESC derived products suitable for clinical practice.

Pluripotency: Unlike mouse embryonic stem cells it is not ethically feasible to test the full developmental potential of a human ES cell by implantation into an intact embryo; thus it can only be hypothesised that human ES cells would be able to contribute to all adult tissues including germ cells. The most stringent means for assessing pluripotency in HESC are currently teratoma assays in which undifferentiated HESC are transplanted into immunodeficient mice. After 3 weeks solid teratomas form which are excised and dissected in order to detect the presence of organised differentiated cells or tissues derived from each of the three developmental germ layers (Muller et al., 2010, Amit et al., 2002, Damjanov et al., 1993). Alternatively HESC can be differentiated as suspended aggregates allowing

the formation of embryoid bodies (EBs) in which the early development of the three germ layers is re-capitulated (Sheridan et al., 2011). Analysis by gene expression, histology and immunohistochemistry has demonstrated the presences of ectoderm, endoderm and mesoderm derivatives in HESC derived EBs (Itskovitz-Eldor et al., 2000, Hopfl et al., 2004).

Longer term directed differentiation protocols have been successful in generating more functionally mature cell types originating from all three germ layers including insulin secreting pancreatic islet cells (Lumelsky et al., 2001), cardiomyocytes (Xu et al., 2002a), and dopaminergic neurons (Chambers et al., 2009) amongst many others. Directed protocols for generating these cells types generally involve supplementing the media with relatively small range of growth factors including TGFβ/activin/nodal, BMP, Wnt and FGF agonists/antagonists, during specific time windows.

Mechanisms of pluripotency: The mechanisms by which HESC remain in an undifferentiated state remain under investigation; it is clear that transcriptional regulation, epigenetic regulation and regulatory miRNAs have important roles to play. Homeodmain transcription factors Oct4, Nanog, and HMG transcription factor Sox2 have been identified as key transcription factors in the pluripotency network (Chen et al., 2008). These transcription factors share target genes and regulate each others expression in feedback and feed forward loops (Boyer et al., 2005) as well as regulating the expression of genes involved in histone and chromatin remodelling complexes (Gan et al., 2007), and genes encoding transcription factors key to early development and differentiation (Chickarmane et al., 2006, Chen et al., 2008). The chromatin in HESC cells is found in a unique, hyperdynamic and permissive state (Gan et al., 2007). This is thought to facilitate the rapid changes in gene expression required to initiate differentiation, a process which is facilitated by the combined action of pluripotency factors and miRNAs (Chen et al., 2008).

HESC pluripotency in culture requires the external stimulation by factors which mediate elements of the pluripotency network including Oct4, Nanog and Sox2. activin/nodal, FGF, IGF and Wnt/β catenin signalling pathways have variously been implicated either alone or in combination with one another (Vallier et al., 2005, Ding

et al., 2010, Bendall et al., 2007). In standard culture conditions these signalling pathways are stimulated by growth factors secreted by MEFs and by the exogenous addition of recombinant FGF (Chin et al., 2007). Activin/nodal is thought to act via SMAD2/3 to maintain the expression of Nanog which then acts as a co-factor in maintaining SMAD2/3 induced transcriptional activity (Brown et al., 2011). The activin/nodal pathway is critical to the maintenance of pluripotency but external stimulation of this pathway alone is insufficient to maintain pluripotency in defined medium and it appears to act through a mechanism in which FGF acts as a competence factor (Vallier et al., 2005). The mechanisms by which FGF acts to maintain pluripotency also remain under investigation. In one study FGF was shown to act indirectly on HESC pluripotency by stimulating IGFII production in a subset of partially differentiated Oct4 negative HESC derived feeder cells that become established adjacent to Oct4 positive undifferentiated HESC cells as part of a regulatory niche that establishes itself in culture (Bendall et al., 2007). Other studies have demonstrated a more direct role of FGF in mediating pluripotency gene expression via MAPK and PI3K signalling pathways (Ding et al., 2010).

Despite the inconvenience of MEFs co-culture, its reliability and relative cost efficiency has meant that it remains the most common method for deriving and sustaining HESC as well as IPSC. An increasing body of knowledge on how these pluripotency networks are regulated has in recent years facilitated the design of defined culture for HESC maintenance (Xiao et al., 2006, Chin et al., 2010). None of these systems entirely prevent spontaneous differentiation however and as a result cultures are heterogeneous, containing both undifferentiated and spontaneously differentiating cells (Narkilahti et al., 2007, Chin et al., 2010). Thus it remains common practice to continually observe HESC cultures and manually 'weed out' colonies with differentiated morphology (Loring et al., 2007).

Prolonged undifferentiated proliferation: HESC are often described as immortal due to their prolonged proliferative potential (Carpenter et al., 2003). HESC population doubling times are between 30-40 hrs (Amit et al., 2000) and pluripotent, karyotypically normal HESC have been maintained in culture for longer than one year or over one hundred and forty passages (Carpenter et al., 2003, Narva et al., 2010). This property is key to their potential wide scale clinical value as it enables

scaled up cell production. Similar to other cell types with extensive replicative capacity (e.g. germ cells, tumour cells) telomerase activity is relatively high in HESC compared to somatic cells, as is the expression of its catalytic component hTERT (Amit et al., 2000, Lebkowski et al., 2001, Thomson et al., 1998). Telomerase reduces and stabilises the telomere shortening which contributes to senescence in somatic cells. Upon differentiation, hTERT expression is down regulated as differentiated HESC derivatives become senescent (Lebkowski et al., 2001). In spite of their proliferative potential there is compelling evidence that HESC populations change over time in culture (Enver et al., 2005, Baker et al., 2007, Harrison et al., 2007, Narva et al., 2010). Although the incidence of gross karyotypic re-arrangements are not necessarily correlated with time in culture (Adewumi et al., 2007, Brimble et al., 2004) more subtle epigenetic adaptations that favour survival and rapid growth are selected for over successive passages (Rossler et al., 2004, Enver et al., 2005). The extent to which these changes occur is not predictable and differences in passaging methods, seeding density, general exposure to stress and individual properties of the cell line may have an impact (Draper et al., 2004, Brimble et al., 2004, Baker et al., 2007). With increasing passage number changes in growth rates and a reduced tendency for early stage spontaneous differentiation have been reported (Enver et al., 2005, Herszfeld et al., 2006). The effects of such changes on long term differentiation yields are yet to be determined.

1.4.2 Origins and characteristics of induced pluripotent stem cells

In 2007 Yamanaka's group and Jamie Thompson's group showed that adult human fibroblasts could be successfully reprogrammed into an embryonic like state by the addition of four transcription factors (Takahashi et al., 2007, Yu et al., 2007). Since then a variety of functional and mature cell types have been differentiated from IPSC including RPE (Meyer et al., 2009, Buchholz et al., 2009, Carr et al., 2009, Hirami et al., 2009). IPSC have both advantages and disadvantages as a cell source over HESC. IPSC share the majority of the critical characteristics of HESC – they retain the ability to differentiate into all cell types over prolonged periods of time in culture, and yet do not require the destruction of a human embryo and can be derived from many kinds of somatic adult tissue. In this way IPSC circumvent the ethical concerns

and limited supply problems associated with HESC. IPSC technology theoretically enables the generation of patient specific, autologous cell lines for cell therapy, as well as providing a unique opportunity to study cellular phenotypes from patients with genetic disorders (Merkle et al., 2013). Some important questions about the differences between HESC and IPSC remain unanswered however. Although the work in this thesis is carried out in HESC, given the rising prominence of IPSC as an alternative source of retinal and RPE cells, some background on IPSC and the recent efforts to differentiate IPSC-RPE and to test their functional/ therapeutic equivalence have been included in this literature review.

Derivation: Induced pluripotent stem cells were originally derived by ectopic expression of a combination of transcription factors OCT4, SOX2, KLF4 and C-MYC by retroviral delivery first into mouse fibroblasts (Takahashi et al., 2006) and then into human fibroblasts (Takahashi et al., 2007) or OCT4, NANOG, SOX2 and LIN28 (Yu et al., 2007). IPSC have since been derived from adult human cell types as diverse as terminally differentiated lymphocytes (Loh et al., 2010) and post mitotic neurons (Kim et al., 2011), although dermal fibroblast obtained from skin biopsies remain the most common source. The choice of donor cell is important as some cell types such as blood (Ohmine et al., 2011) and urine (Zhou et al., 2012) are less invasive to sample, but may have poor reprogramming efficiencies due to their capacity for expansion in culture and/or differentiation status (Eminli et al., 2009). Currently the best quoted efficiencies of human somatic cell to IPSC conversion, using retroviral integration methods remains low at between 0.1-1% (Sommer et al., 2013). The technology is advancing quickly however and efficiencies are improving due to new methods for gene delivery, the discovery of small molecules which enhance reprogramming efficiency (e.g. valporic acid, sodium butyrate) and in some cases transferral to hypoxic conditions (Warren et al., 2010). Of particular interest for therapeutic application are non-integrative reprogramming methods that do not risk insertional mutagenesis or leaky transgene expression which can result in partially reprogrammed cells and/or enhanced tumorigenicity. Integration free methods including episomally maintained plasmids, adenoviral vectors, recombinant DNA, mRNA, and recombinant proteins have proven successful at generating human IPSC lines (reviewed in Stadtfeld et al., 2013) although conversion efficiencies are generally several orders of magnitude lower than with integrating methods (Sommer

et al., 2013). IPSC lines are also being derived in accordance with GMP regulations (Ohmine et al., 2011).

Pluripotency, HESC equivalence: The first IPSC to be derived were found to be similar to HESC in terms of morphology, surface marker expression, methylation status in promoter regions associated with pluripotency and in-vitro differentiation (Takahashi et al., 2007, Yu et al. 2007). Similar to HESC it is not ethically feasible to test the pluripotency of human IPSC by implantation into embryos, however this experiment has been performed in mouse demonstrating the potency of reprogrammed cells. Injection of IPSC into tetraploid blastocycts has been shown to produced chimeric mice and in some cases 'all-IPSC' mice (Boland et al., 2009). IPSCs meet the most stringent criteria of HESC pluripotency in that they form teratomas containing derivatives of all three germ layers when injected into immunodeficient mice (Park et al., 2008). More detailed studies into the equivalence of HESC and IPSC have looked at global gene expression profiles and histone modificiation patterns and found a high degree of similarity between the two (Maherali et al., 2007, Mikkelsen et al., 2008). Reported differences between the two cell types have included less efficient and more variable neuronal differentiation in IPSC (Hu et al., 2010a), premature senescence in IPSC derived cells (Feng et al., 2010, Kokkinaki et al., 2011) and epigenetic memory of the cell type of origin in IPSC (Kim et al., 2010). One report found that IPSC deviate from ES in a recurrent gene expression signature (Chin et al., 2009). Despite these differences, a huge range of functionally mature cell types have been derived from IPSC.

Prolonged undifferentiated proliferation: The formation of IPSC from mature somatic cells requires epigenetic re-programming which is triggered by the transient expression of the reprogramming transcription factors (Takahashi et al., 2007). A recent study comparing the DNA methylation profiles of 22 IPSC lines over long term culture found that continuous passaging reduced the differences between IPSC lines, with multiple appearances and disappearances of hyper-methylation throughout the reprogramming process (Nishino et al., 2011). This is thought to reflect a process of cell lines losing the characteristics derived from their parental cell type and adapting a more embryonic like character. Reprogramming of somatic cells induces telomere length extension and a reactivation of the enzymatic complex telomerase

(Takahashi et al., 2007, Park et al., 2008). Thus reprogrammed cells from donors of any age do not undergo replicative senescence. Whether or not these cells undergo the same process of culture adaptation seen in HESC remains an open question. The identical culturing practices used to maintain IPSC and HESC would suggest that a similar phenomenon is likely to occur.

1.4.3 Embryonic retinal development is mimicked in HESC and IPSC

Spontaneous differentiation into RPE appears to occur reliably in the majority of HESC and, more recently, IPSC lines in standard culture conditions (MEFs, DMEM, 20% KOSR) without the requirement of exogenous growth factors (Odorico et al., 2001, Klimanskaya et al., 2004, Lund et al., 2006, Vugler et al., 2008, Buchholz et al., 2009, Hu et al., 2010, Vaajassari 2011 – see table 1.1). It is generally assumed that the differentiation of HESC into RPE and other retinal phenotypes faithfully mimics the well defined and evolutionarily conserved development program that occurs during human retinogenesis (Vugler et al., 2007). This assertion is based on three lines of evidence in the case of RPE differentiation: 1. the coordinated sequence of gene/protein expression and timing of pigmentation, 2. stage specific responses of differentiating HESC to exogenous growth factors and 3. in vitro observations of structural aspects of optic vesicle morphogenesis in HESC. The melanocytes that make up the retinal pigment epithelium (RPE) have a distinct developmental origin to those which are found in the iris, choroid, inner ear and skin (Nakayama et al., 1997). The RPE cells are uniquely derived from anterior neural plate (Bharti et al., 2006) whereas the other pigmented cells are neural crest derived. Thus the epithelial melanocytes (RPE) derived from long term HESC culture differ from other pigmented cells not only in their terminal morphology and marker expression, but in the developmental stages through which they progress (Fig.1.3)

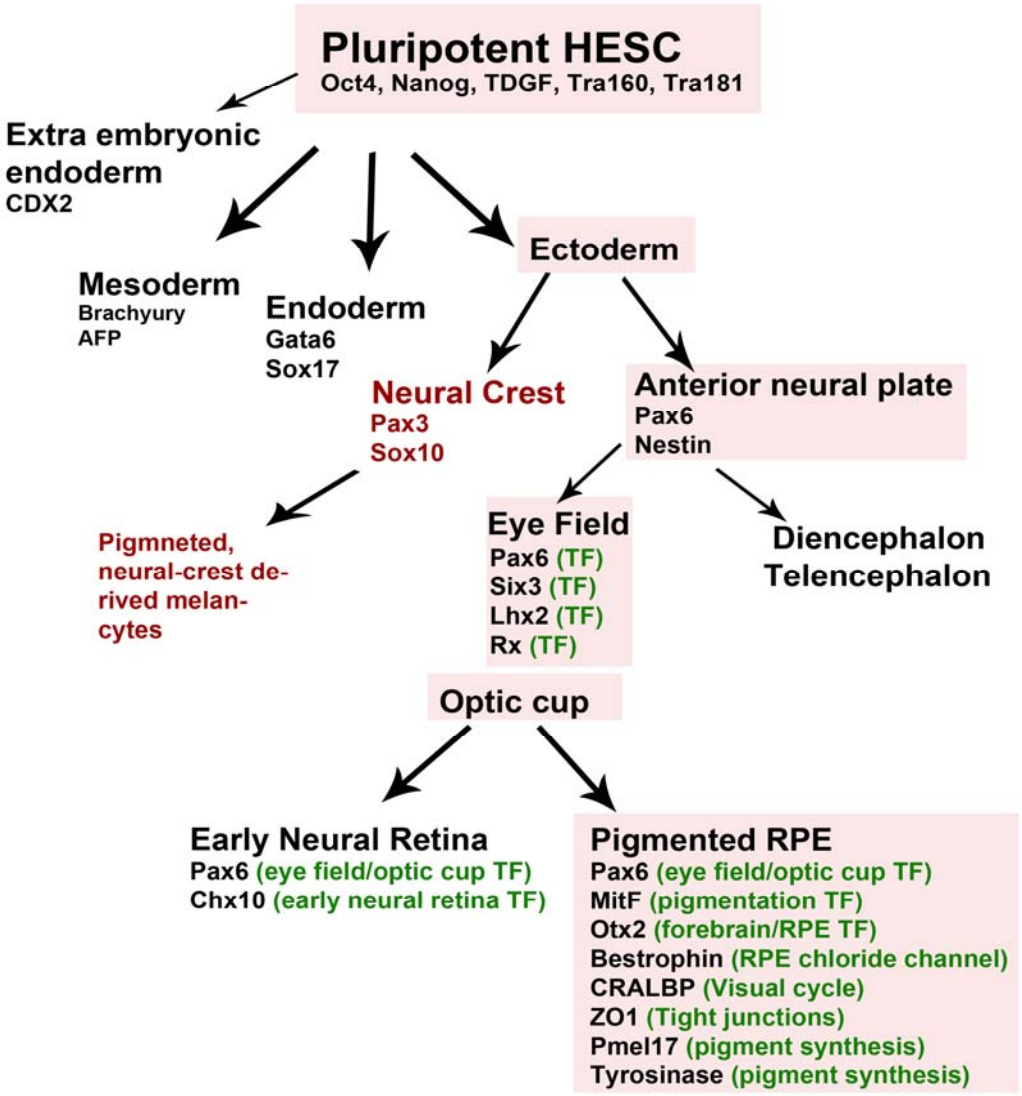

Figure 1.3 Embryonic retinal development is mimicked in HESC. Pigmented RPE emerging in HESC culture have been shown to undergo the same developmental stages seen in vivo. Pluripotent HESC differentiate into derivatives of all three germ layers but under the right conditions a significant proportion adopt an anterior neuroectodermal fate. Some of these cells adopt eye field and subsequently a pigmented, RPE phenotype (boxes). Directed differentiation with appropriately timed external cues can also yield Sox10 and Pax3 positive melanocytes. derived from a neural crest progenitor type cell (chambers et al., 2009), (TF= transcription factor).

Coordinated sequence of gene/protein expression: Using a non-interventionist approach Meyer et al., demonstrated the step wise differentiation of the H9 cell line toward RPE and early retinal progenitors in minimal media (Meyer et al., 2009). Time course experiments revealed a steady increase in Pax6 and Rx gene expression from day 3 and 5 of differentiation respectively, accompanied by a steady increase in the abundance of cells immunopositive for these markers. The expression of other eye field transcription factors (Six3, Six6, Lhx2) was first detectable from days 6-10. Importantly these markers are not detected in undifferentiated HESC from days 0-4 post seeding. In longer time course experiments MitF expression was found to peak at day 37 and Chx10 expression later at day 60 in line with the sequence of these events in vivo (Nguyen et al., 2000). Endogenous expression of BMP and Wnt antagonists Noggin and DKK1 has also been show to increase during early differentiation (Meyer et al., 2009) and Shh and Nodal expression to increase from day 45 onwards (Mellough et al., 2013).

There is considerable variation in the reported timings of pigmentation appearance during spontaneous differentiation ranging from 40-60 days (Meyer et al., 2011, Rowland et al., 2012) to 10-17 days (Vaajassari et al., 2011) (See table 1.1 for timings of all HESC-RPE differentiation protocols published to date). This is likely due to differences in differentiation propensity between cell lines as well as methods for pigmented cell detection. A crude assessment of the published timings (table 1.1) yields a median time to pigmentation of 28 days ± 12 STDEV (N=35) post cell seeding. Pigmentation of the prospective RPE occurs in humans at post ovulatory weeks five to six (days 35-42) and given that HESC are derived from post implantation embryos at day 5-7, the average timing of HESC-RPE emergence falls within the shorter end of the predicted range. A number of protocols employ a cell expansion step in HESC maintenance media during which supposedly undifferentiated HESC proliferation occurs (Vugler et al., 2008, Buchholz et al., 2009, Maruottie et al., 2013) this is often 7-10 days in length. In such cases the spontaneous differentiation of pluripotent cells to pigmented RPE cells occurs more rapidly than in vivo (~18 days). A very recent study has reported the derivation of Pmel17 positive, pigmented RPE in a significantly shorter time period (2 weeks post seeding) by inducing differentiation with several growth factors and small molecules (Buchholz et al., 2013).

Responses to exogenous growth factors: Early addition of BMP4 and Wnt3a to the culture medium prevents the formation of Pax6 and Rx positive neural rosettes (Meyer et al., 2009) affirming the role of inhibition of these pathways in the in vitro equivalent of anterior neural plate formation (Villanueva et al., 2002, Wilson et al. 2004). Similarly IGF1, which is secreted by MEFs (Bendall et al., 2009) and is present in Matrigel and N2/B27 supplement (www.bdbioscences.com), has been shown to be critical to Pax6, Rx and Otx2 expression during early HESC differentiation, and its pharmacological inhibition prevents the formation of stratified retinal neuroepithelium during spontaneous differentiation (Zhu et al., 2012). This is in line with the role of IGF1 in inducing Otx2 expression during specification of the anterior neural plate and eye field (Pera et al., 2001). In another example, the addition of small molecule Wnt agonist CHIR99021 at a later time point in the differentiation (days 18-21) significantly enhances the formation of RPE cells (Nakano et al., 2012), in agreement with the key role of Wnt/βcatenin (in combination with Otx2) in driving MitF expression at the optic vesicle/early optic cup stage in vivo (Westenskow et al., 2010). Finally activin A/TGFβ has been shown to stimulate RPE differentiation when added from day 14 onwards (Idelson et al., 2009, Meyer et al., 2011) as seen in chick optic explants (Furhmann et al., 2000).

Structural aspect of eye morphogenesis: Recently the spontaneous emergence of optic vesicle like structures in HESC differentiating as floating aggregates has been described (Nakano et al., 2012). Using an Rx::Venus HESC reporter line, the formation Rx expressing hollow bulbs was shown following early treatment of HESC aggregates with a Wnt inhibitor. These bulbs developed into Chx10 +ve neural retinal epithelium. Subsequent addition of a Wnt agonist induced the formation of thin MitF expressing epithelium next to the Chx10 positive cells. The Chx10, MitF expressing bulbs then spontaneously invaginated to form a double walled optic cup structure 550μM in diameter in which pigmented RPE and stratified layers of the neural retina could be clearly identified within 24 days of differentiation (Nakano et al., 2012). The size of the optic cup structure is similar to observations in human foetal eye development, and the time taken is only a few days shorter (O'Rahilly et al., 1999). Similar experiments in mouse embryonic stem cells generated a significantly smaller optic cup (~280μM) in a shorter time (9 days) as predicted by observation in mouse foetal development (Nguyen et al., 2000).

1.4.3 Characterisation of HESC and IPSC derived RPE

Pigmentation and distinctive cobblestone morphology enables the identification of HESC-RPE among a background of other cell types in culture. Given that HESC are theoretically capable of producing any cell type including other pigmented cells such as melanocytes, it is necessary to employ assays that eliminate the possibility that the cells have other identities. A number of assays have been developed in order to test the functionality of HESC derived RPE. An important point for investigation has been to establish the equivalent developmental stage which HESC derived RPE most closely resemble.

Gene expression: HESC-RPE expression profiles have been characterised extensively, they express known RPE transcription factors (Otx2, MitF), genes involved in pigment synthesis (Tyrosinase, Pmel17, Tyrp1/2), the visual cycle (CRALBP, RPE65, LRAT), membrane associated protiens (Bestrophin, EMMPRIN) as well as early eye field genes (Pax6, Rx, Six3) (Vugler et al., 2008, Meyer et al., 2009, Buchholz et al., 2009, Vaajasaari et al., 2010). Global gene expression analysis has demonstrated the similarity between HESC derived RPE and foetal RPE (Klimanskaya et al., 2004, Liao et al., 2010). HESC-RPE were found to be more similar to foetal RPE than to the spontaneously immortalised cell line ARPE19. This is in line with observations that ARPE19 cell lines tend to lose expression of critical functional genes such as RPE65, Bestrophin, CRALBP and PEDF over time in culture (Alge et al., 2003).

Newly differentiated HESC-RPE are thought to be in a developmentally immature state. This has implications in terms of the expansion capacity of the HESC derived RPE. The immature status may also be advantageous in terms of their ability to integrate into the degenerating retina; the fundamental importance of controlling the developmental staging of ES derived retinal cells for successful integration has been shown in the degenerating mouse retina (Maclaren et al., 2006, Lamba et al., 2009). Observations that HESC-RPE express early developmental markers in addition to mature markers suggests some heterogeneity within these populations (Liao et al., 2010).

Protein Expression: Shef1 derived HESC-RPE cells stain positively for important RPE proteins involved in the visual cycle (CRALBP), membrane associated channel proteins (Bestrophin), RPE transcription factors (MitF, Otx2), pigment synthesis (Pmel17), tight junction protiens (ZO1, Occludin and Claudin-1) and polarised ion transporters (Na+/K+ ATPase) (Vugler et al., 2008). A number of these markers have since been found in HESC-RPE and IPSC-RPE derived from other cell lines (Ideslon et al., 2009; Meyer et al., 2009; Buchholz et al.,2009; Vjasaari et al., 2010; Kokinakki et al. 2011). The expression of RPE65 protein by HESC-RPE has also been verified by immunohistochemistry and western blot, a protein is usually undetectable in ARPE19 (Vugler et al., 2008, Alge et al., 2003).

Morphological features: In vivo RPE form a highly polarised monolayer. Electron micrographs of RPE expanding on Matrigel clearly show the presence of polarised features such as apical microvilli and basal nuclei (Vugler et al., 2008, Idelson et al. 2009). Mature HESC-RPE feature a basally located nucleus, tight junctions and apically distributed melanosomes with the morphologies indicative of the various stages of melanogenesis (Vugler et al., 2008, Carr et al., 2009, Zhu et al., 2013).

Growth factor secretion: When cultured on transwell plates ESC and IPSC derived RPE demonstrate polarised growth factor secretion as seen in vivo (Maminishkis et al., 2006). A range of growth factors are secreted by HESC-RPE including VEGF, PEDF, BDNF and TGFβ (Sugino et al., 2011). Media samples taken from the upper and lower reservoirs of HESC-RPE seeded on transwell plates show that VEGF is mainly secreted on the basal side, and PEDF mainly on the apical side as seen in vivo in healthy RPE (Kokkinaki et al. 2011; Vjasaari et al., 2011). The secretion of specific growth factors may be critical to the therapeutic benefit of cells transplanted into the ocular environment (Lawerence et al., 2000) and it has been shown that the levels of secretion correlate with the degree of RPE differentiation in cultured human RPE cells with more mature RPE secreting larger quantities (Ohno-Matsui et al., 2001).

Phagocytosis: As detailed in section 1.2.1, an important function of RPE in the retina is to phagocytose rod and cone outer segments. In an attempt to demonstrate this capacity several groups have used a latex bead assay, in which the ability of the cells

to internalise fluorescently labelled latex beads is demonstrated (Klimanskaya et al., 2004; Idelson et al., 2009, Osakada et al., 2008). Carr et al. have subsequently demonstrated the full functionality of Shef1 derived RPE by showing their ability to phagocytose fluorescently labelled outer segments from porcine eyes. The latter is more relevant as defective RPE are not able to phagocytose photoreceptor outer segments but can ingest inert polystyrene/latex beads (Carr et al., 2009b).

Attachment and survival assays: Attachment and survival of the HESC-RPE cells in the ocular environment will be critical to their function in transplantation therapies. Transplantation strategies differ with some favouring direct injection of a cell suspension into the sub-retinal space (Lu et al., 2009, Schwartz et al., 2012) and others seeding cells onto an artificial substrate generating a differentiated RPE monolayer prior to transplantation (Hu et al., 2012 (c), Kearns et al., 2012, Subrizi et al., 2012 – see section 1.5.2-1.5.3). In the former strategy, characterising the ability of the cells to attach and survive in the ocular environment is critical. Sugino et al. compared the ability of HESC-RPE with different degrees of pigmentation to attach and survive on aged human Bruch's membranes. It was found that more pigmented and differentiated HESC-RPE (5 or 10-11 weeks in culture) had improved survival over 21 days relative to less pigmented HESC-RPE (1 week in culture) (Sugino et al., 2011). Conversely, another study determined that less pigmented HESC-RPE had improved survival on gelatine relative to heavily pigmented differentiated cells (Schwartz et al., 2012).

IPSC-HESC RPE equivalence: Several induced pluripotent stem cell lines have been successfully differentiated into RPE cells (Meyer et al., 2009, Buchholz et al., 2009, Hu et al., 2010, Carr et al., 2009, Kokkinaki et al., 2011 – see table 1.1). Differentiating IPSC generate RPE foci within the typical time frames and efficiencies that have been described in HESC (see table 1.1). Significant variability in RPE yields are seen between IPSC lines with one study implicating the reprogrammed cell of origin, and the 'epigenetic memory' of the cells in the relative differentiation efficiency (Hu et al., 2010). In the most extensive study of gene expression profiles to date, purified, first passage IPSC-RPE have been shown to have equivalent expression of 59/89 signature genes (Strunnikova et al., 2010) compared to native RPE by QPCR (Kokkinaki et al., 2011). RPE derived from the

fibroblast IPSC line IMR90, adopt the polarised morphological characteristics typical of native and HESC-RPE including apical mircovilli, basal nuclei, melanosomes, basal lamina and adherens junctions (Carr et al., 2009) as well as expressing appropriately localised proteins such as collagen IV and Na+/K+ ATPase ATP1B1 and RPE proteins MitF, Otx2, Bestrophin, CRALBP and RPE65 (Buchholz et al., 2009, Carr et al., 2009). In another study, IPSC-RPE were shown to have equivalent polarised growth factor secretion, ion transport and membrane potential to an adult human retina. These differentiated RPE were also shown to have rapid telomere shortening and DNA chromosomal damage which may have implications for their expansion capacity and survival post transplantation, this property therefore warrants further investigation (Kokkinaki et al., 2011). The ability of IPSC-RPE to phagocytose fluorescently labelled bovine and porcine photoreceptor outer segments was found to be equivalent to HESC-RPE and foetal-RPE (Buchholz et al., 2009, Carr et al., 2009).

1.4.3 Directed differentiation strategies

In addition to spontaneous differentiation strategies, commonly used cell lines such as H7 and H9 (Thomson et all., 1998) as well as others, have been used in a variety of so called 'directed' retinal differentiation protocols that often aim to mimic the developmental cues that direct eye development in vivo (see section 1.2.2) by the addition of growth factors. In spite of the huge range of methods and reported yields, pigmented cells possessing the typical RPE characteristics described in the previous section are consistently derived.

These 'directed' strategies employ a range of media formulations including growth factors and small molecules in attempts to enhance differentiation yields, reduce the time required to generate the required cell, encourage differentiation into more mature retinal cell types and/or to investigate the synergies with human eye development (section 1.2.2). The number of distinct methods has risen rapidly over the last 4 years since the start of this project, the basic methodologies and findings

are summarised in table 1.1. Here we will discuss in general terms the relative success of these differentiation strategies.

Growth factors and small molecules that are known to enhance early neural specification and specify the anterior neural fate in vivo by interfering with major signalling pathways have been used extensively at the early stages of HESC differentiation protocols. These have included Wnt antagonists (DKK1, CKI7), Nodal antagonists (LeftyA, SB431542) and BMP antagonists (Noggin) as well as Insulin growth factor (IGF) which is thought to specify anterior neural specification (see section 1.2.2). Growth factors DKK1, LeftyA and IGF reportedly increase MitF positive cell yields by 3-5 fold following embryoid body differentiation (Osakada et al., 2008). Their small molecule equivalents (CK17, S431542) have comparable efficacy at a significantly reduced cost (Osakada et al., 2009).

N2 and B-27 supplements are also common to many of the protocols listed in table 1.1. These supplements contain high concentrations of insulin and have been shown to promote neuralization as well as enhancing neural progenitor proliferation (Schuldiner et al., 2000). Mellough et al., found the retinal differentiation promoting effect of these supplements was significantly greater than that of the recombinant growth factors DKK1, LeftyA, IGF1 (Mellough et al., 2013).

Nicotinamide (NIC) is an example of a small molecule shown to robustly enhance RPE yield without directly interfering with RPE specification pathways (Idelson et al., 2009). Idelson et al., found that 10mM NIC added to standard culture medium (14% KOSR, -bFGF) enhanced the number of embryoid bodies containing pigmented cells between 2 and 5.6 fold, dependent on the cell line. This study concluded that the mechanism of Nicotinamide's RPE promoting action was by reducing apoptosis in cells differentiating towards the neuroectoderm lineage. Large scale transcriptional analysis found that NIC specifically enhanced the expression of genes involved in anterior neural specification as apposed to midbrain or caudal markers (Idelson et al., 2009).

At later time points, factors that interfere with neural-retina vs. RPE fate decision at the optic vesicle/optic cup stage are frequently added in an effort to enhance RPE

differentiation. In the study described above, NIC treated cells are further treated with TGFβ superfamily growth factors including activin A and TGFβ (Idelson et al., 2009). When added to standard medium between weeks 3-4 activin A enhanced pigmentation in three cell lines (3- 5 fold increase relative to NIC only). Activin A has been shown to improve RPE yields in optic vesicle like structures (Meyer et al.,. 2011, Zhu et al.. 2013), although in other cell lines it has been reported it to have little effect on pigmentation or RPE gene expression (Buchholz et al., 2013, Zhu et al., 2013), and thus the wide-scale efficacy of activin A in differentiating HESC remains somewhat controversial. As discussed in section 1.2.2, FGF signalling emanating from the surface ectoderm during optic cup formation down regulates MitF and enhances Chx10 expression thereby specifying neural retinal fate (Fuhrmann et al., 2000). The addition of the FGF inhibitor SU5402 from days 16-40 have been shown to increase MitF expression ~12 fold (Meyer et al., 2009). Aside from the TGFβ/FGF signalling pathways, Wnt agonists (days 18-21, Nakano et al., 2012) and Shh agonists (days 15-18, Nakano et al., 2012, days 18-30 Zahabi et al., 2012) have been used to induce pigmentation as well as a small molecule vasoactive intestinal peptide (VIP) (days 6-10, Buchholz et al., 2012) which has been shown to speed up the maturation of cultured primary RPE (Koh et al., 2000).

Apart from the addition or removal of growth factors innovative strategies have been devised to purify cells predicted to be destined to undergo retinal/RPE differentiation. Meyer et al., generated aggregates from neuroepithelial rosettes and were able to identify and manually isolate 'optic-vesicle like' aggregates (~20%) from a mixed population by virtue of their unique morphology (phase bright 'outer mantel' of cells) (Meyer et al., 2011). Interestingly these optic vesicle like aggregates adopted a Chx10 positive neural retinal identity by default; the addition of activin A from days 20-40 induced pigmentation in some of these aggregates.

Many HESC-RPE/retinal differentiation protocols employ an embryoid body (EB) stage in which cells are cultured in suspension for time periods ranging from 7 to 56 days. Protocols for the generation of RPE most commonly feature a subsequent adherent stage where EBs are plated onto various substrates including Laminin, Matrigel, Poly D lysine/laminin/Fibronectin and defined substrates such as Synthemax. Rowland et al., have shown that the choice of substrate is critical to

RPE differentiation and maturation with Matrigel and mouse laminin supporting the highest levels of pigmentation (Rowland et al., 2012).

A commonly cited problem with EB based methods are the losses incurred during the aggregate formation stage (Dang et al., 2002,), this is thought to lead to reduced overall efficiency (Vugler et al., 2008), though to our knowledge this has not been systematically investigated. The tightly connected epithelial cells that form on the surface of EBs presents a limitation to the transfer of growth factors and small molecules generating a gradient of concentrations that causes heterogeneous cell populations (Van winkle et al., 2012). It is also a challenge to derive EBs of equal size, a parameter which affects early lineage specification (Bauwens et al., 2008, Bratt-Leal et al., 2009). Innovative methods to control EB sizes, such as forced aggregation of single cells in defined numbers using Aggrewell^{TM} plates (STEMCELL Technologies) have recently been developed. In addition to these problems it is challenging to monitor differentiating cell morphology and to quantify relative RPE yields in EBs; % pigmented aggregates is often cited (Idelson et al., 2009, Vaajasaari et al., 2011) a parameter which gives no indication as to the number of pigmented cells per aggregate. The lack of reliable methods for quantifying pigmented cell yields have led to a variety of parameters being used to assess relative yields; % MitF positive cells, % pigmented colonies, % PMEL17 positive cells and quantitative PCR for RPE genes are the most commonly used.

Aside from the protocols that rely of spontaneous differentiation on MEFs, relatively few methods have been published using directed, continuous adherent differentiation (Rowland et al., 2012). Zahabi et al., achieved high yields (40% RPE65 positive) from HESC and IPSCs in feeder-free adherent differentiation using inhibition of BMP signalling (Noggin) and subsequent treatment with retinoic acid and Shh (Zahabi et al., 2011). Two additional very recently published studies have used continuous adherent differentiation as an alternative to EB based methods (Maruottie et al, 2013, Buchholz et al., 2013), with the latter employing directed differentiation strategies involving Noggin, DKK1, IGF1, NIC, activin A and VIP and the former relying on spontaneous differentiation but in feeder-free conditions.

In summary an ever increasing number of HESC-RPE differentiation strategies are being published using a large number of HESC and IPSC cell lines. Their ability to generate morphologically indistinguishable pigmented RPE cells underlines the robustness of this spontaneous phenomenon. Despite the many complex differentiation strategies, protocols employing neuroectodermal cell survival factors such as NIC, N2 and B27 may be the most efficacious at improving over all yields. The large variability in timings and methods used to assess relative yields, the absence of quoted yields in untreated controls and the varying responses between cell lines makes it challenging to compare protocols and determine which strategy is the most effective. From a bioprocessing perspective, it will be important to consider not only the yield but the efficiency, cost, reproducibility and scalability of differentiation strategies.

1.5 Clinical trials in HESC/IPSC-RPE therapy for AMD

Given the unlimited expansion capacity of the HESC and the superior functional properties of HESC-RPE, these cells are a promising source for wide scale cell therapy. Their efficacy has been tested extensively in the RCS rat and a safety/tolerability trial is currently underway in patients with dry AMD and Stargardt disease (Schwartz et al., 2012). HESC are a biologically complex source for a therapeutic and their potential tumorigenicity is a concern to regulatory bodies (Blum et al., 2008). One HESC derived therapy consisting of Oligodendricyte progenitor cells for the treatment of spinal cord injury was granted clinical approval in 2011 with five patients enrolled in a 15 year clinical trial carried out by Geron Corp (Menlo Park CA, USA). This trial is currently on hold however due to financial restrictions from the parent company. Thus in spite of significant pre-clinical evidence it was not until 2012 that HESC derived RPE were first injected into patients in a trial operated by Advanced Cell Technologies (ACT). Here we will review the published pre-clinical evidence for efficacy and early reports from phase I trials by ACT as well as upcoming trials by the London Project to Cure Blindness, the Riken institute, Japan and the California project to cure blindness.

1.5.1 HESC/IPSC-RPE in AMD animal models

The ability of the HESC derived RPE to rescue visual function has been tested by several groups in the RCS rat (Lund et al., 2006, Vugler et al., 2008, Lu et al., 2009, Idelson et al., 2009, Zhu et al., 2013). In the first demonstration of HESC-RPE transplantation, batches of $2x10^4$ cells HESC-RPE cells were injected per rat eye. The cells were injected into the sub-retinal space at post-natal day 21 when photoreceptor degeneration was yet to develop. Photoreceptor rescue was demonstrated by improvements in electro-retinography, head tracking experiments and luminance threshold recordings relative to sham injected controls (Lund et al., 2006). These results have since been repeated using a range of dosages (5K-100K/eye) and pigmentation levels (Lu et al., 2009). Injected HESC-RPE have been shown to maintain pigmentation and expression of RPE specific markers (CRALBP, RPE65, Vimentin, Bestrophin) up to 19 weeks post transplantation (Vugler et al.,

2008, Idelson et al., 2009). Transplanted HESC-RPE successfully phagocytose Rhodopsin positive debris in the RCS rat retina, confirming their functionality beyond growth factor secretion (Vugler et al., 2008, Idelson et al., 2009). In all studies, preservation of the photoreceptors outer nuclear layer adjacent to the HESC-RPE graft was seen (up to 19 weeks) and no reported evidence of tumour formation has been found (Lund et al., 2006, Vugler et al., 2008, Idelson et al., 2009).

1.5.2 ACT clinical trial

ACT (Malborough, MA, USA) are in the process of carrying out an early stage clinical trial using HESC-RPE to treat dry AMD and Stargardt disease (Clinicaltrials.gov numbers NCT01345006, NCT01344993). At the time of writing, 12 patients with Stargardt disease and 6 patients with dry AMD have had HESC-RPE transplanted, a preliminary report published 4 months post implantation, details the surgical procedure (Schwartz et al., 2012). Fifty thousand viable RPE cells suspended in a 150µL of balanced salt solution were injected into in the subretinal space in a specific site in the pericentral macular in two patients. Prior to transplantation, batches of RPE cells were assessed according to their overall melanin content and ability to attach to gelatine coated plates following extrusion through the injection cannula to be used in surgery. It was found that lightly pigmented RPE were better able to survive and attach to the surface following extrusion and thus lightly pigmented cells were chosen for transplantation. No abnormal growth or hyper-proliferation has thus far been observed, there were no surgical complications, injected RPE cells were not found outside of the subretinal space and no signs of inflammation have been detected. It is too early to determine whether or not the cells will affect any clinical benefit, as the reported improvement in visual acuity was within the repeatability limits of the visual acuity test used (Huang et al., 2012).

1.5.3 Upcoming clinical trials

Injection of cell suspensions has thus far been the most commonly used method to administer HESC-RPE into the subretinal space in animal models (Lund et al., 2006, Vugler et al., 2008, Lu et al., 2009, Schwartz et al., 2012). This technique, whilst convenient, can result in the formation of isolated cell clumps which fail to form a polarised monolayer and do no function as normal RPE. An alternative approach involves seeding RPE cells on a transplantable scaffold, allowing them to form a polarised monolayer prior to administration (Hu et al., 2012). This approach has several potential advantages in terms of cell survival and functionality and may act as a replacement to the damaged Bruch's membrane (Ramsden et al., 2013). However the transplantation of polarised patches is a more complicated surgical procedure than injection of a cell suspension and requires the use of specially developed tools (Gosh et al., 2002, Thumann et al., 2006, Stanzel et al., 2012). A clinical trial application submitted by the London Project to Cure Blindness (www.thelondonproject.org), using Shef1 derived HESC-RPE cultured on a 3mm by 6mm polyester membrane has been submitted to the UK medicines and Healthcare Regulatory Agency for approval (Carr et al., 2013).

The California project to cure blindness, currently in the pre-clinical stage, plans to use a similar strategy of transplanting sheets of HESC-RPE, this time derived from the H9 HESC line on a vitronectin coated parylene substrate. IPSC derived RPE are also being developed into a trial therapy for dry AMD. The project is being carried out at the RIKEN Centre for Developmental Biology in Kobe, Japan and is expected to gain approval to begin clinical trials in the near future.

1.6 Summary

Age-Related Macular degeneration is the most common form of blindness in the western world and yet there are precious few treatment options for those afflicted. The disease is caused by an age associated break down of the retinal pigment epithelium in the macular region of the retina which may be brought about by chronic, low grade inflammation. Replacing these cells with healthy cells from the periphery or other allogeneic sources has proven to be an effective treatment however the extreme technical complexity of autologous patch graft translocation means there is a high complication rate and the surgery could not at present be a routine treatment option.

With the advent of human embryonic stem cells a potentially unlimited source of highly functional retinal pigment epithelium cells has become available making the wide spread production of allogeneic 'off the shelf' RPE patches for transplantation a possibility.

RPE cells form in confluent HESC culture with minimal intervention. Since the beginning of this project there has been a rapid increase in the number of reports of new methods for deriving RPE, these have been comprehensively reviewed in table 1.1. The methods range from straight forward spontaneous differentiation protocols to complex sequences of growth factor and small molecule additions and withdrawals. In addition many methods include steps to mechanically isolate cells with favourable morphologies..

There are major challenges in garnering widely applicable outcomes from these studies; clearly there are major differences in the behaviour of cell lines – potentially due to genetic makeup, or the methods used to isolate the inner cell mass and establish lines. There are also major differences within cell lines which are cultured in different laboratories. It has been suggested that this may result from individual passaging techniques and culturing practices (feeding regimes, passaging frequency, colony dissection) and in the MEFs feeder cells on which they are grown. Thus in addition to improving differentiation efficiency, a major goal of this thesis will be to

establish and characterise a differentiation protocol that minimizes these obvious sources of variability, with a view to improving reproducibility.

Clinical trials utilizing HESC-RPE commenced last year, and more centres are scheduled to begin their own trials in 2013. Currently the process for generating RPE by spontaneous differentiation is robust within certain cell lines but also highly inefficient. HESC are amongst the most complex biological entities to be proposed as a source of a therapeutic. The wide spread clinical application of HESC derived therapies will depend not only on the of efficacy of the eventual therapy but also on the economic feasibility of said product and the efficiency of the manufacturing process is likely to be a major cost determinant.

Reference	Cell Line	Timing of Pigmentation (days)	Expansion/differentiation media/Substrate	Cell Seeding Density	'Treatment'	RPE yield before treatment	RPE yield after treatment	Purpose
Odorico et al., 2001	**H9**		**EBs (8-14 days) Gelatin**					**Multilineage differentiation**
Kawasaki et al., 2002	**Primate ES (CMK 6,9)**	**21 days**	**Collagen**		**SDIA (surface molecule derived from PA6)**	**None**	**8 ± 4% of colonies**	**Accidental RPE**
Klimanskaya et al., 2004	**H1,H7, H9, MA01,3,4,9,14,40,J1**	**42-56 days**	**MEFs (7-10 days)**		**-bFGF, -LIF (day 7-10)**			**Transcriptional comparison to RPE**
			EBs				**<1% EBs**	
Lund et al., 2006	**H1,H7, H9, MA01,3,4,9,14,40,J1**	**42-56 days**	**MEFs**					**Multiple lines made for HLA match**
			EBs				**<1% EBs**	
Vugler et al., 2008	**Shef1, Shef7**	**17-24 days**	**MEFs**		**-bFGF 10 days confluent**			**Ontogenesis**
Gong et al., 2008		**17-28 days**	**PA6 cells**	**2000/cm^2**	**Day 13 Pax6 +ve neural progenitors on: Matrigel**	**None**	**None**	**Bruch's membrane facilitates RPE differentiation**
					Laminin	**None**	**None**	
					Human Bruch's	**None**	**Best + CRALBP expression**	
Osakada et al., 2008	ES (Monkey)	60 days	SFEB (21 days) Poly D lysine/laminin/ Fibronectin		Days 0-21 DKK1 (Wnt inhibitor) 100ng/.ml LeftyA (Nodal inhibitor) 500ng/ml	10% MitF +ve colonies	55% MitF +ve colonies	Generate photoreceptors from HESC
	KhES1						37% MitF +ve colonies	
Osakada et al., 2009	KhES1 235G1, 201B7 (IPSC)	40 days	SFEB (21 days) Poly D lysine/laminin/ fibronectin	880 clumps/ ml	Days 0-25 CKI7 (Wnt inhibitor) 5µM SB 431542 (Nodal inhibitor)5µM.	8% MitF +ve colonies	28-32% MitF +ve pigmented colonies	Using small moleules in place of growth factors
	201B6 (IPSC)					None	None	

Reference	Cell Line	Timing of Pigmentation (days)	Expansion/differentiation media/Substrate	Cell Seeding Density	'Treatment'	RPE yield before treatment	RPE yield after treatment	Purpose
Lu et al., 2009	H1 H9	-	EBs (7 days) Gelatine MDKB serum free media + 1x B-27					cGMP manufacture
Meyer et al., 2009	H9 IMR90 (IPSC)	30 days	EBs (6 days) Laminin +				25% MitF Cells	Modelling retinal development
			1% B-27, 1% N2, 2 µg/ml Heparin 2%B-27 (Days 4-6)		SU5402 (FGF inhibitor) (day s 16-40)	1 fold MitF mRNA	11.8 Fold MitF mRNA	
Buchholz et al., 2009	**iPS (foreskin)-1 (IPSC)** **iPS (foreskin)-2 (IPSC)**	**21-28 days**	**MEFs or Matrigel +100ng/ml bFGF (7-10 days)**					**Functional RPE from IPSC**
	IMR90-3 (IPSC) **IMR90-4 (IPSC)**	**20-35 days**						
	H9	**20-35 days**	**HFFs (7-10 days)**					
Hirami et al., 2009	201B7 (IPSC) 253G1 (IPSC)	40 days	SFEB (21 days) Poly D lysine/laminin/ fibronectin		DKK1 (Wnt inhibitor) 100ng/.ml LeftyA (Nodal inhibitor) 500ng/ml (days 0-21)		39% Pigmented colonies	Retinal cells from IPSC
	201B6 (IPSC)						None	
Idelson et al., 2009	HES1	28 days	EBs, 14% KOSR		10mM Nicotinamide (vitamin B)day 0 -28	0%EBs pigmented	10% EBs pigmented (6% of each EB)	Directed differentiation with Nicotinamide and TGFβ superfamily members
	HES4	28-35 days				10%	35% of EBs	
	H7					3%	6% of EBs	
	HES1				10mM Nicotinamide + 100ng/ml Activin A (days 14-28)	18%	55% of EBs	
	HES4					35%	60% of EBs	
	H7					6%	32% of EBs	

Reference	Cell Line	Timing of Pigmentation (days)	Expansion/differentiation media/Substrate	Cell Seeding Density	'Treatment'	RPE yield before treatment	RPE yield after treatment	Purpose
Carr et al., 2009	**IMR90-3 (IPSC)**	**28 days**	**MEFs + 100ng/ml bFGF**		**-bFGF 7-10 days confluent**			**IPSC-RPE in vivo model**
Nistor et al. 2010	H7	42 days	Matrigel + Mefs conditioned medium EBs (day 21-28) Collagen/ laminin (days 28-35)		B27, Insulin–Selenite–Transferrin (IST), triiodothyronine (T3), Taurine 2.5 g/l; Hyaluronic Acid (HA) 250mg/l, Dkk1 25ng/ml, LeftyA 50ng/ml, FGF 5ng/ml (days 14-21)			3D RPE/neural progenitor construct created
Yue et al., 2010	**Primate ES cells**	**21 days**	**Co-culture with Sertoli Cells**					**Use inactivated RPE as a feeder layer for differentiating photoreceptors**
Liao et al., 2010	**H1, H9**	**21-28 days**	**MEFs**		**-bFGF 7-10 days confluent**		**20 foci /cm^2**	**Determine RPE 'molecular signature'**
	HUES12, HUES15, HSF1						**15 foci /cm^2**	
	HSF6						**<10 foci /cm^2**	
Hu et al., 2010	H14	32 days	EBs (8 days) Seeded onto 0.1% gelatine		-bFGF		12% colonies pigmented	Epigenetic memory in foetal RPE derived IPSCs.
	IMR90-3 (foetal lung IPSC)	22 days					7%	
	IPS (foreskin)-2 (IPSC)	None					0%	
	A3 (Foetal RPE IPSC)	19 days					72%	
	A4 (Foetal RPE IPSC	19 days					60%	
	A6 (Foetal RPE IPSC)	30 days					2%	

Reference	Cell Line	Timing of Pigmentation (days)	Expansion/differentiation media/Substrate	Cell Seeding Density	'Treatment'	RPE yield before treatment	RPE yield after treatment	Purpose
Meyer 2011	WA09 WA01 IPS-12 (IPSC) IPS-12.4 (IPSC)	40-60 days	EBs (7 days), N2 (1%), Heparin (2 µg/ml), B-27 (2%) (Days 4-6) Neural rosettes isolated at day 16 and grown in suspension		Separate phase bright optic vesicle like EBs (days 20-25)	Pigmentation observe	'rarely observed'	Separation of retinal progenitor cells from early forebrain populations
					Activin A 100ng/ml (days 20-40)	Rarely observed	Pigmented subsets observed. 8 Fold increase in MitF mRNA 5 fold RPE65, 19 fold Bestrophin	
	Lenti IPSC2 (IPSC)				DKK1(100ng/ml) + Noggin (days 2-4)	27% Pax6 +ve 5.1% Chx10 +ve	72% Pax6 +ve 34% Chx10 +ve	
Vaajassari et al., 2011	Regea 08/013,	21 ± 3 days	–bFGF(1-7 days) EBs (days 7-30)		-bFGF		Day 28,10% pigmented aggregates	Screen multiple lines on human feeders (HFFs)
	Regea 08/017,	12 ± 7 days					6%	
	Regea 08/023,	12 ± 5 days					23%	
	Regea 08/056,	10 ± 2 days					22%	
	FiPS 5-7 (IPSC)	11 ± 5 days					24%	

Reference	Cell Line	Timing of Pigmentation (days)	Expansion/differentiation media/Substrate	Cell Seeding Density	'Treatment'	RPE yield before treatment	RPE yield after treatment	Purpose
Jin et al., 2011	K11 (Retinitis Pigmentosa (RP) IPSC)	40-60 days	SFEB Poly D lysine/laminin/ Fibronectin (21 days)	15-20 aggregates per slide	DKK1 (Wnt inhibitor) 100ng/.ml LeftyA (Nodal inhibitor) 500ng/ml (Days 0-21)		At day 60, 16% pigmented area:	Modelling Retinitis Pigmentosa
	K21 (RP- IPSC)						24%	
	K10 (RP- IPSC)						18%	
	K101 (RP- IPSC)						23%	
	P59 (RP- IPSC)						20%	
Sugino et al. 2011	MA01 (H1)	28-30 days	EBs 7-10 days in MDKB media + 1x B27 supplement, Seeded onto 1% gelatine					Attachment and survival on aged Bruch's membranes
Kokkinaki et al, 2011	IMR90-4 (IPSC)	28 days	EBs of defined size in Aggrewells™	1000-2000 cell EBs	10μM NIC (day 1-28), 140ng/ml Activin A + SB431542 (days 21-28)		37% pigmented clusters	Comparison of IPSC and HESC derived RPE.
Zahabi et al., 2011	**Royan H6 hiPSC1 (IPSC)**	**25 days**	**5% KOSR, N2**		**250ng/ml noggin 10ng/ml bFGF (day 0-6)** **bFGF 10ng/ml Retinoi acid 0.2-0.6μM only (day 6-12)** **25ng/ml Shh, 25 ng/ml bFGF (days 12-18)** **18-25 5% KOSR only (days 18-40)**		**40% RPE65 + ve, 40% Bestrophin +ve (Day 40)**	

Reference	Cell Line	Timing of Pigmentation (days)	Expansion/differentiation media/Substrate	Cell Seeding Density	'Treatment'	RPE yield before treatment	RPE yield after treatment	Purpose
Clarke et al., 2012	**H9**	**35 days**	**MEFs cells**		**-bFGF (days 10-35)**		**Day 28, 9% pigmented surface area**	**Clonal isolation (FACS) and characterisation**
		28 days	**PA6 cells**					
Hongisto et al., 2012	Regea 06/040 FiPS5-7 (IPSC)	15-17 days	EBs		Activin A 10ng/ml (day 0 onwards)	Day 28 30% pigmented aggregates	Day 28 70% pigmented aggregates	Activin A mimics RPE promoting action of MEFs
Nakano et al., 2012	Khes1	21 days	SFEB G-MEM 20% KOSR 1mM Pyruvate 10µM Y-27632 Embedded in Matrigel (1%) (days 2-18)	9000 cells/well /EB	IWR1e (Wnt inhibitor) (3µM)(days 0-12) FBS (10%), SAG (Hedgehog /smoothened agonist) (100Nm) (days 12-18)		No pigment	3D optic cup formation and cryopreservation
					CHIR99021 (GSKβ inhibitor) (days 18-21)	No pigment	Pigmented + 3.5 increase in MitF mRNA	
Rowland et al., 2012	**H9**	**51 days**	**HS27 feeders**		**-bFGF (day 7-10)**		**Day 51, ~4.2/cm^2**	**Effect of substrate on RPE differentiation yield**
			Matrigel				**~2.3/cm^2**	
			Mouse Laminin				**~2.1 /cm^2**	
	IMR90-3 (IPSC)	**35 days**	**MEFs**				**0mm^2 / well**	
			Matrigel				**0.28mm^2**	
			Mouse Laminin				**0.30 mm^2**	
Singh et al., 2012	A416K, N296H (Best disease IPSC lines),	30-40 days	EBs (6 days) Laminin + 1% B-27,N2, 2µg/ml Heparin, 2%B-27 (Days 4-6)					Characterising Best disease patient derived IPSC-RPE.

Reference	Cell Line	Timing of Pigmentation (days)	Expansion/differentiation media/Substrate	Cell Seeding Density	'Treatment'	RPE yield before treatment	RPE yield after treatment	Purpose
Mellough et al., 2013	H9 hIPSC-NHDF (IPSC)	20-30 days	EBs 30 days,10% KOSR + B27 (1:50) Poly-L-ornithine/laminin coated slides (30 days) N2 (1:100), B27 (1:50) (day 30-60)		-B27 -N2	~49% RPE65 +ve day 30 ~30% RPE65 +ve day 60	~10% RPE65 +ve day 30 ~30% RPE65 +ve day 60	Screen of staged growth factor addition for retinal differentiation.
					Noggin (1ng/ml), Dkk1 (1ng/ml), IGF (5ng/ml), LeftyA (500ng/ml), Shh (30nM) (Day 0-37) Noggin (10ng/ml), DKK1 (10ng/ml), IGF1 (10ng/ml), FGF (5ng/ml), Retinoic acid (500nM), T3 (40ng/ml), Taurine (2µM), Shh (12nM) (day 37-60)	~49% RPE65 +ve day 30 ~30% RPE65 +ve day 60	~59% RPE65 +ve day 30 ~30% RPE65 +ve day 60	
Krohne et al. 2013	IMR-90 (IPSC), 4F IPSC, (2F) IPSC, (1F) IPSC		EBs		10mM NIC, 62ng/ml Activin A (day 0-28)		'More rapid and efficient' –	Characterising in vivo functionality of 1 factor (1F) reprogrammed IPSC.
Maruottie et al., 2013	**H7 HESC, IPSC (IMR90-4)**	**32-38 days**	**8 Days in mTesR1(single cell seeding) Matrigel or VN-PAS Synthemax DMEM/F12**	**20k/cm2**	**Day 50 passage as single cells, seed at 100K/cm2 (P1), grow for 15-20 days, Passage again seed at 100K/cm2 (P2) for 30 days.**	**16 % RPE 65 +VE**	**97-99% MitF +ve RPE65 +ve (115 days total)**	**Serial passaging of mixed cultures eventually generates pure RPE**

Reference	Cell Line	Timing of Pigmentation (days)	Expansion/differentiation media/Substrate	Cell Seeding Density	'Treatment'	RPE yield before treatment	RPE yield after treatment	Purpose
Buchholz et al., 2013	**H9**	**14 days**	**B27, N2 Matrigel**		**50ng/mlNoggin, DKK1, IGF1, NIC (days 0-2)** **10ng/.ml Noggin, Dkk1, IGF1, NIC +bFGF (day 2-4)** **10ngml DKK1,10ng/ml IGF1 (days 4-6)** **100ng/ml activin a, 10µM SU5402, 1mM VIP (days 10-16)**	**25 %± 2%, PMEL17**	**79% ±1 % PMEL17**	**High yields in short time**
Sridhar et al., 2013	IPSC (IMR90-4)	30 days	EBs (7 days) Synthemax		1% N2, (days 7-17) 2% B-27 (up to 60 days)			Completely xeno free.
Zhu et al., 2013	H9 O27-08 (IPSC)	18-30 days	EBs embedded in 150-300µL matrigel in N2/B27 neural induction medium (5 days) Dissociated into single cells seeded onto matrigel coated transwells	9.6 cm^2 confluent cells into 300µL of matrigel. 2-4 x10^5 differentiated cells per 6.5mm well	100ng/ml Activin A (+20% KOSR) (days 6-25)	Isolated pigmented foci	96% pigmented cells (day 30)	Transplantation of whole RPE aggregates with no selection or purification.
	H1						No effect	
					8µM SB435142 (+20% KOSR) (days 6-25)	Pigmented (~80-90%)	No pigmentation	

Table 1.1 A history of pluripotent stem cells to RPE differentiation Methods used to derive RPE from HESC and IPSC. All cell lines listed are human embryonic stem cell lines unless stated otherwise in brackets. Protocols that use continuous adherent differentiation methods that do not employ a cell detachments and suspension culture step are highlighted in bold. The cell seeding density column is left blank where no information about density is given. Like wise the yield before/after treatment is blank where this information was not recorded, as appose to the word 'none' when the absence of pigment/immunopositive cells is noted. 'Purpose' column summarises the main theme of the study as indicated by the paper's title. 'RPE yield' is assessed by different studies in a variety ways which are denoted (eg. '%MitF +ve' is the percentage of cells which are immunopositive for the early RPE marker MitF). Note '% pigmented aggregates', referring to the relative number of differentiating embryoid bodies that contain pigmented patches of any size, is not equal to '% pigmented cells'. Expansion and differentiation media is standard HESC media (knock out DMEM/F12 + 20% knock out serum, NEAA, glutamine and β mercaptoethanol and bFGF, and any deviations from this are noted (e.g. 5% KOSR). In the 'treatment' section, the '-' prefix signifies the removal of growth factor(s) from the expansion medium to induce differentiation at the specified time.

SFEB = Serum free embryoid body method (Watanabe et al., 2005), cells are cultured in clumps of 5-10 cells in decreasing serum concentrations in G-MEM media (Gibco, Invitrogen) and a final concentration of 5% KOSR. MEFs= mitotically inactivated mouse embryonic fibroblasts. HFFs = human foreskin fibroblasts EBs = embryoid bodies. PA6 are murine, bone marrow derived stromal cells used as an alternative feeder layer to induce neuralization. 'Time to pigmentation' is quoted as the total time since cells are seeded (includes expansion steps). 'Aggrewell' plates are conical bottomed 96 well plates provided by STEMCELL Technologies.

1.6 Summary

Age-Related Macular degeneration is the most common form of blindness in the western world and yet there are precious few treatment options for those afflicted. The disease is caused by an age associated break down of the retinal pigment epithelium in the macular region of the retina which may be brought about by chronic, low grade inflammation. Replacing these cells with healthy cells from the periphery or other allogeneic sources has proven to be an affective treatment however the extreme technical complexity of autologous patch graft translocation means there is a low success rate and the surgery could not at present be a routine treatment option.

With the advent of human embryonic stem cells a potentially unlimited source of highly functional retinal pigment epithelium cells has become available making the wide spread production of allogeneic 'off the shelf' RPE patches for transplantation a possibility.

RPE cells form in confluent HESC culture with minimal intervention. Since the beginning of this project there has been a rapid increase in the number of reports of new methods for deriving RPE, these have been comprehensively reviewed in table 1.1. The methods range from straight forward spontaneous differentiation protocols to complex sequences of growth factor and small molecule additions and withdrawals. In addition many methods include steps to mechanically isolate cells with favourable morphologies. Perhaps unsurprisingly, given the demonstrable importance of the interplay with adjacent tissues, no reports have described close to 100% HESC-RPE conversion efficiencies.

There are major challenges in garnering widely applicable outcomes from these studies; clearly there are major differences in the behaviour of cell lines – potentially due to genetic makeup, or the methods used to isolate the inner cell mass and establish lines. There are also major differences within cell lines which are cultured in different laboratories. It has been suggested that this may result from individual passaging techniques and culturing practices (feeding regimes, passaging frequency,

colony dissection) and in the MEFs feeder cells on which they are grown. Thus in addition to improving differentiation efficiency, a major goal of this thesis has been to establish and characterise a differentiation protocol that minimizes these obvious sources of variability, with a view to improving reproducibility.

Clinical trials utilizing HESC-RPE commenced last year, and more centres are scheduled to begin their own trials in 2013. Currently the process for generating RPE by spontaneous differentiation is robust within certain cell lines but also highly inefficient. HESC are amongst the most complex biological entities to be proposed as a source of a therapeutic. The wide spread clinical application of HESC derived therapies will depend not only of efficacy of the eventual therapy but also on the economic feasibility of said product and the efficiency of the manufacturing process is likely to be a major cost determinant.

1.7 Project Aims

Chapter 2: Methods for assessing pigmented cell yield

A variety of methods have been used to assess RPE cell yield (see table 1.1). The pigmented nature of differentiated RPE makes for a useful marker that can be assessed visually. Commonly used parameters such as '% pigmented aggregates' however are relatively subjective, do not account for the size of pigmented areas, and are laborious to determine, requiring cells to be kept out of the incubator for long periods of time. Thus our initial goal is to develop a rapid, non-destructive, standardized method for reliably assessing pigmented RPE cell yield over time. This method should be such that it can be widely applied to assess the efficiency of differentiation methods in an unbiased, automated fashion.

Chapter 3: MEFs co-culture and feeder-free differentiation: Bioprocess characterisation

In this chapter we aim to establish the differentiation characteristics of two HESC lines Shef3 and 6; to establish whether they are able to differentiate into pigmented RPE expressing the characteristic range of markers using the traditional MEFs co-culture method described by Vugler et al., 2008. We aim to use gene/protein expression assays in relation to morphological observations to characterise the various stages of differentiation from the loss of pluripotency up to the emergence of pigmented cells. Using the methods we develop in chapter 2 we hope to characterise the rate of pigmented cell accumulation in the two cell lines, quantify the typical differentiated cell yields and assess how these characteristics vary over time in culture. The use of MEFs is undesirable for clinical manufacturing of cell therapies, so in the last part of this chapter we will test the ability of Shef3 and Shef6 cells to be differentiated into RPE in feeder-free conditions.

Chapter 4: Differentiation efficiency: the impact of seeding density and single cell dissociation

Starter cell seeding density is one of the 'traditional' bioprocess engineering parameters that have been central to biopharmaceutical process optimization (Kirouac et al., 2008) but it is rarely controlled for in HESC differentiation experiments. In the processing of HESC for cell therapies, in addition to the usual impact on viability and raw material usage, there is evidence suggesting that seeding density may govern early cell fate decisions during differentiation (Bauwens et al., 2008, Chambers et al., 2009). In this chapter we aim to investigate how HESC seeding density affects RPE differentiation yields and its subsequent impact on the overall process efficiency. HESC colonies are usually passaged as clumps of undefined size, a practise that is labour intensive, introduces significant variability and is not amenable to scaled up cell processing. As an alternative, we aim to address whether single cell dissociation, a practise which is suitable for scaled-up culture and automation, can produce acceptable RPE yields. Following this we aim to establish an optimal seeding density following single cell dissociation, in terms of HESC-RPE differentiation efficiency, in feeder-free conditions.

Chapter 5: Enhancing differentiation efficiency using small molecules

Having established robust feeder-free methods for HESC-RPE cell derivation, the aim of this last chapter will be to investigate ways to further enhance yields by directing early cell fate decisions using small molecules. Our literature review indicates that manipulating early differentiation will likely be the most potent strategy in terms of directing differentiation. In order to further understand the mechanisms of HESC-RPE differentiation we will look at the how manipulating the key pluripotency/differentiation signalling pathways impacts on early neuroectoderm conversion, and how this affects long term RPE differentiation.

Chapter 2: Materials and Methods

2.1 HESC maintenance

2.1.1 MEFs isolation, maintenance and preparation of feeders

MEFs were isolated from CF1 mouse embryos at day 13 post coitum. Using sterile tweezers and scissors the heads and internal organs of the embryos were removed before immersing in PBS then 0.05% Trypsin/EDTA (Gibco-Invitrogen, Paisley, UK) and finely mincing the tissue. Additional Trypsin/EDTA was added the material was placed in the 37°C incubator for 5-10 minutes after which MEFs medium was added to quench the reaction, MEFs medium consisted of D-MEM, foetal bovine serum (FBS) (10%v/v), NEAA (1% v/v) (all Gibco-Invitrogen). The partially digested tissue was transferred to centrifuged tubes and large pieces of tissue were allowed to settle the bottom of the tubes. The supernatant was removed and re-suspended in fresh MEFs media, then centrifuged at 1000rpm for 3-5 minutes, the supernatant was then discarded and the pellet re-suspended in MEFs medium before transferring to T75 flasks (NUNC, EasYFlasks, Thermo-Fischer scientific). MEFs were allowed to grow for two population doublings and then viably frozen in cryopreservation media (40% MEFs media, 50% FBS, 10% DMSO (Sigma-Aldrich)) in liquid nitrogen and designated passage zero (P0).

P0 vials were removed from the liquid nitrogen and thawed in the water bath before centrifuging (12,000 rpm, 3 mins) and re-suspending in MEFs medium. MEFs were grown in NUNC T75 EasYFlasks and passaged every 3 days (at 70-80% confluence) with 0.25% Trypsin/EDTA at a split ratio of 1:5-1:2 up to passage 6.

The day before HESC passaging, confluent flasks of MEFs were mitotically inactivated by treatment with mitomycin-C (0.01mg/ml, Sigma-Aldrich). MEFs media was replaced with 7mls of mitomycin C medium (0.01mg/ml of filtered mitomycin C in MEFs media) and incubated for 2 hours. Inactivated MEFs were washed 3x in PBS and dissociated by 3 minutes treatment with 0.05% trypsin/EDTA at 37°C. Cells were counted using a haemocytometer and seeded onto 0.1% porcine Gelatin (Sigma-Aldrich) coated flasks or wells at a density of 9,200/cm^2.

2.1.2 Shef6 and Shef3 maintenance

Undifferentiated Shef3 and Shef6 HESC were obtained from the UK Stem Cell Bank. Cells were maintained in 0.1% Porcine Gelatine (Sigma-Aldrich) coated T25 NUNC EasYFlasks (Thermo-Fischer scientific) on mitomycin-C inactivated mouse embryo fibroblasts (MEFs) in Knockout DMEM supplemented with 20% (v/v) Knockout serum replacement, 2mM Glutamax 1%(v/v) non-essential amino acids, 4ng/mL basic FGF (FGF2) (all Invitrogen) and 0.1mM β-mercaptoethanol (Sigma-Aldrich), filtered through a 0.22μm sterile filter. Cells were cultured in a Sanyo IncuSafe incubator (Sanyo, MCO-18AIC, Leicestershire, UK) at 37℃ and 5%(v/v) CO_2. HESC media (5-6mls/ T25) was exchanged every 24 hours after the first day post passaging. Every 3-4 days HESC colonies were passaged. When the majority of colonies were large enough to fill a 10x objective, cells were treated with 0.125mg/ml collagenase IV (Invitrogen) for four minutes at 37°C. Colonies with undifferentiated HESC morphology were then dissected into smaller clumps under the dissecting microscope using a fine tip Pasteur pipette (Appleton woods, Birmingham, UK). Detached clumps containing around 1000 cells/clump were seeded onto fresh MEFs feeders in HESC media at a split ratio of 1:2.

2.1.3 HESC vitrification and thawing

Shef6 and Shef3 obtained from the stem cell bank were banked in liquid nitrogen at around passage 30. Vitrification straws (MTG, Bruckberg, Germany) containing 6-8 colony pieces were thawed and expanded to produce working banks that were again banked at around passage 35. HESC freezing was achieved by a process of vitrification. HESC colonies were treated with collagenase IV, as above, and cut into small pieces as if for passaging. Using a 20μL Gilson pipette colony pieces were transferred into droplets of 'ES-HEPES' solution (20%v/v FBS, 80% DMEM + 25mM HEPES (Sigma-Aldrich)). After 1 minute, the pieces were transferred to '10% freezing solution' (80% v/v ES-HEPES media, 10% v/v DMSO (Sigma-Aldrich), 10% Ethylene Glycol (Sigma-Aldrich)) and after 40 seconds again transferred this time to '20% freezing solution' (30% v/v ES-HEPES, 30% 1M Sucrose (Sigma-

Aldrich) in PBS, 20% DMSO, 20% Ethylene Glycol (Sigma-Aldrich) for 10 seconds. Following this clumps were sucked up into vitrification straws by capillary action and immersed in liquid nitrogen.

In order to thaw cells, vitrifcation straws were thawed directly onto gelatine and inactivated MEFs coated IVF dishes (Nunc, Thermo Scientific) in HESC media. Cells were left to attach in the incubator with occasional media changes for up to 1 week, at which point sufficient attachment and colony growth had occurred for passaging. Cells were cultured in IVF dishes until 7 IVF dishes were filled with colonies at which point the content of all 7 dishes were transferred into 1 x T25 flask.

2.1.4 Karyoptying and Mycoplasma testing

Every thawed batch of Shef6 and Shef3 were subjected to karyotypic analysis after prolonged passaging (2-3 months) and use. Karyotyping was carried out by TDL genetics (60 Whitfield Street, London) using G banding with up to 20 cells counted per sample. Mycoplasma testing was carried out regularly by Surrey Diagnostics (Cranleigh, UK).

2.2 HESC-RPE differentiation

2.2.1 MEFs co-culture differentiation

Shef6 and Shef3 were mechanically passaged following 4 minutes of collagenase IV treatment at 37 °C (Invitrogen). Unless other wise stated flasks were split at a ratio of 1:2. Where experiments tested more than 2 conditions, cells were split pooled and split at a 1 in 2 ratio. The cells were seeded onto mitomycin inactivated MEFs (1 day post plating) at a density of 9200 MEFs per cm^2. The same batch of MEFs was used for differentiation experiments throughout the whole project. The day of seeding was designated day 0, cells were fed with 6mls of HESC media +bFGF for the first 10 days excluding day 1, on which cells were left in the incubator to settle. On the 10^{th} day the media was changed to HESC media – bFGF (‘differentiation

media'). Thereafter –bFGF differentiation media exchanged every day (4-5mls) until day 50-80. In order to manage multiple asynchronous differentiation experiments, an excel spreadsheet and calendar of time lines and was generated for all experiments.

2.2.2 Feeder free differentiation on Matrigel in Mefs conditioned media/mTeSR1

For feeder free differentiation T25 flasks or 6 well plates were coated growth factor reduced Matrigel (BD Bioscience, San Diego, CA). Matrigel was thawed at 4°C on ice before diluting 1:30 in KO-DMEM. Matrigel coated plates were left wrapped in cling film in the hood for 1 hour before removing the excess and seeding cells onto them. For differentiation experiments Shef6 and Shef3 colonies with undifferentiated morphology were dissected into clumps in standard +bFGF HESC media and transferred to 15ml centrifuge tubes. The colonies were left to settle to the bottom of the tube and the supernatant was aspirated. The colonies were then re-suspended in MEFs conditioned medium (see below) or mTeSR1 medium (StemCellTechnologies, Vancouver, BC). Media was exchanged daily until the 10^{th} day at which time the media was changed to standard HESC media –bFGF (differentiation media) for the remaining 40 days.

2.2.3 MEFs conditioned media

To generate MEFs conditioned media 750,000 mitomycin C treated MEFs were seeded onto gelatinised T75 flasks in standard MEFs media. After 24 hours MEFs media was replaced with 12 mls/T75 of standard hESC media containing 4ng/ml bFGF. After a further 24 hours the MEFs conditioned media was harvested and spun down (12,000rpm, 3 minutes) to remove any detached feeder cells. Batches of MEFs media were frozen at -20°C and stored. At the time of use, conditioned media was thawed overnight in the fridge an additional 4ng/ml of bFGF was added on the day of

use. T75 MEFs feeder flasks were used for 2-3 days maximum (i.e. 2 -3 'harvests'), and only passage 2-4 MEFs were used.

2.2.4 Feeder free differentiation – Embryoid bodies

To generate embryoid bodies, Shef6 and Shef3 cells at day 4 post passage were treated for 4 minutes with type IV collagenase at 37°C then scraped off the surface using a plastic, fine tip Pasteur pipette. Colonies were transferred to 30mm non-adherent bacterial grade culture dishes (Sterilin, Caerphilly, UK) where they formed compacted EBs in 2-3 days. Media was exchanged by allowing EBs to settle in a centrifuge tube and aspirating the supernatant. Media was exchanged every day and switched to –bFGF differentiation media at day 10.

2.2.5 Single cell dissociation differentiation

For single-cell differentiation, flasks of Shef6 and Shef3 ready for passaging (day 3-4) were examined under the microscope and differentiating colonies were mechanically removed using a fine tipped Pasteur pipette (Appleton woods). Cells were then washed with PBS and 2mls of TrypLE select enzyme (Invitrogen) was added per flask, before incubating at 37°C for 10 minutes. After this time flask were tapped vigorously to detach cells. Standard HESC media was added and cells were spun down for 3 minutes at 12,000rpm. Cells were then re-suspended in MEFs conditioned media or mTeSR1 and counted on a haemocytometer before seeding at the specified density onto Matrigel coated plates. MTeSR1 or conditioned media was exchanged daily from the 2nd to the 5^{th} day after which media was switched to –bFGF differentiation media.

2.2.6 Preparation of Growth factor/small molecule differentiation media

Powdered dorsomorphin (Tocris Biosciences, Bristol, UK) was diluted in DMSO to create a 1mM solution which was stored in aliquots at -20°C. Aliquots were added to standard HESC media –bFGF 1µL/ml to achieve a final concentration of 1µM. Similar procedures were carried out with SB431542 (Tocris Biosciences) to achieve a 10µM concentration and PD0325901 (Tocris Biosciences) to achieve a 10µM solution. In all small molecule experiments an equal volume of DMSO was added to control wells from the same batch of cells. Activin A (R&D systems) was added at 100ng/ml to standard HESC media –bFGF. Fresh, small molecule/growth factor containing media was prepared every 3-4 days.

2.2.7 Cell counts

Viable cell counts were performed in triplicate using the Trypan blue exclusion method (Strober et al., 2001). Shef6 and Shef3 cells were seeded onto matrigel in mTeSR1 or MEFs conditioned media at a density of 5000 cells per cm2. Cells were harvested every 2-3 days using TrypLE select (Invitrogen); adherent cells were washed twice in PBS before treating with 1ml/well of TrypLE for 10 minutes at 37°C. Cells were diluted in media to achieve a concentration ranging from 250,000 cells/ml – 2,500,000 cells/ml the optimal range indicated by the haemocytometer manufacturer (LW scientific, Lawrenceville, GA). 0.1mls of 0.4% Trypan Blue stock solution (Invitorgen) was added per 1ml of cells and solutions were sampled three times and counted on eight squares of a haemocytometer.

2.3 RPE Expansion

2.3.1 RPE Isolation

Pigmented foci were mechanically isolated from non-pigmented tissue using at day 50-60. Cells were treated with 1mg/ml collagenase IV (Invitrogen) for 8-10 hours at 37°C. Two autoclaved microsurgical microcresent blades were used to cut non-pigmented tissue away from pigmented foci under the dissection microscope. The foci were then washed in fresh differentiation medium

2.3.2 RPE maintenance

Following isolation, 2-3 pigmented foci were seeded per well onto matrigel coated 24 well plates in a-MEM RPE medium' (a-MEM, 1x N1 supplement, 1X NEAA, 250mg/ml taurine, 13ng/ml Tiiodothyronin, 20ng/ml Hydrocortisone, , 1:100 Penicllin-streptomycin (all Sigma Aldrich), 2mM L-glutamine & 15% FBS (Gibco-Invitrogen). After 3-4 days the serum content was reduced to 5%. After allowing foci to adhere for two days, media was exchanged every 2-3 days.

2.4 Microscopy and Immunocytochemistry

Cells were fixed with 4%(w/v) paraformaldehyde (PFA) (Sigma-Aldrich) at room temperature for 20 minutes. PFA was removed and cells were washed with 0.1M Dulbecco's modified phosphate-buffered saline (DPBS). Cells were then simultaneously permeabilized and blocked in 0.3% v/v Triton-X100, 5% v/v Goat serum in DPBS (all Sigma-Aldrich) for 1 hour at room temperature. For surface markers the Triton X100 was omitted. Primary antibodies were diluted to the specified concentrations in 1% Goat Serum, 0.3% Triton-X100, DPBS solution. 500μL of diluted primary antibody solution was used per well of a six well plate. Primary antibodies, their suppliers and the concentrations used are listed in table 2.2 at the end of this chapter.

Primary antibodies were incubated at room temperature over night. The following day cells were washed 3x in 15 minutes in 500µL per well of DPBS on a shaker. The appropriate secondary antibodies were diluted in 2% goat serum in DPBS and 500µL of diluted secondary solution was used per well. Secondary antibodies are listed in table 2.3, all were supplied by Invitrogen. For each experiment isotype control wells were assigned to which were added species matched isotype control antibodies at the same concentration as the most concentrated primary antibody in each experiment.

Cells were incubated with the appropriate secondary antibody to match the host species and isotype of each primary antibody for 2 hours, covered in foil on a shaker at room temperature. Following this wells were washed 3x in 15 minutes in DPBS. Diamidino-2-phenylindole (DAPI, Invitrogen, 1:1000) in DPBS was then added for 5 minutes before washing the cells 3x again prior to storage at -4°C. Fluorescence and bright field images were acquired using a Nikon, Eclipse TE2000-U microscope and analyzed with NIS-element software (Nikon UK LTD, Surrey, UK).

2.5 Gene expression analysis

2.5.1 RNA isolation and storage

RNA extraction was carried out using Qiagen RNeasy kit (Qiagen, Crawley, UK) according to manufacturer's instructions. Cells were harvested by 10 minutes incubation with TrypLE select. Detached cells were pelleted, washed in PBS and stored at -80°C. Thawed pellets were disrupted with 500µL 'RLT' buffer (Qiagen) before homogenizing by passing 8 times through a 19 guage syringe. Following this, samples were processed according to manufacturer's instructions. Contaminating genomic DNA was digested using RNAse free DNAse (Qiagen). RNA was eluted from the spin columns with 40µL of RNAse free water and the concentration/purity was determined by measuring the 260/280nm absorbance ratio on a spectrophotometer (NanoDrop ND-1000, Thermo Scientific, Epson, UK).

2.5.2 CDNA synthesis

Control and test samples for direct comparison were always subjected to RNA extraction and cDNA synthesis on the same day. CDNA was made using Ambion RETROscript kit 1st strand synthesis kit (Ambion, Warrington, UK) from 1µg of RNA according to manufacturer's instructions with a total reaction volume of 20µL. Random decamers were added to the RNA + RNAse free water and the mixture was incubated at 65°C for 5 minutes before cooling to 4°C. The first strand synthesis reaction was run for 60 minutes at 42°C followed by 92°C for 10 minutes, and cooling to 4°C. CDNA products were stored at -20°C. No reverse transcriptase (NRT) controls were simultaneously generated, containing RNA and all the RetroScript components with the exception of the reverse transcriptase enzyme, the volume of which was replaced with RNAse free water.

2.5.3 Reverse transcription PCR (RT-PCR)

Primer pairs were a kind gift from Dr. Amanda Carr, and are listed in table 2.4 and are designed across exons. CDNA was amplified using Go Taq Polymerase kit (Promega, Southhampton, UK) following manufacturer's instructions. The PCR cycle consisted of a denaturing step at 95 °C for 2 min followed by 37 cycles of denaturation at 95 °C for 30s, annealing at 52°C (or 3 degrees cooler than the melting temperature) for 30s and extension at 72 °C for 30s, an extension step at 72 °C for 2 minutes and final cooling step at 4°C. PCR products were resolved on a 2% agarose/ethidium bromide gel. The identity of single bands was confirmed by comparison to a l Kbp ladder (Promega). NRT controls were included for all samples as well as no template controls (NTC) containing all components except primers. The house keeping gene for TATA binding protein (TBP) was used as an internal control.

2.5.4 Quantitative (real time) PCR (QPCR)

Quantitative real-time PCR was carried out on an Applied Biosystems 7900HT Fast Real-Time PCR system using the SYBR Green method. Master mixes were made containing Power SYBR (Applied Biosystems), Primers and DNAse/RNAse free water. Mini-master mixes (84µL) containing 1µL of cDNA were then made for each sample. 25µL triplicate reactions were carried out in a 96 well plate for each sample. Test and control conditions were always carried out on the same plate such that the plotted relative values reflect changes in gene expression between samples rather than others sources of variation in the assay.

Data from the Q-PCR was normalized to the geometric mean of the expression of three internal control genes in each sample. These genes (POL, MAN, GNB – see table 2.5) were chosen due to their stability across the sample groups, which was determined using the GeNorm algorithm **(**Vandesompele et al*.,* 2002). Forward and reverse primers were designed across exons and kindly lent by Dr Mayaan Semo or purchased from Qiagen's quantitect range (Qiagen, Crawley, UK) see table 2.5. QPCR data was initially analysed using the SDS 1.7 software (Applied Biosystems). Raw fluorescence values were then imported into the 'DATA Analysis for Real Time PCR' (DART PCR) excel workbook (Pierson, 2003). The DART workbook tests amplification efficiencies using the slope of the amplification plot and uses this, in combination with the threshold cycle to calculate the theoretical starting fluorescence, Ro. Based on the formula $Ro = Rct- (1-E)^{-ct}$. Where Rct = the fluorescence at the threhold cycle, E= efficiency and Ct is the threshold cycle. The normalised Ro is then calculated by dividing the target gene Ro by the average house keeping gene Ro (Pfaffl et al., 2001). The DART work book identifies any outliers in terms of relative expression values or amplification efficiency within triplicates by one way ANOVA which, if detected, were excluded from analysis. Normalised Ro values are then expressed relative to the normalised Ro of control samples and the data is plotted as normalised relative fold changes.

$$\text{Relative fold change} = \frac{\text{Efficiency corrected, normalised expression (test condition)}}{\text{Efficiency corrected, normalised expression (control condition).}}$$

2.6 Statistical Analysis

2.6.1 One and two-way ANOVA

One and two way ANOVA were carried out in the excel workbook 'RANOVA'

2.6.2 Paired and Unpaired student's t test

Following one or two way ANOVA, post hoc student's t-tests were performed in excel to test significance within the groups. In QPCR experiments, where control and test conditions were carried out on the same plate, but different biological replicates carried out on different plates, 2- tailed, paired t-tests were used to compare normalized fluorescence values. Unpaired t-tests were used when the subjects between the groups had no specific relation to each other e.g. when comparing gene expression data between two cell lines.

2.7 Measuring Pigmentation and Confluence

Pigmented HESC-RPE cells are clearly visible with the naked eye against a background of non-pigmented cells. This provides an opportunity for rapid on-line, non destructive monitoring of the differentiation progress by image analysis. We sought to develop an assay to rapidly and reproducibly monitor the changing quantities of pigmented cells during hESC-RPE differentiation. By measuring the numbers of individual pigmented foci at specified time points in the differentiation, we were able to quantify the relative conversion efficiency in various differentiation conditions (see results chapters 3-5).

2.7.1 Scanning Flasks and Wells and Importing to Image J

The first challenge was to find a system for reproducibly capturing images of the flasks. Background lighting in the lab changed considerably over the course of the day therefore it was necessary to create a closed system to ensure consistent background illumination. Further criteria are outlined in the table 1.

Requirement	**Reasoning**
Controlled and reproducible illumination of dishes or flasks	Images captured at different times can be compared with confidence
Fixed distance from lens to flask surface	Consistent scaling
Rapid capturing of images	Cells are not removed from incubator for prolonged periods of time
Can tolerate harsh cleaning with Virkon and Ethanol	Must be suitable for use in clean lab

Table 2.1 Image acquisition constraints

With these constraints in mind we designed a system that combined an Epson V750 flat bed scanner (Epson UK Ltd., Hertfordshire, UK) with a custom made flask mounting block and lid designed and constructed in the UCL biochemical engineering workshop (Fig. 2.1A). The mounting block was finished with matt

black walls and the lid was matt white to ensure a light background with which the pigmented foci would contrast (Fig. 2.1B). The block was designed to contain a T25 flask shaped hole so that a flask could be clicked into the same place relative to the captured area every time, facilitating rapid processing of flask images.

Images were acquired using the supplier software 'Silverfast Epson version 6.5 (LaserSoft Imaging, AG, Germany). The settings for image acquisition were as follows:

General Sm: Normal file
Orig:Transparent
Positive/Negative: Positive
Frame: Q factor: 2.5, 192, 3.57 MByte, 480 DPI 48-24 bit colour

Having tested several variations on the above settings, we found this to produce the best contrast between pigmented and background cells, it also acquired images at a suitable resolution (as specified by DPI –dots per inch setting- 480) and size (3.57MB). Scanned images were then opened in Image J (http://imagej.nih.gov/ij/) for further processing.

2.7.2 Auto-counting to determine number of Foci

Pigmented foci are visible to the naked eye and currently the best practice is to count the number of individual foci manually. This is both time consuming and subjective with the size and intensity of pigment undefined. We sought to develop a method for automatically counting the number of foci in a flask that could be applied throughout the project to accurately compare yields between cell lines and differentiation conditions.

Find Edges: The mounting block and lid removes background lighting so that the flask is always illuminated to the same extent. Figure 2.2 shows a typical flask of differentiating shef6 at day 50. When the imported images were converted from colour to grey scale and a threshold is applied, the top and side areas of the flask are obscured due to shadows caused by the narrowing flask neck. This led to non-pigmented areas being darker than the threshold (red areas) so that only the central portion of the flask could be assayed for pigmentation (Fig 2.2A).

We used image J's 'find edges' function to circumvent this problem. This function uses a 'sobel edge detector' to detect sharp changes in intensity in the imported image; applying the 'find edges' function highlighted all pigmented foci irrespective of their position in the flask (Fig 2.2B).

Noise Removal: Flasks and dishes were wiped with a lint free tissue prior to scanning. Despite this, occasionally white flecks appeared on the captured image. These would be detected by the find edges function as an area of sharp change in intensity and thus need to be removed prior to analysing the image.

Image J has a 'noise removal' function (Process> Noise> Remove outliers) which replaces a pixel by the median of the pixels within a specified radius if it deviates by more that a specified value. The radius, which is used for calculating the median, and the threshold, which determines by how much a pixel must deviate from the median were defined in order to remove all white flecks. 'Which outliers' was set to 'bright' so that only pixels brighter than this threshold were corrected. Fig. 2.3 illustrates

how removal of white flecks was achieved when we set the radius to 30 and the threshold set to 15. The white flecks visible in the top panel (red circles) have been removed by application of the 'remove outliers' function and as a result only the black, pigmented areas were detected by the find edges function.

Intensity and Size Threshold: In order to make an accurate estimation of the number of pigmented foci, the size and threshold intensity was defined. Images were converted from colour into an 8 bit grey scale image, which assigns every pixel a value from 1-255 with 255 being the darkest black and 1 being white. By choosing the threshold intensity we assigned the pixels which will be defined as pigmented cells and incorporate into the RPE foci count. Currently the best practice is to manually count the number of foci so the threshold settings chosen were those that most accurately matched those that were counted by eye. We found that setting the threshold to 45/255 selected the pigmented foci (highlighted by the find edges function) and excluded background giving the expected result as determined by manual counting. Fig. 2.4 illustrates a whole flask to which the above processing has been applied. Painstaking manual counting detected 118 individual foci. Thresholding the 'find edges/remove outliers' processed image at 45/255 detected the same number of foci. Close inspection of the highlighted areas revealed accurate highlighting of pigmented areas and exclusion of background (Fig. 2.4 E, F).

2.7.3 Validation with manual counts

In order to validate the auto-counts, the numbers of foci were first counted manually using the Plugins>analyze>cell counter function which allows the user to mark counted areas (Fig. 2.4 B,E). A total of 8 flasks with varying degrees of pigmentation were counted three times on three separate occasions. The same images were subsequently imported into image J and the 'remove outliers', 'convert to 8 bit grey scale', 'find edges' functions were applied as described above. A range of threshold and size cut offs were tested until a combination which matched the manual counts was determined. The threshold was set at 45 so that all pixels lighter than 45 (highlighted by find edges function) were included. The size cut off was set at 18 pixels. The size was an important feature as smaller sizes included areas that were not identified by eye and larger areas missed smaller foci. Figure 2.4 demonstrates how performing these functions and then auto-counting particles greater than 18 pixels in size accurately selected the foci that were also identified by manual counts. This was also accurate over the scale of the whole flask (Fig. 2.4 B,C).

The above functions were then combined into an ImageJ Macro (Fig. 2.4 G). The macro was tested in 8 flasks of Shef6 with varying levels of pigmentation. The numbers of foci in each of the 8 flasks were counted manually on 3 separate occasions. And the macro was used to determine foci numbers on three separate occasions. The results in Fig 2.4 H show how utilising the macro reduces variability in the counted numbers and is accurate over a range of pigmentation levels.

This 'auto-count' marco was applied to images of flasks and wells captured on the scanner throughout all the experiments described in the project.

2.7.4 Determining % pigmented Area

In rare instances where very high RPE yields were generated at day 50, it was not possible to distinguish individual pigmented foci. In order to compare relative RPE yields in these instances, Image J was used to quantify the total pigmented area above a specified threshold. Images were converted to greyscale 8-BIT (black and

white) images using the IMAGE: TYPE submenu. The THRESHOLD function (IMAGE: ADJUST submenu) was then used to select only the pigmented areas. These experiments were carried out in wells in which shadowing due to the shape of the vessel did not exclude large areas, as was the case in T25 flasks (Fig. 2.5A). Thus the find edges function was not required. Close analysis of individual pigmented particles was used to determine the most suitable threshold value (Fig 2.5B). We noticed that media volume and changes in colour due to pH affected the contrast in the wells, something that had not been a problem when the find edges function was applied. Thus a careful routine of exchanging the media and filling to a precise volume of 2mls per well before scanning was obeyed. Following the use of the THRESHOLD function the total % area was determined using the ANALYZE: ANALYZE PARTICLES submenu with the following settings: SIZE: 15–INFINITY, CIRCULARITY: 0–1, SUMMARIZE: On, EXCLUDE ON EDGES: OFF. CIRCULARITY is set to include all shapes, and EDGE EXCLUSION was set to include particles at the perimeter of the selected area. The total well area was selected for analysis, excluding the very edge of the well.

2.7.5 Estimation of cell seeding density following mechanical passaging

In order to visualise undifferentiated HESC colonies, flasks were scanned on an Epson V750 flat bed scanner as before but in with the lid on the mounting device removed. Against the dark background HESC colonies were visible (Fig 2.6A). Acquired images were imported into ImageJ and individual colonies were counted using the Plugins>analyze>cell counter function. In addition the % confluence was determined at day 6 in x flasks before dissociating cells (TrypLE enzyme, 10 mins, 37°C) and counting on a haemocytometer. These measurements were used to generate a calibration curve relating % confluence to actual cell numbers (Fig 2.6B). The scans were carried out at day 6 post seeding. The cell numbers plotted ranges from 1,200,000/25 = 48,000/cm2 to 7,207,000/25 = 288,280/cm2. Assuming a continuous growth rate during the six days, a doubling time of 40 hours after a latent period of 1 day (Park et al., 2010), the cells are likely to undergo approximately (5 x 24)/40 =3 population doublings.

If No = Initial seeding density, Nt= Population at day 6 and n= the number of population doublings in 6 days.

Then $No = Nt / 2^n$

The various split ratios tested in chapter 4 were scanned at day 6 and generated a range of confluence measurements with a minimum of 10.5 % and a maximum of 41.0% confluent. Using the calibration curves the maximum and minimum seeding density tested was determined as follows:

From the equation of the straight line calibration curve (Fig 2.7B):

Total Cell number at day 6 = 128218 (% confluence) + 451296

Therefore for 10.5% and 41.0 % confluence the total cell numbers are 1.8 million and

5.8 million respectively (72,000 - 228,000/cm2).

Applying the formula $No = Nt / 2^n$ where n= 3. The approximate range of seeding densities tested were between 9, 000/cm^2 and 29,000/cm^2.

Primary Antibody	Host/Isotype	Concentration	Supplier
Oct4	Mouse IgG	1:300	Santa Cruz
*Tra160	Mouse IgM	1:300	Millipore
*Tra181	Mouse IgM	1:300	Millipore
*SSEA1	Mouse IgM	1:300	Sheffield*
*SSEA3	Mouse IgG	1:300	Sheffield*
Nestin	Mouse IgG	1:500	Millipore
Pax6	Mouse IgG	1:300	Millipore
Otx2	Rabbit Poly	1:1000	Millipore
MitF	Mouse IgG	1:50	Santa Cruz
Chx10	Rabbit IgG	1:300	Sigma-Aldrich
CRALBP	Mouse IgG	1:300	Thermo Scientific
Bestrophin	Mouse IgG	1:300	Millipore
Pmel17	Mouse IgG	1:300	Abcam
Zo1	Mouse IgG1	1:200	Invitrogen
Isotype Control	Mouse IgM	1:200	Sigma-Aldrich
Isotype Control	Mouse IgG	1:200	Abcam
Isotype Control	Rabbit IgG	1:200	Abcam

Table 2.2. Primary antibody sources and working dilutions. (*antibodies gifts from Peter Andrews's lab at Sheffield university). ** = antibodies raised against cell surface antigen for which the permeabilization step was omitted.

Secondary Antibody, Host/Isotype	Supplier	Concentration
Alexa Flour 488 Goat Anti-mouse IgG	Invitrogen	1:200
Alexa Flour 488 Goat Anti-rabbit IgG	Invitrogen	1:200
Alexa Flour 555 Goat Anti-mouse IgG	Invitrogen	1:200
Alexa Flour 555 Goat Anti-rabbit IgG	Invitrogen	1:200
Alexa Flour 488 Goat Anti-mouse IgM	Invitrogen	1:200
Alexa Flour 555 Goat Anti-mouse IgM	Invitrogen	1:200

Table 2.3. Secondary antibody sources and working dilutions.

Gene	GenBank Accession	Sequence
Otx2	NM_172337	**FOR** TAAACCAGCCCCTCTGTTTG **REV** TCTCGCATGAAGATGTCTGG
Pax6	NM_000280	**FOR** TCAGCTCGGTGGTGTCTTTG **REV** GTCTCGGATTTCCCAAGCAA
MitF	NM_198177	**FOR** AGTTGCTGGCGTAGCAAGAT **REV** ATGGAGGCGCTTAGAGTTCA
Tyrosinase	NM_000372	**FOR** TGCCAACGATCCTATCTTCC **REV** GACACAGCAAGCTCACAAGC
PMEL17	NM_006928	**FOR** GTGGTCAGCACCCAGCTTAT **REV** GAGGAGGGGGCTATTCTCAC
TBP	NM_003194	**FOR** GAACCACGGCACTGATTTTC **REV** CCCCACCATATTCTGAATCT

Table 2.4. RT-PCR primers. Shortened gene name, GenBank accession number of amplified product, forward and reverse sequences. Annealing temperature was set at 52°C.

Gene	GenBank Accession	Sequence
POL	NM_000937	**FOR** GCGGGGTGAAGTGATGAAC **REV** ATCATCGGGATGGGTGCTGT
MAN	NM_016219	**FOR**ACCGTGGAGAGCCTGTTCTA **REV** GTTTGGGTCATCGGAGAAGA
GNB	NM_006098	**FOR** GAGTGTGGCCTTCTCCTCTG **REV** GCTTGCAGTTAGCCAGGTTC
OCT4 (POUF51)	NM_002701	**FOR** GACAACAATGAAAATCTTCAGGA **REV** TTCTGGCGCCGGTTACAGAACCA
Nanog	NM_024865	**FOR** TCCCTCCTCCATGGATCTCGC **REV** CTGAGGCCTTCTGCGTCACA
TDGF	NM_001174136	**FOR** TCCTTCTACGGACGGAACTG

		REV AGAAATGCCTGAGGAAAGCA
Otx2	NM_021728	**FOR** GCGCAGCTAGATGTGCTGGA **REV** CACTGCTGCTGGCAATGGTC
Pax6	NM_000280	**FOR** CCATCAGACCCAGGGCAATC **REV** GGTCTGCCCGTTCAACATCC
Six3	NM_005413	**FOR** CCCAGCAAGAAACGCGAACT **REV** CATTCCGAGTCGCTGGAGGT
Lhx2	NM_004789	**FOR** AGAGCACCTGGACCGTGACC **REV** ACTTGTCCACGCCCGTGTTT
MitF	NM_198177	**FOR** TTGTATCTCAGTTCCGCCGAGC **REV** TGCTTTACCTGCTGCCGTTG
Chx10	NM_182894	**FOR** AAGAAGCGGCGACACAGGACAATG **REV** TTGGCTGACTTGAGGATGGACTCG
Tyrosinase	NM_000372	**FOR** AGAACCTGATGGAGAAGGAATGCTG REV GGTCCCCAAAAGCCAAACTTGC
PMEL17	NM_006928	**FOR** GATGGGCAGGTTATCTGGGTCAAC **REV** GCTGGAATGAGCAAGAGGCACATAG
Bestrophin	NM_004183	QT00023282
CRALBP	NM_000326	QT00001239
Nestin	NM_006617	QT01015301
Brachyury (T)	NM_003181	QT00062314
AFP	NM_00134	QT00085183
Gata6	NM_005257	QT00233331
Sox17	NM_022454	QT00204099
CDX2	NM_001265	QT00027807

Table 2.5. QPCR primers. Shortened gene name, Genbank accession numbers and forward and reverse primer sequences. Some primers were sourced from Qiagen's pre-validated 'Quantitect' range for which the catalogue numbers starting QT are quoted.

Chapter 3: MEFs co-culture and feeder-free differentiation: Bioprocess characterisation

3.1 Introduction

The first and most commonly used method for deriving pure populations of RPE from pluripotent HESC involves 'continuous adherent' culture on mitotically inactivated MEFs, followed by manual isolation of pigmented foci, re-plating and expansion on a substrate such as Matrigel. This method has been used in a number of HESC lines, producing well characterised RPE cells which have been transplanted into animal models of ocular diseases (Klimanskaya et al., 2004, Lund et al., 2006, Vugler et al., 2008, Buchholz et al., 2009, Carr et al., 2009b, Liao et al., 2010). The number of independent studies reporting successful derivation of HESC-RPE using this continuous adherent co-culture method demonstrates that the method is robust. It is not, however, well defined. There remains considerable variation in reported RPE yields (see table 1.1), a number of cell lines which fail to generate RPE and significant differences in the reported time scales required to generate RPE (Rowland et al., 2011, Vaajasaari et al., 2011).

The factors which drive spontaneous formation of HESC-RPE in these culture conditions are not fully understood although the so called 'default model' of neural differentiation in embryonic stem cells (Munoz-Sanjuan et al., 2002) has been implicated (Vugler et al.,. 2002). HESC derived neuroectodermal cells have been shown to adopt anterior neuroepithelial characteristics in the absence of exogenous signalling (Pankratz et al., 2007, Elkabetz et al., 2008). Thus without adding any growth factors or small molecules to direct cell fate, a large proportion of HESC will theoretically differentiate into cells similar to the anterior neural plate from which all retinal cell types are derived during eye development in vivo (Zaghloul et al., 2005). The mitotically inactivated MEFs used in HESC-RPE differentiation do, however, secrete a variety of growth factors including members of the TGFβ superfamily and proteins involved in IGF, BMP and Wnt signalling (Gerber et al., 2007, Prowse et al., 2007, Bendall et al., 2009, Hongisto et al., 2012). A number of these factors are critical to HESC maintenance but may also act to direct efficient RPE differentiation. For example, activin A is actively secreted by MEF feeder cells (Hongisto et al., 2012), in vivo activin A mimics the action of the extraocular mesenchyme and induces RPE differentiation (Fuhrmann et al., 2000) and in HESC culture, exogenous

activin A significantly enhances RPE yields when added to differentiating HESC (Idelson et al., 2009, Meyer et al., 2009, Hongisto et al., 2013).

In a cell culture environment, factors other than the presence of molecules directing cell fate decisions are likely to be equally influential in determining the HESC-RPE differentiation efficiency; such as undifferentiated and differentiated cell survival and proliferation rates. In the following sections, the bioprocess of RPE differentiation using the 'continuous adherent' method in MEFs co-culture is described in two new cell lines (Shef6 and Shef3). The method is also applied to a novel feeder-free continuous adherent differentiation system that facilitates high yielding and animal cell free differentiations. At the time of carrying out these experiments, feeder-free adherent HESC-RPE differentiation had yet to be demonstrated although it has now been shown by others (Zahabi et al., 2011, Rowland et al., 2012, Sridhar et al., 2013).

The initial aims of this study were to determine whether Shef6 and Shef3 were able to generate RPE in MEFs co-culture and in feeder-free conditions, to define the relative quantity of RPE foci generated in defined conditions, to establish time lines and to characterise any significant differences in the process of RPE emergence between the two cell lines. The step wise differentiation process consists of HESC expansion and early differentiation, acquisition of forebrain and eye field characteristics, emergence of pigmented foci, foci isolation/enrichment and RPE expansion. At each stage, gene expression, immunocytochemical and image analysis assays are carried out in order to characterise the phenotypes of the emerging cells (Fig. 3.1).

3.1 Characterisation of HESC lines Shef6 and Shef3

Due to the propensity of HESC to undergo spontaneous differentiation and acquire karyotypic abnormalities in culture (Brimble et al., 2004, Draper et al., 2004), our cell lines, Shef3 and Shef6, were characterised regularly using morphological examination, immunocytochemistry and karyotypic analysis. By comparing the morphologies of colonies to pluripotency marker expression, it was possible to identify and select pluripotent colonies for continued passaging.

3.1.1 Morphology and HESC marker expression

Shef6 and Shef3 were maintained on mitotically inactivated mouse embryonic fibroblasts (MEFs) at a density of 9200 cells/cm^2. Undifferentiated cells in both HESC lines had a similar appearance. The cells were small, round and grew in tightly compacted colonies, with a characteristic high nucleus to cytoplasm ratio (Thompson et al., 1998) (Fig. 3.2 A, D). At the colony edges, cells were slightly larger and more elongated. Colonies were usually passaged onto fresh MEFs feeders when they were large enough to fill a 10x objective (approximately 15,000 cells (Loring et al., 2007)). When colonies were allowed to grow much larger than this or left on old MEFs for prolonged periods, distinctive changes in cell morphology became increasingly common. Cells in the centre of colonies would gradually become larger and less compacted forming a hole like structure surrounded by compacted cells (Fig. 3.2 B, E). After 15 days of continuous culture, the majority of colonies had lost their HESC like morphology and some had formed thick, multi-layered clumps of differentiating cells (Fig. 3.2 C,F).

Immunocytochemistry was carried out on cultures of Shef6 and Shef3, 5 days post passaging. HESC markers including transcription factor Oct4, keratin sulphate-associated antigens Tra160 & Tra181 and the glycosphingolipid antigen, SSEA3, were used to assess undifferentiated phenotype. The majority of colonies observed in Shef6 and Shef3 were immunopositive for all of these HESC markers (Fig. 3.3);

however, a small number of differentiating colonies were also present. These colonies contained cells with reduced expression of HESC markers (Oct4, Tra160, Tra181, SSEA3) and were commonly found at the centres of large colonies (Fig. 3.4 A). Areas where HESC marker expression was absent were immunopositive for SSEA1 (Fig. 3.4 C), a marker of early differentiation in HESC (Draper et al., 2002).

These results illustrate the heterogeneity typical in HESC MEFs co-culture. In an effort to minimise differentiation and improve reproducibility, we selectively passaged only colonies with undifferentiated morphology.

3.1.2 Karyotypic stability

Shef6 and Shef3 cell lines were karyotyped regularly. Karyology was carried out at TDL genetics (60 Whitfield Street, London) using G banding with up to 20 cells counted per sample. In the majority of cases Shef3 had a normal male 46 XY karyotype (Example Fig 3.5 A.) and Shef6 had a normal female 46 XX karyotype (Fig 3.4 B). On one occasion a sub-population of abnormal cells with 47 chromosomes including an extra copy of chromosome 5 (TRISOMY 5) was detected in passage 81 Shef3 (Fig 3.5 C). This same abnormality (TRISOMY 5) was also detected on one occasion in a subpopulation of Shef6 passage 72 cells in addition to a sub-population with an extra copy of chromosome 17 and a translocation between the short arm of one X chromosome and the long arm of one chromosome 18 at breakpoint q11.2. On these occasions no notable differences in cellular morphology, HESC marker expression or RPE differentiation capacity was observed. Within this limited sample size we observed no direct correlation between passage number and the incidence of karyotypic abnormalities; cells as late passage as 103 were found to have a normal karyotype (Fig 3.5 A).

3.2 Shef3 and Shef6 undergo spontaneous differentiation on MEFs forming pigmented foci with varying efficiencies

The Shef6 and Shef3 HESC lines were derived by Harry Moore's group in Sheffield using a microdrop culture system. The same group had previously derived the Shef1 cell line which will be used to derive HESC for clinical trials (Carr et al., 2013) using similar methods (Draper et al., 2004, Aflatoonian et al., 2010). HESC-RPE differentiation in these two cell lines has yet to be reported in a published study. In this section we show, for the first time, that both cell lines are able to produce pigmented RPE. The changes in gene and protein expression during the process of continuous adherent differentiation in MEFs co-culture (Vugler et al., 2008) are described and the differentiation rate and efficiency in the two cell lines is assessed and compared.

3.2.1 Spontaneous differentiation yields a subset of cells with anterior neuroepithelial characteristics

Mechanically passaged clumps (approximately 1000 cells per clump) of Shef6 and Shef3 were seeded onto MEFs where they established typical round and compacted colonies of Oct4 immunopositive cells (Fig. 3.6 B, F). Cells were fed daily with +bFGF HESC expansion media and allowed to proliferate. By day 10, colony borders began to merge and Oct4 expression was lost in the centres of colonies (Fig. 3.6 C, G.). Imaging of whole flasks revealed how individual colonies become increasingly large and opaque with time in culture (Fig. 3.6 A). At day 15, morphological examination revealed an increasing abundance of 'holes' in the centre of colonies containing less compacted Oct4 negative cells (Fig. 3.6 D, H). By day 20, Oct4 expression was almost undetectable by immunocytochemistry; cells had formed multilayered ridges and adopted a variety of distinct morphologies (Fig 3.6 E, I). Imaging of the whole flask at day 20 revealed a thick, opaque layer of cells covering the entire flask surface (Fig 3.6 A).

RNA was extracted from differentiating flasks over the first 15 days of early differentiation and QPCR was used to compare the relative changes in pluripotency gene expression. From days 3-6 there was a relative increase in expression of all HESC markers (Fig. 3.6 J). Relative expression of all HESC markers then decreased from day 6 onwards demonstrating a down regulation in the pluripotency circuitry with time.

At day 20, immunocytochemistry was used to detect the presence of markers of neuroectoderm differentiation, Pax6 (Zhang et al., 2010), and anterior forebrain specification, Otx2 (Boncinelli et al., 1995). These transcription factors are critical to the step wise induction process that will eventually lead to a retinal phenotype (Zaghloul et al., 2005. Meyer et al., 2009). Pax6 and Otx2 proteins were detected in clustered, neural-rosette structures found on multilayered and compacted ridges of cells (Fig. 3.7 A-F). These clusters were abundant in flasks at day 20 (Fig 3.7 G, H). QPCR was carried out on RNA extracted from whole flasks of Shef6 at time points leading up to day 25 (5 flasks all derived from the same starter culture). Pax6 expression increased steadily from day 10 onwards, culminating in a 50 fold increase in relative Pax6 expression by day 25 (Fig. 3.7 I). Otx2 expression did not undergo any large fold changes in gene expression over time (Fig. 3.7 J); this is likely due to the role played by this transcription factor during multiple stages of development including maintenance of the epiblast, forebrain specification and later RPE differentiation (Simeone et al., 1998, Bovolenta et al., 1997). This pattern of Otx2 and Pax6 expression was also found in differentiating cultures of Shef3 by RT PCR up to day 50 (5 flasks derived from same starter culture). The Pax6 RT-PCR primers amplified both the Pax6+5a and Pax6-5a isoforms. Both have distinct DNA binding domains and the larger (Pax6+5a) is thought to be particularly critical to retinal development (Azuma et al., 2005). RT-PCR revealed that the expression of Pax6 increased steadily over time in culture, with the larger fragment (arrow) becoming increasingly strongly expressed over time (Fig 3.7 K).

3.2.2 Pigmented foci first appear around day 30 following an upregulation in eye field and RPE gene expression

Between days 10 and 20 of differentiation a lot of cell death was observed in differentiating cultures and the media would turn an intense yellow colour between daily media changes indicating significant lowering of pH over 24 hours. By day 25 the intense colour changes had subsided and a thick contiguous sheet of cells was seen. Fluid filled bubbles were also frequently observed indicating a fluid pumping action and water-tight connectivity across the cell sheet. In both cell lines, small pigmented foci were first easily detectable by eye between 25 and 32 days post seeding (15-22 days post bFGF withdrawal) (Fig. 3.8 A,B, arrows).

Immunocytochemistry or FACs analysis was challenging at this stage as cells were very difficult to dissociate and a large amount of debris from the extra cellular matrix and dead cells interfered with the fluorescence signal. Extraction of RNA from lysed cells for QPCR was carried out to assess changes in gene expression over this time. The emergence of pigmented cells in Shef3 and Shef6 was accompanied by an increase in expression of Tyrosinase, Pmel17 and MitF from days 20-50 as detected by QPCR time course analysis (Fig 3.8 C-E) and RT PCR (Fig 8F); these genes are critical for the synthesis of pigment in RPE (Bharti et al., 2006). There was a basal level of Pmel17 expression detected in HESC (Fig 3.8 F) but this was upregulated as pigment accumulated. In shef3, the RT-PCR time course suggested an earlier upregulation in MitF expression (day 10) than that detected by QPCR in Shef6 (days 20 onwards). Temporal Tyrosinase expression faithfully followed the visible emergence of pigmented cells in both cell lines.

3.2.3 The kinetics of RPE accumulation in Shef6 and Shef3

In designing a manufacturing process for a biological product an important consideration is the optimal time for harvesting the product. Measuring the emergence of pigmented foci over time allows us to carry out 'on-line' monitoring of HESC-RPE differentiation. The emergence of pigmented foci in Shef6 and Shef3 was measured over up to 84 days of differentiation. Flasks of Shef6 (N=3) from passages 42-48 and Shef3 (N=3) from passages 45-47 were fed daily with differentiation media. Each flask was scanned every 3-5 days from day 25 onwards and images imported into Image J (see chapter 2 methods). Using the foci counting macro developed in Image J the kinetics of RPE accumulation in the two cell lines were established (Fig. 3.9).

Pigmented foci were first detected earlier in Shef3 at Day 25, in Shef6 foci were first detected at day 32 in 3 out of 4 flasks. The rate of foci accumulation per cm^2 from days 30-50 was significantly greater in Shef6 (0.5 foci/cm^2/day, N=4), than Shef3 (0.3 foci/cm^2/day (N=3), (student's unpaired t-test $p<0.05$). In Shef3 the rate of foci accumulation began to decrease from around day 50 onwards at which point each flask contained on average 157 ± 16 foci; in contrast, in Shef6, pigmented foci numbers continued to accumulate rapidly past day 50 (271 ± 13 per flask) up to the last measured time point day 58, (369 ± 38 per flask). Comparing time points at which all flasks were measured, (days 25, 32, 42, 50 and 58), two way ANOVA revealed a significant effect of time ($F(4,20) = 47.5$, $p<0.001$), cell line ($F(1,20) = 18.4$, $p<0.001$) and a significant interaction ($F(4,20) = 14.31$ $p<0.001$), indicating that the cell line effect increased with time in culture. Post-hoc unpaired student's t-test revealed significantly greater numbers of pigmented foci in Shef6 at days 50 and 58 ($p<0.01$).

These data show that the optimal time for harvesting RPE foci differs between the two cell lines; an earlier time point (~ day 50) is optimal in Shef3, whereas a longer time in culture would increase process efficiency in Shef6.

3.2.4 RPE yields are compromised at high HESC passages

Human embryonic stem cells are heralded for their ability to expand indefinitely in culture; in spite of this, several studies have reported changes in cell behaviour over time in culture (Enver et al., 2005, Baker et al., 2007). In order to determine how time in culture might affect the ability of Shef6 and Shef3 to generate RPE, cells from both lines were differentiated using the above protocol over a broad range of passage numbers. In each case, the number of pigmented foci per T25 flask was measured at day 50 using the auto-counting macro in Image J (see methods). All other variables were kept constant (MEFs batch, MEFs seeding density, media volume, media composition, time in culture, flask split ratio at passaging).

Cells were banked in small quantities at passage 30 therefore the earliest passage numbers at which cells were in sufficient quantities to carry out differentiation were between 40 and 45, the oldest passage numbers tested were between 80 and 90 (Fig. 3.10 A,B). Combining the data from both cell lines and grouping the data into passage numbers (p) 40-50, 50-60 and 70-90, a decrease in foci yield was observed with increasing passage number (Fig. 3.10A). Two way ANOVA revealed a significant effect of passage number on foci numbers per cm^2 ($F(2,10)= 70.9$, $p<0.01$) and a significant effect of cell line ($F(1,10) = 5.8$, $p<0.05$), but no significant interaction ($F(2,10)=2.02$, $p=0.23$). Both cell lines produced the highest RPE yields in the p40-50 group (Mean (Shef6 p 40-50) = 10.7 ± 0.9 SEM foci per cm^2, Mean (Shef3 p 40-50) = 6.3 ± 0.7 foci per cm^2). Thereafter a drop off in foci yield was observed, with the combined yields of both cell lines at p50-60, significantly lower than in the p40-50 group (Student's unpaired t-test $p<0.01$) and the combined yields in the 70-90 group significantly lower than the p40-50 group ($p<0.01$) (Mean (p40-50 Shef6+Shef3)= 9.3±1.0 foci/cm^2, (p50-60 Shef6+Shef3)= 3.0±1.0 foci/ cm^2, (p70-90 Shef6+Shef3) =0.2±0.1 foci/cm^2).

These data demonstrate a significant decline in RPE differentiation efficiency with increasing passage number. To our knowledge, this is the first report demonstrating that the length of time for which the HESC have been in culture is a critical factor influencing the expected RPE yield.

3.3 RPE enrichment and Expansion

After 50 days of differentiation we consistently observed large numbers of individual pigmented foci in low passage Shef6 and Shef3. Pigmented cells occupy only ~0.1-2% of the total surface area with foci nestled within a large amount of extracellular matrix and non-pigmented cellular material. The next stage in the bioprocess requires the separation of pigmented foci from surrounding, non-pigmented material.

3.3.1 Pigmented foci are manually isolated and re-plated to form 'cobblestone' pigmented epithelial sheets that are positive for RPE markers.

At day 60 the morphologies of several emerging foci were examined. We found there to be considerable variation in the size and shape of pigmented foci (Fig 3.11). In some cases a monolayer of pigmented cells could be observed fanning out from a 3 dimensional heavily pigmented centre (fig 3.11 A, D); in other cases heavily pigmented, multilayered foci remained in small discrete areas (Fig 3.11 C). These differences are likely related to local spatial constraints and the asynchronous emergence of pigmented foci.

At this time point the contiguous cell sheet was resistant to enzymatic dissociation. Trypsin had very little impact regardless of the concentration or treatment time. Collagenase at a high concentration (1mg/ml) was more effective at breaking apart the cell sheet. Overnight collagenase treatment (1mg/ml, 8-10 hours) facilitated manual dissection of the individual foci with microsurgical blades. Although time consuming, this manual dissection method yielded foci that successfully adhered to Matrigel coated plates and expanded to form largely homogenous, pigmented epithelial sheets.

The adherence and growth of cells from four typical foci was imaged over 35 days. Two days after the initial dissection most of the foci had successfully adhered to the Matrigel coated plates and proliferating cells were visible around the edges (Fig. 3.12

B). By day 7 pigmented cells with epithelial morphology were visible in all wells (Fig. 3.12 C). At day 18 the monolayers had expanded further (Fig. 3.12 D). In one well a contaminating cell type was visible at day 18 (arrow) which appeared to be restricting pigmented RPE proliferation; closer analysis revealed a non pigmented structure from which neuronal projections were emanating (Fig. 3.13 A,B). By day 35 this structure appeared to have receded and pigmented epithelial cells occupied the whole area surround the foci (Fig. 3.13 C,D). The rate at which pigmented cells accumulated in the wells appeared to vary considerably. At day 35 pigmented, epithelial cells occupied the entire field of view in 2 out of the 4 wells (column 1, 4), and less than half of the same area in the remaining two (column 2,3). This did not appear to correlate with the size or rate of attachment of the original foci.

In order to confirm the identity of the pigmented epithelial cells, expanding foci from both Shef6 and Shef3 were immuno-stained with RPE markers. Pigmented, polygonal cells from both cell lines stained positively for mature RPE cell markers CRALBP, Bestrophin, Otx2 and ZO1 (Fig. 3.14 A,B).

Examples of multiple foci expanding in 24 well plates are shown in Fig. 3.15 A, B; the most heavily pigmented areas are visible closest to the original point of foci adherence (marked by arrows). Bestrophin expression was restricted to these heavily pigmented cells found close to the adherent foci (Fig 3.15 D) demonstrating the specificity of the antibody to pigmented, non-proliferating RPE. Stitching multiple 10 x microscope images together further demonstrated the change in pigmentation (high to low) and morphology (polygonal to elongated) with increasing distance from the adherent foci (Fig 3.15 C) as did immuno-staining for tight junction protein ZO1 (Fig. 3.15 E). These characteristics of expanding RPE are consistent with observations in HESC derived from other cell lines (Vugler et al., 2008 (Shef1, Shef7), Liao et al., 2010 (H1, H9)).

3.4 Feeder-free differentiation in Shef6 and Shef3

Mitotically inactivated MEF 'feeders' have been used in derivation and culture of human embryonic stem cells since the discovery of HESC (Thomson et al., 1998) and are an integral part of a number of published HESC-RPE differentiation protocols (Rowland et al., 2011). The use of MEFs may prove problematic in the manufacture of cells for cell therapy by risking the introduction of animal derived pathogens, and impeding the standardization of differentiation protocols (Chin et al., 2007, Akopian et al., 2010). It is, therefore, desirable to generate HESC-RPE in feeder cell free culture environment. In these experiments we test RPE differentiation in the commonly used feeder-free systems employing Matrigel and MEFs conditioned media (CM) (Xu et al., 2001) and the commercially developed defined mTeSR1 media (Ludwig et al., 2006).

At the time of these experiments, feeder cell free HESC-RPE differentiation using the continuous adherent method was yet to be demonstrated. In this section we aimed to answer the following questions:

1. Can feeder-free HESC culture generate RPE in Shef6 and Shef3 using the continuous adherent method without the addition of growth factors or small molecules?
2. What effect does the replacement of MEFs with feeder-free matrices and media have on RPE yields?

3.4.1 Neuroectoderm conversion efficiency at day 15 in feeder cell free conditions

Pax6 is a neuroectoderm fate determinant homeobox gene that is critical to the formation of both neuroectoderm and eye field (Zhang et al., 2010). It has previously been observed that Pax6 expression increases steadily over time during RPE differentiation in MEFs co-culture in both Shef6 and Shef3 (Fig. 3.7 I, K). In order

to assess the neuroectoderm conversion efficiency in feeder-free cultures, Pax6 upregulation in Shef6 and Shef3 was evaluated after 15 days of culture in feeder-free conditions. Shef6 and Shef3 cells were seeded onto MEFs or Matrigel and expanded for 10 days in HESC media or MteSR1 respectively, before switching to –bFGF differentiation media for the remaining 5 days. For comparison, cells from the same starter cultures were also differentiated as floating embryoid bodies, i.e. in the absence of external stimuli from MEFs, mTeSR1 or Matrigel. Experiments in Shef6 and Shef3 were carried out concurrently and over a range of passages in an attempt to decipher the inherent differentiation capacity of the cell lines (Fig. 3.16).

Pax6 expression increased from days 5-15 indicating a degree of neuroectodermal conversion in all conditions. One way ANOVA was used to assess the significance of differences in Pax6 expression following the 3 differentiation methods. In Shef6, there was an overall statistically significant difference between all three methods ($F(2,6)=37.6$, $p<0.01$), with the embryoid body method producing the greatest upregulation (average fold increase 76.9 ± 7.3), followed by feeder-free differentiation on Matrigel with mTeSR1 (average fold increase = 46.1 ± 12.4) and with MEFs co-culture giving the lowest relative upregulation (average fold increase = 4.0 ± 2.2). In Shef3, the embryoid body method also gave the greatest fold increase (Average= 44.5 ± 5.4), though this was significantly lower than the upregulation seen in Shef6 embryoid body differentiation ($p<0.05$, student's unpaired t-test). In Shef3, MEFs co-culture produced a relatively large fold increase in Pax6 expression (Average = 32.5 ± 1.3); this was significantly higher than that seen in Shef6 in similar conditions ($p<0.01$, unpaired t-test) and was higher than (though not significantly different to) the fold increases in Matrigel + mTteSR1 (Average = 13.6 ± 9.9, $p=0.3$, paired t-test) suggesting that Shef3 is more prone to spontaneous rapid neuroectoderm differentiation in MEFs co-culture conditions.

Shef6 and Shef3 cell growth rates were measured in the feeder cell free Matrigel +mTeSR1 condition (Fig 3.16 B). Both Shef6 and Shef3 proliferated successfully in Matrigel + mTeSR1 with viable cell numbers increasing over time. Shef6 however had a significantly higher growth rate than Shef3. Two way ANOVA revealed a significant effect of time ($F(2,18) = 227.5$, $p<0.001$) and the cell line ($F(1,18) = 914.3$, $p<0.001$) on total cell numbers and a significant interaction ($F(2,18)=108.1$,

$p<0.001$) with total viable cell numbers significantly higher at all time points in Shef6 ($p<0.05$, N=4, Student's unpaired t-test).

These results show that optimal conditions for neuroectodermal conversion differ between cell lines. Feeder-free differentiation on Matrigel significantly enhances Pax6 upregulation in Shef6 relative to MEFs co-culture but reduces it in Shef3 within the same time frame. In the absence of external stimuli (embryoid body differentiation), Pax6 is upregulated in Shef6 to a significantly greater degree than in Shef3 suggesting an enhanced innate propensity for neuroectodermal differentiation in Shef6.

3.4.2 Shef3 rapidly differentiate in absence of MEFs or MEFs-conditioned media

In order to further study the impact of feeder-free differentiation, Shef3 colonies were observed during the first ten days of differentiation in MEFs co-culture and feeder cell free conditions on Matrigel.

Cell morphology is very difficult to observe in floating EBs so cells were instead plated onto Matrigel where they adhered and were fed with standard HESC media +bFGF. As before, Shef3 cells were also plated onto Matrigel and fed with MEFs conditioned media (CM) and on MEFs fed with standard HESC media for comparison. Colonies were observed in all conditions at day 3 and day 10 (Fig 3.17 A.). In the Matrigel +HESC media condition, cells with differentiated morphology were abundant at the edges of colonies at day 3; cells grown on Matrigel in the presence of CM, however, formed colonies with typical HESC morphology. Colonies appeared to be larger in the Matrigel + CM condition compared to typical MEFs co-culture; this may be due to the lack of spatial constraints imposed by MEFs or due to enhanced HESC growth rates in Matrigel + CM. At day 10, multilayered cell sheets with a variety of non HESC-like morphologies were visible in the Matrigel only condition in the presence of conditioned media; however, monolayers of compacted HESC-like cells were observed across the flasks. In MEFs, co-culture colonies had grown considerably in size and were beginning to merge but had not yet become completely confluent.

QPCR was carried out on samples of Shef3 differentiating in the three conditions at day 10. As before, Pax6 expression was significantly different in all conditions (one way ANOVA $F(2,6)=150.0$, $p<0.05$). Pax6 expression was higher in the adherent, Matrigel only condition than the other conditions ($p<0.01$, paired student's t-test), demonstrating that rapid differentiation and upregulation of Pax6 occurs in the absence of MEFs or CM whether cells were differentiated in floating embryoid bodies or adhered to Matrigel (Fig 3.17 B).

3.4.3 Temporal gene expression changes during differentiation in feeder cell free conditions

After 10 days expansion in the three conditions, the media was switched to differentiation media (HESC media –bFGF) for the remaining forty days of differentiation. Cells from each condition were harvested at days 5, 10, 20, 30 and 50 of differentiation for RT-PCR analysis (Fig 3.18.).

In MEFS co-culture, Pax6 RNA was detectable at day 10 and continued to increase in abundance up to day 50. In Matrigel+CM a similar pattern was seen although the transcript appeared less abundant at days 10 and 50. In the Matrigel only condition, however, expression was detected at day 10 only to be down regulated thereafter. A similar pattern was seen in Otx2 and Pmel17 expression with expression maintained, increasing over 50 days in the MEFs co-culture and Matrigel+CM condition, but down regulated from day 20 in the Matrigel only condition. MitF expression was also down regulated at day 50 in this condition. Temporal expression of Tyrosinase followed the appearance of pigment first detectable at days 20-30 and increasing in abundance over time in MEFs co-culture and MEFs-CM but virtually absent at days 30 and 50 in the Matrigel only condition.

These results demonstrate that although differentiation in the absence of MEFs or MEFs-CM leads to rapid differentiation (as evidenced by early Pax6 expression), this method fails to sustain the gene expression necessary for long term RPE differentiation.

3.4.4 The effect of feeder-free differentiation on Shef3 RPE yields

RPE foci numbers were counted using the auto-count macro in Image J (see methods) from scans of flasks taken at day 50 following differentiation in the three conditions in three separate experimental runs. It was observed that Shef3 produced significantly greater RPE yields when differentiated in MEFs co-culture relative to the other conditions (One way ANOVA, $F(2,6) = 76.8$, $p< 0.05$, student's unpaired t-test, $p<0.001$) (Fig 3.19 A). At day 50, Shef3 in the Matrigel only conditioned had produced very few foci (Average =0.11± 0.05foci/cm2). Poor cell coverage across the flask was observed with only isolated colonies surviving. Cells in the Matrigel + CM condition had a slightly improved yield (Average= 0.35± 0.27 foci/cm2) but not significantly so ($p=0.43$), despite a thick layer of cells covering the whole flask. QPCR analysis was carried out at day 50 in the three conditions. There was a significant difference in Tyrosinase and Pmel17 expression at day 50 between differentiation conditions (One way ANOVA, $F(2,6)= 26.5$, $p<0.01$, $F(2,6)= 33.7$, $p<0.01$ respectively) with the co-culture method resulting in significantly greater expression than in Matrigel only ($p<0.01$, student's paired t-test) and Matrigel + CM ($p<0.01$). There were no significant differences in gene expression between Matrigel only and Matrigel + CM in either Tyrosinase or Pmel17 expression.

Pigmented foci emerging in Matrigel + CM had a similar appearance to those seen in MEFs co-culture at day 50 (fig 3.19 C). The foci were manually extracted and expanded on Matrigel where they formed monolayers of pigmented cells with typical RPE morphology. The pigmented cells were immunopositive for RPE markers Bestrophin and CRALBP (Fig 3.19 D).

These results back up the findings in early differentiation and time course experiments. Although differentiation in the absence of MEFs or CM leads to rapid neuroectodermal conversion, it is not conducive to the production of high RPE yields. Very few RPE foci were generated in the Matrigel + CM condition relative to MEFs co-culture suggesting that additional growth factors or small molecules will be required to induce high yielding RPE differentiation in feeder-free shef3 culture.

3.4.5 The effect of feeder-free differentiation on Shef6 RPE yields

In contrast to Shef3, differentiation in feeder-free conditions appeared to improve neuroectodermal conversion rates in Shef6, as evidenced by the significantly larger upregulation in Pax6 expression at day 15 in feeder-free conditions (Fig 3.16).

The same conditions tested in Shef3 were tested in long term HESC-RPE Shef6 differentiation experiments; cells were seeded into standard MEFs co-culture or onto Matrigel in HESC media or CM. In addition, the commercially available defined media, mTeSR1, was tested in combination with Matrigel. Colonies were observed at day 2 and day 8. At day 2, HESC-like colonies were present in all conditions (Fig 3.20 A) although the colonies were larger and more compacted in the MEFs co-culture and Matrigel +mTeSR1 conditions. Similar to the observations in Shef3, Shef6 colonies grew into undifferentiated monolayers with compacted, HESC-like morphology by day 8 in all conditions, with the exception of the Matrigel only condition in which differentiating colonies were abundant. Cell proliferation rates were measured in the mTeSR1 vs. CM condition over 8 days in culture (Fig. 3.20 B). Two way ANOVA revealed statistically significant differences in cell numbers over time between cells grown in mTeSR1 and CM; there was a significant effect of the media on cell numbers ($F(1,18) = 17.1$, $p<0.01$), and time ($F(2,18) = 203.5$, $p<0.01$) and a significant interaction ($F(2,18) = 47.7$, $p<0.01$) indicating an increasing effect of the media on cell numbers over time. After the first 3 days, cell numbers were significantly higher in wells fed with MEFs-CM (student's paired t-test $N=4$ $p<0.01$) perhaps reflecting the greater similarity between MEFs co-culture and MEFs-CM and a required period of adaption of cells to the new mTeSR1 media. By day 8, however, cell numbers in mTESR1 fed cells were significantly higher ($p<0.01$, paired student's t-test) which could be a result of the very high bFGF concentration in mTeSR1 (100ng/ml) (Ludwig et al., 2006).

The impact of feeder-free differentiation on Shef6 RPE yields was determined by measuring the number of pigmented foci following 50 days of differentiation in the four conditions (Fig. 3.21). Feeder-free differentiation on Matrigel substantially enhanced RPE yields in Shef6 ($N=2$ passage numbers 42, 54). The greatest RPE

yield was observed when cells were expanded in mTeSR1 media (N=2, Average Foci/cm^2= 15.9 ± 1.1) followed by CM (Average 13.0 ± 6.1 Foci/cm^2), then MEFs co-culture (Average =7.6 ± 2.9 Foci/cm^2). In line with this finding, the normalised, relative expression of RPE genes Pmel17 and Tyrosinase was greatest in the Matrigel + mTeSR1 condition followed by Matrigel + CM, MEFs co-culture and the lowest relative expression in the Matrigel + HESC media condition.

In addition to the differences in RPE foci abundance, we observed differences in the thickness of the cell sheet at day 50 when cells were expanded in the different conditions. Shef6 that were expanded in CM formed a patchy cell sheet at day 50 (Fig 3.22 A) and large areas with sparse cell coverage were visible (Fig 3.22 B,C). Most of the thickened areas, however, contained an abundance of pigmented RPE cells, including large epithelial monolayers in addition to the usual discrete foci (Fig 3.22 D,E). In contrast, cells that were expanded in mTeSR1 had formed thick, opaque sheets at day 50 which were dotted with small but abundant RPE foci (Fig. 3.22 F-H).

Whilst mTESR1 media facilitates rapid growth and undifferentiated maintenance of HESC, it does not contain an identical growth factor compliment to MEFs or CM. MTeSR1 derived pigmented foci were isolated and expanded in RPE medium. The expanding foci displayed typical RPE morphology and were immunopositive for RPE markers CRALBP, Bestrophin and MitF (Fig 3.23) thus confirming the RPE identity of these mTeSR1 derived pigmented cells.

These results back up the findings in early differentiation experiments; Shef6 cells also require an expansion step in CM or mTESR1 and will not generate RPE foci on Matrigel alone. In contrast to Shef3, Shef6 undergo enhanced neuroectodermal conversion in feeder-free conditions relative to MEFs co-culture leading to high RPE foci yields. Both Shef6 and Shef3 have reduced cell sheet thickness and coverage in Matrigel+CM relative to MEFs co-culture, but an expansion step in defined mTeSR1 media increases cell sheet coverage as well as RPE Foci yields.

3.5 Discussion

Continuous adherent differentiation of HESC in MEFs co-culture is one of the most commonly used methods for deriving HESC-RPE; this method continues to produce high pigmented cell yields from a wide range of cell lines (Klimanskaya et al., 2004, Vugler et al., 2008, Buchholz et al., 2009, Carr et al., 2009b, Laio et al., 2010, Clarke et al., 2012). It has been repeatedly shown that pigmented cells derived using this method are akin to native RPE with appropriate morphological characteristics, protein and RNA expression profiles and functional properties (Klimanskaya et al., 2004, Vugler et al., 2008, Buchholz et al., 2009, Carr et al., 2009b, Laio et al., 2010, Clarke et al., 2012). In this chapter we have demonstrated for the first time the derivation of pigmented RPE cells from two new cell lines, Shef6 and Shef3, which expand to form pigmented, 'cobblestone' monolayers of cells expressing a range of typical RPE markers.

Early spontaneous differentiation followed a similar course in the two cells lines; differentiating colonies were found in increasing abundance as the cultures grew over-confluent with differentiating cells first detectable in the centres of large colonies. By day 20 the edges of colonies had formed multi-layered ridges in which Pax6/Otx2 positive neural rosettes formed. The spontaneous emergence of Pax6/Otx2 positive neural rosettes has been described in other cell lines (Pankratz et al., 2007, Chambers et al., 2009, Hu et al., 2010a) and is consistent with the default neural model of human embryonic stem cell differentiation, wherein HESC derived neuroectodermal cells adopt anterior neuroepithelial characteristics in the absence of exogenous signalling (Pankratz et al., 2007, Elkabetz et al., 2008). The RPE is the first differentiated cell type to emerge during development of the human eye and pigmentation is first detected between post ovulatory weeks 5-6 (O'Rahilly, R., 1975). HESC lines are derived from blastocysts at day 5-7; the emergence of pigmented cells in our cultures between days 25 and 32 post seeding, therefore, is a little faster than the timing of RPE emergence in vivo (Meyer et al., 2009) given the 10 day expansion step prior to bFGF withdrawal. It is difficult to assign a specific start point to the differentiation in this protocol, however; the loss of Oct4 expression

was seen during the 10 day expansion step but was asynchronous amongst colonies (Fig 3.6). Our observations are at the shorter end of the range of times described by others using similar protocols; for example, the emergence of pigmented foci has been observed at 17-30 days post seeding (Vugler et al., 2008, Carr et al,. 2009b), and at 35-60 days (Klimanskaya et al., 2004, Lund et al., 2006). Consistency is evidently a problem when generating HESC-RPE by this method. Very careful maintenance of the HESC starter culture and selectively passaging only equally sized colonies with undifferentiated morphology greatly improved reproducibility in our experiments and allowed us to gather meaningful data on the effects of external factors on differentiation yields. Where possible, we tried to keep passage number ranges small within each experiment. Nevertheless, 50 days is a long time in cell culture and we found contamination of the cultures to be a continual problem. GMP accredited clean room facilities and the automation of cell feeding procedures would greatly reduce these risks.

In designing a manufacturing process for a biological product an important consideration is the optimal time for harvesting the product; harvesting the product too early can mean significant losses in potential yield, harvesting too late wastes time and resources as well as incurring unnecessary risks of contamination or other sources of damage to the product (Placzek et al., 2009). In the case of RPE differentiation, the pigmented phenotype lends itself to non-destructive 'on-line' monitoring of emerging RPE by image analysis enabling determination of differentiation rates and thus the optimal time to harvest the RPE product. Determination of the differentiation rates of other morphologically distinct cell types, such as neurons, have been attempted using complex image recognition software and time lapse microscopy systems set up inside incubators (Lappalainen et al., 2010); or, in the case of cardiomyocyte differentiation, by manual counting of visibly contracting areas (Passier et al., 2005). In our case, regular imaging of whole flasks using the scanning device described in chapter 2, followed by automated image processing was a robust, inexpensive and time efficient way to establish HESC-RPE differentiation rates.

We found that the two cell lines used have significantly different RPE differentiation rates. In Shef3, RPE Foci numbers did not increase significantly past day 50.

Continuing to culture Shef3 beyond this time would use up resources without increasing the RPE yield. Shef6 cultures commenced rapid differentiation up to 10 days later, however, and the rate of RPE accumulation was still high up to day 58. Harvesting pigmented foci at the same time in both cell lines would clearly be inappropriate. Our results demonstrate the value of determining differentiation rates for each cell line and incorporating this into the design of manufacturing processes for any HESC derived cell therapy product. Although early clinical studies using HESC derived RPE make use of only one cell line (Schwartz et al., 2012), the advent of IPSC technology and the prospect of generating HLA matched cell therapies is predicted to demand the use of multiple cell lines (Carpenter et al., 2009).

Differentiation-rate analysis in more HESC lines will be required to establish whether the disparity between Shef6 and Shef3 RPE accumulation rates are typical among cell lines or whether one is more typical than the other. We were able find evidence of only one other analysis of RPE differentiation rates in the literature, carried out in the H9 cell line (Rowland et al. 2010). In this study, a steady increase in foci numbers was observed from day 28, reaching up to 4 foci per cm^2 at day 51. The average rate of accumulation was 0.15 foci/cm2/day (days 30-50 post seeding). In our system Shef6 had an RPE accumulation rate of 0.53 ± 0.03 foci/cm^2/day and Shef3 0.27 ± 0.02 foci/cm^2/day (days 30-50 post seeding). Unfortunately, this study did not record the differentiation rate past day 50 so it is unclear if this rate was maintained up to day 60 (as in Shef6), or declined (as observed in Shef3). We were able to monitor differentiation up to day 84 in Shef3; in Shef6 flasks, however, the cell sheet tended to become increasingly fragile over time and frequently began to peel off the culture plastic surface such that measurements could only be taken up to day 58. Cell sheet peeling is a drawback of the continuous adherent method for RPE differentiation; GMP compliant measures to tackle this problem (e.g. tethering the cell sheet) have yet to be described and would be a helpful development in RPE manufacturing methods.

The observation that pigmented cells appeared earlier in Shef3 may reflect a more rapid departure from pluripotency in Shef3. Throughout continuous culture we noted that spontaneous differentiation during routine maintenance was more common in Shef3. It was also observed that the HESC growth rates were significantly lower in

Shef3 (Fig 3.16 B). The higher RPE foci yields that were consistently observed in Shef6, as well as the higher Pax6 expression following EB differentiation, indicate a greater innate preference for neuroectoderm differentiation, as has been described in other cell lines (Osafune et al., 2008). However, the contribution of cell growth rates and spontaneous differentiation rates may be of equal importance in determining differentiated cell yields (Tavakoli et al., 2009).

One of the important advantages of using HESC as a starting material for cell therapies is that the cells can undergo considerable expansion in culture without compromising their pluripotency (Thomson et al., 1998, Reubinoff et al., 2000). In spite of this a number of groups have reported changes in cell behaviour over time in culture (Draper et al., 2004, Enver et al., 2005, Baker et al., 2007). We sought to determine the effect of prolonged culture on HESC-RPE differentiation yields. We observed a significant reduction in RPE yield with increasing passage number. Previously reported differences between high and low passage cells include enhanced growth rates, improved single cell cloning efficiency and a reduction in apoptosis, changes which are attributed to the selective pressures imposed by serial passaging (Enver et al., 2005, Herszfeld et al., 2006). It has also been suggested that culture adapted cells will become increasingly differentiation resistant (Baker et al., 2007) though this has not previously been systematically investigated. Our observation of the gradual decline in RPE yield over time in cultures is, therefore, a novel and important insight into the behaviour of differentiating HESC. A significant reduction in process efficiency with time will be an important consideration in the design of a HESC-RPE manufacturing process. These data indicate that, ideally, only cells from the low passage numbers should be used in HESC-RPE manufacture using the spontaneous differentiation method.

The image analysis methods applied here allows us to determine relative HESC-RPE conversion rates; the absolute number of RPE cells yielded however, will depend entirely on the ability of the operator to mechanically isolate individual foci and the proliferative capacity of individual foci. The mechanical isolation step is critical as non-RPE contaminating cell types could compromise both the safety and efficacy of a cell therapy for AMD. We detected up to 300 individual pigmented foci emerging from a typical low passage Shef6 flask; manual isolation of this many foci is clearly

impractical. This part of the process could also benefit from automation. One promising technology for this purpose is laser-assisted micro dissection and pressure catapulting (LMPC) (Terstegge et al., 2009); this method uses a laser to cut tiny areas of adherent cells and pressure to propel the cut out areas into solution. Another solution may come from a carefully optimised enzymatic dissociation step as has been developed for the isolation of neural rosettes from differentiating HESC cultures (StemDiff™ Neural Rosette Selection (STEMCELL technologies)).

We observed that the rate at which the RPE monolayer expanded from individual foci was highly variable; after a month in culture, pigmented cells filled the whole 4x field of view around some foci, and only half the area in other cases. It would be interesting to determine if the proliferative capacity of individual foci is related to their size or the time at which they first emerge in culture. Since the pigmented foci appear at different time points over a time span of one to two weeks, it is reasonable to assume that the isolated foci have a range of developmental maturity which has been shown to be a function of time in culture and expansion status (Zhu et al., 2013). It has been widely noted that HESC derived RPE have limited proliferative capacity, necessitating their repeated derivation from undifferentiated cells; loss of RPE phenotype has been reported to occur after 3-5 passages with cells losing pigmentation and acquiring a fibroblastic character (Vugler et al.. 2008, Buchholz et al., 2009, Kokkinaki et al., 2011).

Despite variation in proliferation from the adherent foci, pigmented cells derived from our cultures consistently displayed typical RPE morphology and were positive for RPE markers including MitF, CRALBP, Bestrophin, ZO1, Otx2 and Pax6. Pax6 expression in the RPE diminishes over time in vivo (Martinez-Morales et al., 2004) and thus Pax6 expression in our cultures indicates a relatively immature phenotype. This is consistent with observations by others that HESC-RPE has an expression profile similar to foetal RPE (Lu et al., 2009, Liao et al., 2010). The expansion capacity of HESC-RPE will be an important parameter in the design of a manufacturing process and more research is required in this area.

Feeder-free Differentiation:

MEFs 'feeders' are utilised in a clinically approved protocol for the manufacture of HESC-RPE for the treatment of macular degeneration (Schwartz et al., 2012). The use of MEFs entails a number of processing challenges and regulatory complications however including batch to batch variability and xenogeneic contamination. We sought to derive RPE from Shef6 and Shef3 in feeder-free continuous adherent conditions and to asses the impact on relative RPE yields.

It has been proposed that the specific growth factors secreted by MEFs are particularly conducive to RPE differentiation (Vugler et al., 2008). MEFS secrete TGFβ superfamily members including activin A (Hongisto et al, 2012), which enhances MitF expression and pigmentation in vivo (Fuhrmann et al., 2000). They also secrete proteins involved in IGF, BMP and Wnt signalling (Gerber et al., 2007, Bendall et al., 2009) pathways that are involved in the embryonic development and maintenance of RPE (Martinez-Morales et al., 2004). Since the work presented here was carried out, three other groups have reported successful feeder-free HESC-RPE derivation using the continuous adherent method (Zahabi et al. 2012, Rowland et al. 2012, Sridhar et al., 2013) and several have derived HESC-RPE via an EB based protocols that do not require feeder cells (Nistor et al., 2010, Vaajassari et al., 2011, Meyer et al., 2011, Kokkinaki et al., 2011, Nakano et al., 2012, Mellough et al. 2012, Hongisto et al., 2012). In these studies, the feeder-free derived isolated RPE product has proven indistinguishable from those derived in MEFs co-cultures. In this study, we demonstrate that feeder-free differentiation has a significant impact on RPE yield. We found that Shef3 differentiation benefited significantly from the use of MEFs, whereas Shef6 cells were able to produce high RPE yields on Matrigel following expansion in CM or mTeSR1. It remains unclear whether these differences in the responses of the two cell lines are due to the effect of MEFs on growth/survival or specific mechanisms to do with eye field specification. Apart from this study, there has been only one recently published account directly comparing pluripotent stem cells-RPE differentiation efficiency in MEFs co-culture to feeder-free culture (Rowlands et al. 2012). In this study it was found that H9 cells generated ~50% fewer pigmented foci/cm^2 on Matrigel relative to hs27 human feeders. Interestingly in the IPSC line iPS (IMR90)-3, the Pigmented cell yield at was significantly higher

in feeder-free conditions (Matrigel) than in MEFs, similar to our findings in Shef3 and Shef6 respectively.

In spite of the apparently favourable RPE-inducing properties of MEFs, their use in the manufacture of a cell therapy has some obvious disadvantages. Only early passage MEFS seem to be conducive to HESC maintenance, necessitating the repeated extraction and establishment of new MEF cell cultures and introducing significant batch to batch variability (Chin et al., 2007. Akopian et al., 2010). Variability between feeder batches has been shown to cause significant differences in their ability to support HESC growth and in the extent and range of HESC differentiation in the culture dish (Chin et al., 2007), thereby impeding the standardization of stem cell cultures. Undefined components such as MEFs and serum also interfere with studies on the effects of exogenous agents of stem cell differentiation (Vallier et al., 2009). The use of MEFS also carries an associated risk of animal-related pathogenic contaminations which complicates the regulatory landscape in cell therapies destined for human use (Rao et al., 2008). Alternative animal-free strategies for HESC maintenance include the use of human derived foreskin fibroblasts and so called 'autogenic' feeders derived from HESC lines themselves (Richards et al., 2002, Chen et al., 2009) but these carry many of the same problems as MEFs in terms of standardization and reproducibility of stem cell cultures.

A number of feeder-free media formulations for HESC maintenance have been developed but with limited success. MEFs conditioned media (CM) in combination with Matrigel has proven to be a robust method for feeder cell free HESC maintenance (Xu et al., 2001). CM can be manufactured in large quantities, batch tested and stored, but it is only a partial solution to the problems described above. A number of defined feeder-free media formulations have also been developed in recent years. The most prominent of these were comprehensively tested by 4 laboratories in over 10 cell lines as part of the international stem cell initiative (Akopian et al.. 2010). The conclusion of this extensive study was that only two, commercially developed medias, mTeSR1 and STEMPRO are up to the task of robust HESC maintenance comparable to MEFs-CM or MEFs co-culture. At the time of conducting these experiments mTeSR1 in combination with growth factor

reduced Matrigel was the most widely published feeder-free method. MTeSR1 contains high concentrations of the growth factors FGF and TGFβ which stimulate major anti-differentiation signalling pathways. In addition, it contains lithium chloride, a GABA agonist/non specific WNT antagonist (Ludwig et al., 2006). Matrigel is a basement membrane preparation derived from the Englebreth-Holm-Swarm sarcoma, the major components are Laminin, collagen IV, entactin and heparin sulfate proteoglycan (Product specification sheet, BD biosciences). The Matrigel matrix has proven to be particularly good for pluripotent HESC maintenance as well as RPE differentiation and maintenance (Rowland et al., 2012, Nakano et al., 2012, Zhu et al., 2013).

In this study, we used Pax6 upregulation as a method for determining neuroectoderm conversion rates in Shef6 and Shef3 during early differentiation in feeder-free conditions. Our finding that the most rapid neuroectodermal conversion was achieved in the absence of MEFs or MTeSR1/CM was not surprising, given that MEFs and MteSR1 stimulate key pluripotency signalling networks such as FGF and activin/nodal/TGFβ (Beattie et al., 2005, Vallier et al., 2005, Greber et al. 2007, Xu et al., 2008). It was interesting to note that Shef6 EBs had a significantly greater Pax6 upregulation than Shef3 over a range of passages. This suggests that Shef6 has a higher innate propensity for neuroectoderm conversion, which may go some way to explain the larger RPE yields we consistently observed in Shef6. Differences in the propensities of HESC lines to undergo differentiation into particular lineages have been widely noted (Allegrucci et al., 2007, Osafune et al., 2008, Kim et al., 2010, Lappalainen et al., 2010).

Despite the efficient short-term neuroectoderm conversion, we found that Shef6 and Shef3 cells that were plated directly onto Matrigel in the absence of MEFs, CM or mTeSR1 failed to produce RPE foci within 50 days. Temporal gene expression analysis demonstrated a significant down regulation in critical RPE genes from days 20-30 in these cultures. These results suggest that an ‘expansion step’ at the start of the process in the presence of a suitable expansion media (Mefs, CM or mTeSR1) is critical to effective RPE differentiation, in both cell lines.

There are several possible explanations for this. The ratio of RPE foci generated per undifferentiated cell seeded is small, especially in Shef3. In the absence of an expansion medium, there is only a short period of proliferation before cells begin to differentiate, and the colonies do not reach confluence. Several days expansion in a medium such as mTeSR1 or CM prior to growth factor withdrawal may be required to increase the statistical likelihood of consistently generating RPE. A second possibility it that high cell density is a requirement for effective RPE differentiation; others have noted a reduction in neuroectoderm conversion efficiency at low cell density (Chambers et al., 2009). A third possibility is that factors secreted my MEFs and found in mTESR1 specifically prime HESC for RPE differentiation and in their absence the majority of cells differentiate into non-pigmented cell types that do not express Otx2, Mitf, Tyrosinase, or Pax6 past day 30. The finding by others that pigmented RPE form in floating Embryoid bodies in the absence of MEFs, CM or mTeSR1 (Idelson et al., 2009, Meyer et al., 2011) suggests that these media are not intrinsically critical. Nevertheless, the majority of these EB based protocols add supplements and growth factors to stimulate neural/retinal differentiation which is suggestive of poor yields in their absence (Osakada et al., 2009, Nistor et al., 2010, Nakano et al., 2012, Zhu et al., 2013- see table 1.1).

In this study we demonstrate the derivation of HESC-RPE from Shef3 and Shef6 in feeder cell free conditions. Perhaps surprisingly, we observed different responses in the two cell lines to feeder-free differentiation. Shef6 responded to feeder-free conditions by significantly increasing relative Pax6 upregulation and producing enhanced RPE foci yields relative to MEFs co-culture, whereas Shef3 had significantly reduced Pax6 expression and RPE foci yields in the same conditions. Evidently MEF feeders supply Shef3 with growth factors that encourage neuroectodermal and RPE differentiation but are absent in CM/mTeSR1, alternatively a component of Matrigel inhibits RPE differentiation in Shef3. Shef3 had a significantly slower growth rate in Matrigel+mTeSR1 than Shef6, perhaps the Shef3 cultures did not reach sufficiently high densities by the time differentiation was initiated. It has been well documented that significant differences in growth rates exist between HESC lines (Cowan et al., 2004, Tavakoli et al., 2009), in addition genotypic and epigenetic differences between cell lines affect their endogenous expression of FGFs, Nodal, BMPs as well as expression of FGF/ TGFβ

receptors and cell attachment proteins (Akopian et al., 2010). These differences affect the relative ability of different cell lines to proliferate and remain undifferentiated. Our results suggest that the differing growth factor requirements of the two cell lines not only determine their ability to grow and differentiate but also critically impact their capacity to produce RPE in feeder-free conditions.

2.6 Conclusion

Here we describe in detail the generation of HESC-RPE in continuous adherent MEFs co-culture in two new cell lines Shef6 and Shef3. In both cell lines, RPE foci appeared spontaneously around day 25-32 consistent with the appearance of pigmented cells during embryonic development (O'Rahilly 1975). Although both cell lines underwent a similar sequential expression of markers appropriate to the various developmental stages, the rate at which RPE foci began to accumulate in culture differed significantly. The process of spontaneous differentiation in MEFs co-culture is highly variable due to a number of undefined and uncharacterised components in the differentiation set up. The genetically and epigenetically distinct cell lines contribute further to the unpredictability of RPE cell yields. We describe the use of a simple, efficient, semi-automated method for reproducibly measuring differentiation efficiency. This method enabled us to compare RPE yields confidently over time and revealed a distinctive reduction in differentiated cell yields with increasing passage number in both cell lines: a property of HESC in culture that has been implied but never shown (Barker et al., 2007). In addition, we use this method in combination with gene expression analysis to characterise the responses of the two cell lines to feeder-free culture. We found that commonly used feeder-free methods employing Matrigel +conditioned media/mTeSR1 produced significantly higher RPE yields in Shef6 but were insufficient for differentiation in Shef3. We hypothesise that this result is due to inherent differences in autogenous signalling controlling growth factor responses and growth rates and between the two cell lines. HESC expanded on MEFs are already being used in a clinical study aimed at treating macular degeneration (Schwartz et al., 2012). As the field expands and, as predicted, multiple cell lines are used to create patient specific RPE cell therapies, comprehensive characterisation of parameters such as differentiation rates and analysis of the optimal differentiation methods for each cell line will be essential for cost effective manufacturing.

Chapter 4: Differentiation efficiency: the impact of seeding density and single cell dissociation

4.1. Introduction

From a manufacturing perspective, the ideal RPE differentiation process will generate the largest quantity of RPE with the minimal usage of raw materials, physical lab space, labour and time. The critical raw materials in this process include undifferentiated HESC, expansion and differentiation media, tissue culture plastic and mouse/human feeders or Matrigel.

The HESC seeding density is fundamental in determining raw material usage. Higher density seeding will require an input of more undifferentiated HESC per culture unit (T25 flask) but, assuming HESC-RPE differentiation efficiency remains constant, higher density seeding will require less physical lab space, labour and media per RPE foci generated. Therefore an assessment of the relative costs of generating undifferentiated HESC versus the cost of materials used per flask will be required to determine the most financially efficient conditions. In addition it will be necessary to determine what impact, if any, HESC seeding density has on the HESC-RPE conversion rate (differentiation efficiency). Seeding density is a difficult variable to control using standard HESC culturing procedures where HESC colonies are manually cut into clumps of undefined size before seeding. Perhaps as a consequence there have been few studies correlating HESC seeding density with target cell yield or examining the impact of changes in seeding density on differentiation efficiency. There are currently no published studies addressing this issue in HESC-RPE differentiation.

In addition to the impact on raw material usage, there is evidence suggesting that seeding density may govern early cell fate decisions during differentiation protocols; this could be critical to the final RPE product purity. The maintenance of pluripotency in HESC relies on autocrine and paracrine signalling from neighbouring undifferentiated cells (Peerani et al., 2007). The size of cell colonies, their proximity to each other and the overall cell density influences the balance between pluripotency and differentiation as well as cell fate decisions (Chin et al., 2007, Bauwens et al., 2008, Peerani et al., 2007). Bauwens et al. have previously used micro-patterning to establish HESC colonies of defined size and found that larger colonies have higher

Oct4 and Pax6 expression, indicating better conditions for maintenance and an enhanced propensity for neuroectoderm differentiation in larger colonies. Peerani et al. found that higher local cell density had a positive correlation with the expression of pluripotency marker Oct4, and Chin et al. have shown that serial passaging at low cell density increases spontaneous differentiation. This is in part attributed to the active secretion of FGFs, activin A and Noggin by pluripotent HESC. As discussed in chapter 3, these factors play key roles in the maintenance of the pluripotency network and inhibition of differentiation-inducing signals such as BMP. In a study aiming to generate dopaminergic neurons from HESC, it was observed that varying the initial seeding density had a direct impact on the relative proportions of differentiated cells yielded; high plating densities were found to enhance the proportion of cells adopting an anterior neuroepithelial phenotype whereas plating at low density lead to more cells with a neural crest identity when subjected to a multistage directed differentiation (Chambers et al., 2009).

In the HESC-RPE differentiation protocol described by Vugler et al., 2008 (described in chapter 3), differentiation is initiated in part by allowing the cells to become over confluent. Variations in seeding density will also influence the time taken for the monolayer of cells to reach confluence and could thereby affect the rate of differentiation.

Despite the many RPE differentiation protocols devised and published in recent years (Table 1.1), there has been no account of the influence of seeding density on the RPE differentiation process or description of optimum seeding densities for efficient RPE production. Given the importance of this variable in defining raw material usage (and therefore processing costs), as well as its likely impact on lineage decisions, this is an important gap in our understanding of optimum differentiation conditions.

This chapter describes an investigation into the influence of HESC seeding density on RPE differentiation yield in co-culture with MEFs feeders after mechanical passaging and in feeder-free conditions, using single cell dissociation. Experiments are described to test the hypothesis that seeding density has a significant impact on RPE differentiation yield and efficiency. The effects of cell density on pluripotency,

early lineage decisions and eventual RPE yield are examined. A single cell seeding protocol is described which is more amenable to scale up than traditional passaging methods and allows for the establishment of an optimal range of seeding densities that generate the maximal yield per cell seeded and per cm^2.

4.2 Mechanical passaging

4.2.1 Mechanical passaging can lead to uneven colony distribution and variable differentiation rates

Mechanical dissection of HESC colonies with a pipette is the most common method used to passage HESC in order to maintain pluripotency and cell viability (Loring et al., 2007, Watanabe et al., 2007). Dissected HESC colonies (~1000 cells per clump) were transferred to a fresh flask of inactivated MEFs and the flasks were shaken 2-3 times to encourage even distribution of the clumps.

Scanning T25 flasks at day 6 against a dark background enabled visualisation of HESC colonies. It was observed that dissociated clumps would often aggregate, leading to an uneven distribution across the flask surface (fig 4.1 A). This could be partially avoided by seeding at lower density. Immunostaining with Oct4 at day seven showed that HESC in the aggregated clusters appeared to have down-regulated Oct4 relative to those colonies with more space in which to expand; cells in aggregated clusters had also undergone morphological changes (fig 4.1 B). After 50 days of differentiation, pigmented foci were visible. The foci were unevenly distributed in a pattern which mimicked the uneven HESC colony distribution at day 10 (fig 4.2 A). Areas with high HESC colony density produced many RPE foci at day 50 (white circles), whereas areas with low colony density at day 2 had produced no pigmented foci by day 50 (red circles). In these low density areas there was poor cell coverage at day 50 despite visible HESC colonies at day 15 (arrow). This suggests poor cell survival following long-term differentiation in low density areas. Taken together, this demonstrates the necessity for controlled seeding density and even cell distribution in order to synchronise differentiating populations and generate RPE at a consistent and reproducible rate.

4.2.2 HESC colony density and RPE yield

In order to keep a constant seeding density during HESC maintenance the 'split ratio' is often maintained (e.g. one flask is split into two or three at each passage). To determine the impact of different split ratios on RPE yield, undifferentiated Shef6 HESC were mechanically passaged and seeded at three different split ratios: 1 into 4 (low density), 1 into 2 (medium density) and 2 into 1 (high density). The actual number of colonies seeded for each run were counted at day 7 (table 4.1) and the continuous adherent RPE differentiation protocol was carried out for a total of 50 days. The number of pigmented foci in each flask was measured from days 40-50 using the scanning device and auto-count analysis in Image J (see chapter 2, materials and methods). One high density flask was discounted from the analysis due to uneven distribution of HESC colonies following seeding. In all cases the numbers of pigmented foci increased from days 40-50, but there were differences between those seeded at high and low density (Fig. 4.3 B-E).

Two way ANOVA revealed a significant effect of seeding density on pigmented foci number (Fig. 4.3 B). There was a significant effect of time on foci number ($F(3,28) = 49.1$, $P<0.001$) a significant effect of density on foci number ($F(2,28) = 19.4$, $p<0.001$) and a significant interaction ($F(6,28) = 14.1$, $p<0.001$) suggesting that the density effect increased with time in culture. At day 50 the average RPE foci yields were greater in the high seeding density group (mean = 611 ± 106 SEM foci per flask) than in the medium (mean = 234 ± 35) or low density groups (mean = 99 ± 18).

RNA was extracted from the day 50 cultures and QPCR was carried out to determine expression of Tyrosinase and Pmel17, two genes critical to the process of melanin synthesis and RPE differentiation. The expression of Pmel17 and Tyrosinase is shown relative to expression in the low density condition for each of the runs (Fig. 4.4). Expression of both genes correlated with the quantity of visible RPE foci at day 50, with the higher density conditions having the greatest fold increase in Pmel17 and Tyrosinase gene expression.

4.2.3 Differentiation Efficiency per HESC Colony

Having established a relationship between HESC seeding density and RPE yield over time it was next sought to determine which seeding density gave the most efficient differentiation per HESC colony. Split ratio is an arbitrary measurement being entirely dependent on how confluent the starting culture was before splitting – something that may vary over time in culture and between different labs. A more relevant measurement is the number of colonies seeded. To determine this, flasks were scanned against a dark background at day 6 and the number of individual colonies counted using ImageJ software. The variability in number of colonies seeded was particularly large at higher seeding densities (table 4.1).

	Number Of Colonies Seeded		
Flask Split Ratio	1 in 4	1 in 2	2 in 1
Run1 (p44)	302	405	812
Run2 (p45)	322	486	
Run3 (p47)	288	456	701

Table 4.1 Number of colonies at different split ratios over three passages

For each flask, the number of RPE foci per HESC colony seeded was plotted against the number of HESC colonies seeded per T25 flask. Figure 4.5 shows how the efficiency of the differentiation correlated positively with seeding density (R^2 = 0.916). The highest efficiency obtained was 0.88 RPE foci per HESC colony, which was achieved when >800 HESC colonies were seeded per T25 (the highest density tested). The lowest efficiency was 0.24 RPE foci per HESC colony, when 288 colonies were seeded (the lowest seeding density tested) per T25 (Fig. 4.5). In these experiments the same number of MEF feeders/cm^2 were used at all seeding densities and the same volume of culture medium (5ml) was used for daily media changes. Within this range therefore it can be concluded that the higher the seeding density, the more efficient the differentiation, in terms of all raw material usage.

Given the above trend, higher seeding densities (4 in 1) were tested. However, peeling off of the cell sheet prior to the beginning of pigmentation was repeatedly observed at these higher densities (N=3). Variations in the culture system used were therefore examined. A feeder-free differentiation system using a coating of Matrigel, as a substrate instead of MEFs feeders and gelatine was evaluated for its ability to support greater HESC adherence at higher seeding densities.

4.3 Single cell dissociation and feeder-free differentiation

In terms of reproducibility, enzymatic dissociation of colonies into single cells before seeding may afford several advantages. Firstly, single cell dissociation and cell counting allows for tight control of seeding density and improved reproducibility between experiments. Secondly, single cells are less prone to aggregation, and thirdly, each cell is exposed to a more homogeneous environment, as there are no longer distinct populations of cells in the centre, as opposed to at the edges, of colonies (Ellerstrom et al., 2007). With this in mind, HESC-RPE differentiation following single cell dissociation was attempted.

Colonies with obvious differentiation were removed under the dissecting microscope prior to treating whole flasks with TrypLE select enzyme (Invitrogen). Cells in suspension were counted before seeding at defined concentrations onto Matrigel (BD Biosciences). Cells were then expanded for 5 days in MEF-conditioned medium (CM) or mTeSR1 defined medium before undergoing 45 days of differentiation in –bFGF differentiation media.

In order to operate at a similar range of densities to the previous, mechanical passaging experiments, a calibration curve was created to assess the approximate cell numbers in flasks containing HESC clumps of undefined size. This curve relates the number of cells to measurements of % confluence at day 6 (see Chapter 2, Materials and Methods section 2.6.5). From this graph we extrapolated the seeding densities at day 0 and determined that the range was between 9,000 and 29,000 HESC/cm^2 (See materials and methods section 2.6.5). The results from section 4.2 showed the efficiency of the differentiation improving with increasing cell density, but cell sheet peeling interfered with experiments at higher densities. Thus the next sets of experiments were carried out to test a range incorporating higher seeding densities - from 8,500 cells/cm^2 (8.5K) up to 100,000 cells/cm^2 (100K).

4.3.1 Early differentiation following single cell seeding over a range of densities

Single cell seeding allows accurate repetition of the same density between experiments at different passage numbers. Cells were seeded at densities up to 100K/cm^2 and down to 8.5K/cm^2. In the 8.5K/cm^2 condition, cells often did not survive following single cell dissociation; at all other densities cells survived the dissociation process and proliferated in the absence of ROCK inhibitor up to day 15(Fig. 4.6A). At day 15, differences in the architecture of the differentiating cells were visible; thick and compact multilayered ridges forming around 'holes' of less compact cells were visible in the 50-100K conditions. These thick ridges did not form to the same extent in 17-25k plating density conditions (Fig 4.6 A, lower panel). Immunocytochemistry revealed that these thickened ridges contained Pax6 positive cells (Fig. 4.6 B).

QPCR was carried at day 15 on cells seeded over this range of densities (Fig. 4.6 C). Within each set, there was a slight increase in the relative expression of Pax6 at high density peaking at a 2.3 fold increase at 100,000/cm^2. One way ANOVA revealed significant differences in Pax6 expression with density ($F(3,8)=4.5$, $p<0.05$). Specifically Pax6 expression was significantly higher is the 100K/cm^2 than the 25K/cm^2 condition (paired student's t-test, $p<0.05$).

4.3.2 Time course of gene expression reveals the impact of seeding density on the timing of early differentiation.

Following mechanical passaging, it was observed that seeding density affected the rate of RPE differentiation and that the highest seeding density condition differentiated the most rapidly, producing the greatest RPE yield. It was also noticed that areas of the flask with high colony density showed a down-regulation of Oct4 protein relative to low density areas (Fig 4.1B). In order to measure the progress of early differentiation in feeder-free differentiation QPCR was carried out at five time points following seeding at three different densities 50,000/cm^2, 25,000/cm^2 and 17,000/cm^2 (50K, 25K and 17K). The rate of departure from pluripotency was determined by measuring Oct4 mRNA, and the rate of early eye field formation was determined by measuring Rx mRNA.

Cells were expanded for five days in conditioned medium (CM) before switching to –bFGF differentiation medium to initiate differentiation. By day ten (5 days differentiation), Oct4 expression was down regulated relative to the expression at day 0. The extent of this down-regulation was similar in the 50k (0.14 fold) and 25K (0.10 fold) condition but was less pronounced in the low density condition (0.55 fold). From days 15-25, Oct4 expression remained higher in the low density condition, suggesting that high seeding density is required for effective Oct4 down-regulation during differentiation (Fig. 4.7 A).

Rx expression had distinctive peak in both the 25K and 50K condition. In the 25K condition, expression peaked at day 10 (26 fold increase); interestingly in the 50K condition this peak occurred later, at day 15 (26 fold increase), and appeared to be increasing again at day 35 (16 fold). This suggests that cells are entering the eye field stage of differentiation earlier in the 25K condition than in the 50K condition (Fig. 4.7 B).

4.3.3 Seeding density determines pigmentation rate in feeder-free differentiation following single cell dissociation.

Shef6 cells from a range of passages were seeded onto Matrigel-coated plates at a range of seeding densities from 17,000/cm^2 and 100,000/cm^2. Media was changed daily for 5 days using either conditioned medium (CM) (Fig. 4.9 A,B) or mTeSR1 (Fig 4.10 A,B,C,D) and then for the remaining 45 days in standard –bFGF differentiation medium.

4.3.3.1 Conditioned Media (CM)Expansion

Two long-term differentiation experiments were carried out using cells expanded in CM as this media gave the highest yield in previous experiments in Shef6 (chapter 3). In the first run (passage number 60 Fig. 4.9 A), such a large proportion of the surface area became pigmented by day 50 that it was not possible to measure the number of individual foci. At the 17k density pigment appeared in discrete foci, but at higher density large non-discrete areas of pigmenting cells emerged that increased in intensity over time (Fig 4.8). In order to compare RPE yield across the different conditions, therefore, the % pigmented areas, as opposed to the number of foci, were measured. Both the large non-discrete pigmented areas and the small discrete foci stained positively for Otx2 (Fig. 4.8). In this first run, pigmented foci were clearly visible by days 33-35 in the 17-35K conditions (fig 4.9 A), but absent in 50,70 and 100K wells.

Similarly in the second run (passage number 68), pigmentation had begun in 17,25,35 and 50K but was not visible in the 70 and 100k wells from days 33-35 (fig 4.9 B). By days 40-50, the 70K and 100k wells had also begun to pigment but had not reached the same yield in terms of % surface area as the 25 and 35K wells. Peeling and lifting off of the cell sheet had occurred by day 40 in one of the heavily pigmented 25K wells (arrow); this may have affected the measurement in run 1, as

contraction of the cell sheet could increase the pigment intensity in portion that is still attached. Over the range of seeding densities tested 25-35K appeared to be the optimum in both runs following expansion in CM, peaking at 51-62% pigmentation in the first run (passage 60, Fig 4.9 A) and peaking at 4-6% in the second run (passage 68, Fig. 4.9 B).

Cells were harvested at day 50 for QPCR analysis of gene expression. The expression of RPE genes Bestrophin, CRALBP, MitF and PMel17 varied with seeding density in a pattern that mirrored the % pigmentation data (Fig. 4.9A). The expression of these genes peaked at day 25-35K/cm^2 before levelling off at 50-70K/cm^2 and decreasing from 70-100K/cm^2. Expression of the pigment synthesis gene tyrosinase decreased slightly with increasing seeding density. Expression of transcription factor Otx2 likewise decreased slightly down to 0.2 fold at 100K/cm^2 (fig 4.9C).

4.3.3.2 MTeSR1 Expansion

Expansion in conditioned media on Matrigel appeared to be conducive to good RPE yields in shef6 (as described in chapter 3). However there was high variability between the two runs, peaking at 62% in the first run, and only 6% in the second run. This may be partly attributed to the variability in MEF feeders. In an effort to combat this variability the same experiment was carried out using mTeSR1 defined media (Stem Cell Technologies, Vancouver, Canada) for the five day expansion step.

Four further long-term differentiation experiments were carried out using cells expanded in mTeSR1. Peeling of the cell sheet was more common in this system This may be due to the extra stress incurred by changing to/from mTeSR1 medium or the higher growth rates seen in mTeSR1 leading to unsustainable cell densities.. This lead to the loss of several wells over the 50 days time period. In the first run (passage 50, Fig. 4.10 A), cells in the 25-35K wells (the optimum density in the previous CM experiments) did not survive the 50 days differentiation period but cells in the 17, 50, 70 and 100K/cm^2 wells survived and the peak pigmentation (9%) was seen in the 50K/cm^2 condition. Similar to the results in the previous CM experiments, pigmentation was notably reduced in the high density (70-100K/cm^2) wells. In the second run (passage 51, Fig. 4.10 B) wells at 17,25,35 and 50K/cm^2 survived the 50 days. In contrast to the conditioned medium experiments, the peak pigmentation was seen not at 25-35K/cm^2 but at 50K/cm^2 where it reached 2.9%. In the third run (passage 52, Fig. 4.10 C), the pattern at day 35 was similar, with pigmented foci visible in the 17 and 50K/cm^2 cultures and none yet detectable in the 70-100K/cm^2 cultures. Unfortunately contamination prevented measurement at day 50 in the 70-100K/cm^2. In the fourth run (passage 68, Fig 4.10 D) all wells survived but severe peeling prohibited accurate measurement at day 50. However at day 35, peak pigmentation levels were seen between 35 and 50K/cm^2 consistent with the previous runs.

Cells from the first run following mTeSR1 expansion (passage 50, Fig 4.10 A) were harvested at day 50 for QPCR analysis of gene expression. The expression of RPE genes Bestrophin, CRALBP, MitF and Pmel17 also mirrored the % pigmentation pattern seen in Fig 4.10 A with relative expression peaking at 50K before decreasing

from 70–100K. Otx2 expression peaked at a higher density of 70K and, as before, there were little density related changes in Tyrosinase expression.

The results of the above six feeder-free single cell dissociation experiments are summarised in Figure 4.11. The fold changes in pigmentation relative to the lowest density condition (17K/cm2) were calculated for each of the 6 experimental runs. For runs where peeling or contamination prevented measurement at day 50, day 35 measurements were used to calculate fold changes. One way ANOVA revealed that pigmentation levels varied significantly with seeding density ($F(4,17) = 3.0$, $p<0.05$). The overall average peak fold increase was observed at $35K/cm^2$, where % pigmentation was on average 5.6 x higher than at 17K, and on average 6.4 x higher than at $100K/cm^2$. Post Hoc analysis revealed a statistically significant difference between the 35 and $100K/cm^2$ conditions ($p<0.05$ student's, unpaired t-test).

4.3.4 Differentiation efficiency per HESC.

As in section 2.1.3, the data were normalised to the number of cells seeded in order to determine the differentiation efficiency at each seeding density. The % pigmentation data were converted to mm^2 and divided by the number of HESC seeded. Despite the significant variation in yields between runs, within each run the maximum efficiencies were achieved at seeding densities between 17 and 35,000 cells per cm^2 (Fig. 4.12) after which the overall efficiency declined in all runs . The maximum efficiency was observed in the first conditioned media expansion run (passage 68, Fig, 4.9 A) at a seeding density of $25K/cm^2$ and was 2.0 mm^2 pigmented RPE per 1000 HESC seeded.

4.4 Discussion

The data presented in this chapter show unequivocally that seeding density has a significant impact on the rate of RPE differentiation as determined by gene expression and pigmentation data recorded over a ten to fifteen day period in both MEFs feeder, mechanically passaged systems and feeder-cell free enzymatically passaged systems. By comparing the RPE yields at various densities we were able to determine HESC-RPE conversion efficiencies, a previously unreported parameter that is fundamental to bioprocess engineering. In addition we found there to be an optimal range of HESC seeding densities out with which RPE yield is notably compromised.

In the cells passaged by mechanical dissection, within the range tested, higher plating density led to improved differentiation efficiency per HESC colony. This may be due to seeding density governing the rate at which cells reach confluence, exit pluripotency and begin differentiation (i.e. timing), or to do with impact of seeding density on lineage decisions during early differentiation, or both.

During early differentiation, seeding density is likely to have a strong affect on pluripotency, and potentially in priming the cells for a particular differentiation trajectory. Previous studies in HESC have found that higher densities favour differentiation towards neuroectoderm and anterior neuroepithelial fate (Bauwens et al., 2008, Chambers et al., 2009) and are therefore likely to be favourable for RPE differentiation. Another potentially important factor is the effect of seeding density of nutrient depletion. As the cells become more confluent, the availability of nutrients and oxygen may become limiting to cell growth. Where differentiations are carried out in wells or flasks of a defined size and media exchange is carried out every 24 hours, the recommended maximum volume of culture medium per culture vessel puts an upper limit on the availability of nutrients during this period, which will be more or less severe dependent on cell density (King et al., 2007). Nutrient and depravation could drive cells to exit pluripotency and begin differentiating. HESC colonies seeded at higher density may also receive a lower dose per colony of

anti-differentiation molecules emanating from the MEF feeders (Heng et al., 2004) since the same number of MEFs were seeded per flask regardless of colony numbers.

In our system, where there is little extraneous chemical stimulation to initiate differentiation (except for the removal of supplementary FGF from the medium), seeding density will also determine the dosage of anti-differentiation signalling emanating from surrounding undifferentiated HESC, with cells in a higher density environment receiving a higher dose (Peerani et al., 2007). Nutrient depletion may also limit the proliferation of the desired progenitor cells and cause considerable loss of viability (King et al., 2007). Thus there is a case for seeding at both high and low density in terms of inducing rapid, and efficient HESC-RPE differentiation.

In our system, it would appear that nutrient depletion, in addition to spatial restrictions that occur as the cells become confluent, are important driving forces causing cells to exit from pluripotency. This, together with the undefined neuroectoderm-favouring properties of high plating densities, could explain the increased rate at which pigmented foci begin appearing in our system and the enhanced overall RPE yield.

From a manufacturing perspective, a high density seeding strategy is advantageous as the same number of RPE foci can be derived using less medium, less space and less labour. In addition our results in section 4.3 show that the 'efficiency' of the differentiation (per HESC colony) improves with increased cell plating density, with the highest efficiency (0.88 foci/HESC colony) seen at the highest density tested. Thus in addition to the savings in space and raw materials, this strategy reduces the number of HESC required to generate a given amount of RPE. An upper limit to this trend was not reached in these first experiments; however an increased incidence of peeling of the cell sheet was noted at very high density (4 into 1 split ratio). As discussed in Chapter 3, cell sheet peeling can be deleterious to differentiation yields; when cells lift off the surface as one contiguous sheet a tight ball of aggregated cells can form, the interior of which is likely exposed to an environment of sub-optimal oxygen and nutrient transfer. Disturbing the cell sheet with the pipette tip, excessive movement of the flask, time out of the incubator and prolonged culturing appear to

increase the incidence of cell peeling. Preliminary results also suggest that very high seeding density increases the incidence of cell sheet peeling in this system.

Mechanical passaging of HESC is a useful method for weeding out cells with differentiated morphology and maintaining undifferentiated cell stocks (Loring et al., 2007). This method incurs a lot of operator variability however, with the size of resulting colonies dependent on individual passaging technique and the determination as to what constitutes 'differentiated morphology' is open to individual interpretation. It is also challenging to count cell numbers and control the seeding density- factors which we have shown to be critical to the yield. Whilst mouse embryonic stem cells can be trypsinised and form colonies at clonal density, human embryonic stem cells are vulnerable to dissociation induced apoptosis (Ohgushi et al., 2010, Watanabe et al., 2007). This has been an obstacle in the development of technologies to manipulate and control HESC behaviour (Hernandez et al., 2011). The propensity for HESC to undergo apoptosis upon dissociation can be partially overcome by the addition of a Rho-associated kinase (ROCK) inhibitor (Watanabe et al., 2007).

We found that the addition of ROCK inhibitor was not necessary when cells were plated at a density of 17,000/cm^2 or above, although cell death was observed at lower densities. It has been suggested that routine passaging by single cell dissociation puts an extra selective pressure on HESC that can lead to a higher rate of acquisition of karyoptypic abnormalities (Brimble et al., 2004, Draper et al., 2004). In these experiments, Shef6 stocks were maintained by mechanical passaging and enzymatically dissociated with TrypLE express (Invitrogen) before the initiation of differentiation only. Shef6 has been proven to remain karyotypically stable in similar conditions for up to 8 passages (Hernandez et al., 2011) thus we deemed it unlikely that they would accumulate significant karyotypic changes during the 2-3 population doublings that occur during the expansion stage. Transferring cells to a feeder-free defined medium (mTeSR1) system appeared to put an additional strain on cells that may have contributed to the high incidence of cell sheet peeling. In MEFs conditioned media however the cell sheet remained largely intact at all the densities

tested. In future experiments, a gradual adaptation from MEFs feeder - feeder-free differentiation systems may be beneficial.

Seeding HESC as single cells allowed us accurately repeat a large range of plating densities, despite this, there was notable variability in RPE differentiation yield between runs even when using defined media. Fold changes within each run however remained consistent and statistically significant; indicating that the optimum density remained despite differences in the yields between batches of HESC. The optimal yield was achieved when cells were seeded at 35K/cm^2 in which wells yielded on average 5.6 times more pigmentation than in the 17K/cm^2 condition and 6.4 times more than in the 100K/cm^2 condition.

As discussed earlier, high seeding density can have both positive and negative influences on HESC-RPE differentiation. As seen in the mechanical passaging experiments, nutrient depletion and accelerated confluence appeared to increase the rate of differentiation with increasing HESC density from 17K up to 35-50K/cm^2. Increasing plating densities above this point however decreased the rate or HESC-RPE differentiation. This led to a reduced yield at day 50, and reduced differentiation efficiency per 1000 cells seeded as well as reduced expression of RPE markers, in spite of the reported increase in neuroectodermal/anterior neuroepithelium conversion rates at high density (Bauwens et al., 2007, Chambers et al., 2009). Notably, previous studies in HESC have not tested such high densities (e.g. Chambers et al., 2009, maximum density 25K/cm^2).

It is interesting to observe the peak in RPE productivity and it's subsequent decline at very high density; as mentioned earlier putting more cells into each culture vessel reduces the space and raw material requirements but only if the same RPE output can be derived per cm^2. At these very high seeding densities, a high dose of paracrine anti-differentiation signalling emanating from surrounding undifferentiated HESC may delay the onset of differentiation (Peerani et al., 2007). Although the time course of gene expression revealed that Oct4 was down-regulated more rapidly at higher density, the peak in Rx, a gene essential for demarcation of the eye field and optic cup was delayed at high density (50K/cm2). Another indication that the onset of differentiation is delayed at high density comes from looking at the morphology of

cells at day 50. Although dark pigment above the detectable threshold was more abundant in discrete foci at 17-35K/cm^2 densities, inspection of the very high density wells (70-100K/cm^2) revealed large contiguous areas of very lightly pigmented cells that were Otx2 positive and reminiscent of immature RPE. This suggests that given more time or chemical stimulation to differentiate that the 70-100K condition would produce high yields of pigmented cells. In primary RPE cultures (Koh et al., 2000) and more recently differentiating HESC (Buchholz et al., 2013), vasoactive intestinal peptide (VIP) has been shown to speed up RPE maturation in culture; and could be used to enhance the yields in these high density cultures.

Despite the numerous recent studies on HESC-RPE differentiation, HESC to RPE conversion efficiencies are rarely reported. Following single cell dissociation we have shown that greatest amount of RPE produced per 1000 HESC cells occurred when cells are seeded at densities between 17 and 35,000 cells /cm^2. Seeding cells at higher density may reduce raw material usage per mm^2 of RPE generated but, as is clear from these results, will reduce differentiation efficiency per HESC cell and increase the time taken to generate RPE product. Thus the design of an RPE manufacturing process should consider the relative costs of the numbers of HESC, space and raw materials required per RPE foci generated and yet not fail to account for the changes in HESC-RPE conversion efficiency that will occur as these parameters are adjusted.

4.5 Conclusion

Seeding density is rarely controlled for in HESC differentiation experiments, probably due in part to the perceived incapacity of the cells to undergo single cell dissociation and clonal propagation (Watanabe et al., 2007). Here we have devised a method to determine the approximate seeding density in traditional clump passaged HESC and shown how the colony seeding density has a significant impact on the HESC-RPE conversion rate. In addition we have demonstrated that single cell dissociation of our cell line, Shef6, does not lead to widespread cell death provided the density is sufficiently high. Enzymatic single cell passaging is much more amenable to automated and scaled up cell manufacturing processes and facilitates the even seeding of cells at reproducible densities. Here we have shown that single cell seeding can be used to generate high RPE yields, a finding that has been subsequently confirmed by others (Maruotti et al., 2013). Following single cell dissociation we have carried out experiments that show there to be an optimal seeding density above and below which RPE yield and overall HESC-RPE differentiation efficiency is significantly reduced. Differentiation efficiency and HESC seeding density will have significant cost implications in any HESC-RPE manufacturing process and are important targets for research and optimisation; these results show how the HESC-RPE conversion efficiency is highly dependent on the HESC seeding density.

Chapter 5: Enhancing differentiation efficiency using small molecules

.

5.1 Introduction

In the previous chapters we have characterised the process of spontaneous HESC-RPE differentiation in Shef6 and Shef3. We have demonstrated how cell line, time in culture, passaging methods, MEFs vs. feeder-free culture and HESC seeding density have a significant impact on the timing of pigmentation and eventual RPE yield during spontaneous differentiation, underlining the sensitivity of RPE differentiation to changes in processing parameters. We found that the Shef3 cell line was less able to generate high RPE yields in a variety of conditions, possibly due to a reduced innate preference for neuroectoderm conversion. In transferring the differentiation system to feeder-free conditions we showed that Shef3 produced particularly poor RPE yields. In this final chapter we sought to enhance RPE differentiation in these low yielding conditions using small molecules known to induce neuroectoderm conversion in HESC.

In addition to the many descriptions of spontaneous HESC-RPE differentiation (Kawasaki et al., 2002, Klimanskaya et al., 2004, Lund et al., 2006, Vugler et al., 2008, Buchholz et al., 2009, Carr et al., 2009, Liao et al., 2010, Rowland et al., 2012) many published protocols employ growth factors and/or small molecules with the aim of directing differentiation towards the desired retinal lineage. Of these, only a few have gone so far as to characterise the capacity of these growth factors/small molecules to improve the efficiency of RPE generation relative to spontaneous differentiation (see chapter 1, table 1.1). For example, Zahabi et al., report the generation of 40% RPE65+ve cells from H6 HESC line following treatment with noggin, bFGF, Retinoic acid and Shh, but do not report the yield in the absence of these factors. A number of studies have anecdotally reported improvements in MitF positive-cell or pigmented RPE cell yields following treatment with a range of growth factors and/or small molecules, but have not quantified them. At the time of carrying out this work only one study had fully characterised and quantified the 'induced' RPE yields relative to spontaneous differentiation in floating cell aggregates (Idelson et al., 2009) –see chapter 1, table 1.1 for a history of HESC-RPE differentiation methods. Since then others have quantified improvements or otherwise in pigmented cell yields following treatment with factors such as activin A,

(Hongisto et al., 2012, Rowland et al., 2012, Mellough et al., 2013, Buchholz et al., 2013, Zhu et al., 2013)

The rational for HESC-retinal cell differentiation protocols generally comes from our knowledge of vertebrate eye development, with most protocols targeting neuroectodermal differentiation and formation of the anterior forebrain. Protocols for retinal cell derivation commonly use pro-neural factors at the beginning of the differentiation, such as: Noggin (BMP inhibitor), DKK1 (Wnt inhibitor) and LeftyA (Activin/nodal inhibitor); small molecule equivalents such as SB431542, CKI-7 and less targeted neuralizing supplements such as B27, N2 and Nicotinamide (NIC) which are known to enhance neural cell survival during differentiation (Lamba et al., 2006, Osakada et al., 2008, Osakada et al., 2009, Idelson et al., 2009, Nistor et al., 2010, Meyer et al., 2009, Zahabi et al., 2012, Mellough et al., 2012, Buchholz et al., 2013). In addition, some protocols include factors at a later stage that are known to induce early optic vesicle development e.g. IGF, Shh (Lamba et al., 2006, Zahabi et al., 2012, Mellough et al., 2013, Zhu et al., 2013) and pattern the developing retina e.g. Activin A, Wnt antagonist CHRIR90021 (Idelson et al. 2009, Meyer et al., 2011, Nakano et al., 2012, Zhu et al., 2013) or induce maturation of RPE e.g. Vasoactive intestinal peptide (VIP), (Buchholz et al., 2013).

The efficacy of some of these protocols has proven difficult to replicate; a problem that is likely due in part to the innate differences in stem cell lines, as we have discussed in previous chapters. Embryonic stem cells will generally adopt anterior neuroepithelial characteristics in the absence of exogenous signalling (Muñoz-Sanjuán et al., 2002, Pankratz et al., 2007, Chambers et al., 2009). It has been well documented that the rate and efficiency with which different HESC lines undergo spontaneous neuroectodermal differentiation is highly variable (Osafune et al., 2008, Kim et al., 2010, Boulting et al., 2011). We have observed this in our cell lines, with Shef3 appearing to undergo significantly less efficient neuroectodermal differentiation than Shef6 (chapter 3). These variations may be because some cell lines are more resistant to differentiation than others, or because some lines preferentially differentiate into other germ layers.

Inhibition of BMP and activin/Nodal signalling pathways, using growth factors or small molecules, has proven highly effective at inducing efficient neuroectoderm differentiation in a large number of HESC lines regardless of their innate differentiation propensity (Chambers et al. 2009, Patani et al., 2009, Zhou et al., 2010, Kim et al., 2010, Morizane et al., 2011). The use of small molecules, as opposed to recombinant growth factors, to direct differentiation is highly favourable for commercial manufacturing processes; not only are the small molecules significantly less expensive, but they also offer less batch-to-batch variability and avoid the cost and complexity of introducing another xenogeneic component to the manufacturing process (Allsopp et al., 2010). Dorsomorphin is a small molecule protein kinase inhibitor that was discovered during a screen in zebrafish (Yu et al., 2007), it can be used to induce highly efficient neuroectodermal conversion in HESC, either on its own (Zhou et al., 2010), or in combination with other small molecules (Kim et al., 2010, Meyer et al., 2011, Morizane et al., 2011). In addition to blocking BMP type I receptors, (thereby inhibiting SMAD 1/4/8 phosphorylation), dorsomorphin interferes with several TGFβ superfamily type receptors and has been shown to dampen activin/nodal signalling in a BMP independent manner, similar to a low dose of SB431542 (thereby reducing activin-induced phosphorylation of SMAD 2/3) (Zhou et al., 2010). The ability of dorsomorphin to induce 'dual SMAD' inhibition makes it a useful tool for enhancing neuroectodermal differentiation in HESC in a simple, cost-effective, one-step method.

In this study, the efficacy of dual SMAD inhibition was tested in our cell lines. Shef6 and Shef3 were found previously to have significantly different innate propensities for RPE differentiation. The mechanisms that cause Shef6 to respond well to feeder-free differentiation and to consistently produce an enhanced RPE yield relative to Shef3 (chapter 3) are unknown, although higher Pax6 expression during the earliest stages of differentiation suggests the early process of neuroectodermal conversion may be critical. The experiments described in this chapter sought to determine whether small molecules could be used to enhance early neuroectodermal conversion in our cell lines and to investigate whether this intervention could improve RPE differentiation yields. It was of particular interest to determine whether yields could be improved in Shef3, a cell line which we had found previously to be particularly inefficient at generating RPE in feeder-free conditions.

5.2 Dorsomorphin enhances neuroectoderm conversion shef6 and shef3

5.2.1 Small molecule inhibitors effect cell morphology, Pax6 and Oct4 expression

Given the numerous and often conflicting reports on the efficacy of various small molecule combinations in different cell lines, experiments were undertaken to determine a suitable regime for use in Shef6 and Shef3. Three small molecules known to interact with major signalling pathways involved in HESC differentiation and germ layer specification (table 5.1) were tested.

Molecule	**Target Pathway**	**References**
dorsmorphin (DM)	BMP / Smad 1/5/8 (+Activin/Smad 2/3)	Kim et al., 2010 Zhou et al., 2010
SB431542 (SB)	Activin/Smad 2/3	Chambers et al., 2009
PD0325901 (PD)	FGF/ERK	Greber et al., 2011

Table 5.1 Small molecules that interact with major HESC signalling pathways

Shef6 and Shef3 were seeded as single cells onto Matrigel-coated 6-well plates at the previously determined optimal density of 35,000/cm^2 (chapter 4). The cells were expanded for five days in defined mTeSR1 medium. This was followed by ten days of differentiation in –bFGF differentiation media supplemented with one of three small molecule combinations or DMSO only as a control. At the end of this period cells were analysed by immunostaining for markers of pluripotency (Oct4) and neuroectoderm differentiation (Pax6), (Zhang et al., 2010).

In Shef3 control samples at day fifteen, patches of compacted cells containing what appeared to be neural-rosette like structures were visible (Fig. 5.1 A, arrow), though

they were not at this stage Pax6-positive (Fig. 5.1 B). Wells also contained areas of less compacted cells (Fig 5.1 C). There were no Oct4-positive cells detected at this time, suggesting that cells are either differentiating into other germ layers or that they are in an intermediate Oct4-negative and Pax6-negative state. In contrast, wells that had been treated with dorsomorphin contained no rosette-like structures but large contiguous areas of compacted, Pax6 positive cells (Fig 5.1 E,F) interspersed with a few 'holes' of un-compacted, Pax6-negative cells. In the DM+SB condition (Fig. 5.1 I, J) a similar picture of Pax6-positive islands around Pax6-negative holes emerged, with the 'holes' appearing larger than in the DM only condition (Fig. 5.1 I). Finally in the DM+SB+PD condition, Pax6-positive cells appeared in similar sized compacted islands with defined, highly compacted borders (Fig. 5.1 N). In all conditions Oct4-positive cells were not detected at day fifteen.

In Shef6 control samples, thick, dense ridges of cells had formed around 'holes' by day fifteen of differentiation (Fig. 5.2 A-C). Pax6-positive neuroepithelial rosettes were abundant on these dense ridges (Fig. 5.2 B, arrows). Oct4-positive cells were not detectable at this time point (Fig. 5.2 D) indicating that neuroectodermal differentiation was advanced in Shef6 by day fifteen. Similar to what was observed in Shef3, dorsomorphin treated cells had formed contiguous sheets of Pax6-positive cells (Fig 5.2 F). Unlike Shef3 there were no large holes containing Pax6-negative cells. A similar phenomenon was observed in the DM+SB condition, with even more compacted Pax6-positive cell sheets forming (Fig 5.2 I, J). In the DM+SB+PD Pax6-positive cells were sparser, appearing only on thickened islands surrounded by Pax6-negative cells. In all conditions Oct4 immunoreactivity was negligible, with the exception of the dorsomorphin only condition where a faint signal was detected in some areas (Fig. 5.2 H).

These results demonstrate that dorsomorphin treatment alone is sufficiently potent to generate high Pax6 cell yields in both of our cell lines as has been described by others (Zhou et al., 2010). Given a recent report that SB431542 reduces RPE cell yields (Zahabi et al., 2011) and the apparent reduction in Pax6-positive cell numbers upon the addition of FGF/ERK inhibitor PD0325901, it was decided to carry out long-term differentiation experiments using dorsomorphin alone.

5.2.2 Dorsomorphin suppresses the down regulation of pluripotency gene expression in differentiating Shef6 but not Shef3.

One report has described how inhibition of BMP signalling by dorsomorphin can partially suppress differentiation and maintain pluripotent patterns of gene expression at the early stages of HESC differentiation (Morizane et al., 2011). Oct4 protein was largely undetectable in our cell lines following ten days of differentiation with or without dorsomorphin treatment (Fig. 1-2). Nevertheless, QPCR was carried out to determine if pluripotency genes were still being expressed at day 15. Initially the expression at day 15 was assayed relative to expression in hESC at day 0. Expression of pluripotency genes decreased by 40-90 fold in the control wells, but only 5-11 fold in the dorsomorphin treated wells (Fig. 5.3 A).

In order to confirm this effect, pluripotency gene expression at day fifteen was measured in Shef6 (N=3) and Shef3 (N=3) in dorsomorphin and untreated control wells. In Shef3, transcript levels were low at day fifteen and there were no significant differences in expression between dorsomorphin treated and untreated controls for any of the genes tested (Fig. 5.3 B). In Shef6 however, there was an increase in mean Nanog and TDGF expression in dorsomorphin treated wells relative to control wells (Fig. 5.3 B) but little change in Oct4 expression. There was a significant difference in the relative expression of pluripotency genes Nanog and TDGF in response to dorsomorphin treatment between Shef6 and Shef3 (student's unpaired t-test, $p<0.05$, N=3).

5.2.3 Dorsomorphin selectively up regulates neuroectoderm gene expression and down regulates mesoderm, endoderm and trophectoderm gene expression in Shef3 and Shef6.

QPCR was used to monitor the expression of other markers of neuroectoderm differentiation in dorsomorphin treated and control samples. Six3 and Lhx2 are involved in demarcation of the eye field (Zuber et al., 2003) but are also critical earlier in neuroectoderm and forebrain specification (Zhang et al., 2010). Pax6 is a neuroectoderm fate determinant and Nestin is involved in early neuralization. All neuroectoderm markers were robustly upregulated relative to control wells in the presence of dorsomorphin, in both Shef3 and Shef6 (Fig. 5.4).

BMP signalling in HESC can induce mesoderm and trophectoderm differentiation (Xu et al., 2002, Zhang et al., 2008) and Activin/Nodal/TGFβ signalling has been shown to induce endoderm differentiation (D'Amour et al., 2005). The addition of 1μM dorsomorphin to culture media has been shown to interrupt both BMP and Activin signalling. Markers of mesoderm (Brachyury, AFP), endoderm (Gata6, Sox17) and trophectoderm (CDX2) differentiation were all robustly down-regulated in the presence of dorsomorphin relative to control in both cell lines (Fig. 5.4).

One way analysis of variance demonstrated a highly significant difference in dorsomorphin induced changes in gene expression between groups of markers of the various germ layers (neuroectoderm, mesoderm, endoderm and trophectoderm) in both Shef6 ($F(3,26)=13.3$, $p<0.001$) and Shef3 ($F(23,3) = 10.5$, $p< 0.001$). Post hoc analysis (student's unpaired t-test) revealed that fold increases in neuroectoderm gene expression in response to dorsomorphin differed significantly from expression of markers of the other germ layers ($p<0.001$), but that there were no significant differences between the dorsomorphin induced effects on mesoderm, endoderm or trophectoderm gene expression ($p=0.2$-0.4). These results suggest that dorsomorphin treatment has a specific affect on enhancing neuroectoderm gene expression whilst suppressing expression of markers of the other germ layers in both cell lines.

Comparing dorsomorphin induced changes in gene expression between the two cell lines, we found there to be a greater fold down regulation in mesoderm, endoderm and trophectoderm genes in Shef3 (Average fold change = 10.3 fold) than in Shef6 (Average fold change = 3.4), one way ANOVA $F(1,28) = 3.8$ $p<0.05$, but no statistically significant difference in the upregulation in neuroectoderm genes (Shef3 Average = 4.9 fold increase, Shef6 average = 3.5 fold).

5.2.4 Dorsomorphin enhances neuroectoderm differentiation at a range of seeding densities.

Given the critical impact of seeding density on differentiation efficiency, the ability of dorsomorphin to induce Pax6 expression was tested over a range of HESC seeding densities. At all densities there was a distinct difference in cell morphology in dorsomorphin treated vs. control wells: in control wells circular 'holes' of less-compacted cells surrounded by thick compacted ridges were observed (Fig. 5.5 A, marked 'H' and 'R' respectively), whereas in dorsomorphin treated wells, compacted, multilayered sheets covered the whole well regardless of density. Compacted cells found in the dorsomorphin treated cultures and in the 'ridges' formed in control wells were immunopositive for Nestin whereas non-compacted cells found in the circular 'holes' were not (Fig. 5.5 B). Pax6 expression at day 15 was measured in dorsomorphin treated and control wells over a range of cell seeding densities (Fig. 5.5 C, D). The relative up-regulation of Pax6 in dorsomorphin treated cultures declined slightly with increasing seeding density, but the differences were not significant.

On the basis of these results it was concluded that ten days of 1μM dorsomorphin treatment is sufficient to enhance neuroectoderm differentiation and suppress differentiation into other lineages in both Shef3 and Shef6.

5.2.5 Time course of eye field transcription factor expression demonstrates sustained up regulation following DM treatment.

Activin/BMP type signalling has been shown to be critical to RPE differentiation at the optic cup stage of eye development in vivo (Fuhrmann et al., 2000) and to augment RPE yields in a number of HESC models (Idelson et al., 2009, Meyer et al., 2011). With this in mind, dorsomorphin was removed from the medium after ten days to allow the equivalent necessary developmental stages to proceed uninterrupted. In order to determine whether the increases in neuroectodermal gene expression seen at day fifteen were sustained beyond the ten day period of dorsomorphin supplementation, QPCR analysis was carried out over a time course of 35 days. Cells were harvested for QPCR analysis at day 0, 5, 15, 25 and 35 and the normalised quantities of mRNA were expressed relative to the quantity in the starting HESC cultures cell (day 0).

In Shef3: the expression of Six3, a critical eye field transcription factor, increased 50 fold from days 5-15 in dorsomorphin treated wells, peaking at day 15 before decreasing to 30 fold and remaining at that level until day 35. In the control wells Six3 expression increased only 12-15 fold in the same time frame (Fig. 5.6 A). Lhx2, another important eye field transcription factor, expression rose steadily in the dorsomorphin treated samples, reaching a peak at day 25 at 170 fold. The control Shef3 samples however peaked at a much lower level of around 40 fold, also at day 25.

In Shef6: Six3 expression followed a similar pattern but was upregulated 480 fold in dorsomorphin treated wells between days five and fifteen, before decreasing to around 70 fold. In control Shef6 wells Six3 expression increased 70 fold from days five to fifteen, a substantially larger increase than in Shef3 control wells (Fig. 5.6 B). Similarly Lhx2 expression rose rapidly to 170 fold in the dorsomorphin treated sample (similar to the level seen in dorsomorphin treated Shef3), compared to 40 fold in the control, before under going a slow decline to 140 fold over the following

20 days. In the control sample Lhx2 expression peaked at 130 fold at a later time point, between days fifteen and thirty five (Fig 5.6 B).

These data demonstrate peaks in eye field transcription factor expression in both cell lines, as have been reported by others (Meyer et al., 2009); they also demonstrate a much greater upregulation of Six3 mRNA in Shef6 than Shef3. In addition they show that ten days of dorsomorphin treatment enhances expression of eye field transcription factors and that this leads to a sustained up regulation of these genes post dorsomorphin withdrawal in both cell lines.

5.3 Shef3 Dorsomorphin treatment and RPE yield

Having determined that early dorsomorphin treatment enhances neuroectoderm differentiation and sustains the upregulation of genes required for determination of the eye field, we next sought to investigate the effect of on RPE differentiation yields from Shef3 in both MEFs co-culture and feeder-free systems.

5.3.1 Pre-treatment with Dorsomorphin during MEFs-co culture enhances RPE yield

Shef3 cells at a range of passages were split 1:2 and seeded onto inactivated MEFs feeders. After 10 days expansion in standard HESC media +bFGF, 1µm dorsomorphin or DMSO (control) was added to the –bFGF differentiation media for the following ten days. Cells were then fed daily with standard hESC –bFGF media until day 50 of differentiation at which point flasks were scanned and the number of foci determined using the auto-counting method as described (Chapter 2, Materials and Methods). The yield of pigmented foci was enhanced by pre-treatment with dorsomorphin (Fig. 5.7 A, C) and the average fold increase in foci numbers dorsomorphin/control was 4.1 ± 0.4 SEM, N=3, the increase was not found to be statistically significant however. In control samples the yield of RPE per cm^2 typically varied with passage number, with lower passage number cells producing greater yields (Fig 5.7 C), as described in chapter 3. Pigmented foci were extracted from dorsomorphin treated flasks and plated onto Matrigel where they expanded and exhibited typical RPE morphology (Fig. 5.7B).

5.3.2 Dorsomorphin enhances RPE cell yield in high passage 'feeder-free' cultures

The chemical induction step was next tested in the feeder-free system using Matrigel-coated six-well plates, mTeSR1 expansion medium and seeding single cells at the optimal density of (35,000/cm^2). It had previously been observed that Shef3 cells produce relatively poor RPE yields in feeder-free conditions and at high passage numbers (Chapter 3), making this system a good target for a more directed differentiation.

After 5 days expansion in mTeSR1, cells were treated with 1μM dorsomorphin (or DMSO control) in –bFGF differentiation media for 10 days, before switching to standard –bFGF differentiation media for the remaining further 35 days. At day 50, the plates were scanned, pigmentation was measured and cells were harvested for QPCR or re-plated onto Matrigel for immunocytochemistry.

In line with our observations of Shef3 differentiation at high passage and in feeder-free conditions in chapter 3, control wells at day 50 contained few pigmented foci; mostly appearing at the edges of the wells (Fig. 5.8 A,B), however the average number of foci per cm^2 was higher following this single cell dissociation protocol than via the clump passaging method used in chapter 3 (6.7 ± 3.3 foci/cm^2 vs. 0.4 ± 0.3 foci/cm^2 clump passaging, feeder-free conditions).

In the corresponding dorsomorphin treated samples however, pigmentation was abundant and distributed across the whole well surface; appearing both in discreet foci and in larger contiguous areas (Fig. 5.8 A, B). The % pigmentation was significantly higher in dorsomorphin treated wells (Fig. 5.8 C), (one way ANOVA, $F(1,10) = 8.0$, $p<0.01$). The average fold increase in % pigmented area dorsomorphin/control wells was 5.0 ± 0.7 (SEM, N=6). The increase in number of foci/cm^2 was also significant ($F(1,10)=9.6$, $p<0.01$). Pigmented foci were manually extracted from the dorsomorphin treated wells and expanded on Matrigel. Pigmented epithelial sheets exhibiting cobblestone morphology and immunopositive for Otx2,

ZO1, CRALBP and MitF were observed (Fig. 5.9 D), thus confirming the HESC-RPE phenotype of the dorsomorphin derived cells.

QPCR analysis was carried out in order to compare gene expression in dorsomorphin treated and control wells at day 50. Consistent with the increased number of pigmented foci, there was a significant upregulation in the expression of RPE associated markers in dorsomorphin treated wells relative to controls (Pmel17, Otx2 and Pax6 ($N= 4$, $p<0.05$, student's paired t-test) but not MitF ($P=0.09$) (Fig. 5.8E).

5.4 Shef6 Dorsomorphin treatment and RPE yield

In Chapter 3 it was shown how Shef6 has a greater capacity for RPE differentiation than Shef3 in undirected spontaneous differentiation, in a variety of culture systems over a range of passages. Immunostaining revealed that Shef6 cells had produced Pax6 positive neural rosettes more efficiently than Shef3 at day fifteen in feeder free conditions (Fig. 5.1, 5.2). Dorsomorphin treatment was able to induce further augmentation of neuroectoderm gene expression in Shef6 (Fig. 5.3) and differentiation into a near uniform layer of Pax6-positive cells (Fig. 5.2). Thus it was hypothesised that dorsomorphin treatment may be able to enhance RPE differentiation yields in Shef6. In this section, long term differentiation experiments were carried out on dorsomorphin-treated Shef6 to assess the impact of this early increase in neuroectoderm differentiation on RPE yield.

5.4.1 Dorsomorphin has minimal effects on RPE yield in MEFs co-culture

As with Shef3, mechanically passaged flasks of Shef6 from a range of passages were split one in two and, after ten days expansion in +bFGF HESC medium, treated for ten days with either 1μM dorsomorphin or an equal volume of DMSO (control). The flasks were scanned at day fifty and the number of pigmented foci counted using the auto-counting method described (Chapter 2, Materials and Methods). In three separate experiments, a small increase in the number of foci was detected in the dorsomorphin treated flasks, with an average fold change of dorsomorphin/control of 1.3 ± 0.1 SEM (Fig. 5.9 A,C), which was not statistically significant. As in Shef3, pigmented foci extracted from dorsomorphin treated flasks displayed typical RPE morphology following expansion on Matrigel (Fig. 5.9B).

5.4.2 In feeder-free cultures DM treatment significantly reduces pigmentation

Differentiation experiments were next carried out in a defined, feeder-free system. Shef6 were dissociated into single cells and seeded at optimum density (35,000 /cm^2) on Matrigel-coated six-well plates. As with Shef3, cells were expanded for five days in mTeSR1, differentiated for ten days in –bFGF media in the presence of dorsomorphin or DMSO, then a further 35 days differentiation in –bFGF differentiation media.

As described in previous chapters, Shef6 produced high RPE yields in feeder-free culture following single cell dissociation; the control wells contained large numbers of discrete, pigmented foci that were distributed evenly across the wells (Fig. 5.10, A). The average number of foci in control wells was 48.3 ± 4.6 SEM foci /cm^2 (N=6) and the mean pigmented area was 4.0 ± 1.3% SEM (Fig. 5.10 A, B left panel). In stark contrast, dorsomorphin treated wells had significantly reduced numbers of pigmented cells at day fifty (Fig. 5.10 A,B, right panel), in some wells a few foci were visible at day fifty (Fig 5.10 A, arrows). The difference in % pigmentation and number of foci was statistically significant between dorsomorphin and control wells (ANOVA, $F(1,10)= 8.2$, $p<0.01$), (Fig. 10C). Examination of control wells under the microscope revealed pigmented, cobblestone RPE surrounded by a non-pigmented cell type; in the dorsomorphin-treated wells, however, no pigmented foci were visible and cells had a non-epithelial, disordered appearance reminiscent of a neuronal progenitor cell type (Fig. 5.10 B). In order to check that differentiation was not merely delayed by the addition of dorsomorphin, two wells were allowed to differentiate for up to sixty days. At this time point there were still no traces of pigmented RPE or epithelial morphology (data not shown).

The large decrease in pigmented cell yield was accompanied by a down-regulation in RPE genes Pmel17, Otx2, MitF and Tyrosinase (Fig. 5.10D). Interestingly there was no decrease in Pax6 expression, a gene that is expressed in both the early RPE and

neural retina during formation and patterning of the optic cup (Martinez-Morales et al., 2004, Bharti et al., 2012).

One way ANOVA revealed a statistically significant difference in the effect of dorsomorphin on RPE gene expression (MitF, Pmel17, Otx2) between Shef3 (average fold change DM/control =10.3 ± 3.6 SEM), and Shef6 (average = 0.5 ±0.1 SEM), $F(1,19) = 5.5$ $p<0.01$).

5.4.3. Comparison of MitF and Chx10 expression suggests a neuroretinal phenotype is emerging in Dorsomorphin treated Shef6*.*

The large up regulation in eye field transcription factors seen in dorsomorphin-treated Shef6 over the thirty five day gene expression time course (Fig. 5.6 B) suggests that the treatment is not inhibiting but augmenting differentiation towards early retinal cell types. Both the RPE and neural retina are derived from the optic neuroepithelium. During the optic vesicle stage of vertebrate development, bi-potent retinal progenitors differentiate into pigmented RPE or neuroretinal progenitors depending on their position and exposure to signals emanating from surrounding tissues (Fuhrmann et al., 2000), a similar phenomenon has been observed in HESC models (Meyer et al., 2009, Nakano et al., 2012). The RPE-neural retina cell fate decision is largely governed by differential expression of Chx10 and MitF (Horsford., et al. 2005) and the relative proportions of neural retina vs. RPE in HESC have proven highly sensitive to exogenous signalling (Meyer et al., 2011, Nakano et al., 2012). In order to investigate whether dorsomorphin-treated Shef6 were adopting a neuroretinal identity at the expense of RPE, the expression of these two transcription factors in Shef6 and Shef3 were compared.

Expression of MitF and Chx10 was found to be mutually exclusive in day fifty Shef6 samples, with MitF localised to pigmented, epithelial RPE and Chx10 localised to an adjacent, non pigmented cell type (Fig. 5.11 A). QPCR was used to measure the relative expression of MitF and Chx10 in whole wells of Shef6 and Shef3 at day 50.

In Shef3, Chx10 was only slightly upregulated in dorsomorphin-treated wells (1.4 fold ± 0.1 SEM, N= 4), whereas in Shef6 there was a larger average upregulation (dorsomorphin/Control 5.2 fold ± 1.0 SEM, N=3), and the difference between dorsomorphin induced Chx10 augmentation in Shef6 and Shef3 was found to be significant (ANOVA, $F(1,5) = 15.0$, $p<0.05$). In contrast, MitF expression was upregulated in dorsomorphin treated Shef3 (3.0 fold ± 0.8, N=3) and downregulated in dorsomorphin-treated Shef6 relative to control wells (0.7 fold ± 0.13, N=3). Again,

the difference between Shef3 and Shef6 was statistically significant (ANOVA, $F(1,5) = 2.4$, $p<0.05$). To confirm the upregulation of Chx10 at the protein level, Shef6 cells were taken from day 50 wells and expanded on Matrigel. The non pigmented cells taken from dorsomorphin treated Shef6 were almost uniformly positive for Chx10 whereas pigmented, cobblestone RPE cells from the corresponding control wells were Chx10-negative (Fig. 5.11 D, E).

These results suggest that dorsomorphin treatment is enhancing differentiation towards a Chx10-positive, early neuroretinal phenotype in Shef6 and doing so at the expense of differentiation towards pigmented RPE.

5.4.4 Activin A supplementation does not induce RPE differentiation in DM treated cultures

Signalling from adjacent tissues has proven critical to patterning of the retina during ocular development (Fuhrmann et al., 2000, Eiraku et al., 2011). Members of the TGFβ superfamily of signalling molecules secreted from the adjacent extraocular mesenchyme trigger MitF transcription and RPE differentiation, where as FGFs from the surface ectoderm upregulate Chx10, initiating neuroretinal differentiation (Fuhrmann et al., 2000). Activin A has been shown to mimic the action of signalling from the extraocular mesenchyme and enhance RPE differentiation yields in animal models as well as differentiating hESC (Fuhrmann et al., 2000, Idelson et al., 2009, Meyer et al., 2011).

It was therefore sought to determine whether the addition of activin A to dorsomorphin-treated Shef6 could skew the balance in favour of RPE differentiation. 100ng/ml of activin A was added to dorsomorphin treated Shef6 from days twenty to forty, a time window within which the *in vitro* equivalent of the optic vesicle stage of eye development is thought to occur (Meyer et al., 2009, Idelson et al., 2009). Whilst untreated controls and activin A supplemented wells became heavily pigmented by day 50 (Fig. 5.12 A, B), activin A added to dorsomorphin-treated wells contained little to no pigmentation as in the dorsomorphin only wells (Fig. 5.12 C, D). In addition, activin A treatment alone (no dorsomorphin pre-treatment) had no significant impact on RPE yields (N=3, Fig. 12 E). From these results we can conclude that activin A at this concentration, added in this time window, was not sufficient to stimulate RPE differentiation.

5.5 Discussion

Our findings from previous chapters have been brought together in the design of a density optimised, feeder-free differentiation protocol for generating HESC-RPE. We have shown that single cell dissociation and differentiation on Matrigel following an expansion step in mTeSR1 reproducibly generates high RPE yields in Shef6. Spontaneous differentiation of Shef3, however, generated poor RPE yields in feeder-free conditions, potentially due to inefficient neuroectoderm conversion in the absence of MEFs feeders. In this chapter we sought to induce efficient neuroectoderm conversion using dual SMAD inhibition in a simple, one-step method, employing small molecules.

The cell lines used in this study (Shef6 and Shef3) have demonstrated highly divergent capacities for neuroectodermal differentiation and RPE differentiation, with Shef6 consistently yielding more pigmented cells regardless of differentiation methods. As discussed in chapter 3, a number of studies have highlighted the variable 'innate' differentiation capacity of different HESC and IPSC lines (Osafune 2008 et al., Hu et al., 2010a, Lappalainen et al., 2010, Kim et al., 2011). Variability in RPE yields across cell lines has also been noted (Idelson et al., 2009, Vjasaari et al., 2011, Zhu et al., 2013). These variations in differentiation behaviour have been attributed to endogenous signalling and growth factor responsiveness brought about by genetic variation (Boulting et al., 2011, Abeyta et al., 2004), epigenetically inherited adaptations to culture and passaging methods (Akopian et al., 2010, Enver et al., 2005, Tavakoli et al., 2009) and in the case of IPSCs, an epigenetic 'memory' of their cell type of origin (Hu et al., 2010b, Buchholz et al., 2009).

Irrespective of the reasons for it, the significant variability in target cell yields when different cell lines are subjected to the same expansion and differentiation protocol is highly problematic and hampers the standardization of research in this field. The advent of IPSC technology and the prospect of generating HLA matched HESC based therapies is predicted to demand the use of multiple cell lines (Carpenter et al.,

2009) and the varying responses of different cell lines to culture conditions is likely to prove challenging in the design and costing of manufacturing processes.

Some recent studies have proposed the idea of a short induction step to coax resistant cell lines towards the desired lineage (Kim et al., 2011, Boulting et al., 2011). Dual inhibition of BMP and activin/nodal signalling pathways (dual SMAD inhibition) is an efficient method for inducing neuroectoderm differentiation (Chambers et al. 2009, Patani et al., 2009, Zhou et al., 2010, Kim et al., 2010, Morizane et al., 2011). For example treatment of differentiating HESC with BMP antagonist noggin (targeting SMAD 1/5/8) and the Activin/Nodal inhibiting drug SB431542 (targeting SMAD 2/3) has been shown to produce a population of over 80-90% Pax6 +ve cells, (Chambers et al. 2009, Zhou et al., 2010). This so called 'dual SMAD inhibition' method produces neuroepithelial cells that are Otx2 and FoxGB1 positive, confirming an anterior neural identity (Chambers et al., 2009). These studies led us to consider 'dual SMAD inhibition' to induce efficient neuroectoderm differentiation and enhance RPE differentiation in the previously low RPE-yielding Shef3.

Dorsomorphin is a small molecule protein kinase inhibitor that was discovered during a screen in zebrafish for small molecules that perturb dorsal-ventral axis patterning (Yu et al., 2007). It has been used to induce highly efficient neuroectodermal conversion in HESC via dual SMAD inhibition (Zhou et al., 2010, Kim et al., 2010, Meyer et al., 2011, Morizane et al., 2011). Zhou et al., found that treating HESC with 1μm dorsomorphin for ten days generated 80-90% Pax6 positive cells, similar to the potency of noggin and SB431542. Small molecules such as dorsomorphin are cheaper, more stable and better able to penetrate large cell masses that recombinant growth factor equivalents such as Noggin. Their use is highly favourable for commercial manufacturing processes in that they also offer less batch-to-batch variability and avoid the cost and complexity of introducing another xenogeneic component to the manufacturing process (Allsopp et al., 2010).

Others have found the efficacy or dorsomorphin to improve when combined with activin/nodal inhibitors SB431542 (SB) (Morizane et al., 2011) or with a downstream inhibitor of FGF signalling, PD325901 (PD) (Greber et al., 2011). Thus three small molecule antagonists of major signalling pathways were tested for their

ability to improve the efficiency of neuroectoderm differentiation and RPE differentiation in Shef3, and their responses compared to Shef6. We observed that dorsomorphin on its own was capable of eliciting a large increase in Pax6-positive cells in both Shef6 and Shef3. In view of a recent report that SB431542 treatment can reduce RPE yields (Zahabi et al., 2011), it was decided to carry out long-term differentiation experiments using dorsomorphin only.

Dorsomorphin treatment specifically and significantly enhanced neuroectoderm gene expression in both cell lines and at a range of cell seeding densities in both defined (mTeSR1) and MEFs-conditioned medium. This was accompanied by a significant down regulation in genes involved in the developing mesoderm, endoderm and trophectoderm. This is consistent with the reported requirements for BMP and activin/nodal type signalling to induce endoderm/trophectoderm and mesoderm differentiation respectively (Vallier et al., 2009, Pera et al., 2004, Xu et al., 2002) and dorsomorphin's ability to block these signals.

Expression of pluripotency genes was appropriately downregulated relative to HESC by day 15, although there was a notable difference in the dorsomorphin-induced response between the cell lines. Dorsomorphin treatment appeared to reduce the time dependent down regulation of some pluripotency genes (Nanog, TDGF) relative to controls in Shef6, whereas it had no such affect in Shef3. The reasons for this disparity are unclear. BMP signalling is a major pro-differentiation mechanism acting in early HESC, causing differentiation towards trophectoderm and primitive endoderm lineages via SMAD 1/5/8 phosphorylation (Xu et al., 2002, Pera et al., 2004). The action of BMPs are normally countered by BMP antagonists (noggin, gremlin) secreted by MEFs feeder cells or MEFs-conditioned medium (Xu et al., 2005), or by high quantities of FGF and TGFβ such as are present in mTeSR1 medium (Ludwig et al., 2006). In the absence of MEFs or mTeSR1, a BMP antagonist such as dorsomorphin could reduce the rate of differentiation; why this occurs in one cell line and not the other remains unclear. We have noted previously that Shef3 is more prone to spontaneous differentiation than Shef6, which is likely to do with differing levels of endogenous signalling in the two cell lines; perhaps Shef6 has higher autocrine FGF or Activin/Nodal signalling, which is not adequately suppressed by this dose of dorsomorphin. This question requires further investigation,

ideally by comparing dorsomorphin-induced reduction in SMAD2/3 and 1/5/8 phosphorylation in the two cell lines.

In spite of the slight pluripotency sustaining activity of dorsomorphin in Shef6, this cell line underwent more efficient neuroectodermal conversion. Time course analysis assessing the relative upregulation from the start of differentiation in the expression of eye field transcription factors (Six3 and Lhx2) in each cell line demonstrated a greater fold increase in Shef6, suggesting that a greater proportion of the cells are differentiating towards the early eye field phenotype in Shef6. These time course studies also demonstrate that the effect of the treatment lasted beyond the ten day period during which dorsomorphin was added to the medium. This is consistent with the theory that retinal specification progresses via a series of steps that gradually restrict fate potential, starting with the expression of eye field transcription factors from a subset of neuraly-induced embryonic cells, the numbers of which are increased by dorsomorphin treatment (Zaghoul et al., 2005).

A highly significant increase in the appearance of pigmented RPE in Shef3 in feeder-free conditions was observed in dorsomorphin treated wells, and an accompanying upregulation in RPE gene expression. In the control conditions few pigmented areas were visible; the addition of dorsomorphin, however, prompted a five fold increase in the total pigmented area. Whilst it is difficult to accurately compare protocols, due to the different methods used to assess yield, Osakada et al., found that DKK1 and LeftyA treatment yielded a similar fold increase in MitF positive monkey ES cells (Osakada et al., 2008). Similarly, Idelson et al. reported variability between HESC lines but HES1 showed an increase of 13% - 51% of aggregates containing pigmented clusters following the addition of activin A – a 3.8 fold increase (Idelson et al., 2009). Other more recent studies also report similar increases (Hongisto et al., 2012, Buchholz et al., 2013, Mellough et al., 2013 - see table 1.1).

Although the dorsomorphin based induction appeared to increase the RPE foci yield in MEFs co-culture also, there was fairly substantial variation in RPE yields. This may be due to the large range of passages over which these differentiation experiments were carried out – a variable which we have previously noted to have a profound affect on differentiation yields (chapter 3). The fold increase in foci

numbers was consistent across passages however (fold increase dorsomorphin/control = 4.13 ± 0.4 foci/cm2, N=3).

The success of dorsomorphin treatment in the otherwise low yielding, high passage Shef3 raises the possibility that small molecule based neural induction could be used to substantially increase the useful lifespan of HESC lines (i.e. the number of passages over which they are productive), provided karyotypic stability was not compromised. This could lead to significant cost savings. In addition, cell lines that generally produce poor RPE yields could be coaxed into productive differentiation. This type of strategy may become particularly important with the advent of IPSC technology, where the idea of patient-specific cell lines for personalised cell therapies is being proposed. In this scenario there would be a need for strategies that guarantee good RPE yields in all cell lines, regardless of their innate propensity for RPE differentiation in feeder-free, clinically appropriate differentiation conditions. Boulting et al. have already shown how a short, dual SMAD inhibition based neural induction step prior to an extensive directed differentiation can promote good yields of functional motor neurons in otherwise 'recalcitrant' IPSC lines (Boulting et al., 2011).

In chapters 3 and 4 we have demonstrated highly efficient RPE differentiation in Shef6 in MEFs co-culture and feeder-free, without the need for chemical induction. The differentiation efficiency was severely compromised at high passage numbers however (chapter 3, Fig. 3.10). Thus we tested the ability of dorsomorphin treatment to improve RPE yields further.

In stark contrast to its beneficial effect in Shef3, Dorsomorphin severely inhibited pigmentation in Shef6 and significantly reduced RPE yields in feeder-free conditions. dorsomorphin treatment of Shef6 produced a highly enriched, homogeneous population of Pax6-positive cells at day 15 but failed to generate pigmented cells within the normal time frame or up to 60 days after seeding, despite inducing a sustained upregulation of genes critical to eye development. At day 50, a homogeneous sheet of non-pigmented cells were found in the dorsomorphin treated wells which were immunopositive for the neuroretinal marker Chx10; this was accompanied by a significant increase in Chx10 mRNA and a down regulation in

MitF mRNA. These results show that dorsomorphin reproducibly induces neuroretinal differentiation at the expense of pigmented RPE in Shef6. This surprising result reveals some interesting features of spontaneous HESC-RPE differentiation. It has been shown in chick optic explants that RPE will not develop normally in the absence of the extraocular mesenchyme, which normally lies adjacent to the developing retina (Fuhrmann et al., 2000). Subsequently, a similar phenomenon has been described in mouse ESC derived optic cup structures derived from mouse ESC aggregates. Eiraku et al. have shown that separating the 'optic cup' like structure from attached non-retinal cells resulted in a failure to produce RPE, causing all cells to express Chx10 and adopt a neuroretinal fate (Eiraku et al., 2011).

Dorsomorphin enhanced neuroectoderm conversion in the Shef3 cell line, but some Pax6-negative cells remained at day fifteen (Fig. 5.1), in Shef6, however, dorsomorphin generated a relatively homogenous population of Pax6+ve cells (Fig. 2); in the absence of MEFs feeders or Pax6-negative, non-neuroectodermal cells therefore, differentiation into the RPE pigmented cell type may not be induced. These Pax6 negative, non-neuroectodermal cells may be critical to the normal process of RPE differentiation, carrying out a function akin to the BMP/Activin producing extraocular mesenchyme in eye development. The exact identity of these cells has not been determined in this study, comprehensive characterisation of these cells and the nature of the cytokines they secrete could make for fruitful future work.

Similar observations, of a population of Chx10 positive neuroretinal progenitors in place of RPE has recently been reported in EB based systems (Meyer et al., 2011, Nakano et al., 2012). Nakano et al. found that Wnt/Shh induced EBs contained Chx10 positive and MitF negative emerging neuroepithelium. They showed that augmentation of Wnt signalling was required to turn otherwise neuroretina-primed cells into pigmenting RPE. In our system a large increase in expression of the eye field transcription factor Six3 was seen in Shef6 (500 fold at day fifteen compared to 50 fold in Shef3). Six3 has been shown to mediate suppression of Wnt signalling in the anterior neural plate in a process that enhances neuroretinal specification (Liu et al. 2010). Six3 mediated Wnt inhibition may be an important mechanism contributing to the suppression of RPE and augmentation of the neuroretinal phenotype in dorsomorphin treated Shef6.

Interestingly, in the experiments described here, dorsomorphin treatment proved more effective in Shef6 in the MEF co-culture system. Whilst it did not cause a substantial increase in RPE yield, there was a slight increase in yield (average 1.3±0.1 foci/cm^2), and the treatment did not halt pigmentation altogether as seen in the feeder-free cultures. Hongisto et al., have recently demonstrated that a low level of activin A is secreted by MEF feeder cells and that this enhances RPE differentiation in co-culture systems. The same process may be occurring in Shef6 MEFs co-culture, promoting RPE differentiation in an otherwise neural retina favouring environment. As discussed in previous chapters, feeder cells are undesirable for robust, scaled up HESC-RPE manufacture; however, these results suggest that in the absence of feeders there may be a limit to the purity of RPE cells that can be generated from HESC differentiation.

A potential solution to this problem may be to simulate the action of extraocular mesenchyme by the addition of recombinant growth factors or small molecules that mimic its action; the appropriate timing and concentrations of the relevant factors will need to be determined. Various reports have demonstrated that it is possible to coax RPE differentiation from isolated or pure retinal progenitor cultures by the addition of exogenous growth factors from the BMP or TGFβ/activin family between days 20-40 of differentiation (Meyer et al., 2011, Eiraku et al., 2011). We hoped to replicate this result in our cultures with the addition of 100ng/ml of Activin A from days 20-40 in dorsomorphin induced Shef6, but this was not effective in stimulating pigmentation. The fact that activin A treatment alone was also ineffective at increasing RPE yields in control samples suggests that cells at this time point were not correctly primed to respond to activin A treatment in this culture system at this concentration. A very recent study has reported that supplementing feeder-free cultures with significantly lower concentrations of activin A at much earlier time point (10ng/ml, day 0-28) restores pigmentation levels to that of MEFs co-culture (Hongisto et al., 2012). It would be interesting to determine whether earlier activin A stimulation could restore pigmentation in our dorsomorphin induced Shef6 cultures.

There have been some conflicting reports regarding the efficacy of activin A treatment for RPE differentiation. One study reported that the molecule has little

impact on RPE yield unless cells had first been primed by the addition of NIC (Idelson et al. 2009). In another report, however, the same concentration of activin A was shown to significantly enhance RPE differentiation in optic vesicle-like structures (Meyer et al., 2011). Large differences have also been found in activin A responsiveness between the H7 and H9 cell lines with the latter responding dramatically to 100ng/ml activin A (a reported 98% pigmented cells generated) and the former being responsive only to its inhibition with SB431542 (Zhu et al., 2013). Another report found activin A treatment alone to have little impact of MitF gene expression (Buchholz et al., 2013). More recently, additional factors have proven to induce RPE differentiation in neuroretinal primed cultures. Wnt agonists (CHIR99021, or Wnt3a-expressing L cells) have been shown to have a dramatic affect on directing RPE differentiation from HESC derived optic vesicle-like structures (Nakano et al., 2012). Turning the problem on its head, it would be interesting to experiment with molecules that interfere with the FGF signalling cascade. This pathway is know to stimulate neural retina (Martínez-Morales et al., 2004) and its inhibition (using FGF inhibitor SU5402) has been shown to act on the reciprocal relationship between MitF and Chx10, swinging the balance in favour of MitF and subsequent RPE differentiation (Meyer et al., 2009, Buchholz et al., 2013).

It is likely that, as is the case in drawing comparisons between almost all HESC differentiation protocols, the enormous variability between cell lines and their hypersensitivity to variations in methods, both for their maintenance and differentiation, mean that extensive screening of growth factor and small molecule combinations, timings of application and concentrations will be required for every cell line and differentiation protocol. Here we have demonstrated a method for reproducibly generating high RPE yields from a previously resistant cell line, in a simple, one-step method employing small molecules and feeder-free culture. In addition we have shown how a short neural induction step can induce neuroretinal differentiation in previously RPE favouring conditions.

5.6 Conclusion

Having investigated how cell line and passage number, MEF feeders vs. feeder-free culturing, single cell dissociation and cell seeding density impact on HESC-RPE differentiation, we sought to investigate if RPE yields could be improved by directing early differentiation using small molecules that interfere with key signalling pathways involved in HESC differentiation and development of the human eye.

The study was restricted to looking at early cell fate decisions, specifically neuroectodermal conversion, hypothesising that early intervention is likely to have the greatest impact. Small molecules were used rather than recombinant growth factors, upon the reasoning that they are more stable, less costly, suffer from less batch to batch variability and are potentially better able to penetrate thick cell masses than recombinant growth factors (Allsopp et al., 2010). We have shown that neuroectodermal differentiation can be efficiently enhanced in a feeder-free system in two cells lines using ten days of treatment with a single small molecule BMP / activin inhibitor, dorsomorphin, presumably via a mechanism of dual SMAD inhibition. In addition, we have shown that enhancing neuroectoderm conversion leads to a robust increase in RPE yields in feeder-free conditions, in the otherwise low yielding Shef3. In feeder-free, density optimised, monolayer culture, dorsomorphin treatment enhanced RPE yields five fold, which is comparable the improvements seen by the addition of growth factors by others. In the usually high RPE yielding cell line Shef6 however, the same neural induction step enhanced neuroretinal differentiation – at the expense of RPE differentiation. This method could be widely applied to generating RPE or neural retina from poorly performing cells lines, and to extend the useful life span of HESC cells, making them productive even at high passages. Future work could focus on the use of small molecules to manipulate differentiation during the in vitro equivalent of the patterning of the optic vesicle stage, when the identity of the neural retina and RPE are specified and consolidated.

Chapter 6: Summary, Discussion and Future Work

6.1 Summary of findings

In the course of this work, several different lines of investigation have identified parameters that can be varied to improve the RPE yield and conversion efficiency. The results from the experimental work are summarised in the table below, expressed as average RPE foci yields per cm^2 in each cell line from experiments carried out at 'normal' seeding density (1:2 split ratio or 35,000/cm^2).

Shef6: Condition (Passage number)	Average RPE Foci /cm2	Fold Change Relative to MEFs co-culture
Shef6, MEFs co-culture (p40-60)	8.7 ± 1.2/cm^2 (N=9)	1
Shef6, MEFs co-culture (p60-85)	0.2± 0.1/cm^2 (N=3)	0.02
Shef6, Matrigel + Conditioned Media (p50-70)	13.0 ± 6.1/cm^2 (N=2)	1.5
Shef6, Matrigel + MteSR1 (p50-70)	15. 9 ± 1.1/cm^2 (N=2)	1.8
SC Shef6 Matrigel + Conditioned Media (p50-70)	35-50 /cm^2 (N=4) *	4.0-5.7
SC Shef6 Matrigel + mTeSR1 (p50-70)	48.2 ± 4.6 /cm^2 (N=6)	5.5

Shef3: Condition (Passage number)	Average RPE Foci /cm2	Fold Change Relative to MEFs co-culture
Shef3, MEFs co-culture (p40-60)	4.1 ± 1.3 /cm^2 (N=7)	1
Shef3, MEFs co-culture (p60-85)	0.2 ± 0.1 /cm^2 (N=7)	0.04
Shef3, Matrigel + Conditioned Media (p40-50)	0.35 ± 0.27/cm^2 (N= 3)	0.08
SC Shef3 Matrigel + MTeSR1 (p60-80)	6.7 ± 1.3/cm^2 (N=6)	1.6
SC Shef3 Matrigel + mTeSR1+ Dorsomorphin (p60-80)	17.7± 3.3/cm^2 (N=6)	4.3

Table 7.1 Summary of differentiation yields.

* homogenous pigmented coverage, single foci indistinguishable, SC = single cell dissociation and seeding.

Both cell lines Shef3 and Shef6 demonstrated increased RPE yields following single cell dissociation and seeding onto Matrigel + mTeSR1 media.

Shef6 produced an average of 8.4 ± 1.8 foci/cm^2 (N=6, p48-70) in traditional MEFs co-culture, following clump passaging. The cell line responded well to transferral to matrigel in feeder-free medium generating an average of 13-16 foc/cm^2 (N=4). Our single cell dissociation protocol increased the yield further with wells generating on average 48.2 ± 4.6 pigmented foci/cm^2 (N=6, p 50-70) in defined, feeder-free conditions. The addition of a dorsomorphin induction step significantly reduced pigmentation in Shef6, instead yielding Chx10 +ve cells resembling neural retinal progenitors.

Shef3 produced on average 2.3 ± 2.1 /cm^2 (N=7, p40-80), and despite reduced yields following feeder-free differentiation in conditioned media following clump passaging, saw an increased yield in matrigel +mTeSR1 following single cell dissociation up to 6.7 ± 1.3/cm^2 (N=6, p60-80), which was then further increased by the addition of a dorsomorphin induction step up to 17.7 ± 3.3/cm^2 (p60-80).

6.2 Process characterisation and feeder-free differentiation

In this study, HESC-RPE differentiation, using traditional HESC-MEFs co-culture, was carried out in two cell lines, Shef6 and Shef3. A novel method for non-destructive, semi-automated measurement of HESC-RPE differentiation rates was created using a flat bed scanner and a simple program developed in using an open-source software package, ImageJ. This system enabled automated analysis of images of whole flasks and wells of differentiating HESC. The program quickly and reliably distinguished pigmented cells from non-pigmented background and used these measurements to count the number of individual HESC-RPE differentiation events (number of foci) and the overall % surface pigmentation. Morphological and immunocytochemical analysis of these pigmented cells confirmed their universal HESC-RPE identity. In addition to image analysis, quantitative gene expression for RPE markers (Pmel17, Bestrophin, CRALBP, Tyrosinase, MitF, Otx2) were used throughout this project as a measure of relative target cell yields in the various differentiation conditions.

Detection of pigmented cells by image analysis allowed the real time assessment of pigmented cell yields without interfering with the progress of differentiation. Data was collected over a 30-80 day time span, revealing important differences in the differentiation rates between the two cell lines. It was found that Shef3 cells consistently produced pigmented foci faster than Shef6, but that Shef6 continued to accumulate pigmented foci over a longer stretch of time. As a result Shef6 had a significantly greater overall yield. This experiment emphasised the heterogeneous differentiation rates between distinctive HESC lines, and helped to define a suitable time scale over which to carry out further long term differentiation studies (usually 50 days). These results may help to explain large ranges in the reported time required for pigmentation in other studies (table 1.1), with different cell lines responding differently to the same conditions. In terms of industrial HESC-RPE manufacture, it

would be advantageous to determine the rate of differentiation for each individual cell lines, such that the optimal RPE harvesting time can be determined.

In using a flat bed scanner to record pigmentation, culture vessels were removed from the incubator for under a minute, much less time than is required for manual counting (Idelson et al., 2009, Kokkinaki et al., 2011, Vaajassaro et al., 2011, Hongisto et al., 2012,) or microscopic imaging of individual pigmented foci (Rowlands et al., 2012). This is important as the drop in temperature resulting from prolonged time out of the incubator has been shown to cause a drop in the media pH, affecting both cell proliferation and differentiation (Veraitch et al., 2008).

The specially designed T25 mounting device reduced the influence of ambient lighting and helped to standardize image acquisition, thereby reducing the requirement for further processing and allowing for comparison of images acquired over the time span of the project. Data was collected on the changes in RPE yields with increasing passage number over the span of the project. A significant drop-off in differentiated cell yield over time in culture was observed in both cell lines: on average, cells produced 9 foci per cm^2 at passage 40-50, but only 0.2 per cm^2 at passage 70-90. HESC are heralded for their purportedly infinite expansion capacity (Hoffman et al., 2005), and although subtle changes in HESC behaviour over time in culture have been noted (Baker et al., 2007), this drop-off in differentiated RPE cell yield has not previously been reported and will be an important consideration in the design of any manufacturing processes using HESC.

Interestingly, later in this study it was found that the usually low yielding, high passage Shef3 cells could be coaxed into more efficient differentiation. Passage 60-80 Shef3 could produce on average ~18 RPE foci/cm^2 when subjected to a dorsomorphin induction step. This suggests that cells become resistant to differentiation with prolonged time in culture, rather than loosing their pluripotency altogether.

The use of feeder cells, murine or human, is undesirable in the manufacture of cells for cell therapy. Not only do they pose a risk in the potential transmission of pathogens and present an additional regulatory burden, but they also add significant

logistical complications to culturing practices and compromise reproducibility and standardization (Akopian et al., 2010, Chin et al., 2007). In this study, the ability of HESC to generate RPE in commercially available feeder-free systems was assessed. HESC-RPE with pigmentation, classical morphology and RPE marker expression were observed in feeder-free conditions in both cell lines. During the course of this project, feeder-free derivation has been demonstrated by others (Vaajassari et al., 2011, Rowland et al., 2012, Buchholz et al., 2013, Sridhar et al., 2013). To our knowledge, there has been only one other recent comparison of differentiated cell yields between feeder cell co-culture and feeder-free differentiation protocols (Rowland et al., 2012). Significantly reduced RPE yields were observed in our study on matrigel in feeder cell free conditions following clump passaging in Shef3. Similarly, another group has reported differentiation of H9 cells generated ~50% fewer pigmented foci/cm^2 on Matrigel relative to hs27 human feeders (Rowland et al., 2012).

In addition to being a highly supportive environment for HESC growth and differentiation, MEFs secrete growth factors that are implicated in in-vivo eye development such as activin A and IGF1 (Hongisto et al., 2012, Gerber et al., 2007, Bendall et al., 2009), which have been proposed to contribute to the relatively high rate of RPE derivation in standard HESC culture conditions (Vugler et al., 2008). The results of this study may reflect the absence/reduced quantity of these RPE inductive factors in feeder-free culture. Apart from the impact on cell fate decisions, the effect of feeder-free culture on cell growth rates may be of equal importance in determining differentiated cell yields (Tavakoli et al., 2009). In this study it was shown that neither Shef6 nor Shef3 could produce RPE in continuous, adherent differentiation on matrigel in the absence of an expansion step in which the cells reached confluence, indicating the importance of high local cell density.

In these, circumstances, where an undefined and complex culturing practice produces the highest product yields, the construction of a financial and bioprocessing modelling tool would be beneficial (Placzek et al., 2009). This could enable comparisons of the raw material/labour requirements vs. the relative process efficiency to determine the most cost-effective strategy.

One surprising finding of this study was that unlike Shef3, when Shef6 were subjected to feeder-free culture, they underwent significantly more efficient RPE differentiation. This difference may stem from the divergent growth factor requirements and endogenous signalling levels in the two cell lines. It may also be a reflection of the relative adaptability of the two cell lines. Significantly reduced cell proliferation rates were observed in Shef3 when cells were transferred to the feeder-free culture relative to Shef6. These finding underline the necessity to carry out screening and optimisation studies for every new HESC or IPSC line.

6.3 Seeding density and process efficiency

One aim of this study was to quantify the RPE foci generated per quantity of HESC within a given time and volume of raw material, in various different differentiation conditions.

The number of individual HESC colonies seeded into each flask could be quickly established using the flat bed scanner, mounting device and Image J. This information was used to calculate the number of RPE foci derived per HESC colony over a number of differentiation runs and hence to establish the HESC-to-RPE conversion efficiency. Importantly the conversion efficiency was shown to vary significantly with seeding density (from 0.22 to 0.88 RPE foci/HESC colony). Not only did the higher density flasks produce more RPE, more rapidly, but the proportion of HESC colonies that generated RPE actually increased. This is the first study to our knowledge reporting this relationship in HESC-RPE differentiation and is in line with findings in other HESC differentiation protocols suggesting that high density cultures are conducive to anterior neuroectoderm differentiation (Chambers et al., 2009). An ideal HESC-RPE manufacturing process should generate the largest number of RPE foci, using the smallest amount of lab space, time, manual labour and raw materials (including HESC). Given that the same quantity of media, incubator space and manual labour was used for both low and high density flasks, there are clearly significant cost savings to be made by optimising seeding density.

These density optimisation experiments were repeated using a single cell dissociation protocol covering a larger range of densities. Single cell dissociation in HESC is usually avoided due to reportedly low viability (Watanabe et al., 2007). In this study it was shown that survival, proliferation and differentiation of both Shef6 and Shef3 following single cell dissociation is possible following a gentle enzymatic treatment and seeding at relatively high densities. It was observed that only very low density conditions (8500 cells/cm^2) were not permissive to cell survival. Using this new approach it was shown that the trend for increased process efficiency with increased HESC density reached a peak at 35,000 HESC/cm^2, above which, RPE yields per HESC cell were compromised. Establishing the optimum seeding density for large scale manufacturing will require the modelling of raw material and processing costs against the changing differentiation efficiencies reported here.

6.4 Dorsomorphin induced neuroectoderm conversion

We hypothesised that the low RPE differentiation yields seen in Shef3 could be improved by prompting neuroectodermal conversion with small molecules. Small molecules which interfere with key signalling pathways are powerful tools in stem cell research. Compared to growth factors they are less vulnerable to degradation in culture, are significantly cheaper and suffer from less batch to batch variability (Allsopp et al., 2010), properties which make them excellent tools for industrial application. Early treatment with the BMP/Activin/Nodal inhibitor dorsomorphin selectively upregulated neuroectoderm gene expression and simultaneously suppressed mesoderm, endoderm and trophectoderm expression, in both cell lines. In feeder-free, density optimised and defined differentiation conditions, the dorsomorphin induction step consistently enhanced Shef3 RPE yields. The Shef3–RPE cells derived from these cultures displayed typical pigmented cobblestone morphology and stained positively for classical RPE markers.

The ability to induce high RPE yields from otherwise recalcitrant cell lines may become important with the advent of IPSC technology, where the idea of patient-specific cell lines for personalised cell therapies is being proposed. In this scenario there would be a need for strategies to induce RPE differentiation in feeder-free,

clinically appropriate differentiation conditions regardless of the cell line's innate propensity for RPE differentiation (Boulting et al., 2011, Buchholz et al., 2009).

Shef6 consistently generated higher RPE yields than Shef3. When Shef6 were subjected to the same early dorsomorphin treatment however, pigmentation and RPE gene expression were suppressed and an upregulation in neural retinal marker Chx10 was observed. The reason for this disparity between cell lines requires further investigation; the neuroectoderm conversion may be too efficient in Shef6 in the presence of dorsomorphin and in the absence of MEFs or non neuroepithelial cells which secrete growth factors that mimic the environment of the extraocular mesenchyme, RPE differentiation is not induced (Hongisto et al., 2012, Meyer et al., 2011).

6.5 Future work

Despite the significant improvements in yield and reproducibility using the new protocols developed here, sources of variability clearly remain. We can only presume that the varying differentiation states of the seeded HESC are behind this variability. Although a protocol was developed to differentiate cells in density controlled, feeder-free conditions, they were expanded by traditional clump passaging in MEFs feeder co-culture and thus subject to the variations in environment that go with this method. It may prove to be beneficial to expand cells in feeder-free conditions for several passages prior to differentiation. Currently the high costs of mTeSR1 and other defined media formulations would make this challenging in a standard laboratory environment. .

Although the numbers of individual foci generated per HESC cell/ HESC colony and the % pigmented surface area were determined, a protocol that generated a suspension of single cells from differentiated flasks at day 50 without suffering significant cell losses was not established, due to the time available. As a result, the actual number of pigmented cells generated was not determined in this study. This did not interfere with our ability to compare differentiation efficiencies between protocols, as was the aim of this study, but it could hamper further process development. Thus, if given more time or resources we would focus the next part of the study on developing scalable and clinically appropriate methods to separate the pigmented foci from the non-pigmented background and in characterising the expansion capacity of the isolated foci. In a very recent study a strategy of clonal propagation and serial passaging claims to enrich for RPE cells generating up to 99% pigmented RPE cells, simply by repeated passaging (Maruottie et al., 2013). This is a promising strategy in terms of its scalability, however the limited proliferation capacity of HESC-RPE is well documented and thus the maintenance of RPE identity would need to be verified. The exact identity of the heterogeneous population of non-pigmented cells which co-emerge with RPE in standard HESC culture is unclear and presumably subject to the same level of sensitivity to culture conditions. Other studies have identified non-pigmented co-emerging cells as having characteristics of early forebrain derivatives (Meyer et al. 2011). From a validation

and safety perspective, it will be important to verify that these cells are removed prior to clinical implantation.

During the course of this project, loss of experiments due to cell sheet peeling and contamination was a significant problem. Transferring these protocols to dedicated clean room facilities would most likely reduce such occurrences. The protocol that we describe here is more amenable to automation that traditional current best practice methods. Whilst clump passaging is challenging to automate, HESC maintenance in a fully automated robotic platform using single cell passaging has been demonstrated (Thomas et al., 2008). In addition, flow rate controlled feeding could reduce losses due to disturbances of the cell sheet. The prolonged time required to generate pigmented cells (see table 1.1, median time to pigment = 28 days), combined with the daily media exchange requirement makes for a labour intensive and therefore expensive process. Automated cell feeding could lead to significant improvement in processing efficiencies. Incorporating automated cell culture into an imaging system for recording pigmentation could lead to the development of a high throughput screening platform, enabling rapid assessment of the optimal differentiation conditions for each cell line.

In a very recent report, pigmented RPE cells were generated from the H9 cell line in the significantly reduced time frame of 14 days, by the addition of several growth factors and small molecules (Buchholz et al., 2013, see table 1.1), thus proving that in vitro RPE differentiation need not follow the same time course as seen in vivo. This development, if applicable to multiple cell lines is a step forward that could lead to significant cost savings.

The expansion capacity of HESC make them ideal source for large scale production, but they present a number of unique challenges e.g. the long time scales required for RPE generation, karyotypic instability, the complexity of culturing methods, spontaneous differentiation, reliance on expensive recombinant growth factors and serum. In addition the use of HESC for commercial therapies is an ethical concern for some. The discovery and rapid developments in IPSC technology is likely to provide a less contentious alternative source of RPE in the future (Buchholz et al., 2009, Carr et al., 2009). In terms of manufacturing it is worth noting that IPSC

currently have similarly complex cell culturing requirements, on top of which the efficiency of their derivation from somatic cells is very poor (e.g. less than 0.001%, Hasegawa et al., 2010). Alternative methods for generating RPE may include somatic cell conversion strategies, which promise more rapid fibroblast-RPE conversion by bypassing the pluripotency stage (Zhang et al., 2013).

6.6 Conclusion

Since the serendipitous discovery in 2002 by Kawasaki and colleagues of Pax6 pigmented foci spontaneously appearing in cultures of primate ES cells (Kawasaki et al., 2002), RPE have been derived from a number of HESC and IPSC lines (table 1.1) . Until recently, there has been surprisingly little research focused on improving RPE differentiation yields using scalable and reproducible differentiation methods. A diverse range of protocols generate RPE from HESC and IPSC, including differentiating cells on a monolayer, growing them as suspended aggregates, directing differentiation with growth factors and small molecules or by spontaneous differentiation. Although the eventual number of RPE cells required per therapy is likely to be small (estimated at ~100,000 cells per therapy (Carr et al., 2013)), the cost and complexity of HESC culturing, coupled with the long time scales required for cells to differentiate, will mean that the HESC-RPE conversion efficiency is likely to be a key driver in the economic feasibility of any potential therapies. In this project the relative conversion efficiency of the HESC-RPE differentiation process was analysed and evaluated following a number of process changes aimed at improving the scalability, reproducibility and target cell yield. Several critical parameters were identified that could help develop a robust, scalable and cost-effective strategy for wide-scale HESC-RPE manufacturing. It is hoped that these process improvements will become widely adopted and will have the predicted beneficial effects on reducing the costs of RPE generation. Reduced manufacturing costs will ultimately increase the availability of RPE implantation as a therapy to ameliorate common and incurable forms of blindness.

Appendix : Validating changes to HESC-RPE differentiation process

A.1 Introduction

This chapter has been included to meet the requirements of the Validation II module of the EngD programme; in it the key validation issues relating to the research presented in this thesis will be outlined and discussed. Clinical approval for the use of HESC-derived RPE at the London Project to cure Blindness has recently been granted, demonstrating that the regulatory and validation requirements have been met using the current process for HESC-RPE manufacture. Thus this chapter concerns the regulatory requirements incurred by changes to the manufacturing procedure and critically assesses their potential value in a scaled up manufacturing process.

The objective of this research has been to understand and improve the efficiency of the current processes for manufacturing RPE from HESC for the treatment of AMD. The finished product of the RPE manufacturing procedure is a 3mm by 6mm polyester patch seeded with approximately 100,000 pigmented RPE cells derived from the Shef1 cell line (Carr et al., 2013). The procedure currently used at The London Project to generate and expand HESC-RPE is sufficient to produce material for small scale animal studies; however significant challenges may arise in designing and validating a more economical, scaled up process. At present the quantity of material produced per batch is highly variable, and the key process parameters that cause this variability are not fully understood. It was the aim of this thesis to investigate some of the sources of variability in the process and their respective impact on RPE derivation, with a view to optimising HESC-RPE manufacture. These improvements in manufacturing procedures ultimately aim to reduce the cost of goods (COG) which can be achieved via several mechanisms:

1. Improving the over all HESC-RPE differentiation efficiency
2. Reducing the cost and/or quantity of raw materials required
3. Reducing the time and physical lab space required to create the final product
4. Reducing the manual labour requirement
5. Reducing the regulatory burden

The outcomes of this study as well as the recent work of others have identified several process parameters which have a significant impact on HESC-RPE differentiation yield and over all process efficiency:

- Cell line characteristics
- Differentiation method (Embryoid body, continuous adherent culture, single cell seeding etc.)
- Feeder cell co-culture vs. feeder-free differentiation
- The substrate used for RPE differentiation and expansion phases
- Addition/withdrawal of growth factors and/or small molecules from the growth and differentiation medium
- Separation and enrichment of pigmented RPE cells from contaminating non-pigmented cells.

Adjusting these parameters, whilst improving differentiation efficiency and reducing processing costs, will have significant validation and regulatory implications the nature of which are discussed in this chapter.

A.2 Validation Issues

In order to validate any changes to the HESC-RPE manufacturing procedure, the goal will be to create a set of specifications that, when met, ensure the product is equivalent to that generated using current processes, in terms of both safety and efficacy. These criteria should be used to test the manufacturing processes and ensure that all processes are kept within pre-determined windows of operation. When adhered to, these process validation criteria should help to minimise batch-batch variability in the product. Planning the IQ, OQ and PQ will only be possible once the process has been further defined, developed and optimised. This will involve establishing process robustness, determining the windows of operation, and testing the operating extremes. The following summarises the key validation issues that are likely to arise as changes to the manufacturing procedure are implemented.

A.2.1 Additional pluripotent cell line characterisation

Although early clinical studies using HESC derived RPE currently make use of only one cell line (Schwartz et al., 2012, Carr et al., 2013), if early clinical studies prove successful, patient specific IPSC derived RPE or HESC derived, HLA matched cell therapies may be required which will demand the use of multiple cell lines (Carpenter et al., 2009). When validating new cell lines for clinical use an important property to assess is karyotypic stability. HESC cells in culture will occasionally undergo random chromosomal rearrangements, which may cause them to become more abundant in culture than cells with normal karyology (Baker et al., 2007). This may affect the propensity of the cells to differentiate into the desired phenotype and could pose a safety risk (e.g. by giving the cells cancerous properties) (Blum et al., 2008). The rate at which these events occur may vary considerably between cell lines. In order to account for this, a percentage of the growing cells must be regularly karyotyped for validation purposes. It may be necessary to undergo this testing at the beginning of expansion, and at the end of the expansion phase. Karyotypic changes

occur during cell division and accumulate during prolonged growth periods (Baker et al., 2007); differentiated HESC-RPE cells undergo few cell divisions when spatially constricted. If the cells prove to be normal after expansion therefore, they will not undergo any further karyotypic changes prior to administration. Karyotypically normal cells can be banked by cryopreservation in vials which can be defrosted and expanded as required in a defined number of passages. If all culturing conditions are kept constant and the cells are not put under any undue stress, this should reduce the probability of karyotypically abnormal cells becoming abundant in culture.

In this study we have demonstrated innate variability in the differentiation rates of different cell lines. This will be an important consideration in the validation of new cell lines. Of particular concern is the rate at which cells depart from the pluripotent state as the transplantation of pluripotent cells may pose a significant risk to patients (Lu et al., 2009). With current protocols, Shef1 derived RPE are cultured for prolonged periods of time following their initial emergence in culture (5-6 weeks) which partly serves to reduce the risk of pluripotent cells remaining; the required time to negate this possibility in new cells lines will have to be assessed and validated.

Another finding of this study was that different cell lines produced significantly different RPE yields over the same time period in culture. This could indicate differences in the relative proportions of contaminating cell types between different cell lines. It may be necessary to apply additional testing confirming the absence of non-RPE cell types in the mechanically isolated pigmented foci. This should include testing for pigmented cell types than are not RPE such as neural crest derived melanocytes; although these cells do not appear in standard culture conditions in Shef1 nor Shef6/3, they may arise in as yet uncharacterised cell lines each with distinct innate differentiation preferences.

If multiple cell lines are going to be used for tailor made HLA matched HESC-RPE or IPSC-RPE therapies, a plethora of sample segregation protocols will have to be implemented. These will include issues surrounding lot segregation, area clearance, material tracking and lot paperwork review and approval (Mason et al., 2007).

A.2.2 Feeder-free derivation and Raw Materials

A number of the materials currently used to derive and grow HESC cells are animal derived (table 6.1). These present a validation challenge in terms of controlling batch to batch variability and, for regulatory purposes, demonstrating the absence of animal derived pathogens/immunogenic components. Human foreskin fibroblasts (HFFs) are now used is place of MEFs in the preparation of Shef1 RPE for clinical trials, which reduces the risk of xenogeneic contamination. Never the less significant logistical and validation challenges remain in the use of an additional feeder cell line including the necessity of proving batch to batch equivalence in the feeder cells. Validating the use of these materials is likely to require the regular sampling and associated paperwork at significant cost.

Material	**Xenogenic component**
Mouse embryonic fibroblast layer	Derived from CF1 mice
Knockout serum replacement	Contains bovine serum albumin
Gelatine	Derived from Porcine Skin

Table A.1.Xenogeneic materials in standard HESC culture

In this study we have demonstrated feeder cell free HESC differentiation using defined media mTeSR1 and matrigel matrix which is derived from the Englebreth-Holm-Swarm sarcoma. New xeno-free, human-derived, good manufacturing practice- compliant medias and matrices have since become commercially developed (Table 2.) Assuming HESC-RPE can be successfully derived in these new medias/matrices (as is the case with mTeSR1 and Matrigel), switching to feeder-free differentiation will significantly reduce the regulatory burden as well as simplifying cell culturing logistics. It will be necessary to batch test new matrices and media to demonstrate lot-lot equivalence and sterility.

Current component	Feeder-free alternative	Source
MEFs or HFFs, DMEM/ 20% KOSR	TeSR2 media	Stemcell technologies, Vancouver, Canada
	StemPro media,	Invitrogen, Paisley, UK
	NutriStem Media*	Stemgent, MA, USA
	CELLstart matrix,	Invitrogen, Paisley, UK
	Synthemax* matrix	Corning, NY, USA

Table A.2 Xeno-free materials developed for HESC culture with potential use in 'feeder-free' HESC-RPE differentiation. (* These materials have very recently been used for completely Xenogeneic component free retinal differentiation of IPSCs, see discussion (Sridhar et al., 2013)).

In this study we have demonstrated the phenotypic equivalence of feeder cell free derived RPE, in terms of morphology and marker expression. For industrial validation of this new technique however it will be necessary to carry out a more comprehensive set of characterisation experiments to determine equivalence of the finished product (see section 7.2.5).

A.2.3 Differentiation yield assessment by image analysis

In this study we have demonstrated how differences in culture conditions (density, cell line, feeder-free differentiation etc.) can alter the rates of RPE emergence. This is an important area for process optimisation and could lead to significant cost and efficiency savings. In order to monitor the differentiation rates we have developed a semi automated image capture and analysis system. This has the potential to be incorporated into a cGMP environment so that on-line monitoring of the differentiation progress can be achieved. In addition to the potential cost and efficiency savings, monitoring the timing of foci emergence may have important implications on product consistency. It has been well documented that HESC derived RPE have limited proliferative capacity, gradually de-differentiating and eventually irreversibly de-pigmenting and adopting mesenchymal characteristics. Thus it is desirable from a validation perspective to isolate the emerging RPE at a defined time point following their emergence in culture. In addition to undertaking the required

cleaning procedures and associated documentation to make the scanning device cGMP compliant, the image recognition capacity should be validated in relation to biological assays. Individual foci detected by the image analysis should be isolated and global gene expression analysis used to assess their relative differentiation states.

A.2.4 Cell separation

In the current process pigmented RPE cells are separated from a mixed background of cells (both undifferentiated stem cells and various other differentiated phenotypes) via a process of manual dissection using microsurgical blades. Pigmented regions are identified by the operator and the surrounding non-pigmented cells are dissected away from it. The pigmented foci are then plated onto matrigel for further expansion. This manual separation is not very amenable to validation since the quality of cell separation is highly dependent on the operator.

Differences in RPE differentiation yield may also affect the suitability of pigmented foci isolation procedures at the end of the differentiation. For example whilst one operator may be able to comfortably isolate the 100 or so foci that typically arise in one cell line, another cell line producing 300-400 will require additional time in the cGMP facility, additional operators and potentially a entirely new foci isolation strategy. These changes will have to be validated and incorporated into the manufacturing plan when new cell lines are included.

There is potential to use fluorescence activated cell sorting (FACS) or magnetic activated cell sorting (MACS) to isolate the desired cell type. However after 3 weeks of differentiation, cells are entangled in a tough extra-cellular matrix, this presents significant problems in making the single cell suspension necessary for FACS and could lead to large product losses. Should further optimisation of the enzymatic dissociation render this method more efficient, its accuracy and reliability would have to be validated as well as any enzymes used included in the list of raw materials to be approved for clinical use. FACS based selection has the advantage that cells

could be sorted on the basis of pigmentation, avoiding the need to include and validate the use of primary and secondary antibodies in the manufacturing. An alternative separation technique could employ semi-automated laser-assisted micro dissection (Terstegge et al., 2009). In this case image recognition software and laser micro-dissection would have to be proven to meet acceptable standards of accuracy and reliability.

A.2.5 Characterization of HESC RPE

The ultimate goal of a validation strategy is to ensure that the finished product will reliably be both safe and efficacious. As we have seen in this study, alterations in differentiation methods and materials can have a dramatic effect on the RPE differentiation yield; our characterisation studies however suggest when isolated and re-plated the expanded RPE cells have very similar characteristics irrelevant of how they were derived. For clinical use however a very comprehensive set of assays will be required to ensure product equivalence. Having established equivalence, batch release criteria should be drawn up. When met these criteria should confirm the identity of the cell population as fully differentiated and functional RPE. In the current process pigmented cells are manually isolated from the differentiating Shef1 HESC before being plated onto CELLstart for expansion over 5-6 weeks. During this time the cells de-differentiate and re-differentiate as they proliferate and over time express an increasing number of markers typical of native human RPE cells. This process of maturation can be monitored by way of gene expression and proteomic analysis. Validation might involve taking samples from dissociated HESC-RPE which have been identified as ‘mature’ by analysis of morphology or level of pigmentation. These samples could then be analysed by way of quantitative PCR (QPCR) and western blot analysis. In this instance the release criteria for a batch could be the fold increase in expression of ‘mature’ RPE genes such as RPE65, CRALBP, Bestrophin, PEDF and Tyrosinase and the concurrent fold decrease in expression of stem cell associated genes such as Oct4, Nanog and Sox2. QPCR is a particularly useful technique in that many genes can be analysed concurrently on a 96 well plate using very small quantities of sample. This analysis could be confirmed

by western blotting; comparing the expression of RPE related genes in the HESC-RPE line to that of an established RPE cell line or foetal RPE. In addition to QPCR, assessing levels of pigmentation by image analysis is a good technique for assessing cell confluence and relative maturation. The presence of mature RPE specific proteins such as PMEL17 could also be assessed by immunocytochemistry performed on patches from a particular batch. The specific quantities which determine the lot release criteria could be established by relation to functional assays such as phagocytosis assays which tests the cells ability to phagocytose fluorescently labelled rod and cone outer segments (Carr et al., 2009), assays to measure PEDF and VEGF secretion (Maminishkis et al., 2006) and studies in rodent models. These gene expression and proteomic assays would have to be performed on samples from each batch. Image analysis is a non-destructive monitoring technique and could be performed on each individual patch.

A.2.6 Storage and handling

Although not within the scope of this thesis, storage and transportation will be a key validation issue in the large scale production of HESC-RPE. If the RPE cells are to be manufactured at a centralised facility prior to transportation, the storage and handling during transfer must be carefully planned. This might include a process of freezing the cells in which case cell viability after thawing must be accounted for. The temperature of the transportation vessel must be monitored and kept within pre-determined limits e.g. 1-2 degrees Celsius for live cells and 2-5 degrees for cryopreserved cells.

A.3 Key Regulatory Issues

Human embryonic stem cell based therapies are very much in their infancy with only two therapies granted approval to enter clinical trials in the US and UK. It will be necessary to define with the regulatory authorities a reasonable set of regulations with which a HESC derived product must adhere.

The regulatory issues applicable to HESC-RPE will concern the safety and efficacy of the cell product. In terms of safety, immunogenicity and tumorigenicity will be primary concerns. In terms of efficacy, designing clinical trials that will prove that HESC-RPE can ameliorate the effects of macular degeneration to an extent that justifies the risk and cost to the patient will be the aim. In addition establishing the potency of the cells and regulating/optimising the dose will be a primary concern.

Immunogenicity:

This HESC-RPE therapy for AMD would be allogeneic i.e. cells derived from one donor will be implanted into all patients. This has obvious implications in immunogenicity of the implanted cells. It is often stated that the eye is an 'immune-privileged site' owing to the blood-retinal barrier separating the retina; however this barrier can be compromised in diseased retinas (Da Cruz et al., 2007). It has been proposed that a course of anti-inflammatory, immunosuppressive drugs could be prescribed after the initial surgery and then stopped after the implantation site has healed (Schwartz et al., 2012).

Aside from the potential immunogenicity of the transplanted cells themselves, regulators will require proof that no contaminating agents (viruses, bacteria, mycoplasma) have been incorporated into the product during the processing which may proliferate inside a host or illicit an immune response. This concerns the HESC, the mouse embryonic feeder layer and any animal derived media components such as serum replacement. This will be of particular concern when products are bovine derived. All cell handling must be carried out in state of the art clean room facilities

to avoid contamination. This should include the use of fully validated ISO class 5 bio safety cabinets in a fully validated ISO class 7 clean room under environmental control. In addition regular testing during processing should be used to confirm the absence of contamination in cells and materials.

Teratoma formation:

One of the primary concerns regarding HESC based therapies is the ability of HESC cells to form teratomas in vitro. These are benign tumours consisting of a mix of unwanted cells. They form when undifferentiated stem cells are administered into a live animal or when cells have acquired a karyotypic change that affords them a growth advantage and tumorigenic characteristics. The chance of teratoma formation increases in proportion with the specific number of undifferentiated cells administered (Blum et al., 2008). It will be essential to regulate the removal of undifferentiated cells from the product, and to demonstrate the absence of tumorigenesis during early pre-clinical trials, in order to satisfy regulators.

HESC spiking studies could be performed throughout the differentiation process to assess the survival of any undifferentiated cells. Undifferentiated cells can be detected by way of antibody staining owing to the specific antigens residing on an undifferentiated cell's surface. An alternative might be the use of antibodies which specifically bind to and induce apoptosis of undifferentiated HESC. The potential toxicity of this type of molecule however means that safety data would have to be gathered and an effective method for its removal established.

Clinical trial design:

There is currently no viable treatment for dry macular degeneration and patients usually become legally blind within 10 years of the onset of notable visual impairment. In designing an appropriately controlled clinical trial for a HESC-RPE therapy, it will be necessary to consider the nature of the disease and of this potential treatment. HESC-RPE would be administered to patients preferably with early stage AMD on a 2 by 3mm polyester patch. The hope is that the HESC-RPE will prevent further degeneration of vision, but it is unlikely to restore vision that has already

been lost. Therefore a clinical trial would have to monitor the decline or otherwise in visual acuity of HESC-RPE transplanted patients over the duration of at least 10 years. The trial design will be challenging as the disease progresses differently in different patients and it would be unethical to implant an empty graft into the control group. However, the disease is common, and there is no alternative cure; meaning that finding sufficient volunteers to assemble age-matched and disease phenotype-matched controls should be possible. It is relatively easy to monitor the state of the retina using Fundus photography. This is helpful for physiological examination of the disease progress once the cells have been administered. Methods for examination would have to be standardised to guarantee the acquisition of comparable data between patients.

A.4 Conclusion

The current processes for deriving HESC-RPE for early clinical trials can generate sufficient material for small scale studies. Subsequent advancements in techniques for HESC maintenance and differentiation have the potential to improve upon the efficiency of RPE manufacture substantially, which could lead to reduced processing and product costs. This can be achieved by improving differentiation yield, reducing the raw material costs and reducing the labour and time requirements. The results chapters of this thesis have demonstrated how small changes to cell processing can dramatically affect the RPE yield, although the identity of the final product appears unchanged. In order to gain regulatory approval for any cell processing changes, a set of assays which comprehensively prove RPE product equivalence will be required. These assays should focus on survival and functionality, particularly pigmentation, growth factor secretion and phagocytosis. Of particular concern to the regulator will be proving the absence of undifferentiated HESC and adventitious agents such as viruses and mycoplasma.

References

Abeyta MJ, Clark AT, Rodriguez RT, Bodnar MS, Pera R, Firpo MT. (2004). Unique gene expression signatures of independently-derived human embryonic stem cell lines. *Human molecular genetics*,13(6):601–8.

Adler R, Canto-Soler MV. (2007). Molecular mechanisms of optic vesicle development: complexities, ambiguities and controversies. *Developmental biology*.,305(1):1–13.

Aflatoonian B, Ruban L, Shamsuddin S, Baker D, Andrews P, Moore H. (2010). Generation of Sheffield (Shef) human embryonic stem cell lines using a microdrop culture system. *In vitro cellular & developmental biology. Animal*.,46(3-4):236–41

Akopian V, Andrews PW, Beil S, Benvenisty N, Brehm J, Christie M, Ford A, Fox V, Gokhale PJ , Healy L, Holm F, Hovatta O, Knowles B, Ludwig TE McKay RDG , Miyazaki T , Nakatsuji N, Oh SKW, Pera MF , Rossant J, & Stacey GN, Suemori H. (2010). Comparison of defined culture systems for feeder cell free propagation of human embryonic stem cells. *In vitro cellular & developmental biology. Animal*,46(3-4):247–58.

Alge CS, Suppmann S, Priglinger SG, Neubauer AS, May CA, Hauck S, Lussen U, Ueffing M, Kampik A. (2003). Comparative proteome analysis of native differentiated and cultured dedifferentiated human RPE cells. *Investigative Ophthalmology and Visual Science,* 44: 3629–3641

Algvere P V, Berglin L, Gouras P, Sheng Y. (1994). Transplantation of fetal retinal pigment epithelium in age-related macular degeneration with subfoveal neovascularization. *Graefe's archive for clinical and experimental ophthalmology,* 232(12):707–16.

Allegrucci C & Young LE. (2007). Differences between human embryonic stem cell lines. *Human reproduction update*. 13(2):103–20.

Allsopp TE, Bunnage ME, Fish PV. (2011). Small molecule modulation of stem cells in regenerative medicine: recent applications and future direction. *MedChemComm*. 1(1):16.

Allikmets, R. (2000). Simple and complex ABCR: genetic predisposition to retinal disease.*American Journal of Human Genetics,*67, 793–799.

Alva JA, Lee GE, Escobar EE, Pyle AD. (2011). PTEN Regulates the Pluripotent State and Lineage Fate Choice in Human Embryonic Stem Cells. *Stem Cells*, 29(12):1952-62

Amit M, Carpenter MK, Inokuma MS, Chiu CP, Harris CP, Waknitz MA, Itskovitz-Eldor J, Thomson JA. (2000). Clonally derived embryonic stem cell lines maintain pluripotency and proliferative potential for prolonged periods in culture. *Developmental Biology,*227, 271-278.

Azuma N, Tadokoro K, Asaka A, Yamada M, Yamaguchi Y, Handa H, Matsushima S, Watanabe T, Kida Y, Ogura T, Shimamura K, Nakafuku M. (2005). The Pax6 isoform bearing an alternative spliced exon promotes the development of the neural retinal structure. *Human molecular genetics*.,14(6):735–45.

Baker DEC, Harrison NJ, Maltby E, Smith K, Moore HD, Shaw PJ, Heath PR, Holden H, Andrews PW. (2007). Adaptation to culture of human embryonic stem cells and oncogenesis in vivo. *Nature biotechnology*.,25(2):207–15

Bailey T.J, El-Hodiri, H, Zhang, L, Shah, R, Mathers, P.H, Jamrich M. Regulation of vertebrate eye development by Rx genes. (2004). *International Journal of Developmental Biology,* 48(8-9): 761-70.

Bauwens CL, Peerani R, Niebruegge S, Woodhouse KA, Kumacheva E, Husain M, Zandstra PW. (2008). Control of human embryonic stem cell colony and aggregate size heterogeneity influences differentiation trajectories. *Stem cells (Dayton, Ohio)*,26(9):2300–10.

Beattie, G. M., Lopez, A. D., Bucay, N., Hinton, A., Firpo, M. T., King, C. C., & Hayek, A. (2005). Activin A maintains pluripotency of human embryonic stem cells in the absence of feeder layers. *Stem cells (Dayton, Ohio)*, *23*(4): 489–95

Beatty, S. Koh H, Phil M, Henson D, Boulton M. (2000). The role of oxidative stress in the pathogenesis of age-related macular degeneration. *Survey of Ophthalmology,* 45: 115–134.

Bendall SC, Stewart MH, Menendez P, George D, Vijayaragavan K, Werbowetski-Ogilvie T, Ramos-Mejia V, Rouleau A, Yang J, Bossé M, Lajoie G, Bhatia M. (2007). IGF and FGF cooperatively establish the regulatory stem cell niche of pluripotent human cells in vitro. Nature, 448: 1015-1023

Bendall, S. C., Hughes, C., Campbell, J. L., Stewart, M. H., Pittock, P., Liu, S., Lajoie, G. (2009). An enhanced mass spectrometry approach reveals human embryonic stem cell growth factors in culture. Molecular & cellular proteomics : MCP, 8(3): 421–32.

Bharti, K., Nguyen, M.T, Skuntz, S., Bertuzzi, S, & Arnheiter, H. (2006). The other pigment cell: specification and development of the pigmented epithelium of the vertebrate eye. *Pigment cell research*, *19*(5): 380–94.

Binder, S., Stolba, U., Krebs, I., Kellner, L., Jahn, C., Feichtinger, H., Krugluger, W. (2002). Transplantation of autologous retinal pigment epithelium in eyes with foveal neovascularization resulting from age-related macular degeneration: a pilot study. *American journal of ophthalmology*, *133*(2): 215–25.

Binder, S, Krebs I, Hilgers RD, Abri A, Stolba U, Assadoulina A, Kellner L, Stanzel BV, Jahn C, Feichtinger H. (2004). Outcome of transplantation of autologous retinal pigment epithelium in age-related macular degeneration: a prospective trial. *Investigative Ophthalmology and Visual Sciences*, 45: 4151–4160.

Bird, A.C & Marshall J. (1986). Retinal pigment epithelial detachments in the elderly. *Transaction of the ophthalmological society UK*, 105 (6): 674–682.

Blum, B. & Benvenisty N. (2008). The tumorigenicity of Human Embryonic Stem Cells. *Advances in Cancer Research,* 100: 133-158.

Boland MJ, Hazen JL, Nazor KL, Rodriguez AR, Gifford W,Martin G, Kupriyanov S & Baldwin KK. (2009). Adult mice generated from induced pluripotent stem cells. *Nature.* 461: 91–94

Boulton, M, Marshall, J., Mellerio, J., (2001). The role of retinal pigment epithelium: topographical variation and ageing changes. *Eye,* 15(3), 384-9.

Boulting, G. L., Kiskinis, E., Croft, G. F., Amoroso, M. W., Oakley, D. H., Wainger, B. J., Eggan, K. (2011). A functionally characterized test set of human induced pluripotent stem cells. *Nature biotechnology*, *29*(3), 279-286

Boncinelli E & Mallamaci A. (1995). Homeobox genes in vertebrate gastrulation. *Current Opinion in Genetics and Development*, 5, 619–628.

Boyer, L. a, Lee, T. I., Cole, M. F., Johnstone, S. E., Levine, S. S., Zucker, J. P., Young, R. (2005). Core transcriptional regulatory circuitry in human embryonic stem cells. *Cell*, *122*(6), 947–56.

Bovolenta, P., Mallamaci A, Briata P, Corte G, Boncinelli E (1997). Implication of OTX2 in pigment epithelium determination and neural retina differentiation. *The Journal of neuroscience : the official journal of the Society for Neuroscience*, 17(11), 4243-52.

Bratt-Leal, A.M., Carpenedo RL, Ungrin MD, Zandstra PW & McDevitt TC (2009). Engineering the embryoid body microenvironment to direct embryonic stem cell differentiation. *Biotechnology Progress*, 25(1), 43-51.

Bressler, N.M. (2000). Age related macular degeneration: new hope for a common problem comes from photodynamic therapy. *British Medical Journal,* 321, 1425-1427.

Brown S, Teo A, Pauklin S, Hannan N, Cho CH, Lim B, Vardy L, Dunn NR, Trotter M, Pedersen R, Vallier L. (2011). Activin / Nodal Signalling Controls Divergent Transcriptional Networks in Human Embryonic Stem Cells and in Endoderm Progenitors. *Stem cells*, 29, 1176-1185.

Buchholz, D. E., Hikita, S. T., Rowland, T. J., Friedrich, A. M., Hinman, C. R., Johnson, L. V, & Clegg, D. O. (2009). Derivation of functional retinal pigmented epithelium from induced pluripotent stem cells. *Stem cells, 27*(10), 2427–34.

Buchholz, D. E., Pennington, B. O., Croze, R. H., Hinman, C. R., Coffey, P. J., & Clegg, D. O. (2013). Rapid and efficient directed differentiation of human pluripotent stem cells into retinal pigmented epithelium. *Stem cells translational medicine*, *2*(5), 384–93.

Canto-Soler, M. & Adler R. (2006). Optic cup and lens development requires Pax6 expression in the early optic vesicle during a narrow time window. *Developmental Biology,* 294, 119–132.

Carr, A.J., Vugler, A. a, Hikita, S. T., Lawrence, J. M., Gias, C., Chen, L. L. & Coffey, P. J. (2009). Protective effects of human iPS-derived retinal pigment epithelium cell transplantation in the retinal dystrophic rat. *PloS one*, *4*(12).

Carr, A.J., Vugler, A., Lawrence, J., Chen, L. L., Ahmado, A., Chen, F. K & Coffey, P. J. (2009). Molecular characterization and functional analysis of phagocytosis by human embryonic stem cell-derived RPE cells using a novel human retinal assay. *Molecular vision*, *15*(January), 283–95.

Carr, A-J. F., Smart, M. J. K., Ramsden, C. M., Powner, M. B., da Cruz, L., & Coffey, P. J. (2013). Development of human embryonic stem cell therapies for age-related macular degeneration. *Trends in neurosciences*, *36*(7), 385–95.

Carpenter, M.K., Rosler E & Rao MS. (2003). Characterization and Differentiation of Human Embryonic Stem Cells. *Cloning and Stem Cells*, 5(1), 79-89.

Carpenter, M. K., Frey-Vasconcells, J & Rao, M. S. (2009). Developing safe therapies from human pluripotent stem cells. *Nature biotechnology*, *27*(7), 606–13.

Chambers, S. M., Fasano, C. A., Papapetrou, E. P., Tomishima, M., Sadelain, M. & Studer, L. (2009). Highly efficient neural conversion of human ES and iPS cells by dual inhibition of SMAD signalling. *Nature Biotechnology*, 27(3), 275 – 280.

Chen, L. & Daley GQ. (2008). Molecular basis of pluripotency. *Human Molecular Genetics*. 17(1), 23-27.

Chen, H.-F., Chuang, C.-Y., Shieh, Y.-K., Chang, H.-W., Ho, H.-N., & Kuo, H.-C. (2009). Novel autogenic feeders derived from human embryonic stem cells (hESCs) support an undifferentiated status of hESCs in xeno-free culture conditions. *Human reproduction, 24*(5), 1114–25.

Chickarmane, V., Troein, C., Nuber, U. a, Sauro, H. M., & Peterson, C. (2006). Transcriptional dynamics of the embryonic stem cell switch. *PLoS computational biology*, *2*(9), e123.

Chin M.H, Mason M.J, Xie, W, Volinia S, Singer M, Peterson C, Ambartsumyan G, Aimiuwu O, Richter L, Zhang J, Khvorostov I, Ott V, Grunstein M, Lavon N, Benvenisty N, Croce CM, Clark AT, Baxter T, Pyle AD, Teitell MA, Pelegrini M, Plath K, Lowry WE., 2009. Induced pluripotent stem cells and embryonic stem cells are distinguished by gene expression signatures. *Cell Stem Cell* 5, 111–123.

Chin, A. C. P., Fong, W. J., Goh, L.-T., Philp, R., Oh, S. K. W., & Choo, A. B. H. (2007). Identification of proteins from feeder conditioned medium that support human embryonic stem cells. *Journal of biotechnology*, *130*(3), 320–8.

Chin, B., Liu, H. U. A., Rufaihah, A. J., & Cao, T. (2006). Human Embryonic Stem Cell (hES) colonies display a higher degree of spontaneous differentiation when passaged at lower densities. *In vitro cellular & developmental biology animal*, 42(3), 54-57.

Chin, A. C. P., Padmanabhan, J., Oh, S. K. W., & Choo, A. B. H. (2010). Defined and serum-free media support undifferentiated human embryonic stem cell growth. *Stem cells and development*, *19*(6), 753–61.

Chopdar, A., Chakravarthy, U., & Verma, D. (2003). Age related macular degeneration. *BMJ (Clinical research ed.)*, *326*(7387), 485–8.

Chow, R. L., Altmann, C. R., Lang, R. a, & Hemmati-Brivanlou, a. (1999). Pax6 induces ectopic eyes in a vertebrate. *Development (Cambridge, England)*, *126*(19), 4213–22.

Chow, R.L & Lang RA. (2001). Early eye development in vertebrates. *Annual Review Of Cell and Developmental Biology*, 17, 255–296.

Clarke, L., Ballios, B. G., & van der Kooy, D. (2012). Generation and clonal isolation of retinal stem cells from human embryonic stem cells. *The European journal of neuroscience*, *36*(1), 1951–9.

Coffey PJ, Gias C, McDermott CJ, Lundh, P, Pickering, M, Sethi, C Bird, A, Fitzke, FW, Maass, A, Chen, L, Holder, G, Luthert, P J, Salt, T E Moss, S E & Greenwood, J (2007). Complement factor H deficiency in aged mice causes retinal abnormalities and visual dysfunction. *Proc. Natl. Acad. Sci.* 104(42):16651–6

Coffey PJ., Girman, S, Wang, SM , Hetherington L, Keegan, DJ, Adamson, P, Greenwood, J., Lund, R D (2002). Long-term preservation of cortically dependent visual function in RCS rats by transplantation. *Nature Neuroscience* 5, 53–56.

Cowan CA, Klimanskaya I, McMahon J, Atienza J, Witmyer J, Zucker JP, Wang S, Morton CC, McMahon AP, Powers D, Melton DA. (2004). Derivation of embryonic stem cell lines from hu man blastocysts. *New England Journal of Medicine* 350, 353–356.

Crook, J. M., Peura, T. T., Kravets, L., Bosman, A. G., Buzzard, J. J., Horne, R. & Colman, A. (2007). The Generation of Six Clinical-Grade Human Embryonic Stem Cell Lines. *Cell stem cell*, *1*(5), 490–494. doi:10.1016/j.stem.2007.10.004

Cskay K. (2003). Anti-Vascular Endothelial Growth Factor Therapy for Neovascular Age-related Macular Degeneration, Promises and Pitfalls. *Ophthalmology. 110(5), 879-881.*

Curico C.A., Sloan KR., Kalina RE, Hendrikson & AE. (1990). Human photoreceptor topography. *Journal of Computational Neurobiology,* 292, 497-523.

Da Cruz, L, Chen FK, Ahmado A, Greenwood J, and Pete Coffey. (2007). RPE Transplantation and Its Role in Retinal Disease. *Progress in retinal and eye research* 26(6): 598–635.

Damjanow, I. (1993). Teratocarcinoma: neoplastic lessons about normal embryogenesis. *International Journal of Developmental Biology,* 37, 39-46.

D'Amour, K. a, Agulnick, A. D., Eliazer, S., Kelly, O. G., Kroon, E., & Baetge, E. E. (2005). Efficient differentiation of human embryonic stem cells to definitive endoderm. *Nature biotechnology*, *23*(12), 1534–41.

Dawson, D.W., Volpert OV, Gillis P, Crawford SE, Xu H, Benedict W, Bouck NP.(1999). Pigment epithelium-derived factor: a potent inhibitor of angiogenesis. *Science,* 285, 245–248,

Dang, S.M, Kyba M, Perlingeiro R, Daley GQ, Zandstra PW (2002). Efficiency of embryoid body formation and hematopoietic development from embryonic stem cells in different culture systems. *Biotechnology and Bioengineering,* 78, 442–453.

D'Cruz, P.M, Yasumura, D.,Weir, J., Matthes, M T., Abderrahim, H., LaVail, M M., Vollrath, D. (2000). Mutation of the receptor tyrosine kinase gene Mertk in the retinal dystrophic RCS rat. *Human Molecular Genetics*, 9, 645–651.

Ding, V.M., Ling, L., Natarajan, S., Yap, MG., Cool, SM., & Choo AB. (2010). FGF-2 Modulates Wnt Signalling in Undifferentiated hESC and iPS Cells through Activated PI3-K/GSK3β signalling. *Journal of Cellular Physiology*, 417-428.

Draper, J. S., Pigott, C., Thomson, JA, & Andrews, P. W. (2002). Surface antigens of human embryonic stem cells: changes upon differentiation in culture. *Journal of anatomy*, *200*(Pt 3), 249–58.

Draper, J. S., Moore, H. D., Ruban, L. N., Gokhale, P. J., & Andrews, P. W. (2004). Culture and characterization of human embryonic stem cells. *Stem cells and development*, *13*(4), 325–36

Edwards AO, Abel, KJ, Manning A, Panhuysen C, Farrer LA. (2005). Complement factor H polymorphism and age-related macular degeneration. *Science.* 308 (5720), 421–424.

Eiraku, M., Takata, N., Ishibashi, H., Kawada, M., Sakakura, E., & Okuda, S. (2011). Self-organizing optic-cup morphogenesis in three-dimensional culture. *Nature*, *472*(7341), 51–56.

Elkabetz, Y., Panagiotakos, G., Shamy, G. Al, Socci, N. D., & Tabar, V. (2008). Human ES cell-derived neural rosettes reveal a functionally distinct early neural stem cell stage, 152–165.

Ellerström, C., Strehl, R., Noaksson, K., Hyllner, J., & Semb, H. (2007). Facilitated expansion of human embryonic stem cells by single-cell enzymatic dissociation. *Stem cells (Dayton, Ohio)*, *25*(7), 1690–6.

Eminli S, Foudi A, Stadtfeld M, Maherali N, Ahfeldt T, Mostoslavsky G, Hock H & Hochedlinger K. (2009). Differentiation stage determines potential of hematopoietic cells for reprogramming into induced pluripotent stem cells. *Nature Genetics* 41: 968–976.

Enver, T, Soneji, S, Joshi, C, Brown, J, Iborra, F, Orntoft, T, Thykjaer, T, Maltby, E.,Smith, K.,Dawud, RA.,Jones, M.,Matin, M.,Gokhale, P.,Draper, J & Andrews, P. W. (2005). Cellular differentiation hierarchies in normal and culture-adapted human embryonic stem cells. *Human molecular genetics*, *14*(21), 3129–40.

Engelhardt, M., Bogdahn, U & Aigner, L. (2005). Adult retinal pigment epithelium cells express neural progenitor properties and the neural precursor protein doublecortin. *Brain research*, 1040(1-2), 98-111.

Esteve, P. & Bovolenta P. (2006). Secreted inducers in vertebrate eye development: more functions for old morphogens. *Current Opinion in Neurobiology*. 16, 13–19.

Feng Q, Lu SJ, Klimanskaya I, Gomes I, Kim D, Chung Y, Honig, GR, Kim KS & Lanza R. (2010). Hemangioblastic derivatives from human induced pluripotent stem cells exhibit limited expansion and early senescence. *Stem Cells,* 28, 704–712.

Fuhrmann, S., Levine, E. M., & Reh, T. a. (2000). Extraocular mesenchyme patterns the optic vesicle during early eye development in the embryonic chick. *Development (Cambridge, England)*, *127*(21), 4599–609.

Friedman, D. S., O'Colmain, BJ., Muñoz, B., Tomany, SC., McCarty, C., de Jong ,PT., Nemesure, B., Mitchell, P. & Kempen J. (2004). Prevalence of age-

related macular degeneration in the United States. Archives of Ophthalmology, 122, 564-572.

Gao, H., & Hollyfield, J. G. (1992). Aging of the human retina. Differential loss of neurons and retinal pigment epithelial cells. *Investigative ophthalmology & visual science*, *33*(1), 1–17.

Gan, Q., Yoshida, T., McDonald, O. G., & Owens, G. K. (2007). Concise review: epigenetic mechanisms contribute to pluripotency and cell lineage determination of embryonic stem cells. *Stem cells ,25*(1), 2–9.

Gelisken, F., Voelker, M., Schwabe,R., Besch, D., Aisenbrey, S., Szurman, P., Grisanti, S., Herzan, V & Bartz-Schmidt, KU. (2007). Full macular translocation versus photodynamic therapy with verteporfin in the treatment of neovascular age-related macular degeneration: 1-year results of a prospective, controlled, randomised pilot trial. *Graefes archive for clinical and experimental ophthalmology,* 245, 1085–1095

Giritharan, G., Ilic, D., Gormley, M., & Krtolica, A. (2011). Human Embryonic Stem Cells Derived from Embryos at Different Stages of Development Share Similar Transcription Profiles. *PLoS ONE*, *6*(10), e26570.

Grisanti, S. & Guidry C. (1995). Transdifferentiation of retinal pigment epithelial cells from epithelial to mesenchymal phenotype. *Investigative ophthalmology & visual science* 36: 391–405

Gonzalez, R., Lee, J. W., Snyder, E. Y., & Schultz, P. G. (2011). Dorsomorphin promotes human embryonic stem cell self-renewal. *Angewandte Chemie (International ed. in English)*, *50*(15), 3439–41.

Gosh, F. & Arner., K. (2002). Transplantation of full-thickness retina in the normal porcine eye. *Retina,* 22, 478–486.

Greber, B., Lehrach, H., & Adjaye, J. (2007). Fibroblast growth factor 2 modulates transforming growth factor beta signaling in mouse embryonic fibroblasts and human ESCs (hESCs) to support hESC self-renewal. *Stem cells (Dayton, Ohio)*, *25*(2), 455–64.

Greber, B., Coulon, P., Zhang, M., Frank, S., Jose, A., Han, D. W., Hans-Christian, P. & Scho, H. R. (2011). FGF signalling inhibits neural induction in human embryonic stem cells. *Molecular Biology*, 1–11.

Gullapalli, V. K., Sugino, I. K., Van Patten, Y., Shah, S., & Zarbin, M. a. (2005). Impaired RPE survival on aged submacular human Bruch's membrane. *Experimental eye research*, *80*(2), 235–48

Gullapalli V.K. (2008). *Albert & Jakobiec's Principles & Practice of Ophthalmology*. Philadelphia: Saunders.

Hageman, G. S., Anderson, D. H., Johnson, L. V, Hancox, L. S., Taiber, A. J., Hardisty, L. I., Hageman, JL., Stockman, HA., Borchardt, JD., Gehrs, KM., Smith, RJH., Silvestri, G., Russell, SR., Klaver, CCW., Barbazetto, I., Chang, S.,Yannuzzi, L.,Barile, GR., Merriam, JC., Smith, RT., Olsh, AK., Bergeron, J.,Zernant, J.,Merriam, JE.,Gold, B.., Dean, M & Allikmets, R. (2005). A common haplotype in the complement regulatory gene factor H (HF1/CFH) predisposes individuals to age-related macular degeneration. *Proceedings of the National Academy of Sciences of the United States of America*, *102*(20), 7227–32.

Hall, M.O., Basigner, SF., Bock, D. (1973). Studies on the assembly of rod outer segment disc membranes. *Biochemistry and Physiology of Visual Pigments,* 319-321.

Haruta, M., Sasai, Y., Kawasaki, H., Kaori, A., Otoo, S., Kitada, M., Kitada, Masaaki,S., Hirofumi,N., Nakatsuji, N., Chizuka, I, Yoshito, H & Takahashi, M. (2004). In Vitro and In Vivo Characterization of Pigment Epithelial Cells Differentiated from Primate Embryonic Stem Cells. *Investigative Ophthalmology & Visual Science*, *45*(3), 1020–1025.

Harrison, N.J., Baker, D. & Andrews PW. (2007). Culture adaptation of embryonic stem cells echoes germ cell malignancy. *International Journal of Andrology,,* 30, 275–281.

Hasegawa, K. Zhang, P., Wei, Z., Pomeroy, JE., Lu, W & Pera, MF. (2010). Comparison of reprogramming efficiency between transduction of reprogramming factors, cell–cell fusion, and cytoplast fusion. *Stem Cells,* 28 (8), 1338–1348.

Heng, B.C. Liu, H & Cao, T. (2004). Feeder cell density- a key parameter in human embryonic stem cell culture. *In Vitro Cell and Developmental Biology Animal*, 40(8-9), 255-257.

Hernandez, D., Ruban, L. & Mason, C. (2011). Feeder-Free culture of human embryonic stem cells for scalable expansion in a reproducible manner. *Stem cells and development*, 20(6), 1089-1098.

Herszfeld, D., Wolvetang, E., Langton-Bunker E, Chung TL, Filipczyk AA, Houssami S, Jamshidi P, Koh K, Laslett AL, Michalska A, Nguyen L, Reubinoff BE, Tellis I, Auerbach JM, Ording CJ, Looijenga LH & Pera MF. (2006). CD30 is a survival factor and a biomarker for transformed human pluripotent stem cells. *Nature Biotechnology.* 24, 351–357.

Hopfl, G., Gassmann, M., Desbaillets, I., (2004). Differentiating embryonic stem cells into embryoid bodies. *Methods in Molecular Biology,* 254, 79-98.

Hongisto, H., Mikhailova, A., Hiidenmaa, H., Ilmarinen, T., & Skottman, H. (2012). Low level of activin A secreted by fibroblast feeder cells accelerates early stage differentiation of retinal pigment epithelial cells from human pluripotent stem cells, *Stem cell Discovery, 2*(4), 176–186.

Horsford, D.J., Nguyen, MT., Sellar, GC., Kothary, R., Arnheiter, H., McInnes, RR. (2005). Chx10 repression of Mitf is required for the maintenance of mammalian neuroretinal identity. *Development,* 132, 177–187.

Huang J, McAlinden C, Wang Q, Jin Z-B & Pesudovs K (2012). Embryonic stem-cell-derived retinal pigment epithelial cells for macular degeneration. *Lancet*. 2012;379(9831):2050; author reply 2050–1.

.

Hu, B.Y., Weich, JP., Yu, J., Li-Xiang, M., Zhang, XQ., Thomson, JA., Zhang, SC. (2010a). Neural differentiation of human induced pluripotent stem cells follows developmental principles but with variable potency, *PNAS*, 107(9), 4335-4340

Hu, Q., Friedrich, A. M., Johnson, L. V, & Clegg, D. O. (2010). Memory in induced pluripotent stem cells: reprogrammed human retinal-pigmented epithelial cells show tendency for spontaneous redifferentiation. *Stem cells, 28*(11), 1981–91.

Hu, Y., Liu, L., Lu, B., Zhu, D., Ribeiro, R., Diniz, B. Padmaja B.T., Ashish A.K., Hinton, DR.,Yu-Chong, T., Hikita S, Johnson, LV., Clegg DO.,Thomas, B & Humayun, MS. (2012a). A novel approach for subretinal implantation of ultrathin substrates containing stem cell-derived retinal pigment epithelium monolayer. *Ophthalmic research*, *48*(4), 186–91.

Hughes B.A., Gallemore RP. & Miller SS. (1998). Transport mechanisms in the retinal pigment epithelium. *The Retinal Pigment Epithelium*, *New York: Oxford University Press,* 103–134.

Idelson, M., Alper, R., Obolensky, A., Ben-Shushan, E., Hemo, I., Yachimovich-Cohen, N., Khaner, Hanita, Smith, Y., Wiser, O.,Gropp, M.,Cohen, M.,Even-Ram, S., Berman-Zaken, Y., Matzrafi, L., Rechavi, G., Banin, E. & Reubinoff, B. (2009). Directed differentiation of human embryonic stem cells into functional retinal pigment epithelium cells. *Cell stem cell*, *5*(4), 396–408.

Ishibashi, T., Hata Y, Yoshikawa H, Nakagawa K, Sueishi K & Inomata H. (1997). Expression of vascular endothelial growth factor in experimental choroidal neovascularisation. *Graefes Archive for Clinical and Experimental Ophthalmology,* 235, 159–167.

Itskovitz-Eldor, J. Schuldiner M, Karsenti D, Eden A, Yanuka O, Amit M, Soreq H & Benvenisty N.(2000). Differentiation of human embryonic stem cells into embryoid bodies compromising the three embryonic germ layers. *Molecular Medicine*, 6, 88-95.

Jager, J.D., M.D., William F. Mieler, M.D., and Joan W & Miller, M.D. (2008). Age-related macular degeneration. *New England Journal of Medicine,* 358, 2606-2617.

Joussen, A. M., Heussen, F. M. a, Joeres, S., Llacer, H., Prinz, B., Rohrschneider, K., Maaijwee, KM, Jan Van Meurs & Kirchhof, B. (2006). Autologous translocation of the choroid and retinal pigment epithelium in age-related macular degeneration. *American journal of ophthalmology*, *142*(1), 17–30.

Kawasaki, H., Suemori, H., Mizuseki, K., Watanabe, K., Urano, F., Ichinose, H., Haruta, M., Takahashi, M.,Yoshikawa, K.,Nishikawa, S, Nakatsuji, N. & Sasai, Y. (2002). Generation of dopaminergic neurons and pigmented epithelia from primate ES cells by stromal cell-derived inducing activity. *Proceedings of the National Academy of Sciences of the United States of America*, *99*(3), 1580–5.

Kearns, V., Mistry, A., Mason, S., Krishna, Y., Sheridan, C., Short, R., Williams, RL. (2012). Plasma polymer coatings to aid retinal pigment epithelial growth for transplantation in the treatment of age related macular degeneration. *Journal of Materials Science: Materials in Science,* 23, 2013–2021

Kessler, D.S. & Melton, D.A. (1994). Vertebrate embryonic induction: mesodermal and neural patterning. *Science* 266, 596–604.

Kim K, Doi A,Wen B, Ng K, Zhao R, Cahan P, Kim J, Aryee MJ, Ji H, Ehrlich LI, Yabuuchi A, Takeuchi A, Cunniff KC, Hongguang H, McKinney-Freeman S, Naveiras O, Yoon TJ, Irizarry RA, Jung N, Seita J, Hanna J, Murakami P, Jaenisch R, Weissleder R, Orkin SH, Weissman IL, Feinberg AP & Daley GQ (2010). Epigenetic memory in induced pluripotent stem cells. *Nature.*, 467(7313), 285-290

King, J. & Miller W.M. (2007). Bioreactor development for stem cell expansion and controlled differentiation. *Current Opinion in Chemical Biology*. 11, 1–5.

Klein, R. J., Zeiss, C., Chew, E. Y., Tsai, J.-Y., Sackler, R. S., Haynes, C., Henning, AK., SanGiovanni, JP., Mane, SM., Mayne, S., Bracken, M., Ferris, F., Ott, Jurg., Barnstable, C. & Hoh, J. (2005). Complement factor H polymorphism in age-related macular degeneration. *Science.* 308(5720), 385–9.

Klimanskaya, I., Hipp, J., Rezai, K. A., West, M., Atala, A., & Lanza, R. (2004). Derivation and Comparative Assessment of Retinal Stem Cells Using Transcriptomics. *Cloning and Stem Cells*, *6*(3). 217-245.

Kolb, H. (2005). Simple anatomy of the retina. Webvision: the organization of the retina and visual system. Salt Lake City (UT): University of Utah health sciences centre.

Kokkinaki, M., Sahibzada, N., & Golestaneh, N. (2011). Human induced pluripotent stem-derived retinal pigment epithelium (RPE) cells exhibit ion transport, membrane potential, polarized vascular endothelial growth factor secretion, and gene expression pattern similar to native RPE. *Stem cells , 29*(5), 825–35.

Koh, S.M. (2000). VIP enhances the differentiation of retinal pigment epithelium in culture: From cAMP and pp60(c-src) to melanogenesis and development of fluid transport capacity. *Progress in Retinal Eye Research*, 19, 669–688.

Kozmik, Z. (2005). Pax genes in eye development and evolution. *Current opinion in Genetics and Development,* 15(4), 430-438.

Krohne, T.U., Westenskow, PD., Kurihara T., Friedlander DF., Lehmann M, Dorsey AL, Li W, Zhu S, Schultz A, Wang J, Siuzdak G, Ding S, Friedlander M (2012). Generation of Retinal Pigment Epithelial Cells from Small Molecules and OCT4 Reprogrammed Human Induced Pluripotent Stem Cells. *Stem cells and translational medicine*, 1, 96-109.

Lappalainen, R. S., Salomäki, M., Ylä-Outinen, L., Heikkilä, T. J., Hyttinen, J. a K., Pihlajamäki, H., Suuronen, R., Skottman, H & Narkilahti, S. (2010). Similarly derived and cultured hESC lines show variation in their developmental potential towards neuronal cells in long-term culture. *Regenerative medicine*, *5*(5), 749–62.

Lamba, D. A., Karl, M. O., Ware, C. B., & Reh, T. a. (2006). Efficient generation of retinal progenitor cells from human embryonic stem cells. *Proceedings of the National Academy of Sciences of the United States of America*, 103(34), 12769–74.

Lamba, D. A, McUsic, A., Hirata, R. K., Wang, P.R., Russell, D., & Reh, T.A. (2010). Generation, purification and transplantation of photoreceptors derived from human induced pluripotent stem cells. *PloS one*, *5*(1), e8763.

Lamba, D.A. & Reh T.A. (2011). Microarray Characterization of Human Embryonic Stem Cell-Derived Retinal Cultures. *Investigative Ophthalmology and Visual Science*, 52(7), 4897-4906.

Lawrence JM., Sauvé Y, Keegan DJ, Coffey PJ, Hetherington L, Girman S, Whiteley SJ, Kwan AS, Pheby T, Lund RD (2000). Schwann cell grafting into the retina of the dystrophic RCS rat limits functional deterioration. *Investigative Ophthalmology and Visual Sciences,* 41, 518–528.

Lebkowski, J.S., Gold, J, Xu, C, Funk, W, Chiu, CP, & Carpenter, MK. (2001). Human embryonic stem cells: culture, differentiation, and genetic modification for regenerative medicine applications. *The Cancer Journal*, 7, 83-93.

Lewis, H., Straatsma BR, Foos RY & Lightfoot DO. (1985). Reticular degeneration of the pigment epithelium. *Ophthalmology,* 92, 1485–1495.

Liang, FQ. & Godley BF. (2003). Oxidative stress-induced mitochondrial DNA damage in human retinal pigment epithelial cells: a possible mechanism for RPE aging and age-related macular degeneration. *Experimental Eye Research*. 76 (4), 397-403.

Liao, J., Yu, J., Huang, K., Hu, J., Diemer, T., Ma, Z., Dvash, T., Yang, X.,Travis, G.,Williams, D.,Bok, D. & Fan, G. (2010). Molecular signature of primary retinal pigment epithelium and stem-cell-derived RPE cells. *Human Molecular Genetics*, 19(21), 4229-4238.

Ludwig, T. E., Levenstein, M. E., Jones, J. M., Berggren, W. T., Mitchen, E. R., Frane, J. L., Crandall, L.,Daigh, C.,Conard, K.,Piekarczyk, M.,Llanas, R., Thomson, J.A. (2006). Derivation of human embryonic stem cells in defined conditions. Nature biotechnology, 24(2), 185–7.

Liu, W. Lagutin, O., Swindel,l E., Jamrich, M & Oliver, G. (2010) Neuroretina specification in mouse embryos requires Six3-mediated suppression of Wnt8b in the anterior neural plate. *Journal of Clinical Investigation,* 120, 3568-3577.

Loring, J.F. & Peterson, S.E. (2007). Human Stem Cell Manual, A Laboratory Guide. London: Elsevier. 6-9

Lu, B., Malcuit, C., Wang, S., Girman, S., Francis, P., Lemieux, L., Lanza. R., Lund, R. (2009). Long-term safety and function of RPE from human embryonic stem cells in preclinical models of macular degeneration. *Stem cells 27*(9), 2126–35.

Loh Y, Hartung O, Li H, Guo, Chunguang,S,Manos, D,Urbach, A Heffner, G,Grskovic, M,Vigneault, F,Lensch, M W,Park, IH,Agarwal, S,Church, GM,Collin, JJ,Irion, S,Daley, GQ. (2010) Reprogramming of T cells from human peripheral blood. 7(1):15–19.

Lu, B., Wang S, Girman S, McGill T, Ragaglia V & Lund R. (2010). Human adult bone marrow-derived somatic cells rescue vision in a rodent model of retinal degeneration. *Experimental Eye Research* 91, 449-455.

Ludwig, T. E., Bergendahl, V., Levenstein, M. E., Yu, J., Probasco, M. D., & Thomson, J. A. (2006). Feeder-independent culture of human embryonic stem cells. *Source*, *3*(8), 637–647.

Lumelsky, N., Blondel O, Laeng P, Velasco I, Ravin R & McKay R. (2001). Differentiation of embryonic stem cells to insulin-secreting structures similar to pancreatic islets. *Science*, 292, 1389–1394.

Lund, R. D., Wang, S., Klimanskaya, I., Holmes, T., Ramos-Kelsey, R., Lu, B., Girman, S., Bischoff., N,Sauvé, Y. & Lanza, R. (2006). Human embryonic stem cell-derived cells rescue visual function in dystrophic RCS rats. *Cloning and stem cells*, *8*(3), 189–99. doi:10.1089/clo.2006.8.189

Lund, R. D. Wang, S., Lu, B., Girman, S., Holmes, T., Sauvé., Y, Messina DJ, Harris, IR., Kihm, AJ., Harmon, AM., Chin, FY., Gosiewska, A. & Mistry SK. (2007). Cells isolated from umbilical cord tissue rescue photoreceptors and visual functions in a rodent model of retinal disease, *Stem Cells* 25, 602-611.

MacLaren, R.E. Uppal GS, Balaggan KS, Tufail A, Munro PM, Milliken AB, Ali RR, Rubin GS, Aylward GW, Da Cruz L (2007). Autologous transplantation of the retinal pigment epithelium and choroid in the treatment of neovascular age-related macular degeneration. *Ophthalmology*, 114, 561–570

Maherali N, Sridharan R, Xie W, Utikal J, Eminli S, Arnold K, Stadtfeld M, Yachechko R, Tchieu J, Jaenisch R. (2007). Directly reprogrammed fibroblasts show global epigenetic remodeling and widespread tissue contribution. *Cell Stem Cell*, 1, 55–70.

Maminishkis, A., Chen, S., Jalickee, S., Banzon, T., Shi, G., Wang, F. E., Ehalt, T., Hammer, JA. & Miller, S. S. (2006). Confluent monolayers of cultured human fetal retinal pigment epithelium exhibit morphology and physiology of native tissue. *Investigative ophthalmology & visual science*, *47*(8), 3612–24.

Marmorstein, A.D. (2001). The polarity of the retinal pigment epithelium. *Traffic,* 2, 867–872.

Martin, M. J., Muotri, A., Gage, F., & Varki, A. (2005). Human embryonic stem cells express an immunogenic nonhuman sialic acid. *Nature medicine*, *11*(2), 228–32.

Maruotti, J., Wahlin, K., Gorrell, D., Bhutto, I., Lutty, G., & Zack, D. J. (2013). A simple and scalable process for the differentiation of retinal pigment epithelium from human pluripotent stem cells. *Stem cells translational medicine*, *2*(5), 341–54.

Martínez-Morales, J. R., Rodrigo, I., & Bovolenta, P. (2004). Eye development: a view from the retina pigmented epithelium. *BioEssays : news and reviews in molecular, cellular and developmental biology*, *26*(7), 766–77.

Martinez-Morales, J.R., Dolez V, Rodrigo I, Zaccarini R, Leconte L, Bovolenta P, & Saule S (2003). Otx2 activates the molecular network underlying retinal pigment epithelium differentiation. *Journal of biological chemistry,* 278 (24), 21721-21731.

Martins-Taylor, K. & Xu, RX. (2012). Concise Review: Genomic Stability of Human Induced Pluripotent Stem cells. *Stem cells*, 30, 22-27.

Merkle FT & Eggan K. (2013) Modelling human disease with pluripotent stem cells: from genome association to function. *Cell Stem Cell*. 12(6): 656–68.

Meyer, J. S., Shearer, R. L., Capowski, E. E., Wright, L. S., Wallace, K. A, McMillan, E. L., Zhang, S.C & Gamm, D. M. (2009). Modeling early retinal development with human embryonic and induced pluripotent stem cells. *Proceedings of the National Academy of Sciences of the United States of America*, 106(39), 16698–703.

Meyer, J. S., Howden, S. E., Wallace, K. A., Verhoeven, A. D., Wright, L. S., Capowski, E. E., Pinilla, I., Martin, JM.,Tian, S. & Stewart, R. (2011). Optic Vesicle-like Structures Derived from Human Pluripotent Stem Cells Facilitate a Customized Approach to Retinal Disease Treatment. *Developmental Biology*, (608).

Mellough, C. B., Sernagor, E., Moreno-Gimeno, I., Steel, D. H. W., & Lako, M. (2012). Efficient stage-specific differentiation of human pluripotent stem cells toward retinal photoreceptor cells. *Stem cells*, *30*(4), 673–86.

Miceli, M.V., Liles MR, & Newsome DA (1994). Evaluation of Oxidative Processes in Human Pigment Epithelial Cells Associated with Retinal Outer Segment Phagocytosis. *Experimental Cell Research*, 214 (1), 242-249

Mikkelsen TS, Hanna J, Zhang X, Ku M, Wernig M, Schorderet P, Bernstein BE, Jaenisch R, Lander ES & Meissner A. (2008). Dissecting direct reprogramming through integrative geno-mic analysis. *Nature,* 454, 49–55.

Morizane, A., Doi, D., Kikuchi, T., Nishimura, K., & Takahashi, J. (2011). Small-molecule inhibitors of bone morphogenic protein and activin/nodal signals promote highly efficient neural induction from human pluripotent stem cells. *Journal of neuroscience research*, *89*(2), 117–26. doi:10.1002/jnr.22547

Muller, F.J. Goldmann, J., Loser P. & Loring JF. (2010). A call to standardize teratoma assays used to define human pluripotent cell lines. *Cell stem cell*, 6 (5), 412-414.

Muñoz-Sanjuán, I., & Brivanlou, A. H. (2002). Neural induction, the default model and embryonic stem cells. *Nature reviews. Neuroscience*, *3*(4), 271–80.

Nakano, T., Ando, S., Takata, N., Kawada, M., Muguruma, K., Sekiguchi, K., Saito, K, Yonemura, S., Eiraku, M., & Sasai, Y. (2012). Self-formation of optic cups and storable stratified neural retina from human ESCs. *Cell stem cell*, 10, 771-785

Nakayama, A, M T Nguyen, C C Chen, K Opdecamp, CA Hodgkinson, and H Arnheiter. (1998). Mutations in Microphthalmia, the Mouse Homolog of the Human Deafness Gene MITF, Affect Neuroepithelial and Neural Crest-Derived Melanocytes Differently. *Mechanisms of development* 70(1-2), 155–66.

Narkilahti, S., Rajala, K., Pihlajamäki, H., Suuronen, R., Hovatta, O., & Skottman, H. (2007). Monitoring and analysis of dynamic growth of human embryonic stem cells: comparison of automated instrumentation and conventional culturing methods. *Biomedical engineering online*, 6, 11.

Närvä, E., Autio, R., Rahkonen, N., L., Itskovitz-Eldor, J., Rasool, O., Dvorak, P.,Hovatta, O., Otonkoski, T., Tuuri, T., Cui, W., Brüstle, O., Baker, D., Maltby, E., Moore, H.D., Benvenisty, N., Andrews, P.W.,Yli-Harja, O., Lahesmaa, R. (2010). High-resolution DNA analysis of human embryonic stem cell lines

reveals culture-induced copy number changes and loss of heterozygosity. *Nature biotechnology*, 28(4), 371–7.

Nguyen, N.T. & Arnheiter, H et al., (2000). Signaling and transcriptional regulation in early mammalian eye development: a link between FGF and MITF. *Development* 127(16), 3581-3591.

Niederkorn, J.Y. (1990). Immune privilege and immune regulation in the eye. *Advanced Immunology.* 48, 191-226.

Niehrs, C. (2004). Regionally specific induction by the Spemann-Mangold organizer. *Nature Reviews Genetics*, 5, 425-434.

Nishino K, Toyoda M, Yamazaki-Inoue M, Fukawatase, Y, Chikazawa, E Sakaguchi, H, Akutsu, H, Umezawa, A (2011). DNA methylation dynamics in human induced pluripotent stem cells over time). *PLoS genetics.*7(5), e1002085.

Nistor, G., Seiler, M. J., Yan, F., Ferguson, D., & Keirstead, H. S. (2010). Three-dimensional early retinal progenitor 3D tissue constructs derived from human embryonic stem cells. *Journal of neuroscience methods*, *190*(1), 63–70.

Niwa, H., Toyooka, Y., Shimosato, D., Strumpf, D., Takahashi, K., Yagi ,R. & Rossant J. (2005).,Interaction between Oct3/4 and Cdx2 determines trophectoderm differentiation. *Cell,* 123, 917–929.

Odorico, J. S., Kaufman, D. S., & Thomson, J. a. (2001). Multilineage differentiation from human embryonic stem cell lines. *Stem cells*, *19*(3), 193–204.

Ohmine S, Dietz AB, Deeds MC, Hartjes, Katherine A, Miller, DR, Thatava, T Sakuma, T, Kudva, YC, Ikeda, Yasuhiro (2011)Induced pluripotent stem cells from GMP-grade hematopoietic progenitor cells and mononuclear myeloid cells. *Stem Cell Research and Therapeutics.* 2011;2(6):46

Ohno-Matsui, K, Morita, I., Tombran-Tink, J., Mrazek, D., Onodera, M., Uetama, T., Hayano, M., Murota, SI. & Mochizuki, M. (2001) Novel mechanism for age-related macular degeneration: an equilibrium shift between the angiogenesis factors VEGF and PEDF. *Journal of Cell Physiology.* 189, 323–333.

Osakada, F., Ikeda, H., Mandai, M., Wataya, T., Watanabe, K., Yoshimura, N., Akaike, A., Akaike., A.Sasai., Y, Takahashi, M. (2008). Toward the generation of rod and cone photoreceptors from mouse, monkey and human embryonic stem cells. *Nature biotechnology*, *26*(2), 215–24.

Osafune, K., Caron, L., Borowiak, M., Martinez, R. J., Fitz-Gerald, C. S., Sato, Y., Cowan, C.A., Chien, K.R., Melton, D. A. (2008). Marked differences in differentiation propensity among human embryonic stem cell lines. *Nature biotechnology*, *26*(3), 313–5.

O'Rahilly, R. (1975). The prenatal development of the human eye. *Experimental Eye Research*, 21(2), 93-112.

Owen, C. G., Jarrar, Z., Wormald, R., Cook, D.G., Fletcher, A.E. & Rudnicka, A.R., (2012). The estimated prevalence and incidence of late stage age related macular degeneration in the UK. *British Journal of Ophthalmolgy*. 96, 752-756.

Pankratz, M. T., Li, X.-J., Lavaute, T. M., Lyons, E. a, Chen, X., & Zhang, S.-C. (2007). Directed neural differentiation of human embryonic stem cells via an obligated primitive anterior stage. *Stem cells. 25*(6), 1511–20.

Park I-H, Zhao R, West JY, Akiko, Huo, H Ince, TA Lerou, PH Lensch, MW, Daley, GQ. (2008). Reprogramming of human somatic cells to pluripotency with defined factors. *Nature*. 2008; 451(7175):141–6.

Patani, R., Compston, A., Puddifoot, C. A, Wyllie, D. J, Hardingham, G. E., Allen, N. D., & Chandran, S. (2009). Activin/Nodal inhibition alone accelerates highly efficient neural conversion from human embryonic stem cells and imposes a caudal positional identity. *PloS one*, *4*(10), e7327.

Passier, R., Oostwaard, D.W., Snapper, J., Kloots, J., Hassink, R.J., Kuijk, E., Roelen, B., De La Riviere, A.B., Mummery, C. (2005). Increased Cardiomyocyte Differentiation from Human Embryonic Stem Cells in Serum-Free Cultures. *Stem Cells*, 23, 772-780.

Peirson, S.N., Butler, J.N., Foster, R.G. (2003). Experimental validation of novel and conventional approaches to quantitative real-time PCR data analysis. *Neuroscience*, 31(14), e73.

Peerani, R., Rao, B. M., Bauwens, C., Yin, T., Wood, G. a, Nagy, A. Zandstra, P. W. (2007). Niche-mediated control of human embryonic stem cell self-renewal and differentiation. *The EMBO journal*, *26*(22), 4744–55.

Pennesi ME, Neuringer M, & Courtney RJ. (2012) Animal models of age related macular degeneration. *Molecular Aspects of Medicine* .33(4):487–509.

Pera E.M., Wessely, O., Li, S.Y., & De Robertis, E.M. (2001). Neural and Head Induction by Insulin-like Growth Factor Signals. *Developmental Cell,* 1, 655–665.

Pera, M.F., Andrade, J., Houssami, S., Reubinoff, B., Trounson, A., Stanley, EG., Ward-van, O.D. & Mummery C. (2004). Regulation of human embryonic stem cell differentiation by BMP-2 and its antagonist noggin. *Journal of cell science*, 117(Pt 7), 1269-1280.

Pfaffl, M.W. (2001). A new mathematical model for relative quantification in real time RT-PCR. *Nucleic Acids Research*. 29(9), 2003-2007.

Pfeffer, B.A. Clark, V,M., Flannery, J.G. & Bok, D. (1986). Membrane receptors for retinol-binding protein in cultured human retinal pigment epithelium. *Investigative Ophthalmology and Visual Science.* 27, 1031–1040.

Placzek, M. R., Chung, I.-M., Macedo, H. M., Ismail, S., Mortera Blanco, T., Lim, M. & Mantalaris, A. (2009). Stem cell bioprocessing: fundamentals and principles. *Journal of the Royal Society, Interface / the Royal Society*, *6*(32), 209–32.

Puck, B. & Marcus, P,I. (1954). A Rapid method for viable cell titration and clone production with HeLa cells in tissue culture: The use of x irradiated cells to supply conditioning factors. *PNAS,* 41, 432-437

Purves, D. et al., 2001. Neuroscience, 2nd Addition, Sunderland (MA) Sinauer Associates pp.

Ramsden CM, Powner MB, Carr A-JF, Smart MJK, da Cruz L & Coffey PJ. (2013). Stem cells in retinal regeneration: past, present and future. *Development*, 140(12):2576–85.

Rao, M. (2008). Scalable human ES culture for therapeutic use: propagation, differentiation, genetic modification and regulatory issues. *Gene therapy*, 15(2), 82-88.

Reubinoff BE, Pera MF, Fong CY, Trounson A & Bongso A. (2000). Embryonic stem cell lines from human blastocysts: somatic differentiation in vitro. *Nat. Biotechnol,* 18(4), 399–404.

Richards, M. Fong C, Chan WK, Wong PC & Bongso A (2002). Human feeders support prolonged undifferentiated growth of human inner cell masses and embryonic stem cells. *Nature biotechnology,* 20, 933-936

Roberts, W. & Palade, GE. (1995). Increased microvascular permeabil- ity and endothelial fenestration induced by vascular endothelial growth factor. *Journal of Cell Science,* 108, 2369–2379.

Rosler ES, Fisk GJ, Ares X, Irving J, Miura T, Rao MS & Carpenter MK. (2004). Long term culture of human embryonic stem cell in feeder-free conditions. *Developmental dynamics*, 229, 259-274.

Rowland, T.J. Buchholz DE & Clegg DO (2011). Pluripotent Human Stem Cells for the Treatment of Retinal Disease. *Journal of Cellular Physiology,* 227(2), 457-466.

Rowland TJ, Blaschke AJ, Buchholz DE, Hikita ST, Johnson L V & Clegg DO. (2012). Differentiation of human pluripotent stem cells to retinal pigmented epithelium in defined conditions using purified extracellular matrix proteins. *Journal of Tissue Engineering and Regenerative Medicine*, 7(8), 642-5.

Schoenwolf, G.C. Gary C; Larsen, WJ. (2009). Larsen's Human Embryology. 4th ed. Philadelphia: Churchill Livingston Elservier. 602-615.

Schuldiner, M, Yanuka O, Itskovitz-Eldor J, Melton D & Benvenisty N (2000). Effects of eight growth factors on the differentiation of cells derived from human embryonic stem cells. *PNAS*, 97, 11307–11312..

Schwartz, SD, Valentina FC, Pan, CK Ostrick, RM Mickunas, E Gay, R Klimanskaya, I & Lanza, R (2012). Embryonic stem cell trials for macular degeneration : a preliminary report. *The lancet*, 6736(12), 1-8.

Sheridan, SD, Surampudi V, & Rao RR. (2011). Analysis of embryoid bodies derived from human induced pluripotent stem cells as a means to assess pluripotency. *Stem Cells International.* Vol 2012, article 738910.

Shi, Y & Clegg DO. (2008). Chapter 1 Retinal Pigment Epithelial cells. *Stem cell Research and Therapeutics*. Springer Science and Business Media B.V. Chapter 1, 1-21.

Simeone, A. (1998). Otx1 and Otx2 in the development and evolution of the mammalian brain. *EMBO, members review*. 17(23), 6790-6798.

Singh, S, Woerly S & McLaughlin BJ. (2001). Natural and artificial substrates for retinal pigment epithelial monolayer transplantation. *Biomaterials*, 22(24), 3337-3343.

Siqueira, R, Messias A, Voltarelli JC, Scott IU & Jorge R. (2011). Intravitreal injection of autologous bone marrow-derived mononuclear cells for hereditary retinal dystrophy: a phase I trial, *Retina*. 31, 1207-1214

Slack, JMW (2006). *Essential Developmental Biology*. Oxford: Blackwell publishing, 202-205.

Sommer C & Mostoslavsky G. The evolving field of induced pluripotency: recent progress and future challenges. (2013). *Journal of Cellular. Physiology.*. 228(2):267–75.

Sridhar, A, Steward M, & Meyer JS. (2013). Nonxenogeneic Growth and Retinal Differentiation of Human Induced Pluripotent Stem Cells. *Neurosciences Research*, (2), 255-264.

Stanga, PE, Kychenthal A, Fitzke FW, Halfyard AS, Chan R, Bird AC, Aylward GW (2002). Retinal pigment epithelium translocation after choroidal neovascular membrane removal in age-related macular degeneration. *Ophthalmology,* 109, 1492–1498.

Stone, EM, Braun TA, Russell SR, Kuehn MH, Lotery AJ, Moore PA, Eastman CG, Casavant TL & Sheffield VC. (2004). Missense variations in the fibulin 5 gene and age related macular degeneration. *New England Journal of Medicine,* 351 (4), 346-353.

Strauss, O. (2005). The retinal pigment epithelium in visual function. *Physiological reviews*, 85(3), 845-881

Strober, W. (2001). Trypan blue exclusion test of cell viability. *Current protocols in Immunology*. 21 A3B.1-A.3B.

Strunnicova NV, Maminishkis A, Barb JJ, Wang F, Zhi C, Sergeev Y, Chen W, Edwards AO, Stambolian D, Abecasis G, Swaroop A, Munson PJ, & Miller SS. (2010). Transcriptome analysis and molecular signature of human retinal pigment epithelium. *Human Molecular Genetics.* 19, 2468-2486.

Subrizi, A. Hiidenmaa H, Ilmarinen T, Nymark S, Dubruel P, Uusitalo H, Yliperttula M, Urtti A, & Skottman H. (2012). Generation of hESC-derived retinal pigment epithelium on biopolymer coated polyimide membranes. *Biomaterials,* 33, 8047–8054

Sunness, JS & Applegate CA. (2005). Long-term follow-up of fixation patterns in eyes with central scotomas from geographic atrophy that is associated with age-related macular degeneration. *American. Journal of Ophthalmology*. 140, 1085–1093.

Stanzel BV, Liu Z, Brinken R, Braun N, Holz FG & Eter N. (2012). Subretinal delivery of ultrathin rigid-elastic cell carriers using a metallic shooter instrument and biodegradable hydrogel encapsulation. *Investigative Ophthalmology and Visual Sciences,* 31, 490–500.

Takahashi K & Yamanaka S. (2006). Induction of pluripotent stem cells from mouse embryonic and adult fibroblast cultures by defined factors. *Cell* 126, 663–676.

Takahashi K, Tanabe K, Ohnuki M, Narita M, Ichisaka T, Tomoda K, Yamanaka S. (2007). Induction of pluripotent stem cells from adult human fibroblasts by defined factors. *Cell,* 131, 861-872.

Tavakoli, T, Xu X, Derby E, Serebryakova Y, Reid Y, Rao, M, Mattson MP & Wu M (2009). Self-renewal and differentiation capabilities are variable between human embryonic stem cell lines 13,16 and BG0IV. *BMC Cell Biology*, 10(44), 1-15.

Thomas, RJ Anderson D, Chandra A, Smith NM, Young LE, Williams D, Denning C. (2009). Automated, scalable culture of human embryonic stem cells in feeder-free conditions. *Biotechnology and Bioengineering*, 102 (6), 1636–1644.

Thumann, G. Aisenbrey S, Schaefer F, Bartz-Schmidt KU (2006). Instrumentation and technique for delivery of tissue explants to the subretinal space. *Opthalmologica,* 220(3), 170–173.

Treumer F, Bunse A, Klatt C & Roider J (2006). Autologous RPE–choroid sheet transplantation in AMD. Morphological and functional results. *British Journal of Ophthalmology*, 91, 349–353.

Tuo, J, Bojanowski, CM, & Chan CC. (2004). Genetic factors of age-related macular degeneration. *Progress in Retina and Eye Research*, 23(2), 229-249.

Vallier, L, Touboul T, Chng Z, Minodora B, Hannan, N, Millan, E, Smithers, L, Trotter, M, Rugg-Gunn, P,Weber, A, Pedersen, R. (2009). Early Cell Fate Decisions of Human Embryonic Stem Cells and Mouse Epiblast Stem Cells Are Controlled by the Same Signalling Pathways. *Plos One*, 4(6), e6082.

Vandesompele J, De Preter K, Pattyn F, Poppe, B, Van Roy, N, De Paepe, A, & Speleman F. (2002). Accurate normalization of real-time quantitative RT -PCR data by geometric averaging of multiple internal control genes. *Genome*, 1-12.

Van Winkle AP, Gates ID & Kallos MS. (2012). Mass transfer limitations in embryoid bodies during human embryonic stem cell differentiation. *Cells Tissues Organs,* 196(1), 34-37.

Villanueva, S, Glavic A, Ruiz P, & Mayor R. (2002). Posteriorization by FGF, Wnt, and retinoic acid is required for neural crest induction. *Developmental Biology* 241(2), 289-301.

Vaajasaari H, Ilmarinen T, Juuti-Uusitalo K, Rajala, Kristiina K, Onnela, N, Narkilahti, S, Suuronen, R, Hyttinen, J, Uusitalo, H & Skottman, H (2011). Toward the defined and xeno-free differentiation of functional human pluripotent stem cell-derived retinal pigment epithelial cells. *Molecular vision*, 17, 558-575.

Vogel-Hopker, A, Momose T, Rohrer H, Yasuda K, Ishihara L & Rapaport DH. (2000). Multiple functions of fibroblast growth factor-8 (FGF-8) in chick eye development. *Mechanisms of Development.* 94, 25–36.

Vugler, A. Carr AJ, Lawrence J, Chen LL, Burrell K, Wright A, Lundh P, Semo M, Ahmado A, Gias C, da Cruz L, Moore H, Andrews P, Walsh J, & Coffey P (2008). Elucidating the phenomenon of HESC-derived RPE: anatomy of cell genesis, expansion and retinal transplantation. *Experimental neurology*, 214(2), 347-61.

Vugler, A. Lawrence J, Walsh J, Carr A, Gias C, Semo M, Ahmado A, da Cruz L, Andrews P & Coffey P. (2007). Embryonic stem cells and retinal repair. *Mechanisms of development*, 124(11-12), 807-829

Wada, M. Ogata N, Otsuji T & Uyama M. (1999). Expression of vascular endothelial growth factor and its receptor (KDR/flk-1) mRNA in experimental choroidal neovascularization. *Current Eye Research* 18 pp 203–213.

Wang, N.K, Kasanuki JM, Chou CL, Kong J, Parmalee N, Wert KJ, Allikmets R, Lai CC, Chien CL, Nagasaki T, Lin CS, Tsang SH (2010). Transplantation of

reprogrammed embryonic stem cells improves visual function in a mouse model for retinitis pigmentosa. *Transplantation*, 89(8), 911-919.

Warren L, Manos PD, Ahfeldt T, Loh YH, Li H, Lau F, Ebina W, Mandal PK, Smith ZD, Meissner A, DaleyGQ,Brack AS, Collins JJ,CowanC, SchlaegerTM & Rossi DJ. (2010). Highly efficient reprogramming to pluripotency and directed differentiation of human cells with synthetic modified mRNA. *Cell Stem Cell* 7:618–630.

Watanabe, K., Kamiya D, Nishiyama A, Katayama T, Nozaki S, Kawasaki H, Watanabe Y, Mizuseki K & Sasai Y. (2005). Directed differentiation of telencephalic precursors from embryonic stem cells. *Nature. Neuroscience*, 8, 288–296.

Watanabe K, Ueno M, Kamiya D, Nishiyama A, Matsumura M, Wataya T, Takahashi JB, Nishikawa S, Nishikawa S, Muguruma K, and Sasai Y (2007). A ROCK inhibitor permits survival of dissociated human embryonic stem cells. Nature biotechnology, 25(6), 681-686.

Weiter, JJ, Delori FC, Wing GL, Fitch KA. (1986). Retinal pigment epithelial lipofuscin and melanin and choroidal melanin in human eyes. *Investigative ophthalmology & visual science*, 27(2), 1451-52.

Weiter, JJ (1987). Phototoxic changes in the retina. *Clinical light damage to the eye*, 79–125.

Wen, R. Song Y, Cheng T, Matthes MT, Yasumura D, LaVail MM, Steinberg RH. (1995). Injury-induced upregulation of bFGF and CNTF mRNAS in the rat retina. *Journal of Neuroscience,* 15, 7377–7385.

Westenskow, P, Piccolo S, & Fuhrmann S. (2009). Beta-catenin controls differentiation of the retinal pigment epithelium in the mouse optic cup by regulating MitF and Otx2 expression. *Development*, 136, 2505-2510.

Wilson, SW & Houart C. (2004). Early steps in the development of the forebrain. *Developmental Cel,* 6 (2), 167-81.

Wimmers, S, Karl MO & Strauss O. (2007). Ion channels in the RPE. *Progress in Retinal Eye Research*, 26, 263–301.

Wu, H. Xu J, Pang ZP, Ge W, Kim KJ, Blanchi B, Chen C, Südhof TC, & Sun YE (2007). Integrative genomic and functional analyses reveal neuronal subtype differentiation bias in human embryonic stem cell lines. *Proceedings of the National Academy of Sciences of the United States of America*, 104(34), 13821-13826.

Xiao, L. Yuan X & Sharkis SJ (2006). Activin A maintains self-renewal and regulates fibroblast growth factor, Wnt, and bone morphogenic protein pathways in human embryonic stem cells. *Stem cells ,* 24(6), 1476-1486.

Xu, C. Inokuma MS, Denham J, Golds K, Kundu P, Gold JD, & Carpenter MK. (2007).Feeder-free growth of undifferentiated human embryonic stem cells. *Nature biotechnology*, 19(10), 971-974.

Xu, C, Police S, Rao N, & Carpenter MK. (2002)(a). Characterization and enrichment of cardiomyocytes derived from human embryonic stem cells. *Circulation research*, 91, 501–508.

Xu, RH, Chen X, Li DS, Li R, Addicks GC, Glennon C, Zwaka TP & Thomson JA. (2002) (b). BMP4 initiates human embryonic stem cell differentiation to trophoblast. *Nature biotechnology*, 20(12), 1261-1264.

Xu, RH, Peck RM, Li DS, Feng X, Ludwig T & Thomson JA. (2005). Basic FGF and suppression of BMP signalling sustain undifferentiated proliferation of human ES cells. *Nature Methods*, 2(3), 185-190.

Xu RH, Sampsell-Barron TL, Gu F, Root S, Peck RM, Pan G, Yu J, Antosiewicz-Bourget J, Tian S, Stewart R & Thomson JA. (2008). NANOG is a direct target of TGFbeta/activin-mediated SMAD signalling in human ESCs. *Cell Stem Cell*, 3, 196–206.

Yang X.J. (2004). Roles of cell-extrinsic growth factors in vertebrate eye pattern formation and retinogenesis. *Seminars in Cell and Developmental Biology,* 15(1), 91-103

Yanai A, Laver CR, Joe AW, Viringipurampeer IA, Wang X, Gregory-Evans CY & Gregory-Evans K. (2013). Differentiation of Human Embryonic Stem Cells using Size-Controlled Embryoid Bodies and Negative Cell Selection in the Production of Photoreceptor Precursor Cells. , *Tissue Engineering*, 9(10), 755-64.

Yoo YD, Huang CT, Zhang X, Lavaute TM, & Zhang SC. (2011). Fibroblast Growth Factor (FGF) Regulates Human Neuroectoderm Specification Through ERK1/2-PARP-1 Pathway. *Stem cells,* 29, 1975–1982

Young, RW & Bok, D. (1960). Participation of the retinal pigment epithelium in the rod outer segment renewal process. *The journal of cell biology,* 42(2), pp 392-403.

Young R.W. (1975). The renewal of rod and cone outer segments in the rhesus monkey. *Journal of cellular biology,* 49, 303-318.

Young, R.W. 1987. Pathophysiology of age-related macular degeneration. *Surveys in Ophthalmolgy*, 31, 291–306.

Yue F, Johkura K, Shirasawa S, Yokoyama T, Inoue Y, Tomotsune D, & Sasaki K (2010). Differentiation of primate ES cells into retinal cells induced by ES cell-derived pigmented cells. *Biochemical and biophysical research communications*, 394(4), 877-883.

Yu J, Vodyanik MA, Smuga-Otto K, et al. Antosiewicz-Bourget J, Frane JL, Tian S, Nie J, Jonsdottir GA, Ruotti V, Stewart R, Slukvin II, Thomson JA. Induced pluripotent stem cell lines derived from human somatic cells. *Science.* 2007, 318, 1917-1920

Yu PB Hong CC, Sachidanandan C, Babitt JL, Deng DY, Hoyng SA, Lin HY, Bloch KD & Peterson RT (2008). Dorsomorphin inhibits BMP signals required for embryogenesis and iron metabolism. *Nature Chemical Biology*, 4(1), 15-16

Zaghloul, N. Yan B, Moody SA (2005). Step-wise specification of retinal stem cells during normal embryogenesis. *Biology of the cell / under the auspices of the European Cell Biology Organization*, 97(5), 321-337.

Zahabi A, Shahbazi E, Ahmadieh H, Hassani SN, Totonchi M, Taei A, Masoudi N, Ebrahimi M, Aghdami N, Seifinejad A, Mehrnejad F, Daftarian N, Salekdeh GH, Baharvand H (2012). A New Efficient Protocol for Directed Differentiation of Retinal Pigmented Epithelial Cells from Normal. *Stem Cells and Development,* 21(12), 2262-2272.

Zeiss CJ. Animals as models of age-related macular degeneration: an imperfect measure of the truth. (2010). *Vetinary Pathology*. 47(3):396–413.

Zhang, P. Li J, Tan Z, Wang C, Liu T, Chen L, Yong J, Jiang W, Sun X, Du L, Ding M, Deng H (2008). Short-term BMP-4 treatment initiates mesoderm induction in human embryonic stem cells. *Blood*, 111, 1933– 1941.

Zhang, X, Huang CT, Chen J, Pankratz MT, Xi J, Li J, Yang Y, Lavaute TM, Li XJ, Ayala M, Bondarenko GI, Du ZW, Jin Y, Golos TG & Zhang SC. (2010). Pax6 Is a Human Neuroectoderm Cell Fate Determinant. *Cell Stem Cell*, 7(1), 90-100.

Zhang K, Liu GH, Yi F, Montserrat N, Hishida T, Rodriguez Esteban C, Izpisua Belmonte JC (2013). Direct conversion of human fibroblasts into retinal pigment epithelium-like cells by defined factors. *Protein and Cell*, (Epub ahead of print).

Zhao S, Hung FC, Colvin JS, White A, Dai W, Lovicu FJ, Ornitz DM, Overbeek PA (2001). Patterning the optic neuroepithelium by FGF signalling and Ras activation. *Development,* 128, 5051–5060.

Zhou, J. Su P, Li D, Tsang S, Duan E & Wang F (2010). High-Efficiency Induction of Neural Conversion in hESCs and hiPSCs with a Single Chemical Inhibitor of TGF-beta Superfamily Receptors. *Stem cells*, 1741-1750.

Zhou T, Benda C, Dunzinger S, Huang, Y, Ho, J, Yang, J, Wang, Y, Zhang, Y, Zhuang, Q, Li, Y, Bao, X, Tse, H, Grillari, J, Grillari-Voglauer, R, Pei, D & Esteban, M. (2012). Generation of human induced pluripotent stem cells from urine samples. *Nature protocols.*;7(12), 2080–9.

Zhu Y, Carido M, Meinhardt A, Kurth T, Karl MO, Ader M &Tanaka EM (2013). Three-Dimensional Neuroepithelial Culture from Human Embryonic Stem Cells and Its Use for Quantitative Conversion to Retinal Pigment Epithelium. *PlOS One* 8(1), 54552.

Zuber, ME, Gestri G, Viczian AS, Barsacchi G & Harris WA (2003). Specification of the vertebrate eye by a network of eye field transcription factors. *Development*, 130(21), 5155-5167.

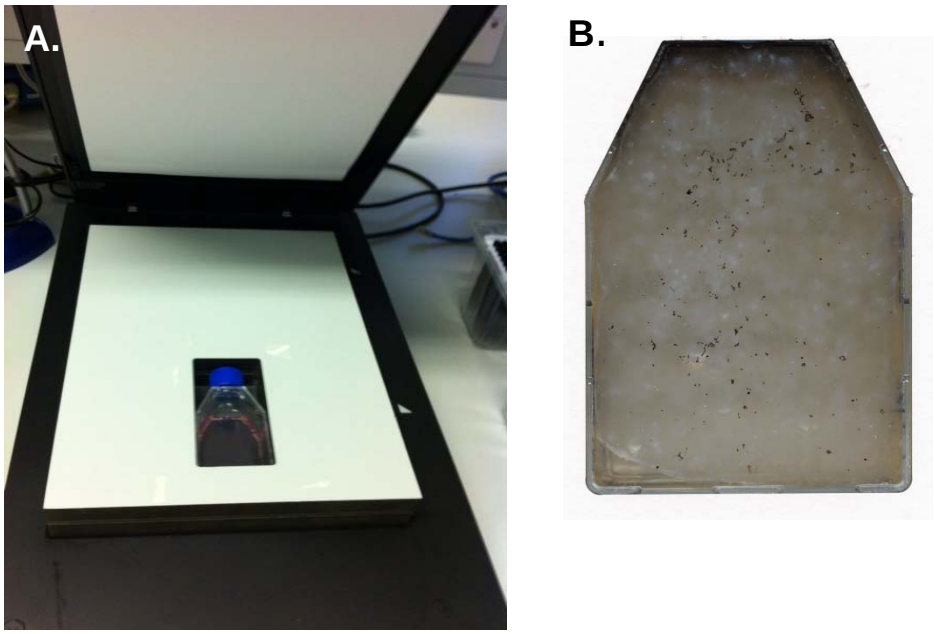

Fig 2.1. Epson V750 flat bed scanner and custom made flask mounting block designed to fit one T25 flask in a fixed position. (A) The mounting block is finished with matt black walls and a matt white lid was designed to ensure a light background with which the pigmented foci would contrast (B).An example of the image acquired using the scanner and mounting block, with pigmented foci clearly visible against a background of non-pigmented cells.

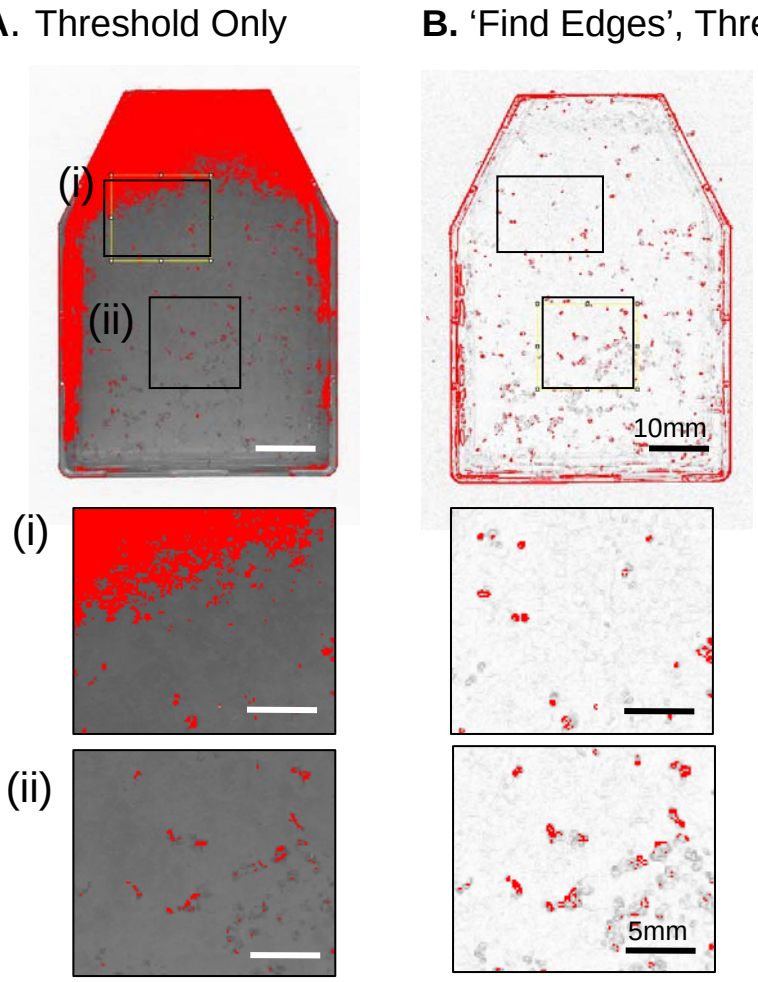

Figure 2.2 Image J 'find edges' function detects pigmented areas in images acquired from the EPSON V700 scanner. Shadows from the edges and top necessitate the use of Image J's 'find edges' function to detect pigmented foci in at the top (i) and side edges of the flask. (A) A Threshold applied to whole flask highlights areas in shadow (i) due to the shape of the T25 flask as well as pigmented foci (ii). (B) The find edges function applied to the same flask (Shef6, day 45) detects pigmented cells in the previously shadowed region. Scale bar = 10mm, 5mm.

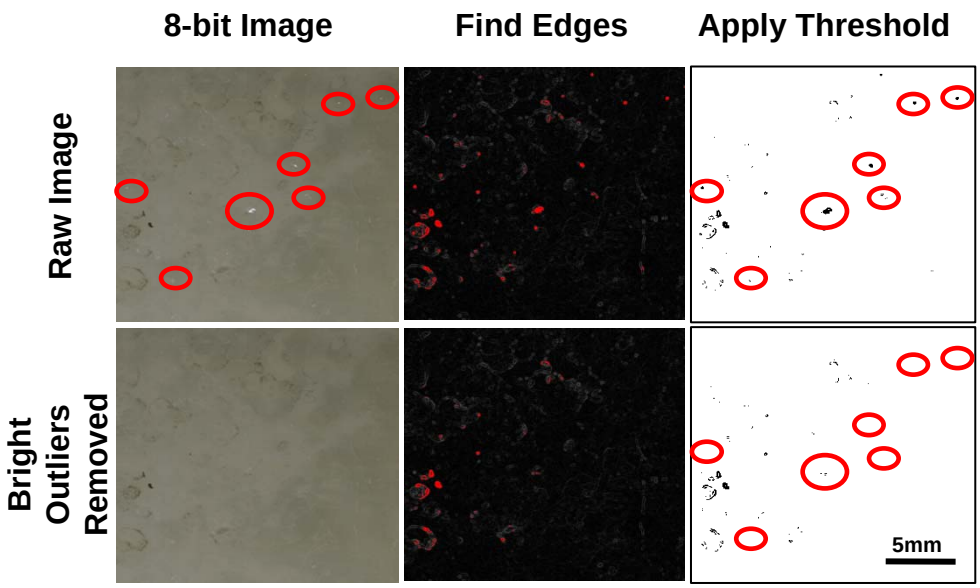

Figure 2.3. White flecks are digitally removed prior to applying 'find edges' function. Samples of scans of Shef6 cells containing pigmented foci, before (top) and after (bottom) removing bright outliers and applying find edges and threshold functions. Top Panel: Red circles highlight areas where white dust has been left on flask surface, these are picked up by find edges function and included when a threshold is applied. Bottom panel: Bright flecks are removed using 'remove outliers' function with the radius set to 30 pixels and the threshold set to 15. The white flecks are removed and no longer picked up when the threshold is applied as seen by the empty red circles in the last column. The pigmented regions are still picked up as seen by the remaining black areas in the last column.

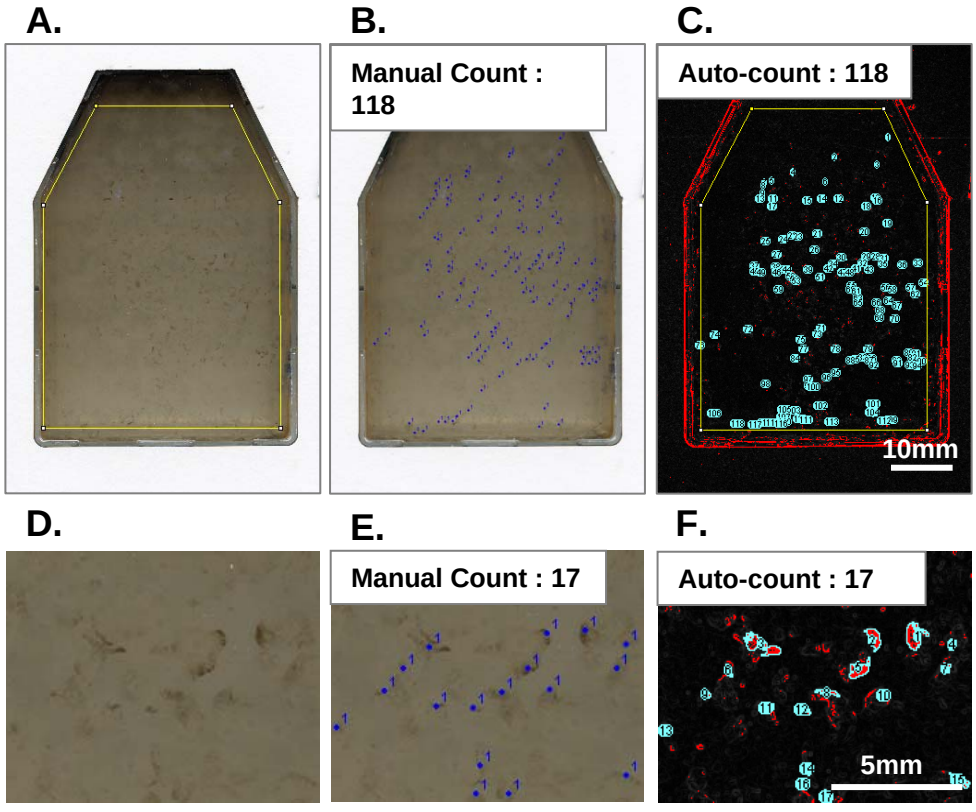
A.
B.
Manual Count : 118
C.
Auto-count : 118
10mm
D.
E.
Manual Count : 17
F.
Auto-count : 17
5mm

G.

```
run("8-bit");
run("Remove Outliers...", "radius=30 threshold=15 which=Bright");
run("Find Edges");

setAutoThreshold();
//run("Threshold...");

setThreshold(45, 255);
run("Convert to Mask");
run("Restore Selection");
run("Analyze Particles...", "size=18-Infinity circularity=0.00-1.00 show=Nothing
display include summarize record add");
```

H.

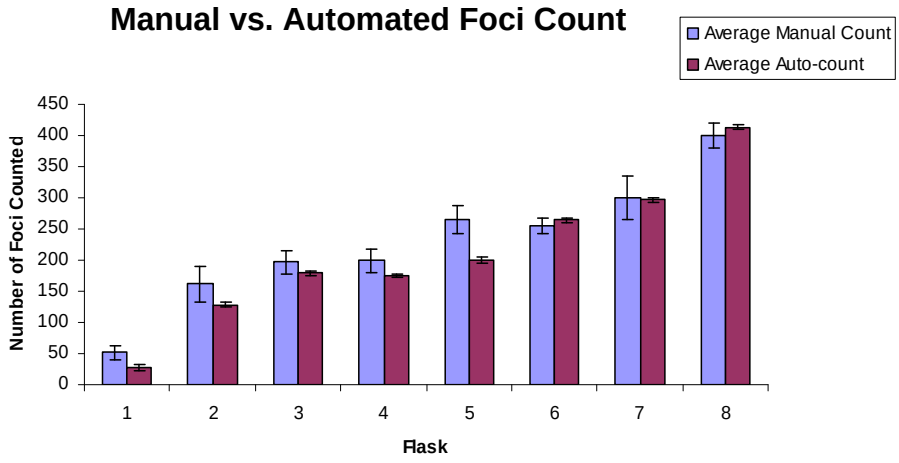

Figure 2.4 Comparing auto-counting method to manual counts. (A). A typical scan of Shef6 at day 50 containing pigmented RPE foci. (B) Manually selecting and counting pigmented foci using the ImageJ cell counter function determines 118 individual foci in the flask. (C) Auto-count using 'find edges' function, thresholding at 45 and including particles >18 pixels in size returns 118 particles in the same flask, scale bar =10mm (D-F) Close up sections of the flasks above, containing with manual and auto-counts labelled, each returning 17 particles, scale bar = 5mm. (G) The combined functions were then assimilated into an ImageJ Macro. The 'autocount macro' generates a value for the total number of pigmented foci above a specified size and pigment intensity threshold. (H) A total of 8 flasks with varying degrees of pigmentation were counted three times on three separate occasions using both manual counting and auto-counting methods applying the macro. Error bars were reduced using the auto-counting macro. For smaller foci numbers, manual counting over estimated the number of foci relative to auto-counting, for larger foci numbers manual counting underestimated the numbers relative to auto-counting.

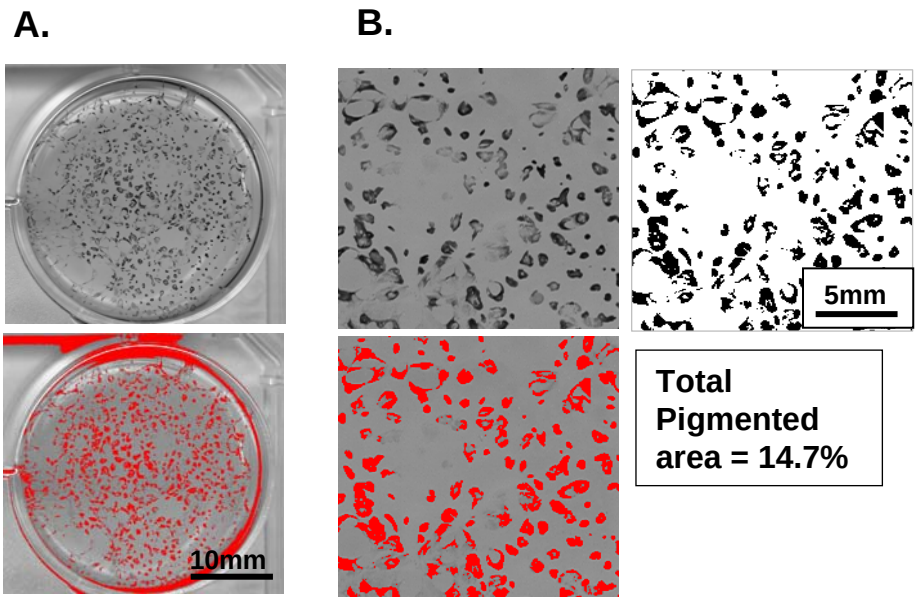

Figure 2.5 Percent pigmented area. Percent pigmented area was used as an alternative to foci numbers to compare relative yields in six well plates where yields were particularly high and individual foci could not be easily distinguished. (A). Scanned images of a typical well at day 50 containing 14.7% pigmented surface area, a circular area as close to the edge of the well as possible was selected, without incorporating side shadows, scale bar = 10mm (B) Enlarged area of the well in A, scale bar = 5mm. 8 bit images were thresholded at 120/255, selecting only pigmented areas and excluding background. The area fraction darker than 120 was then selected, and the % coverage was calculated in image J 'analyse particles' function.

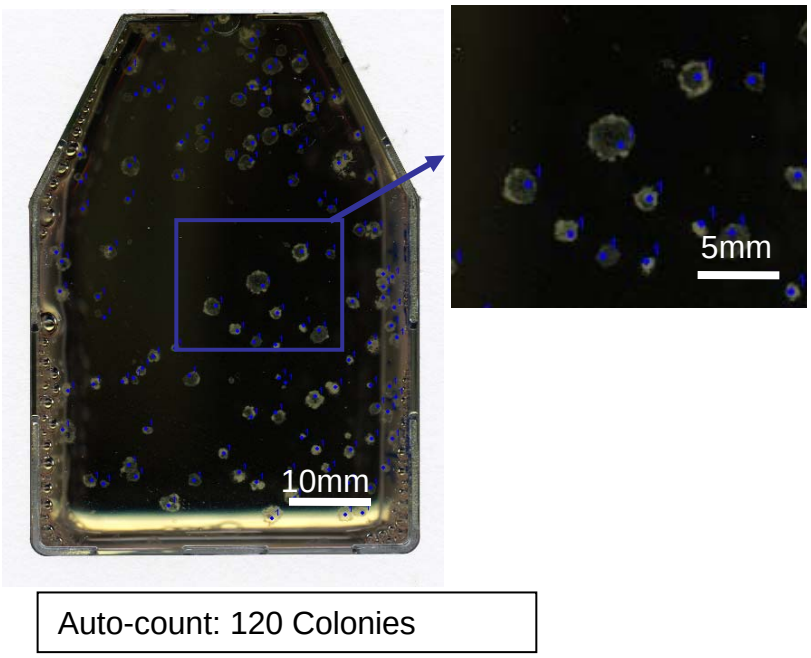

Fig 2.6 Visualisation of HESC colonies at day 6. Examples of scanned image of a flask with the lid removed from the mounting device allowing visualisation of individual HESC colonies at day 6. Colonies were counted using Plugins>analyze>cell counter function.

A.

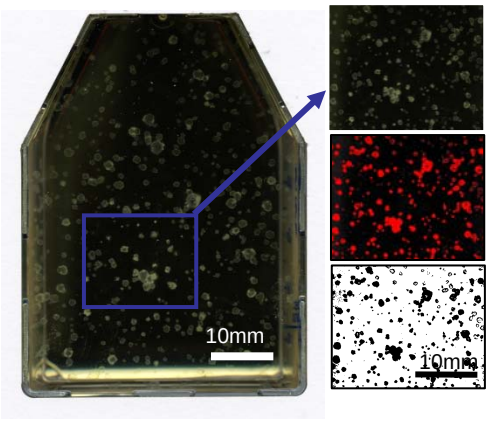

15.1% Confluent

B. **% confluence vs. cell number**

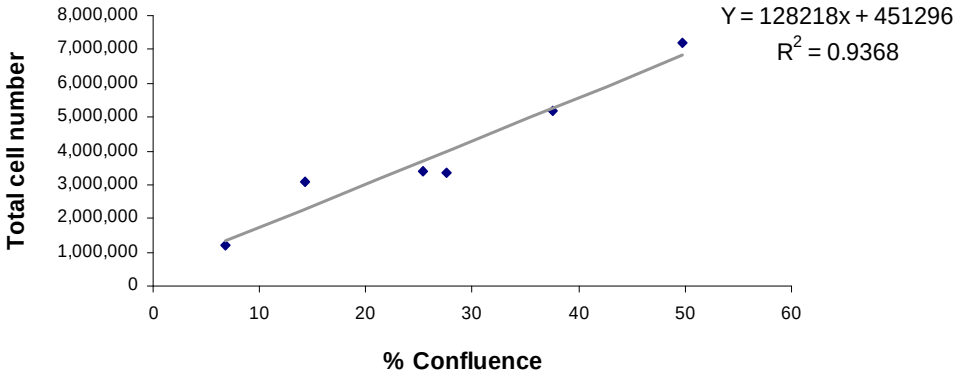

Sample	Total Number of cells	% confluency Image J
Shef6 p50 A	3,350,000	27.6
Shef6 p50 B	3,375,000	25.4
Shef6 p50 C	3,087,500	14.25
Shef 6 p51 A	5,193,000	37.6
Shef6 p51 B	7,207,000	49.8
Shef 6 p52	1,200,000	6.83

Figure 2.7 Confluence vs. Cell number correlation curve (A) A threshold was applied to the scanned images enabling an approximation of the % confluence. (B) Six flasks of shef6 HESC were scanned at day 6 before dissociating into single cells and counting. The results were used to construct a calibration curve that allowed for the approximate determination of cell seeding density.

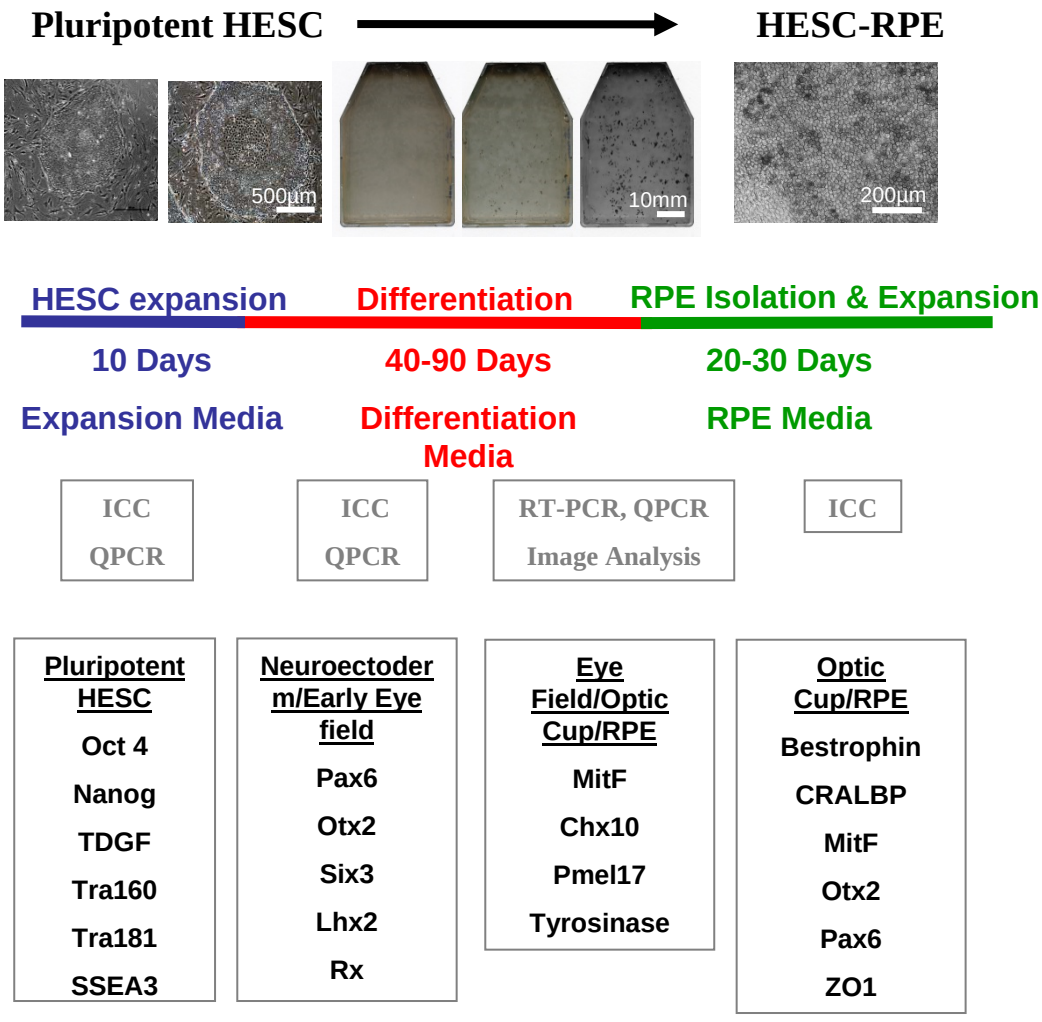

Fig 3.1 HESC-RPE Differentiation using the continuous adherent MEFs co-culture method. The 'continuous adherent' method of differentiation involves plating undifferentiated pluripotent HESC onto mitotically inactivated MEF feeders ('MEFs'). During the HESC expansion phase (first 10 days) cells grow to confluence in expansion medium containing 20% KOSR and 4ng/ml bFGF, during this period immunocytochemistry (ICC) and real-time quantitative PCR (QPCR) is carried out to monitor the expression of pluripotency markers over time. After 10 days the medium is switched to 'differentiation medium' containing 20% KOSR but no bFGF. During differentiation, acquisition of neuroectoderm, eye field and finally pigmented RPE characteristics are monitored with ICC, QPCR, standard reverse transcriptase PCR (RT-PCR) and Image analysis. From day fifty onwards, pigmented foci are large enough to be mechanically extracted. Isolated pigmented foci are then re-plated onto Matrigel coated plates and fed with a-MEM based RPE medium for 20-30 days. Pigmented RPE monolayers are characterised by immunocytochemisty for RPE markers. Scale bars (left to right) 500µm, 10mm, 200µm.

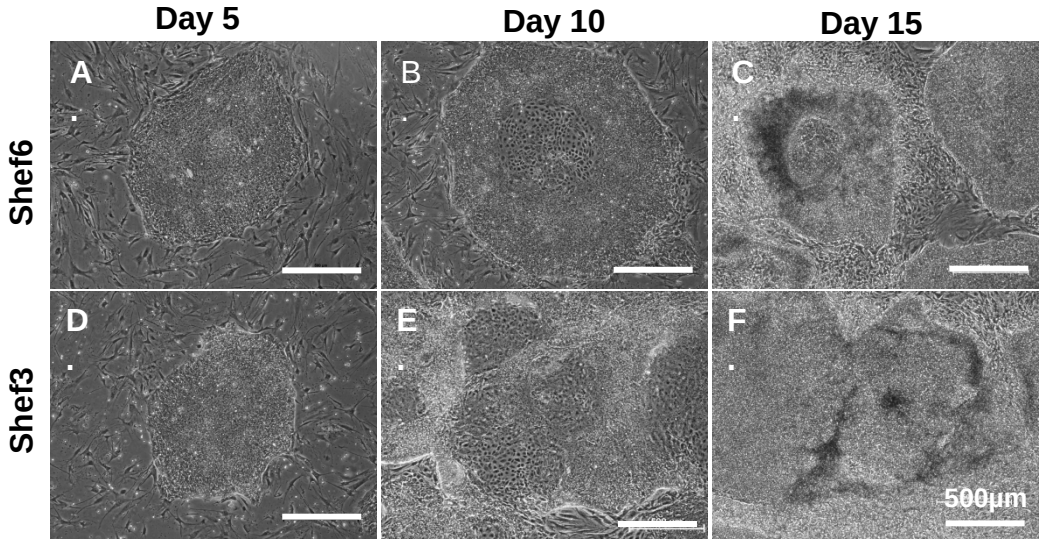

Figure 3.2 HESC morphology. Phase-contrast photographs showing the varying morphology of pluripotent and differentiating shef3 and 6 on MEFs feeders. If colonies are left to expand without passaging their morphology begins to change indicating the loss of pluripotency and beginning of differentiation, (A-C) Typical Shef6 colonies at day 5 (A) and day 10 (B) and day 15 (C) post passaging.. (D-E) Shef3 at day 5 (D), day 10 (E) and day 15 (F) post passaging .Scale bar = 500µm

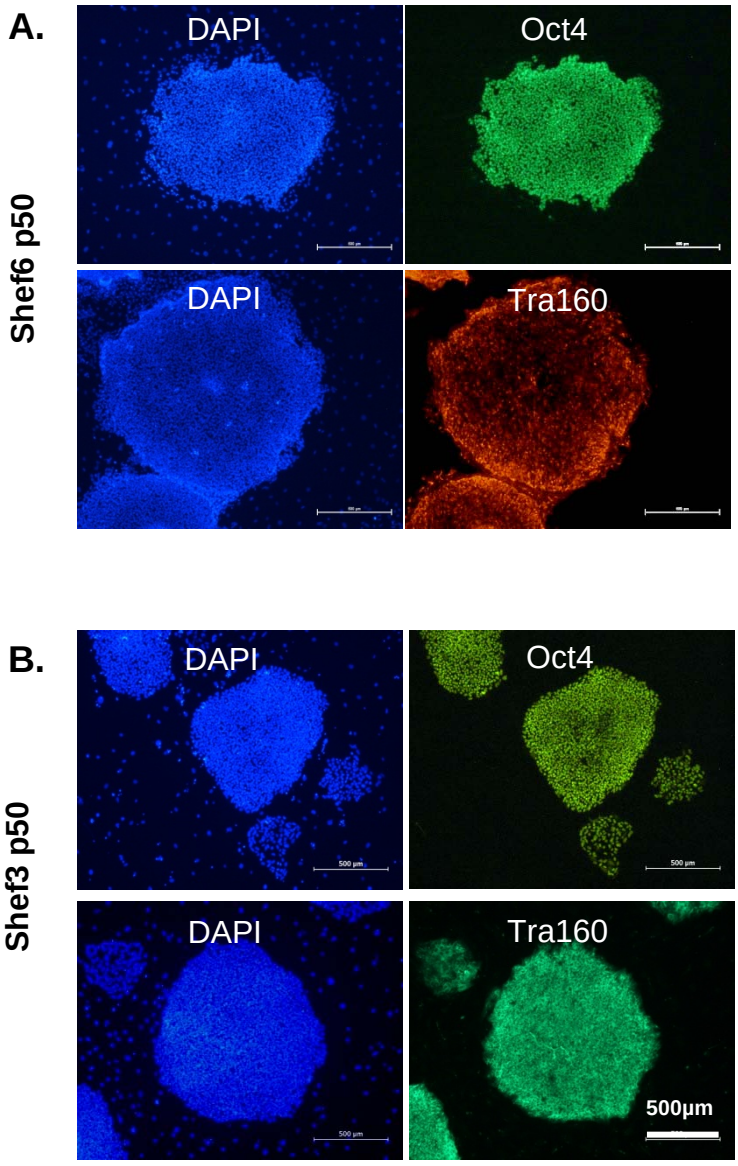

Figure 3.3 Pluripotency marker expression at day 5. The majority of HESC colonies are round, tightly compacted and stain positively for pluripotency markers Oct4 and tra160.(A)Shef6 passage 50 (B) Shef3 passage 50. Scale bar = 500µm.

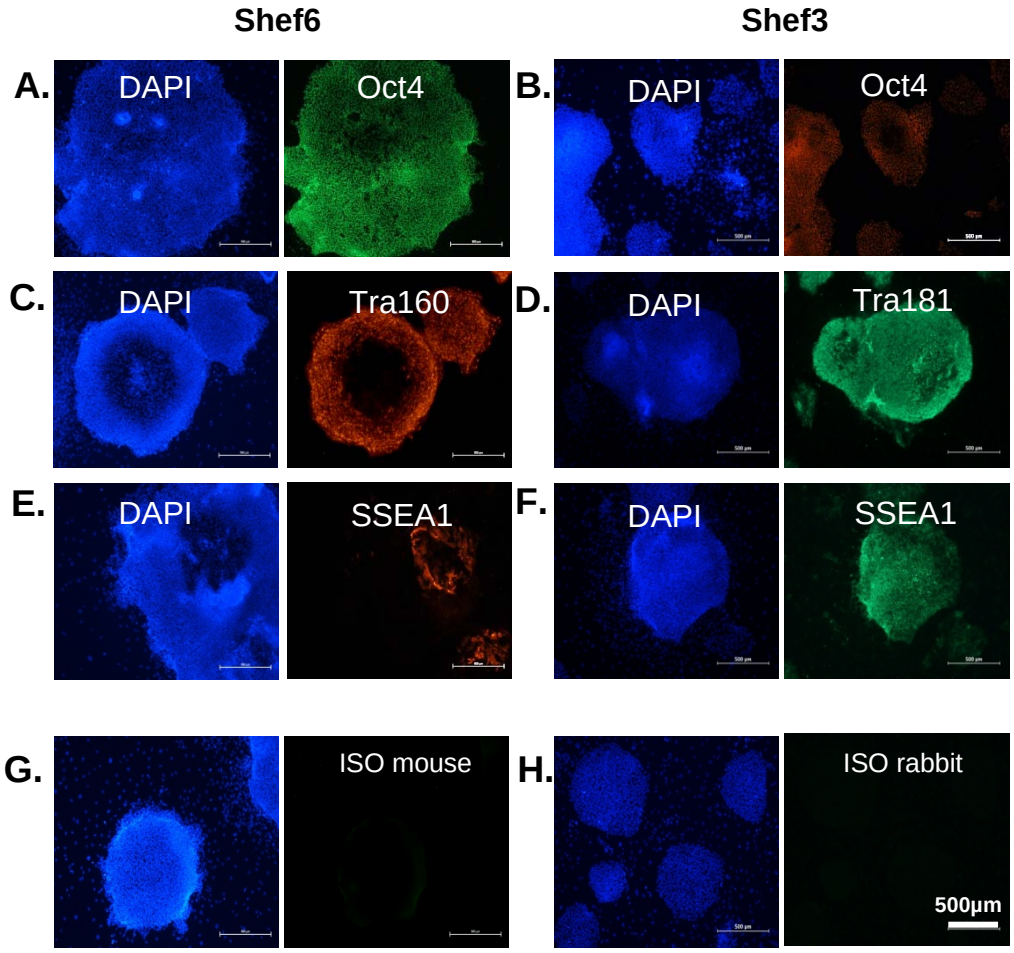

Figure 3.4 Heterogeneous HESC cultures contain some differentiating colonies at day 5. Immunocytochemistry using pluripotency markers (Oct4, tra160, tra181) demonstrates the loss of pluripotency marker expression in spontaneously differentiating colonies of Shef6 and Shef3. (A) Oct4 expression down regulated at one edge of a large Shef6 colony. (B) Oct4 down regulation in a small Shef3 colony at day 5. (C) Tra160 expression is reduced in the centre of a large Shef6 colony. (D) Tra181 is down regulated in the centres of two large Shef3 colonies. (E) SSEA1, a marker of early differentiation in HESC is expressed in the centre of a differentiating colony of Shef6. (F) SSEA1 is expressed across one edge of a differentiating Shef3 colony. (G-H) Isotype controls antibodies (mouse, rabbit) + Alexa 488 secondary. Scale bars = 500µm.

A. SHEF 3 (XY)

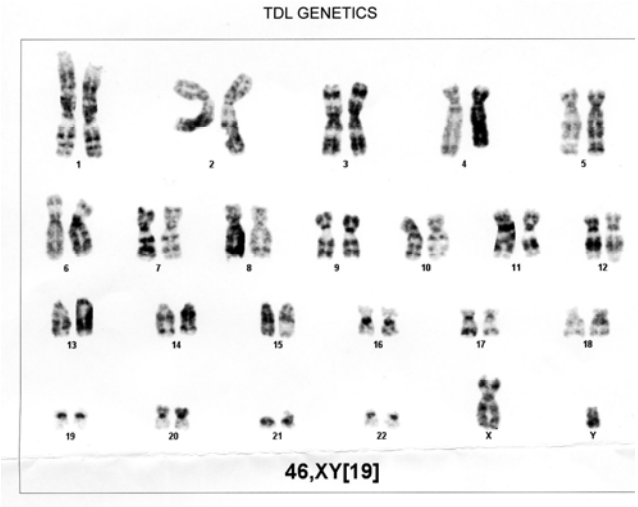

B. SHEF 6 (XX)

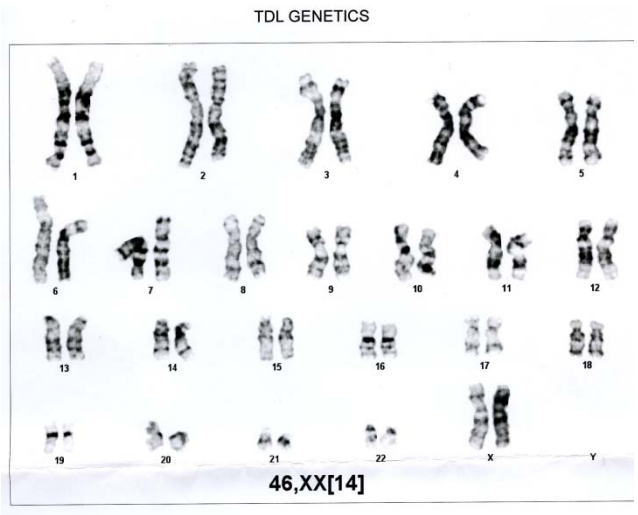

Figure 3.5 Karyotypic Analysis of Shef6 and Shef3 cell lines. Karyotypic analysis using standard G banding was carried out regularly (TDL genetics, Whitfield street, London). (A) G banded chromosomes of Shef3 at passage 103. In the majority of cases Shef3 had a normal 46 XY karyotype. On one occasion a subpopulation of TRISOMY 5 cells was detected. (B) G banded Shef6 chromosomes at passage 62 showing a normal 46 XX karyotype. On one occasion a TRISOMY 5 and TRISOMY 17 sub population of cells were also detected in Shef6.

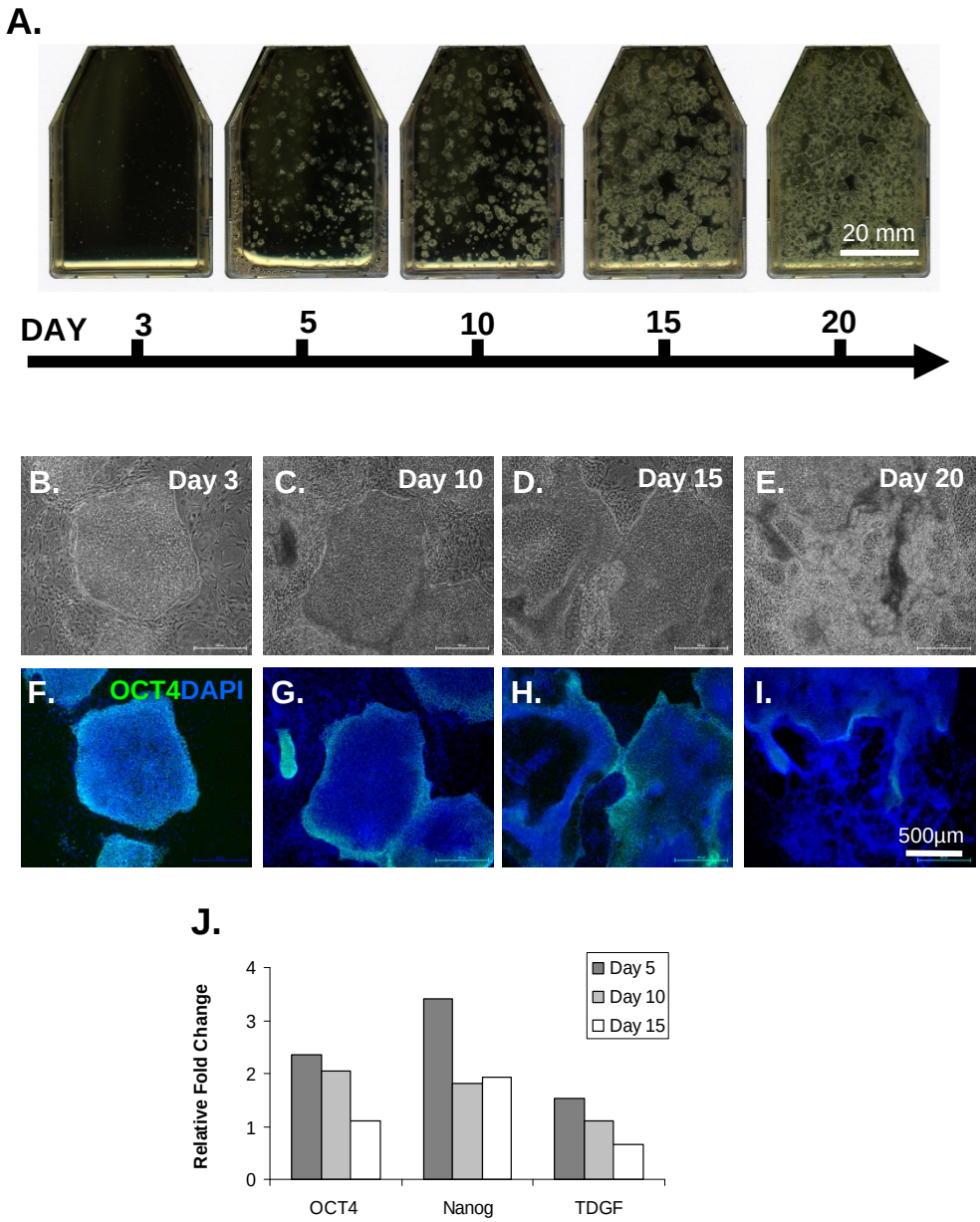

Figure 3.6 Spontaneous differentiation of HESC in MEFS co-culture. (A) Scanned images of whole flasks show how individual colonies expand over time to fill a T25 culture flask. (B-E) Bright field images show the changes in cell morphology that accompany early, spontaneous differentiation after prolonged culture on MEFs and withdrawal of bFGF at day 10, scale bar = 500µm. (F-I) Immunofluorescence images of OCT4 and DAPI over the time course of early differentiation show the progressive loss of Oct4 immunoreactivity. (J) QPCR for HESC markers (OCT4, NANOG, TDGF) show a gradual decrease in expression over the first 15 days of differentiation post seeding. Bars represent the normalised fold change in gene expression relative to day 3.

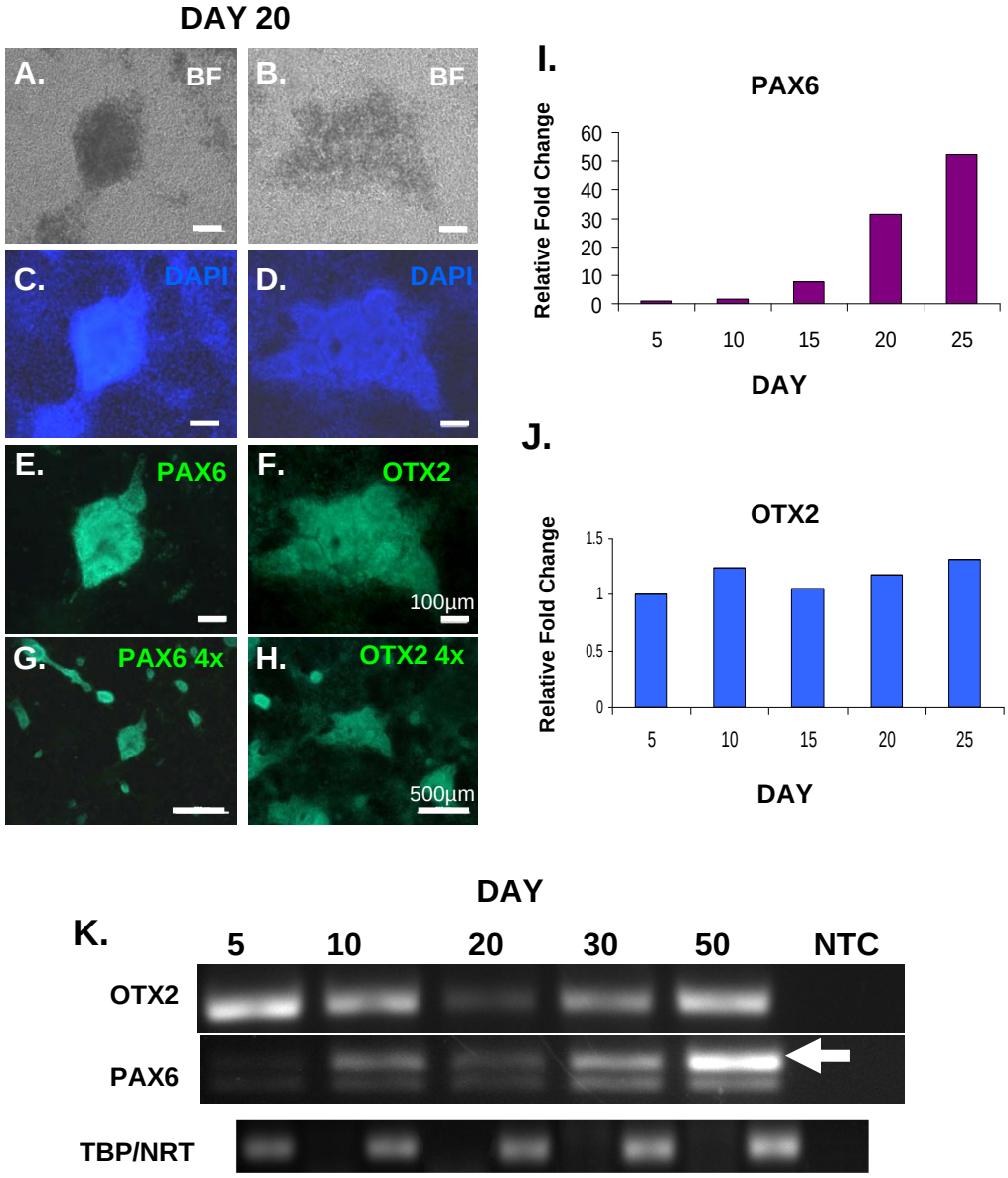

Figure 3.7 Spontaneous differentiation yields thickened ridges containing Pax6 and Otx2 positive neuroepithelial rosettes. (A-H) Bright field and immunofluorescence images taken at day 20 of continuous adherent differentiation on MEFs. Thickened, multilayered clumps of cells containing rosette structures are Pax6 and Otx2 positive, scale bar = 100µm. (G-H) The clumps and ridges are found in abundance across the flasks as seen in 4x magnification images, scale bar = 500µm. (I) QPCR time course over 25 days in shef6 bars show the expression of Pax6 and Otx2 at each day relative to day 5. (K) RT-PCR at days 5,10,20,30 and 50 of differentiation in Shef3 shows the expression of Otx2 and Pax6 relative to the house keeping gene TBP as well as no reverse transcriptase (NRT) and no template controls (NTC). Pax6 primers amplify both the larger +5a (arrow) and smaller -5a Pax6 isoforms, the former of which is more critical to retina formation (Azuma et al., 2005).

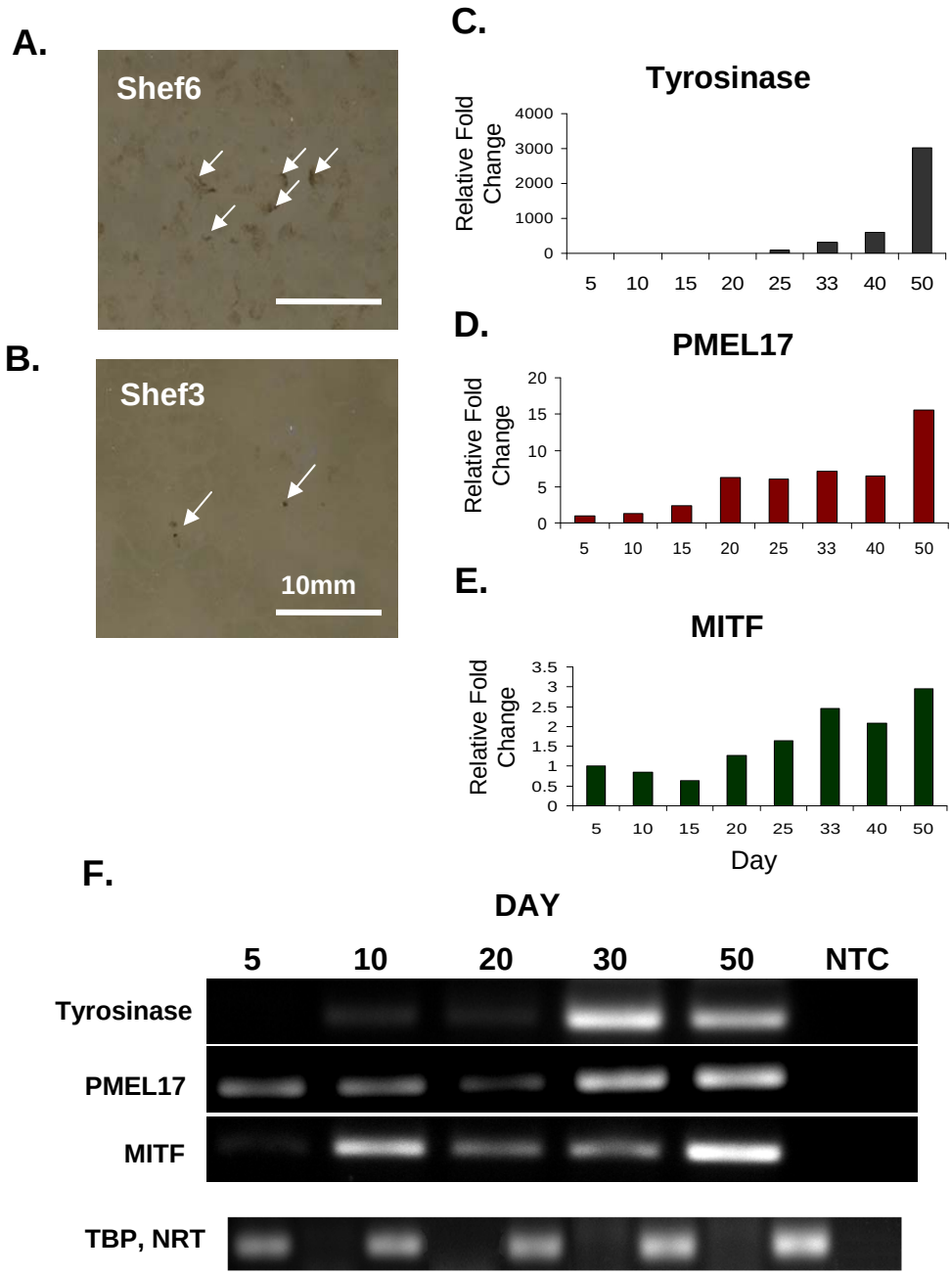

Figure 3.8 Pigmented foci being to appear between days 25 and 32 post HESC seeding. (A,B) Scanned images of Shef6 and Shef3 flasks at day 40 showing the pigmented foci, scale bar = 10mm. (C-E) QPCR time course of gene expression in whole flasks over 50 days of Shef6 differentiation from HESC demonstrates the relative fold increases in expression RPE/Pigmentation genes Tyrosinase (C), PMEL17 (D) and MitF(E). (F) RT-PCR time course of Shef3 differentiation showing a similar pattern of Tyrosinase and Pmel17 up regulation over time. An increase in MitF expression is detected earlier in Shef3 at day 10.(NTC = no template control, TBP = house keeping gene, NRT= no reverse transcriptase control).

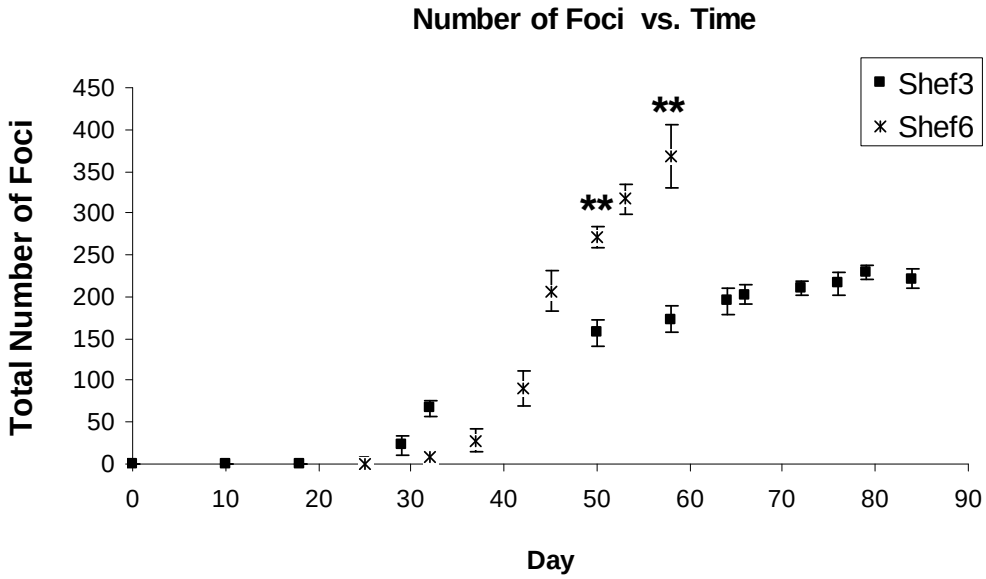

Figure 3.9 Kinetics of RPE accumulation over time. The numbers of individual foci were determined from scanned images of flasks taken at several time points using the image J macro (see chapter 2 methods) over 84 days (Shef3, N=3) or 58 days (Shef6 N=3) of HESC-RPE differentiation. Error bars = SEM. In both cell lines numbers of foci accumulated rapidly from days 30-50 in Shef3 at a rate of 0.27 $\pm$ 0.02 foci/cm^2/day and in Shef6 at 0.53$\pm$0.03 foci/cm2/day. Two way ANOVA revealed a significant effect of time ($F(4,20) = 47.5$, $p<0.001$), Cell line ($F(1,20) = 18.4$, $p<0.001$) and a significant interaction ($F(4,20) = 14.31$ $p<0.001$), indicating that the cell line effect increased with time in culture. At days 50 and 58 there were significantly greater numbers of pigmented foci in Shef6 relative to Shef3 (**$p<0.01$ unpaired student's t-test).

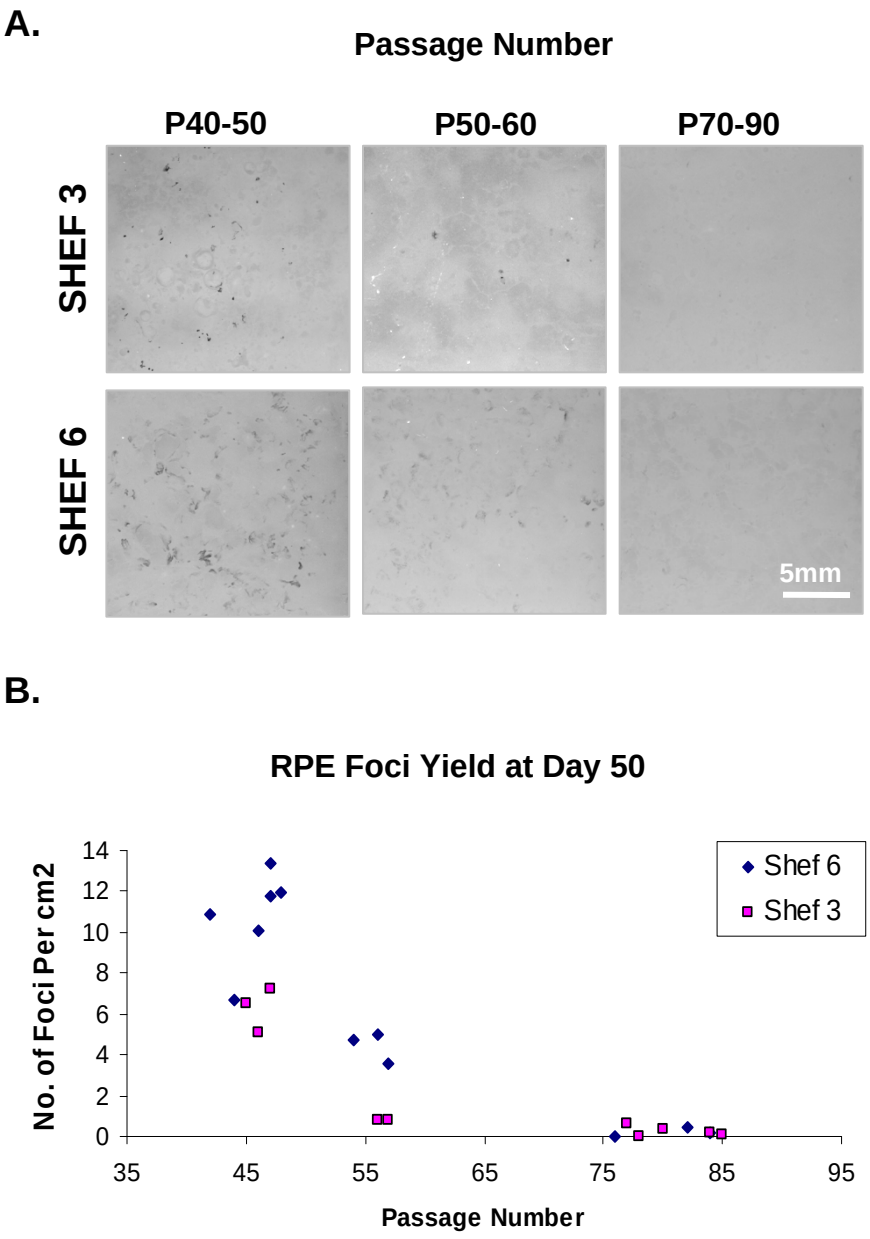

Figure 3.10 RPE yield is compromised at high passage numbers. (A) Representative scanned areas of typical flasks of Shef3 (top panel) and Shef6 (lower panel) at day 50 at low (p40-50), medium (p50-60) and high (p70-90) passage numbers illustrating difference in typical foci numbers. (B) Scatter graph of number of foci per cm2 at day 50 vs. starter HESC culture passage number. Average (p40-50 Shef6+Shef3)= 9.3±1.0 foci/cm2, (p50-60 Shef6+Shef3)= 3.0±1.0 foci/ cm2, (p70-90 Shef6+Shef3) =0.23±0.08 foci/cm2). Two way ANOVA revealed a significant effect of passage number ($F(2,10)= 70.9$, $p<0.01$) and cell line ($F(1,10) = 5.8$, $p<0.05$) but no significant interaction ($F(2,10)=2.02$, $p=0.23$).

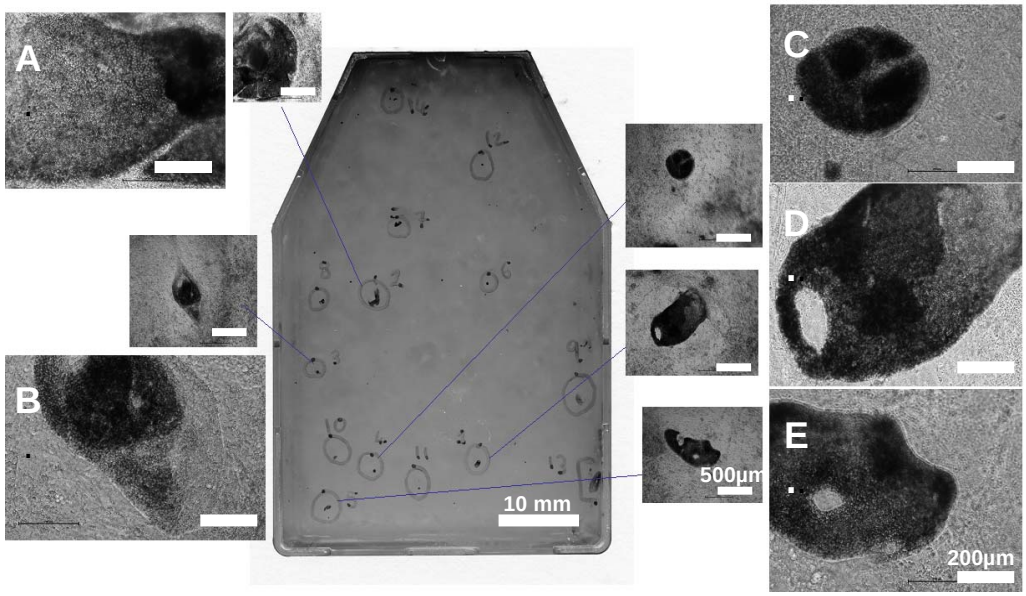

Figure 3.11 Pigmented foci adopt a range of sizes and morphologies. Scan of a whole T25 flask at day 60 containing several pigmented foci with the corresponding 4x and 10x bright field microscope images of individual foci labelled (A-E). In some areas, a pigmented monolayer of cells 'fan out' from a central focus (A), in other areas foci are small and discrete (C). Differences are likely due to local spatial constraints and asynchronous differentiation. Scale bars (large) = 200µm, (small) = 500 µm.

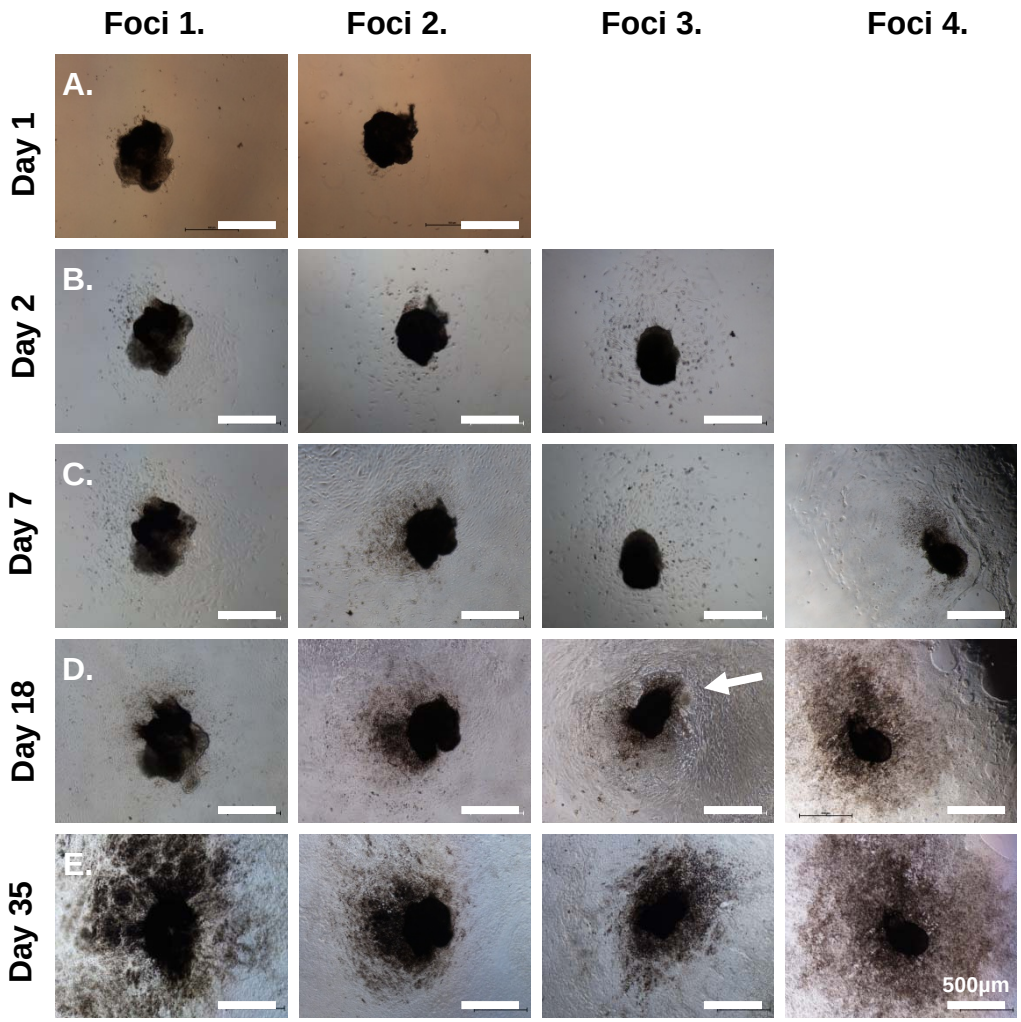

Figure 3.12 Manually isolated foci adhere to Matrigel coated plates and proliferate forming monolayers of pigmented cells with 'cobblestone morphology'. Bright field microscope images taken at 4x magnification. Four pigmented foci were manually extracted from typical day 60 cultures using microsurgical blades and re-plated onto Matrigel coated plates in aMEM- RPE medium. By day 3 the foci had adhered to the coated plates and cells had begun to proliferate away from the attached foci. By day 18 heavily pigmented cells were visible, though a contaminating cell type with neuronal projections was visible in one well (Foci 3, arrow). By day 35 extensive monolayers of heavily pigmented cells with classical, polygonal RPE morphology had formed around each foci but the total area occupied by pigmented cells was variable. Scale bars = 500µm

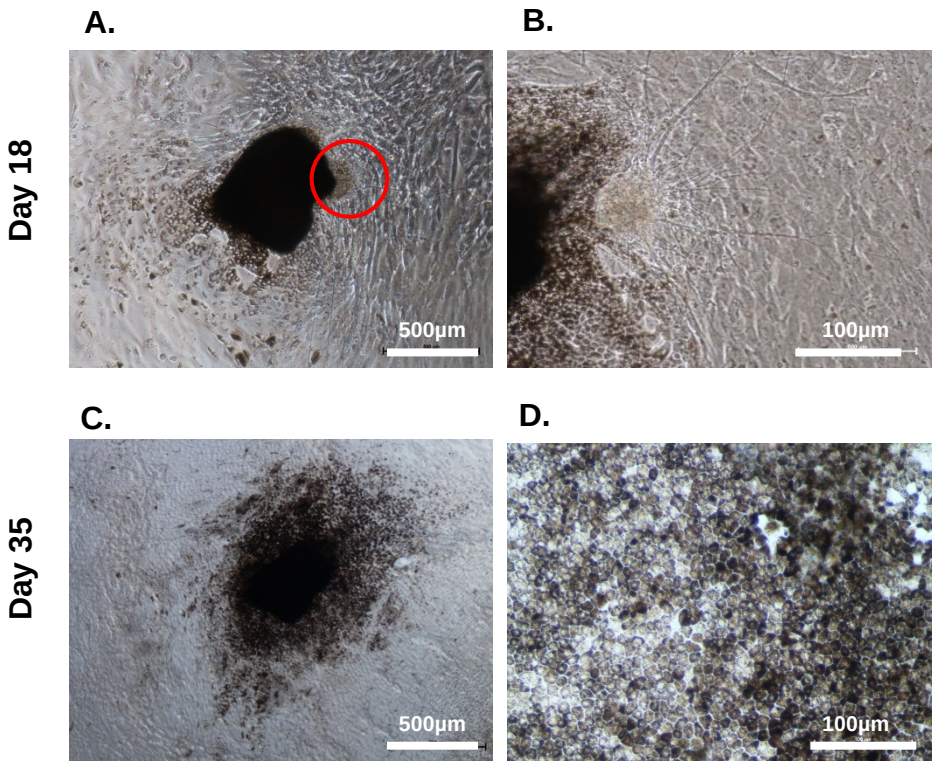

Figure 3.13 Contaminating, non pigmented cell types were occasionally visible in the manually extracted foci. Microscope images of an expanding foci at day 9 and day 35 at 4x (A,C) and 20x (B,D) magnification. (A) In addition to the usual cells with a cobblestone, pigmented phenotype, a cluster of non pigmented cells from which neuronal projections were visible was observed (enlarged image B). By day 35 these cells had receded and the area was overtaken by expanding RPE (C,D).

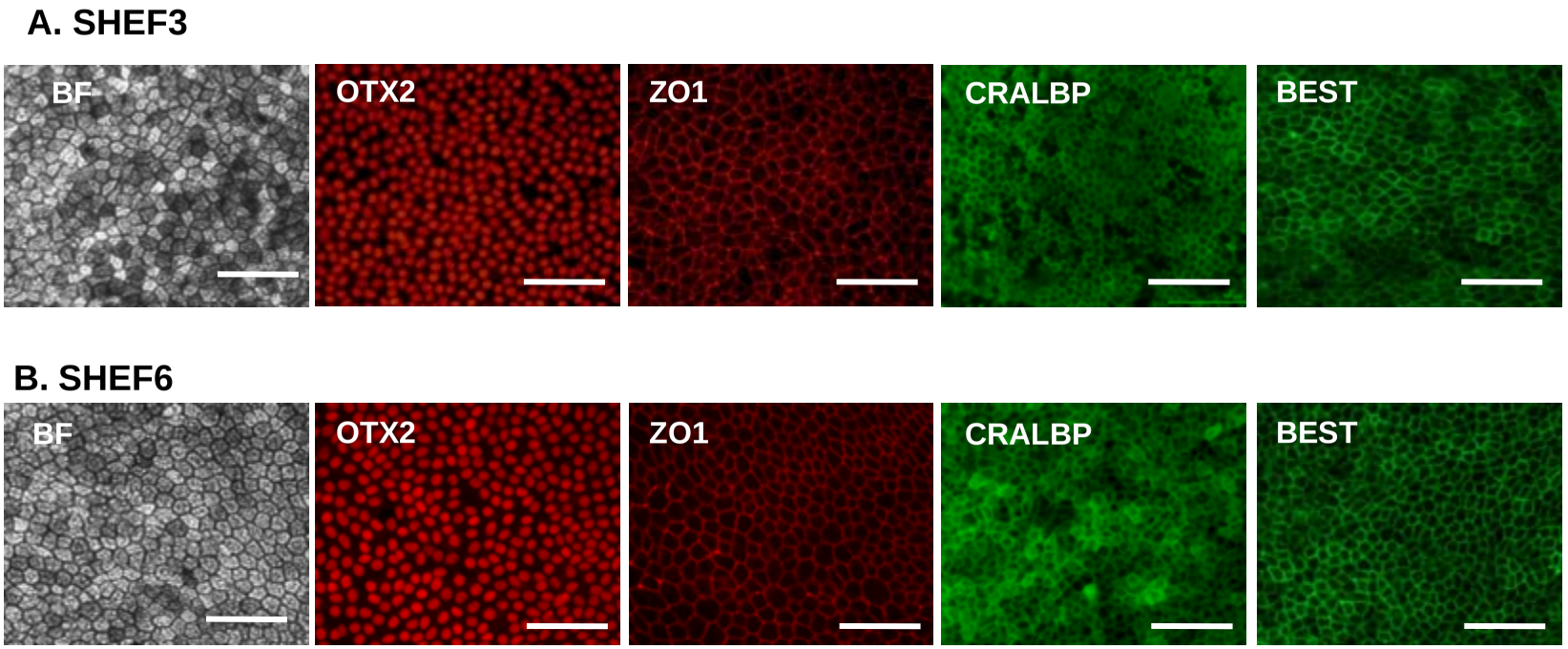

Figure 3.14 Phase contrast and fluorescence images of expanding RPE from Shef6 and Shef3. Pigmented cells derived from Shef3 and Shef6 foci have typical RPE morphology and are immunopositive for RPE markers. Pigmented foci were manually extracted from day 50 cultures of Shef3 (A) and Shef6 (B) and re-plated onto Matrigel coated plates where they were left to expand in aMEM RPE medium for 3-5 weeks. Brightfield images (BF) Shef3 and Shef6 foci derived cells, heavily pigmented and with polygonal, 'cobblestone' morphology typical of RPE. Immunostaining demonstrates the homogeneous expression of RPE markers Otx2, ZO1, CRALBP and Bestrophin in pigmented cells derived from both cell lines.

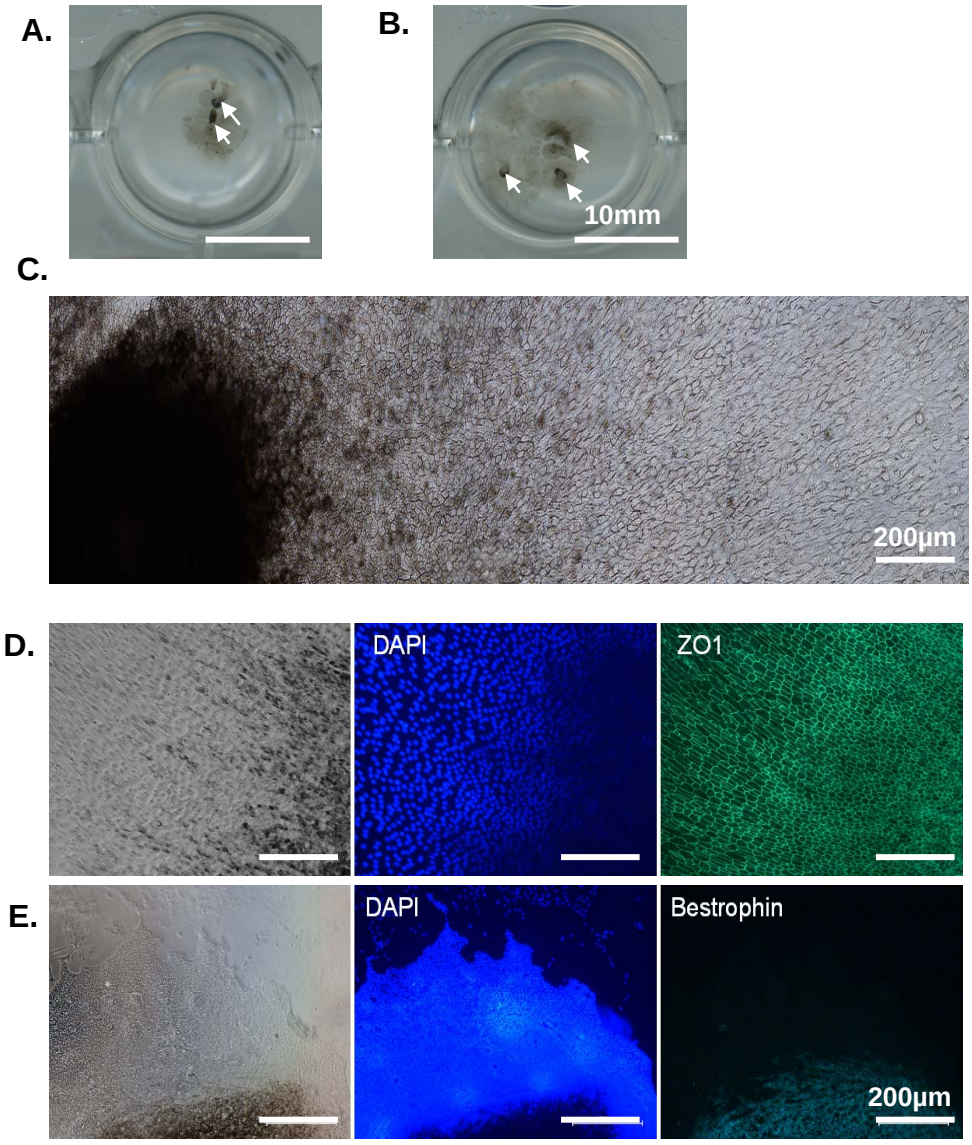

Figure 3.15 Proliferating RPE de-pigment, adopt an elongated morphology and down regulate RPE marker expression. (A,B) Scanned images showing typical wells containing expanding pigmented foci (day 35) scale bar = 10mm. The attached pigmented foci are clearly visible (arrows) and are surrounded by an expanding monolayer of RPE with the intensity of pigment decreasing with distance from the central foci. (C) Microscope images stitched together showing changes in cell morphology and pigmentation with distance from the adherent foci. Cells close to the central foci are pigmented and have typical cobblestone morphology, whereas at the proliferating edge cells are de-pigmented and have a more elongated morphology, scale bar =200µm. (D,E) Brightfield and immunocytochemisty at the leading edge. (D) ZO1 expression indicates the presence of tight junctions across the expanding RPE but a clear change in morphology towards a more elongated phenotype at the leading edge. (E) Bestrophin is only expressed in the compacted, heavily pigmented cells close to the central foci. DAPI nuclear staining is obscured in heavily pigmented cells, scale bar = 200µm

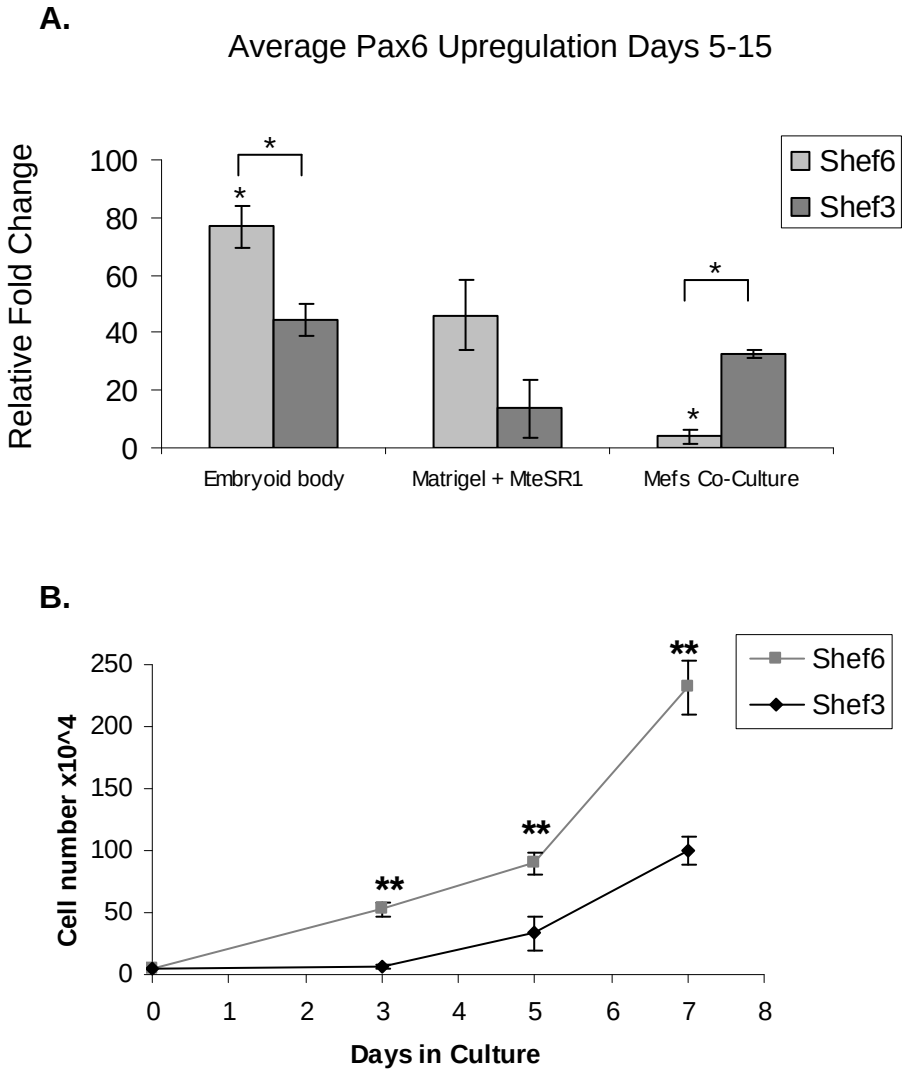

Figure 3.16. Pax6 up regulation and cell growth rates in Shef6 and Shef3 in feeder-free differentiation. (A) QPCR showing relative fold up regulation in Pax6 from days 5-15 in Shef6 and Shef3 cells taken from a range of passages (passage numbers 50-80). Cells were split three ways and allowed to expand and differentiate in three separate systems: 1. On low attachment plates as embryoid bodies (EBs) in HESC media +bFGF 2. On Matrigel in MTeSR1 media 3.In MEFs co-culture and HESC media +bFGF. After 10 days expansion and 5 days in differentiation media (-bFGF), cells were harvested for QPCR. The graph shows the average relative up regulation in Pax6 expression from days 5- 15. In Shef6 there were statistically significant differences between the differentiation methods (one way ANOVA, $F(2,6)=37.6$, $p<0.01$), but not in Shef3. In the EB method Shef6 up regulation was significantly higher in Shef6 than Shef3. In contrast , in MEFs co-culture differentiation, Pax6 up regulation was significantly higher in Shef3 (* $P<0.05$ student's t-test error bars =SEM). (B) Shef3 and Shef6 cell growth rates were measured over 7 days in feeder-free Matrigel+mTeSR1 conditions. There was a significant difference between cell lines (2 way ANOVA) with shef6 cell numbers significantly greater than Shef3 at days 3, 5 and 7 (* $P<0.05$, N=4, Student's unpaired t-test).

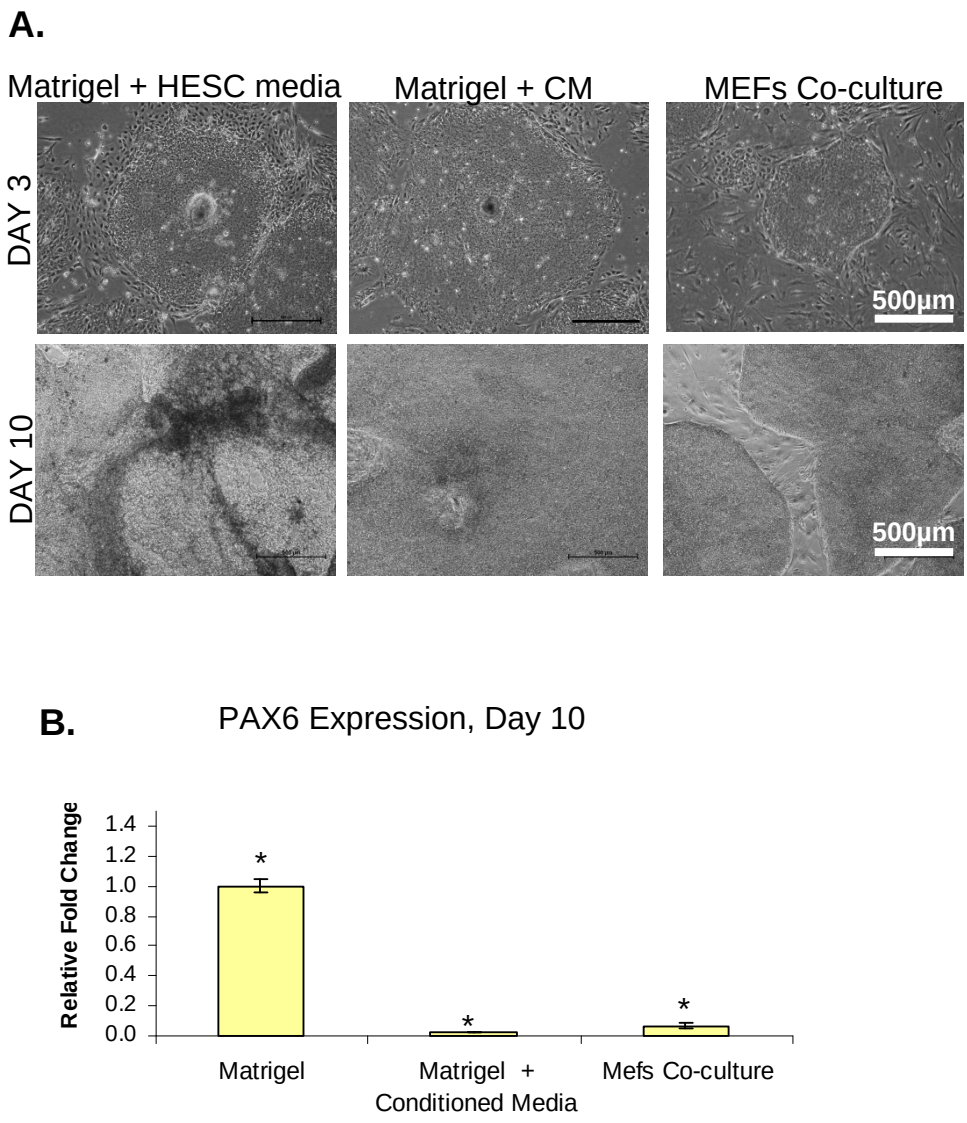

Figure 3.17. Shef3 expanding in MEFs and feeder free conditions . (A). 4x phase contrast images of typical Shef3 cultures at day 3 and day 10 in three differentiation conditions; on Matrigel in HESC media, on Matrigel in MEFs conditioned media, and in MEFs co-culture. MEFs conditioned (CM) media maintains undifferentiated HESC morphology similar to that seen in MEFs co-culture although colonies tended to expand to larger sizes. Cells grown on Matrigel in standard HESC media rapidly differentiated adopting non HESC-like morphologies. Scale bar = 500µm. (B) Similar to differentiation by the embryoid body method (Fig 3.16), Pax6 expression is significantly higher at day 10 in cells grown on Matrigel with standard HESC media (one way ANOVA, $F(2,6)= 150$, $P<0.05$) this reflects the rapid differentiation of HESC in the absence of MEFS or MEFS conditioned medium regardless of whether cells are differentiating as floating EBs or adhered to Matrigel.

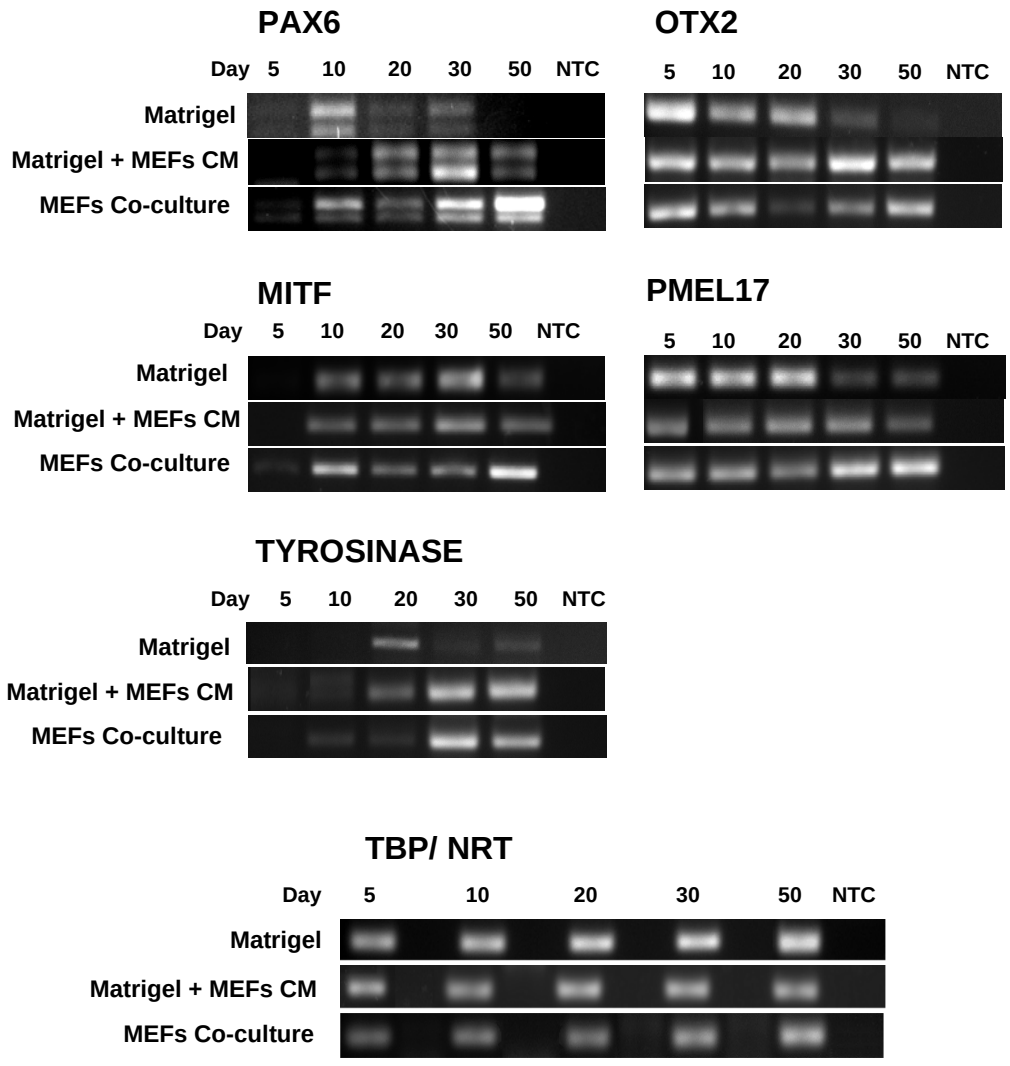

Figure 3.18 Time course of gene expression over 50 days Shef3 differentiation in MEFs co-culture and in feeder cell free conditions. RNA was harvested at 5 times points from Shef3 differentiating in three conditions; on Matrigel in HESC medium (+bFGF), on Matrigel in MEFS conditioned media (CM) or in MEFS co-culture, bFGF containing media (or CM) was replaced with –bFGF differentiation media from day 10 onwards. In the absence of MEFs or MEFs conditioned medium, genes critical to RPE formation (Pax6, Otx2, MitF, Tyrosinase, Pmel17) are down regulated over time. In the presence of MEFs CM (middle row) the temporal gene expression pattern is similar to that seen in HESC differentiating in MEFs co-culture (bottom row).

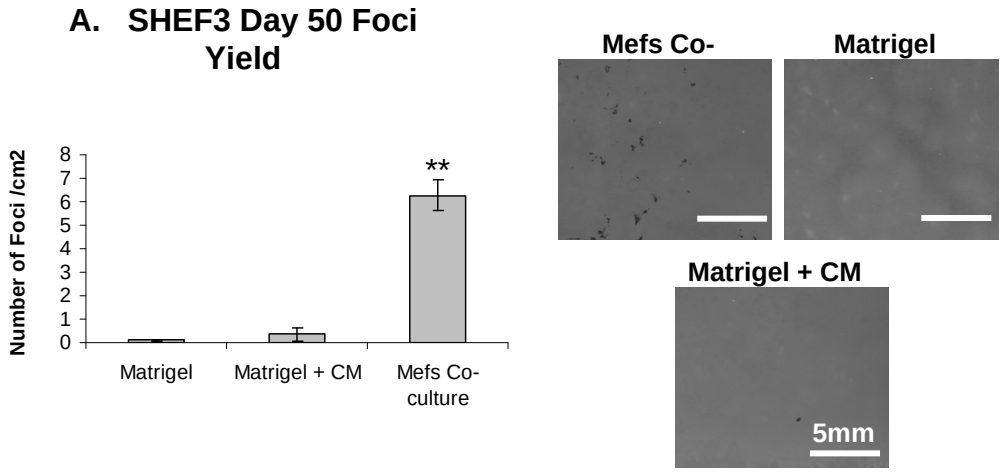

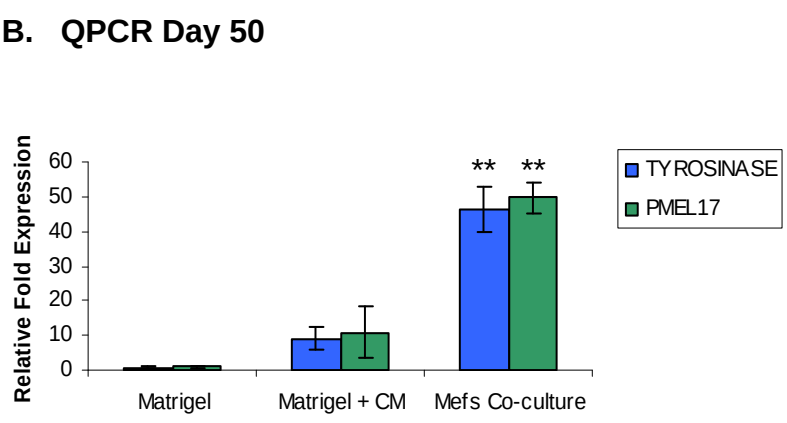

Figure 3.19 RPE yields in Feeder free culture. RPE foci numbers were counted using the auto-count macro (see methods) from scans of flasks taken at day 50 (N=3 passage numbers 45-48). (A) Shef3 produced significantly greater RPE yields when differentiated in MEFs co-culture relative to the other conditions (one way ANOVA, $F(2,6) = 76.8$, $p < 0.05$, student's paired t-test, $^{**}p<0.001$). Cells seeded onto Matrigel in standard HESC media had poor survival and produced very few RPE per cm2, when seeded onto Matrigel with MEFs conditioned media the yield improved slightly but not significantly. (B) QPCR analysis following 50 days of Shef3 differentiation. There were significant differences in Tyrosinase and Pmel17 expression at day 50 (One way ANOVA, $F(2,6)= 26.5$, $p<0.01$, $F(2,6)= 33.7$, $p<0.01$ respectively) with the expression of both genes significantly higher in MEFs co-culture (student's paired t-test, $^{**}P<0.01$). The differences in expression between Matrigel + CM and matrigel only were not significant. Error bars = SEM.(C) Bright field images of emerging pigmented foci in day 50 cultures of Shef3 in feeder-free Matrigel+CM and MEFs co-culture differentiation. (D) 'Feeder free' Matrigel+CM derived foci were mechanically isolated and re-plated. Typical cobblestone RPE monolayers formed with pigmented cells that were positive for RPE markers Bestrophin and CRALBP, scale bar = 50µm.

C. Matrigel + CM MEFs co-culture

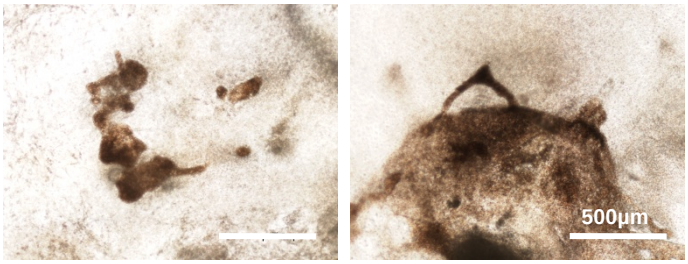

D. Matrigel + CM expanding RPE Foci

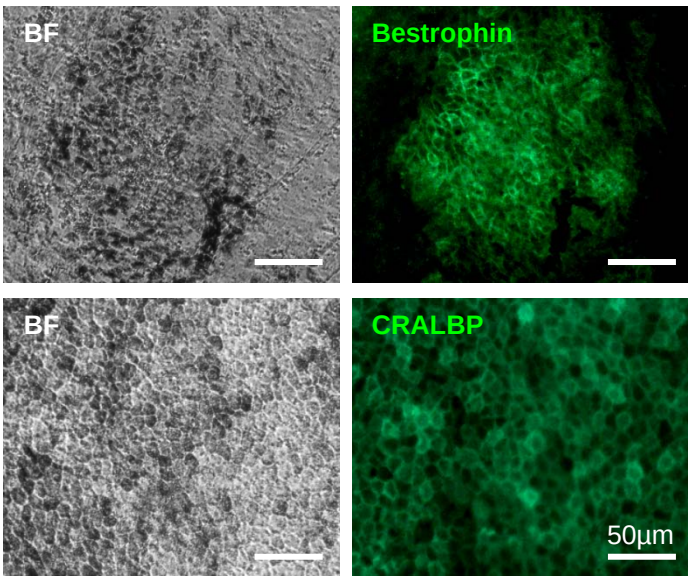

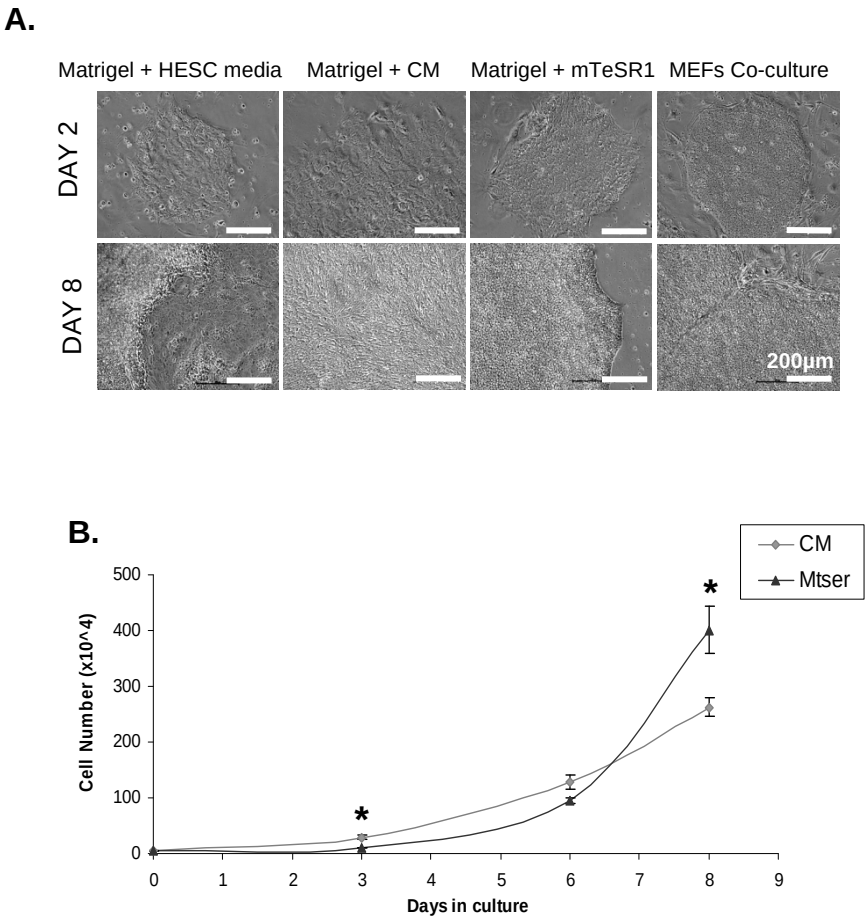

Figure 3.20 Shef6 expanding in feeder-free conditions. (A) Bright field microscope images at day 2 and day 8 showing Shef6 colony morphology in different conditions. Typical HESC morphology as seen in standard MEFs co-culture is apparent when cells are seeded on Matrigel+ conditioned media, or mTeSR1 media. In absence of MEFs, MEFs-CM or mTeSR1 however, when cells are grown in standard HESC media +bFGF, distinctive changes in cell morphology are apparent by day 8 (bottom left panel), scale bar = 200µm (B) Growth curves of Shef6 expanding on Matrigel in MEFs-CM and in defined mTeSR1 media over 8 days in culture. There were statistically significant differences in cell numbers between cells lines which increased over time (2 way ANOVA, $F(2,18) = 47.7$, $p<0.001$), specifically there were more cells in the MEFs-CM condition at day 3 but more cells in mTeSR1 by day 8 (unpaired, student's, t-test N=4, * $P<0.01$), possibly reflecting a period of adaptation to mTeSR1 media. Error bars = SEM.

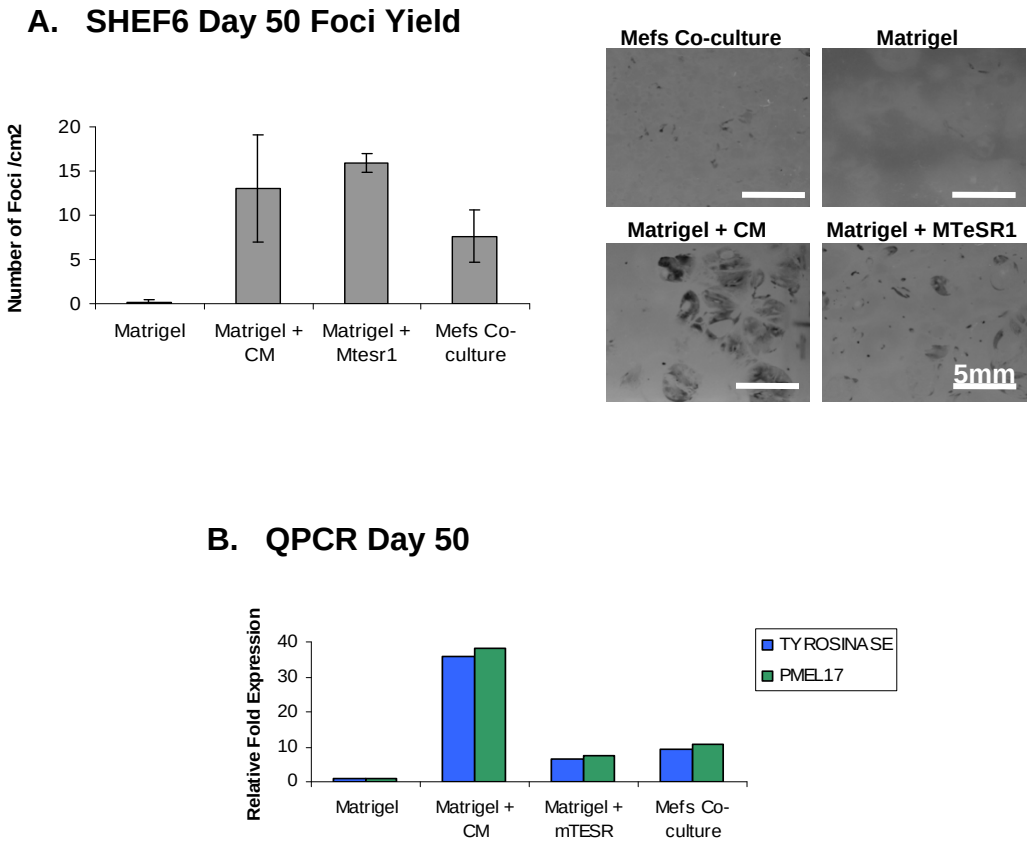

Figure 3.21 Shef6 RPE yield in feeder-free culture. (A) The average number of pigmented foci /cm2 in Shef6 cells at day 50, following differentiation in four conditions (N=2 passage numbers 42, 54). In Matrigel + standard HESC media, Matrigel + MEFs conditioned media, Matrigel + mTeSR1 media and in MEFs co-culture, error bars = SEM. Areas taken from scanned images of flasks at day 50. (B) QPCR analysis reveals differences in Tyrosinase and Pmel17 expression at day 50, following expansion in the different feeder-free conditions.

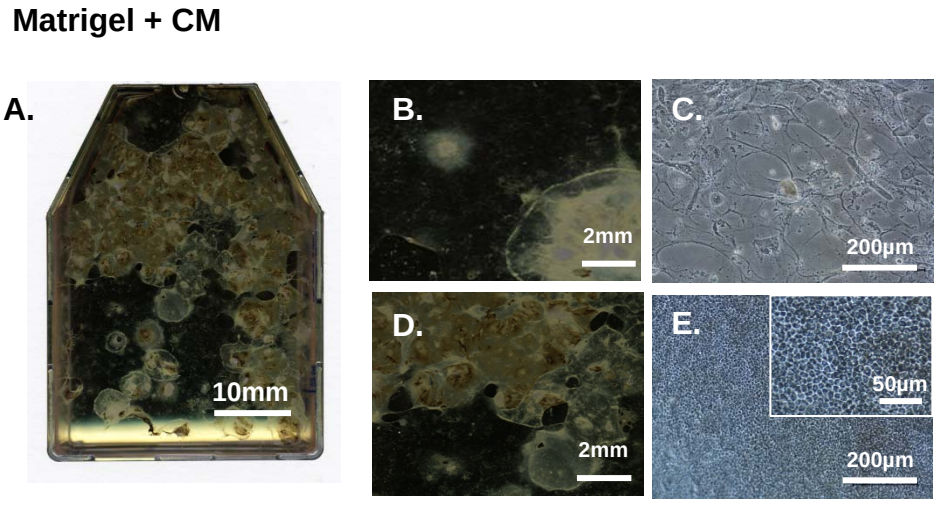

Figure 3.22 Variation in cell sheet coverage and thickness at day 50 dependent on expansion medium. Scanned images of flasks at day 50 showing opaque white areas covered with thick cell sheets, and dark, translucent areas with little cellular material. (A) Shef6 expanded in CM had formed a patchy cell sheet at day 50. (B,C) Large areas with sparse cell coverage were visible. (D,E) large areas of expanding pigmented RPE were also visible (F-H) Shef6 cells that were expanded in mTeSR1 media formed a thick multi-layered sheet in which abundant pigmented foci were embedded. Scale bars (left to right) = 10mm, 2mm, 200µm.

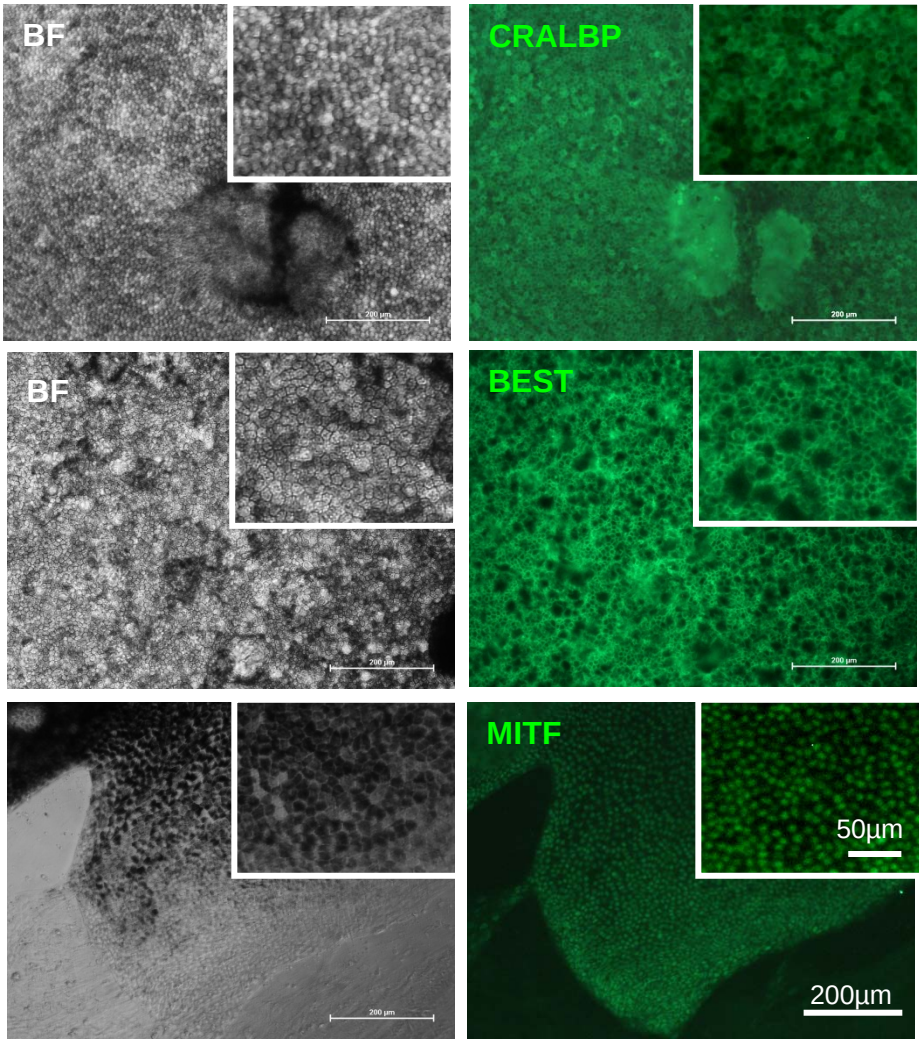

Figure 3.23 Shef6 feeder-free derived RPE. Pigmented foci were isolated at day 50 from Matrigel + mTeSR1 flasks and plated onto Matrigel for expansion. After three weeks, sheets of pigmented cells with classical cobblestone, RPE morphology were expanding away from the adhered pigmented foci. Pigmented cells were positive for RPE markers CRALBP, Bestrophin and MitF. Scale bars = 200µm and 50µm (insert).

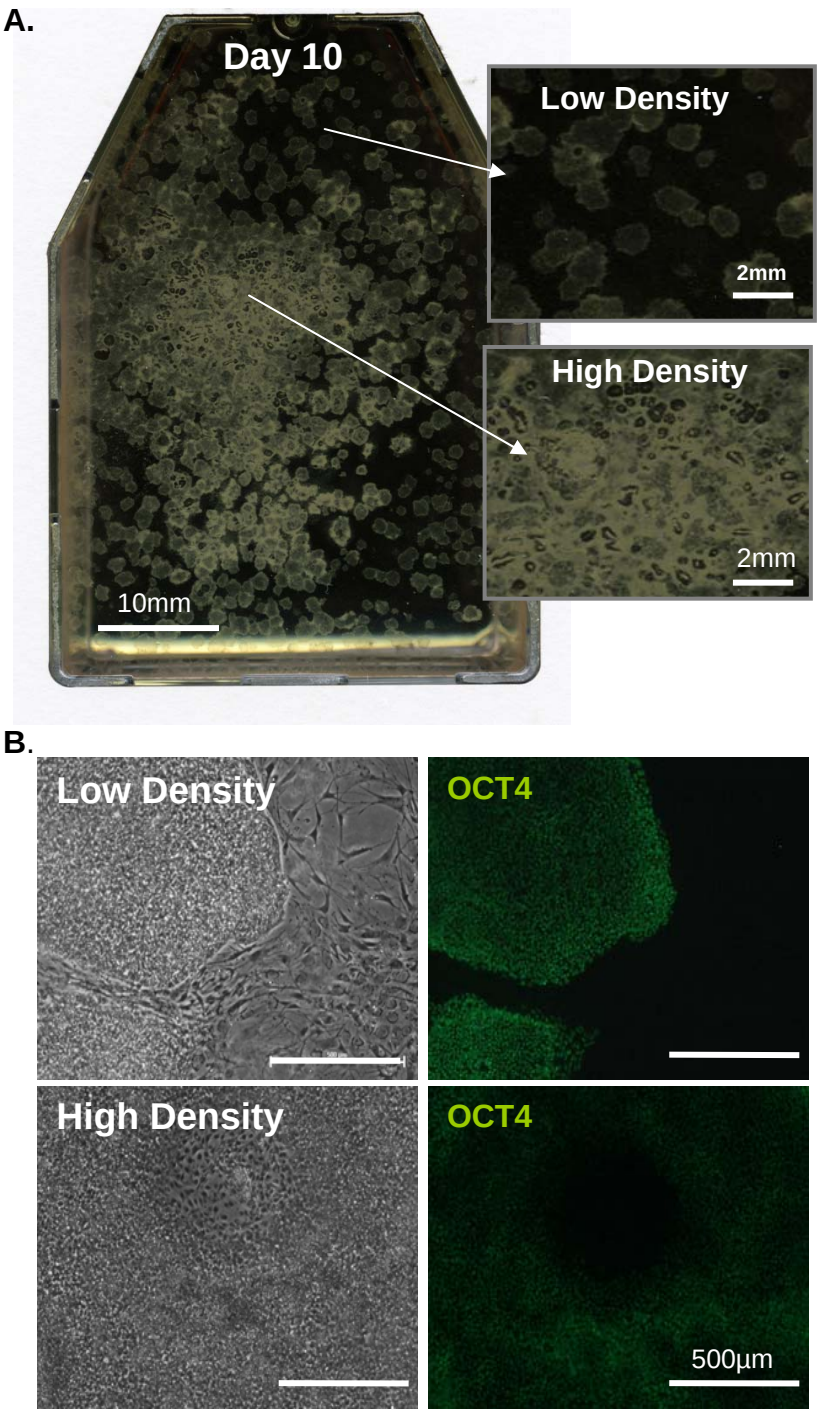

Figure 4.1 Mechanically passaged colonies tend to aggregate at high density leading to an uneven distribution. A. T25 containing areas of low and high colony density. B. Bright field and fluorescence images taken in areas of different local cell density. Colonies in lower density areas proliferated and maintained Oct4 expression and undifferentiated morphology by day 10 whereas highly confluent areas of the same flask (lower panel) began to differentiate and loose Oct4 expression. Scale bar = 500µm

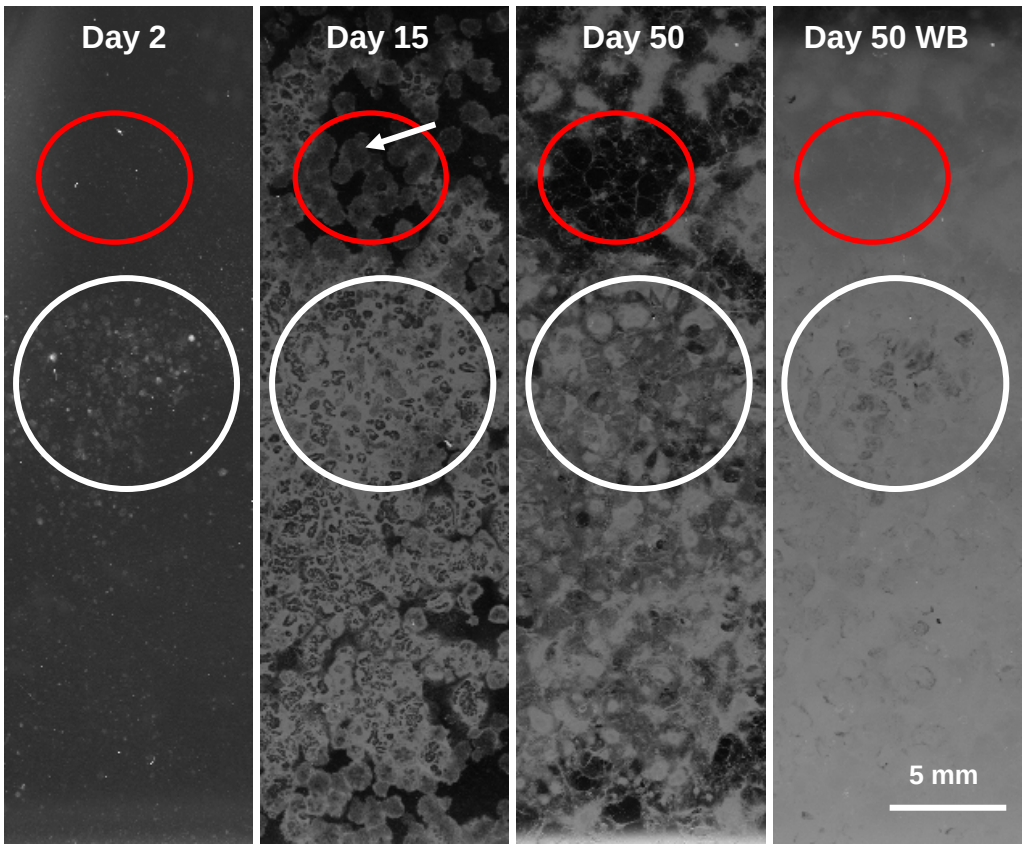

Figure 4.2 Uneven colony distribution leads to an uneven distribution of pigmentation at day 50. Vertical sections of scanned T25 flasks of differentiating cells taken at days 2,15 and 50. Areas of high seeding density have produced pigmented RPE (white circles). Areas with low seeding density have produced no pigment and appear to be devoid of surviving cells at day 50 (red circles). Scale bar = 10mm

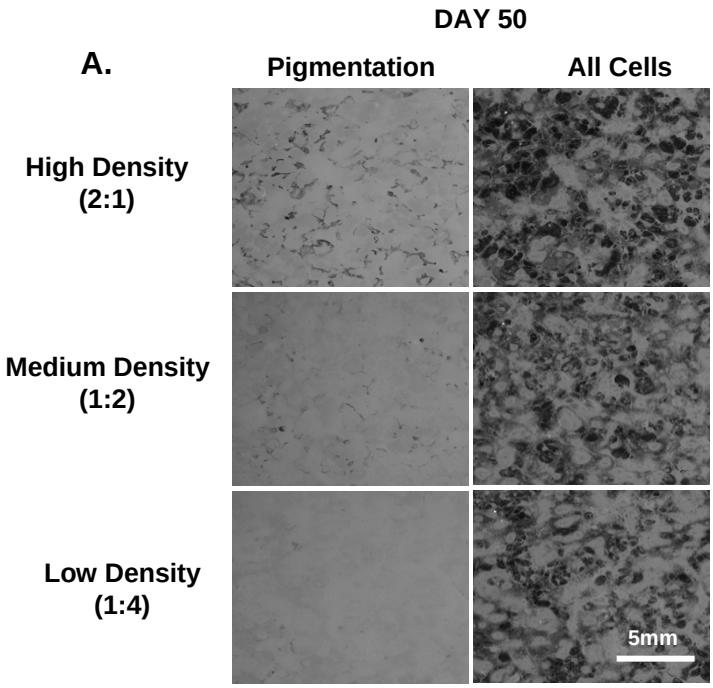
DAY 50
A.
Pigmentation
All Cells
High Density
(2:1)
Medium Density
(1:2)
Low Density
(1:4)
5mm

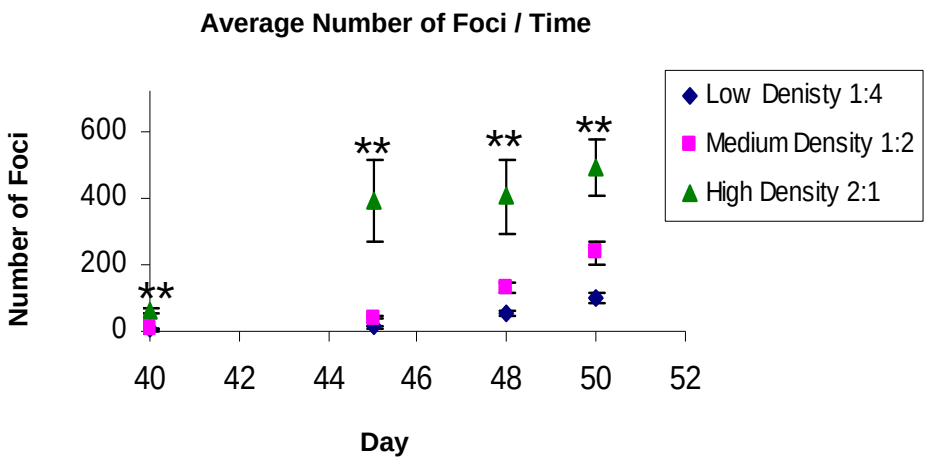
B.
Average Number of Foci / Time
Number of Foci
600
400
200
0
40
42
44
46
48
50
52
Day
**
**
**
**
Low Denisty 1:4
Medium Density 1:2
High Density 2:1

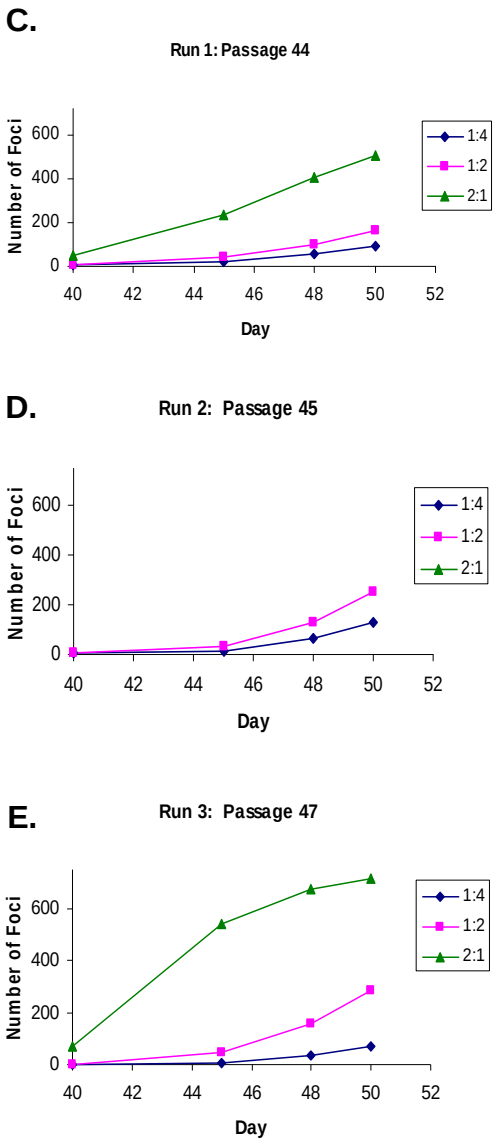

Fig 4.3 Time course of differentiation at different seeding densities. Higher seeding density consistently produced a greater RPE yield over 3 passages (p44-47) (A) Close ups of the scanned images at day 50 at the different seeding densities. Scanning with a white background (left panel) clearly shows the pigmented cells. Removing the white backing before scanning (right panel) shows the density of the cell sheet with multilayered thick areas appearing opaque white. Scale bar = 5mm. (B) Average number of Foci per T25 flask from days 40-50 analysed using the auto-counts method (chapter 2) from scanned images of flasks seeded at three different densities (split ratios low density 1:4, medium density 1:2 and high density 2:1). Two way ANOVA revealed a significant effect of density ($F(2,28) = 19.4$, $p<0.001$) , time ($F(3,28) = 49.1$, $P<0.001$) and a significant interaction ($F(6,28) = 14.1$, $p<0.001$) . At all time points, high density seeded flasks has significantly greater foci numbers than low or medium density seeded flasks (** $p < 0.001$, student's unpaired t-test,). Error bars =SEM.(C-E) Individual graphs from each experimental run, passage numbers 44, 45 and 47.

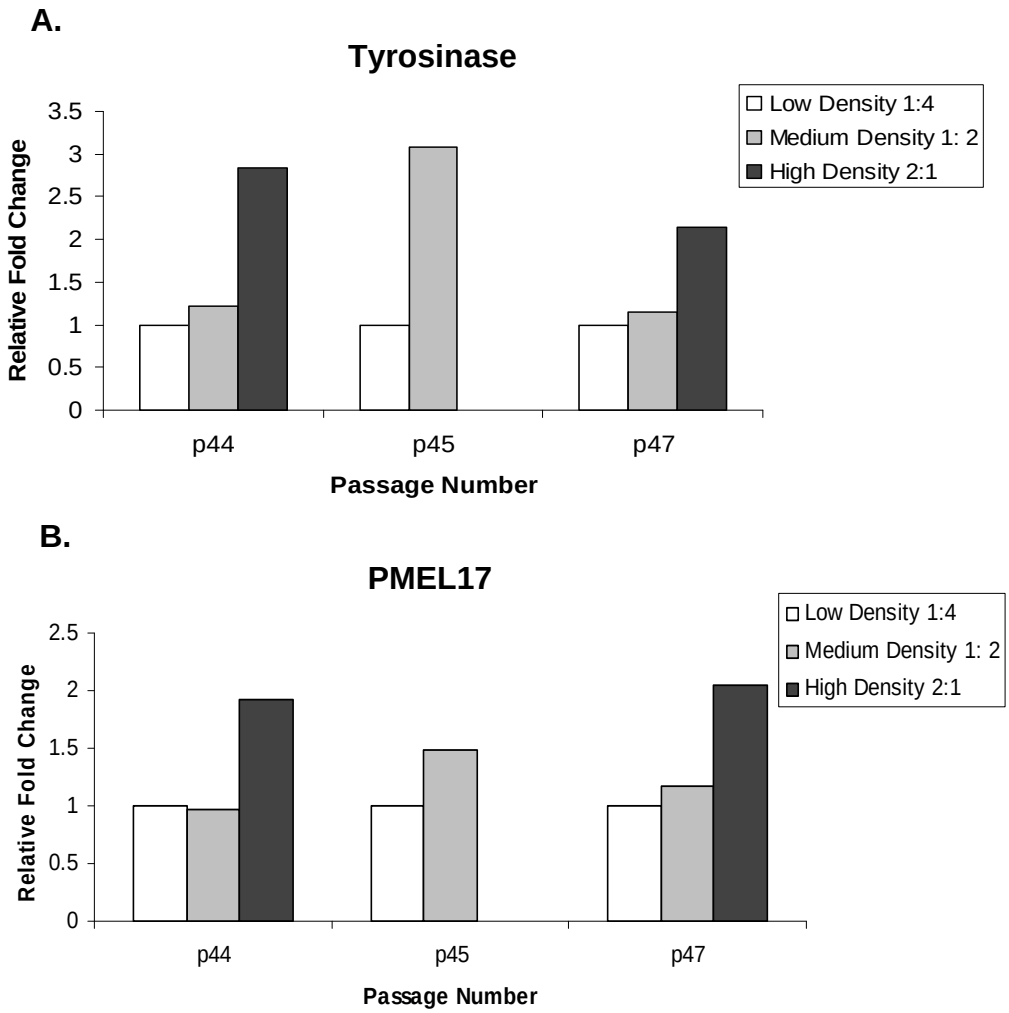

Fig 4.4 HESC seeding density effects the expression of RPE pigmentation genes at day 50. QPCR analysis of Tyrosinase (A) and PMEL17 (B) expression at three densities across three passages (p44, 45 and 47). Bars represent the fold change in expression relative to the lowest density (1:4) within each experimental run. Relative gene expression follows the pattern of relative pigmentation. All QPCR expression data was normalised to the mean expression of house keeping genes POL, MAN and GNB (chapter 2 methods).

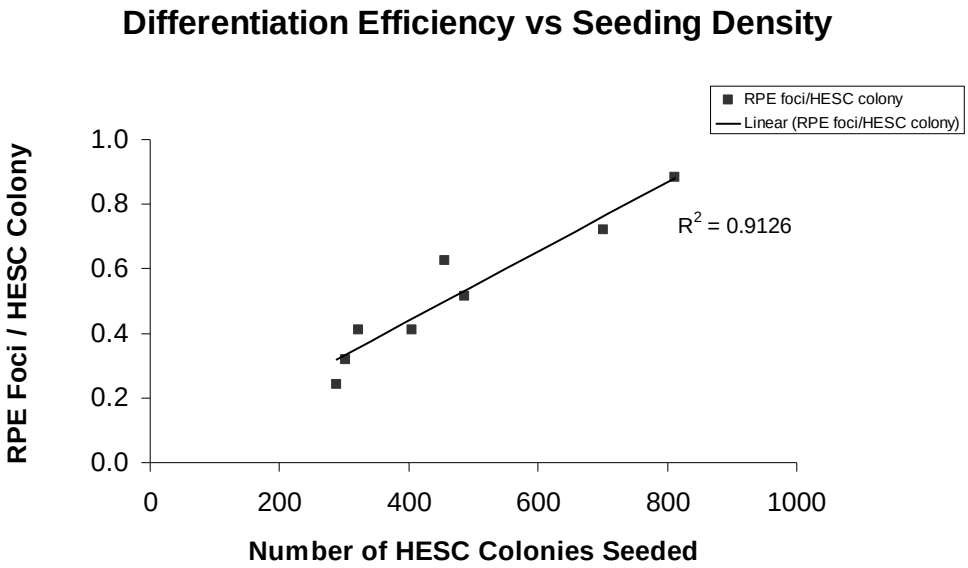

Figure 4.5 Number of RPE foci per HESC colony vs. seeding density. The total number of foci at day 50 was divided by the total number of HESC colonies seeded as determined at day 7. This indicates the differentiation efficiency and clearly shows a correlation between the number of colonies seeded per flask (seeding density) and the differentiation efficiency (RPE foci formed per HESC colony). R squared value = 0.9126.

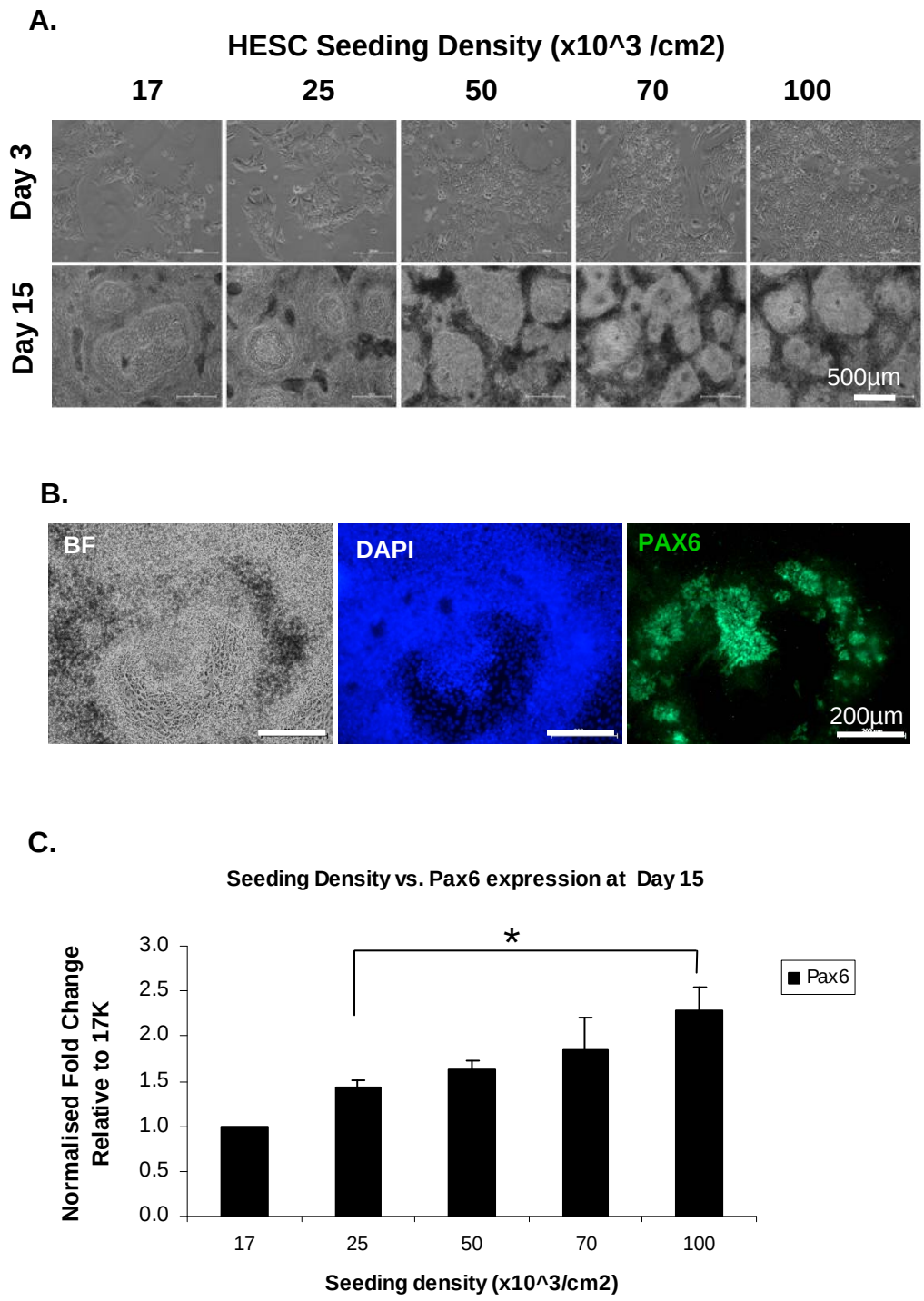

Figure 4.6. Seeding density affects early differentiation. (A) Photomicrographs at day 3 showing dissociated cells surviving and proliferating after seeding at a range of densities (upper panel). At day 15 thick ridges had formed between 'holes' of less compacted cells, these were more pronounced at higher densities (50-100k/cm2), scale bar= 500µm. (B) Immunocytochemistry showing the presence of Pax6 positive neuroepithelial rosettes on these thickened ridges, scale bar = 200µm. (C) QPCR analysis at day 15, bars represent the fold increase in Pax6 expression relative to the 17K/cm2 condition, normalised to three house keeping genes (Error bars = SEM, N=3).. One way ANOVA revealed a significant difference in Pax6 expression with seeding density ($F(3,8) = 4.5$, $*p<0.05$).

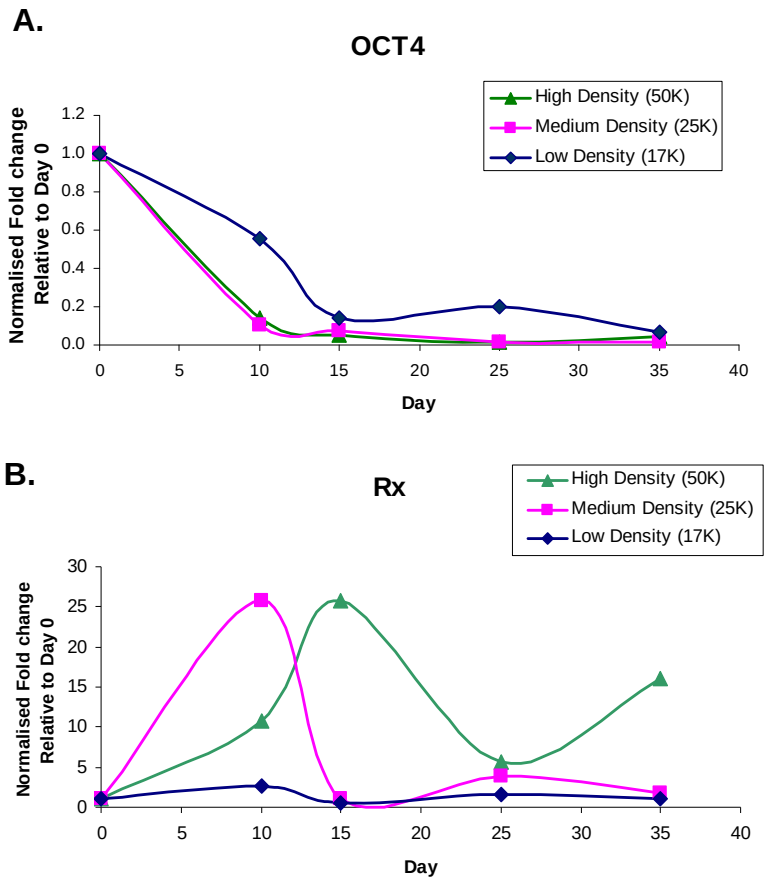

Figure 4.7. Time course of gene expression during early differentiation. QPCR analysis of gene expression of cells differentiating following seeding at three different plating densities (50,25 and 17K/cm2). Cells were harvested at 5 time points up to day 35 of differentiation. Lines represent the normalised fold change in gene expression relative to the day 0 starter cultures. (A) Oct4 expression decreases over time in culture as the cells differentiate, the rate of down regulation is reduced at low density (17K /cm2) and similar in the 25 and 50 K/cm2 condition. (B) Rx expression increases as cells differentiate and adopt an eye field fate. The peak in Rx expression occurs later at high density (50K/cm2) compared to medium density (25K/cm2).

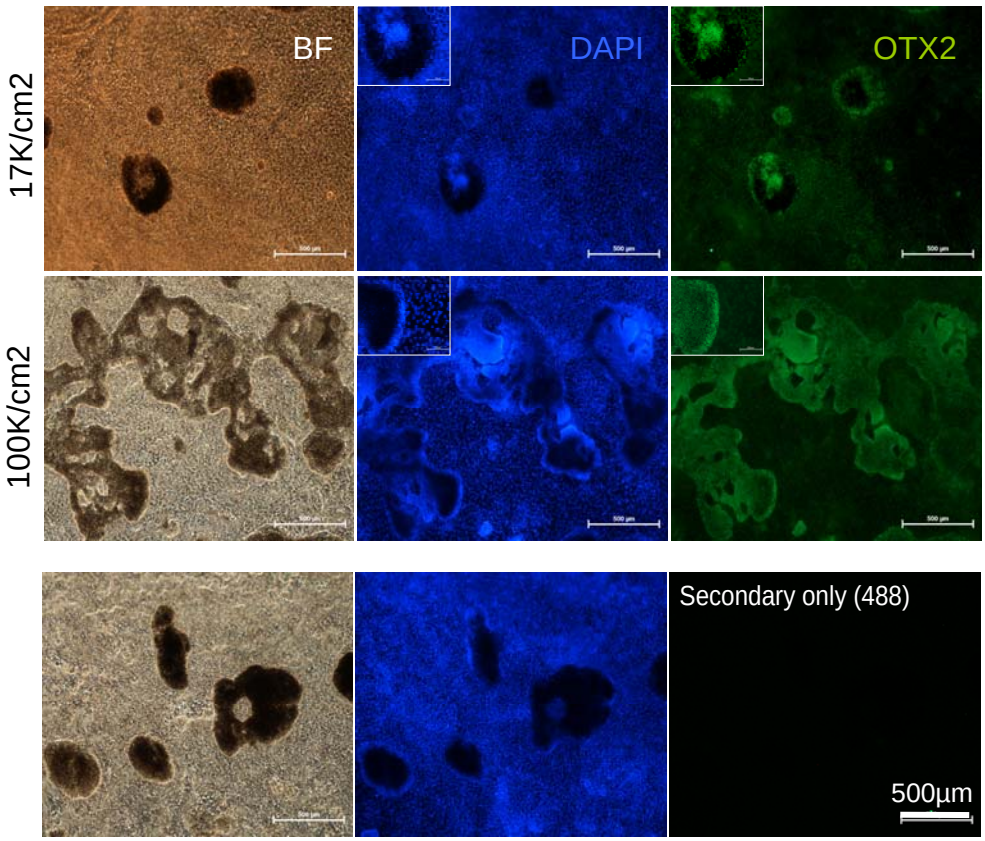

Figure 4.8. Pigmented RPE morphology at 17K and 100K/cm2 seeding densities. Photomicrographs and immunohistochemistry at day 50 in wells seeded with 17 and 100k/cm2 HESC. In wells that were seeded with 100K/cm2, Otx2 positive pigmented cells appear as contiguous flattened sheets (middle panel). At 17K/cm2 Otx2 positive pigmented cells appear in small, slightly raised and compacted foci in which the highly concentrated pigment partially obscures the fluorescence signal (top panel).

A. Shef6 Passage 60

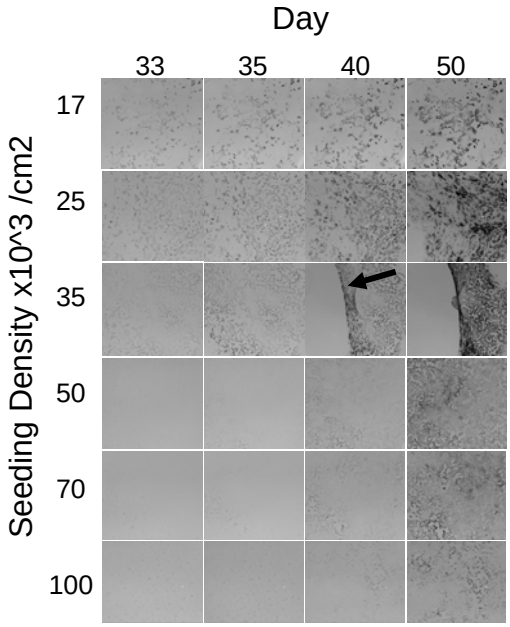

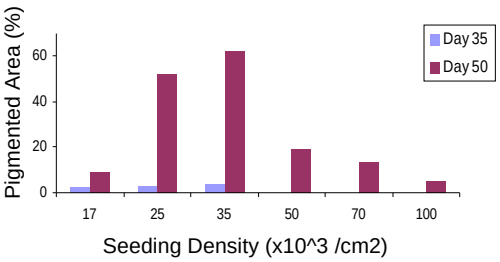

B. Shef6 Passage 68

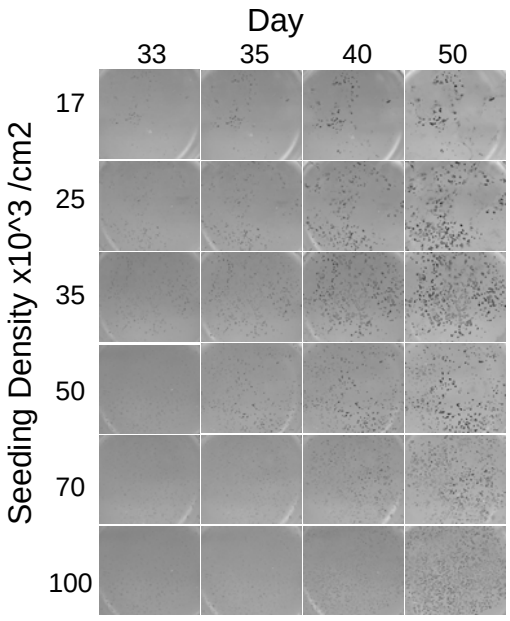

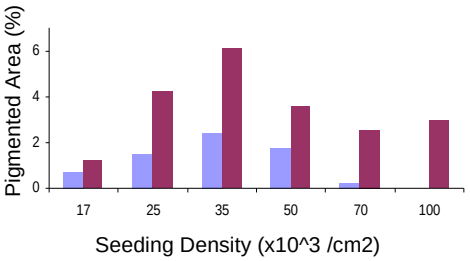

C.

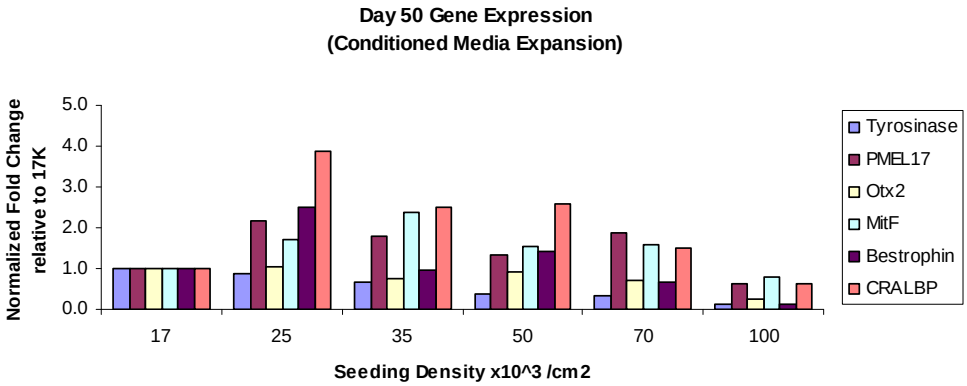

Fig 4.9 Seeding density and rate of pigmentation following conditioned media expansion. Panels show scanned images of the wells seeded at different densities (17k-100k /cm2) showing the increase in pigmentation over time from days 33-50. Graphs show % surface pigmentation at days 35 (blue) and 50 (red) as assessed in Image J (See Chapter 2, materials and methods. (A) Scans and % pigmentation data from run 1, using passage 60 Shef6. (B) Scans and % pigmentation data from experimental run 2, using passage 68 shef6. (C) QPCR analysis of RNA extracted at day 50 of differentiation from passage 60 Shef6. Each bar represents the normalised expression of an RPE marker (Tyrosinase, Pmel17, Otx2, MitF, Bestrophin, CRALBP) at day 50 relative to its expression at day 50 in the lowest seeding density condition (17k/cm2).

A. Shef6 Passage 50 – mTeSR1 Expansion

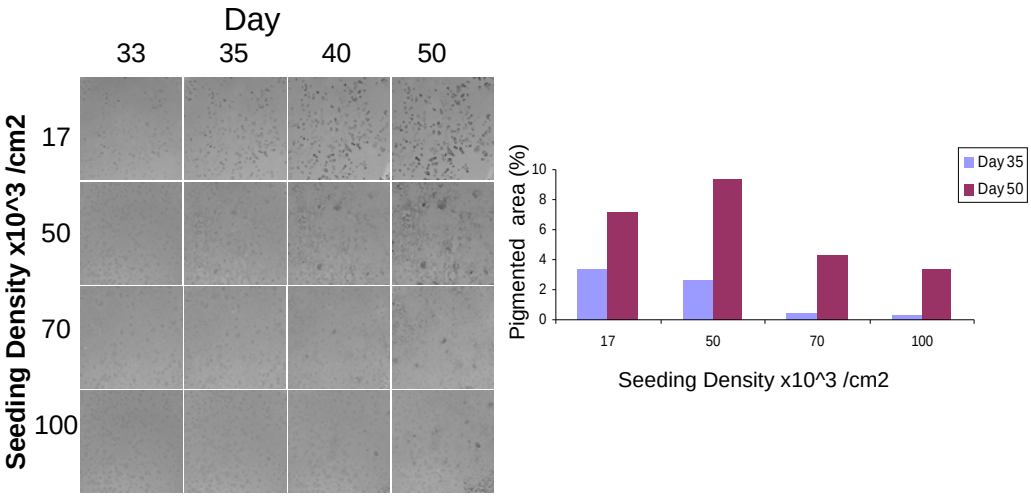

B. Shef 6 Passage 51 –mTeSR1 Expansion

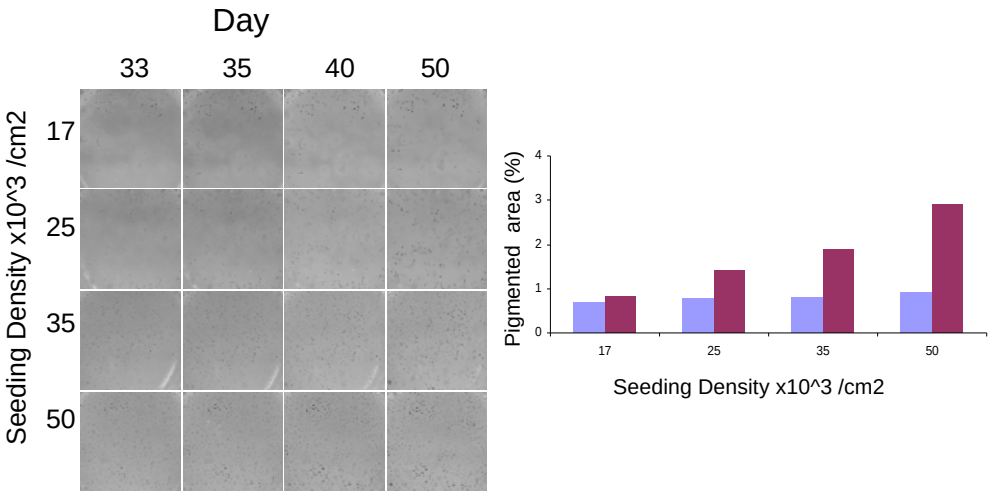

C. Shef6 Passage 52 –mTeSR1 Expansion

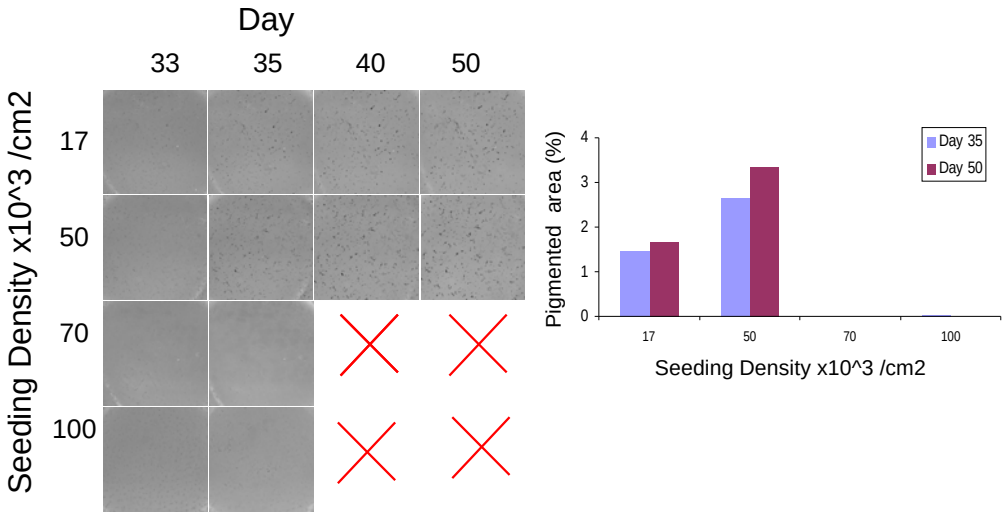

D. Shef6 Passage 68 –mTeSR1 Expansion

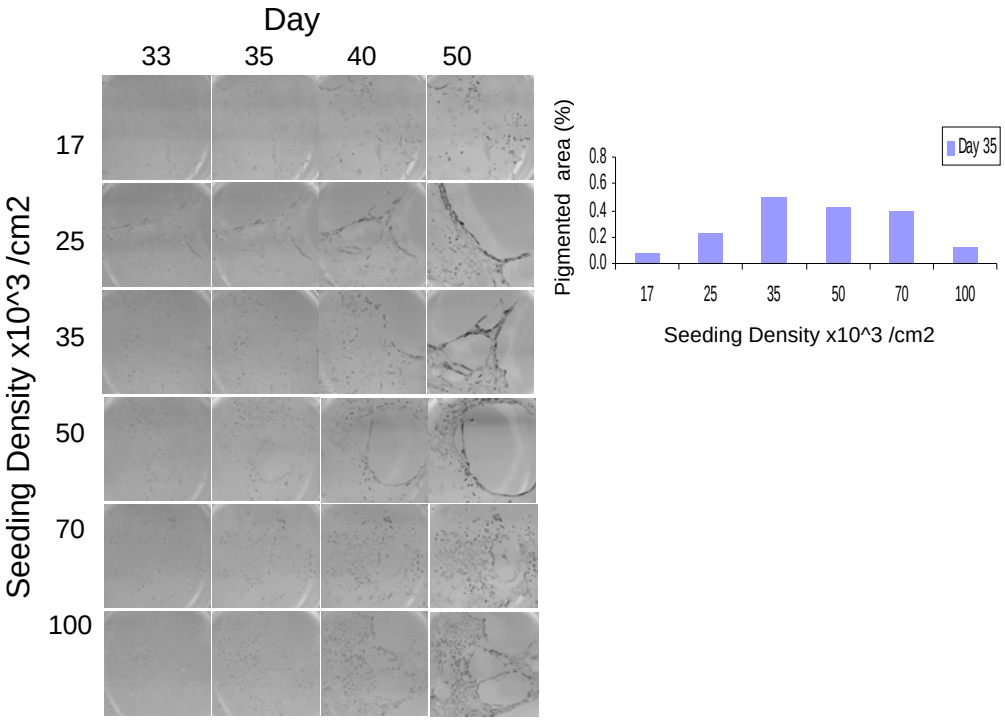

E.

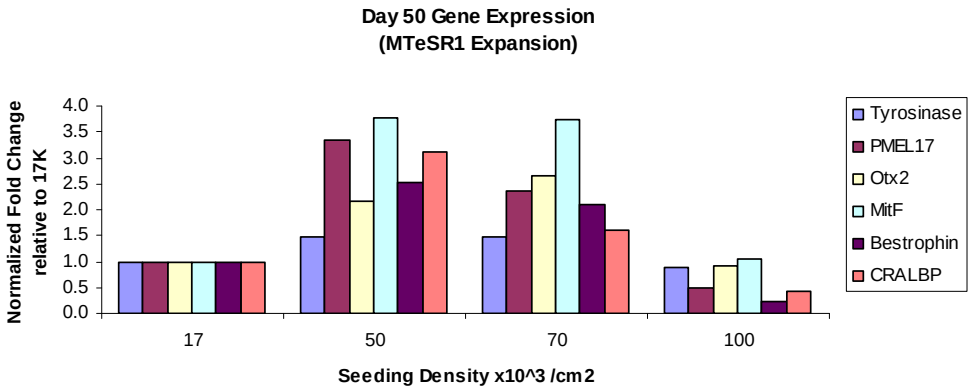

Figure 4.10 Seeding density and rate of pigmentation following mTeSR1 expansion. Panels show scanned images of the wells seeded at different densities (17k-100k /cm2) from days 33-50 using cells at passage 50(A), and 51 (B), 62 (C) and 68 (D). Red crosses indicate wells lost before day 50 to contamination (C). Graphs show % surface pigmentation analysis in Image J at days 35 (blue) and 50 (red). In (D) day 50 measurements could not be taken due to cell sheet peeling. QPCR analysis of RNA extracted at day 50 of differentiation from passage 50 Shef6. Each bar represents the normalised expression of an RPE marker (Tyrosinase, Pmel17, Otx2, MitF, Bestrophin, CRALBP) at day 50 relative to its expression at day 50 in the lowest seeding density condition (17k/cm2).

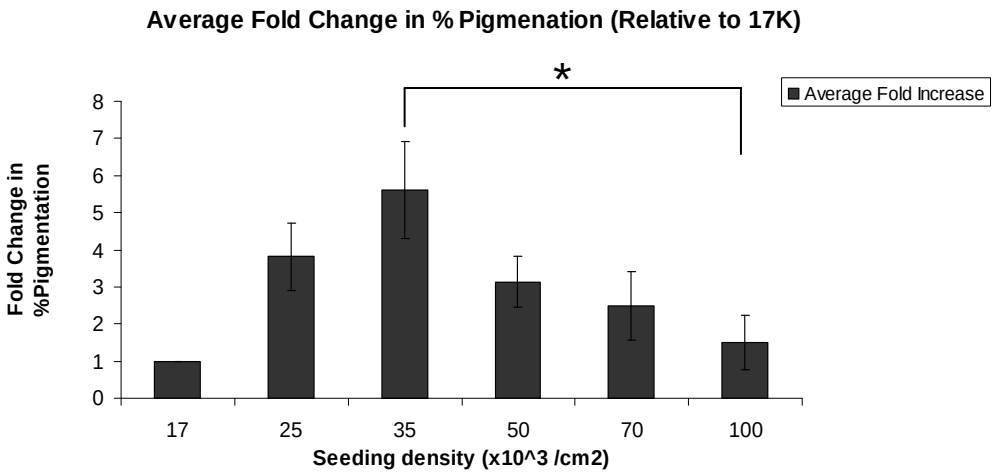

Figure 4.11 Average fold change in pigmentation. The % pigmentation data from all 6 feeder-free single cell dissociation experiments were collated. Bars represent the fold change in % pigmentation relative to % pigmentation in the 17K/cm2 condition in each of the 6 runs. (Error bars = SEM, N=4-6). One way ANOVA revealed a significant difference in fold increases in pigmentation with seeding density ($F(4,17)=3.0$, $p<0.05$),. Post hoc t-tests found that the fold changes at 35K/cm2 were significantly higher than those at 100 K/cm2 , ***** = $P<0.05$ (student's unpaired t-test).

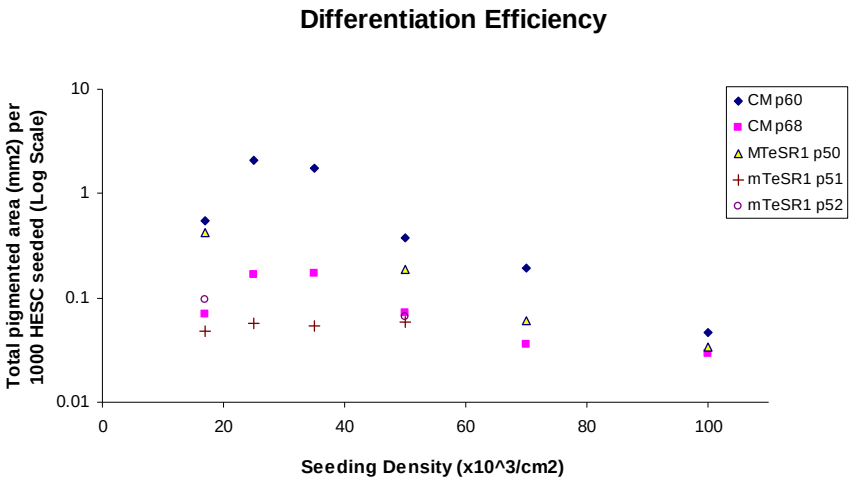

Fig 4.12. RPE Differentiation Efficiency per HESC cell. Scatter plot showing the changes in HESC conversion efficiency with increasing cell seeding density for each experimental run. Each dot represents the total pigmented cell area in a well at day 50 ($mm^{2)}$ divided by the number of cells seeded (in thousands) versus number of cells seeded (x10^3/cm2). In each run, the peak efficiency occurs at a seeding density between 17-35,000 cells/cm2, with higher densities giving reduced efficiency. NB. wells that were lost before day 50 are not included (mTeSR1 passage 68, mTESR1 passage 52 (70-100K wells)).

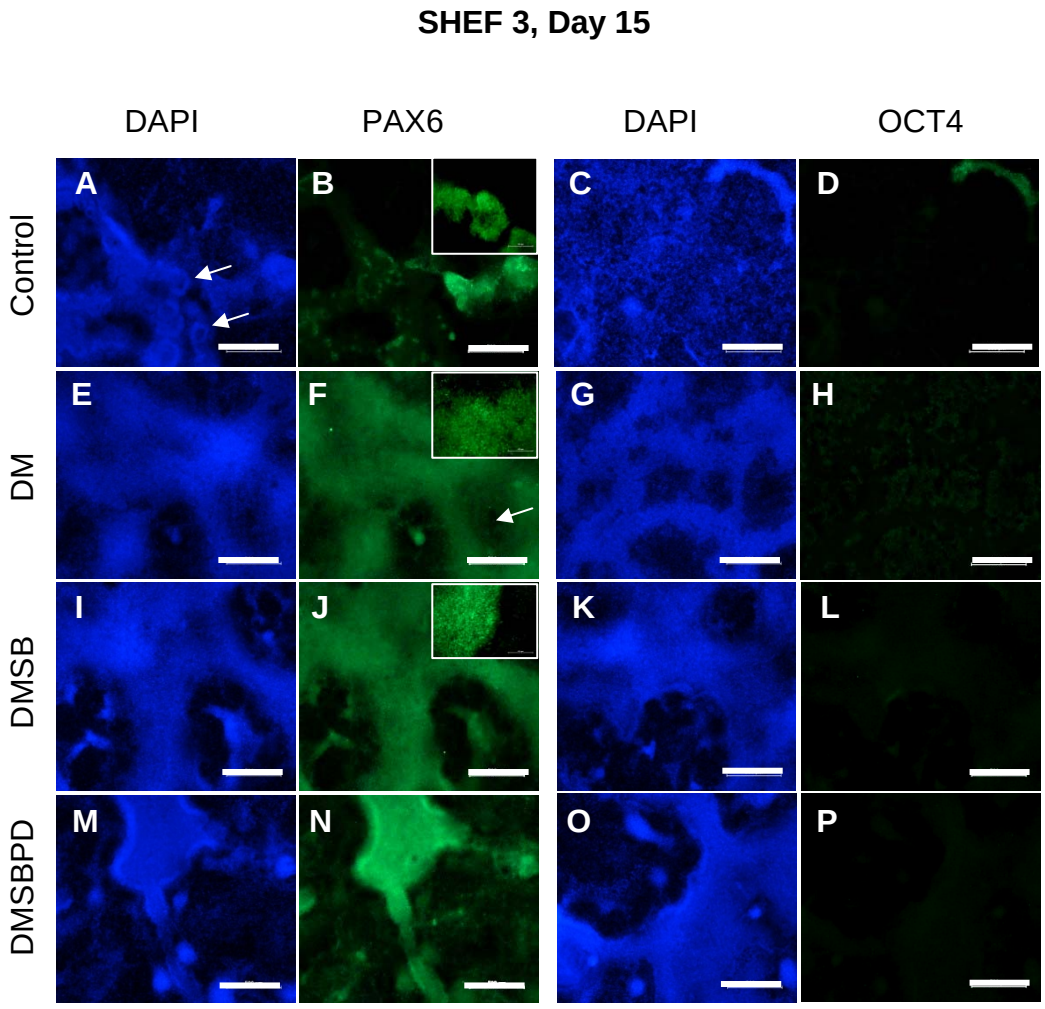

Figure 5.1 Small molecule inhibitors enhance neuroectoderm differentiation in Shef3. Immunocytochemistry for Pax6 and Oct4 following ten days of differentiation in the presence of small molecules. (A-D) Control samples (DMSO only), some neural rosettes are visible (A, arrows) but many are not Pax6 positive at this time point (B), Oct4 is not detectable . (E-H) BMP/activin inhibitor dorsomorphin (DM) 1µm only, Pax6 positive cells are now abundant though not arranged in rosette like structures. Some Pax6 –ve cells remain in hole like structures (F, arrow). Oct4 is again not detected (G,H). (I-L) 1µm dorsomorphin + activin/nodal inhibitor SB431542 10 µm, a similar picture to dorsomorphin only with Pax6 positive sheets interspersed with Pax6-ve holes (J). (M-P) 1µm Dorsomorphin + 10 µm SB431542 + FGF/ERK inhibitor PD0325901 1µm Pax6 positive cells appeared in more tightly compacted islands surrounded by larger Pax6 negative holes (M,N), again Oct4 was not detected (O,P).

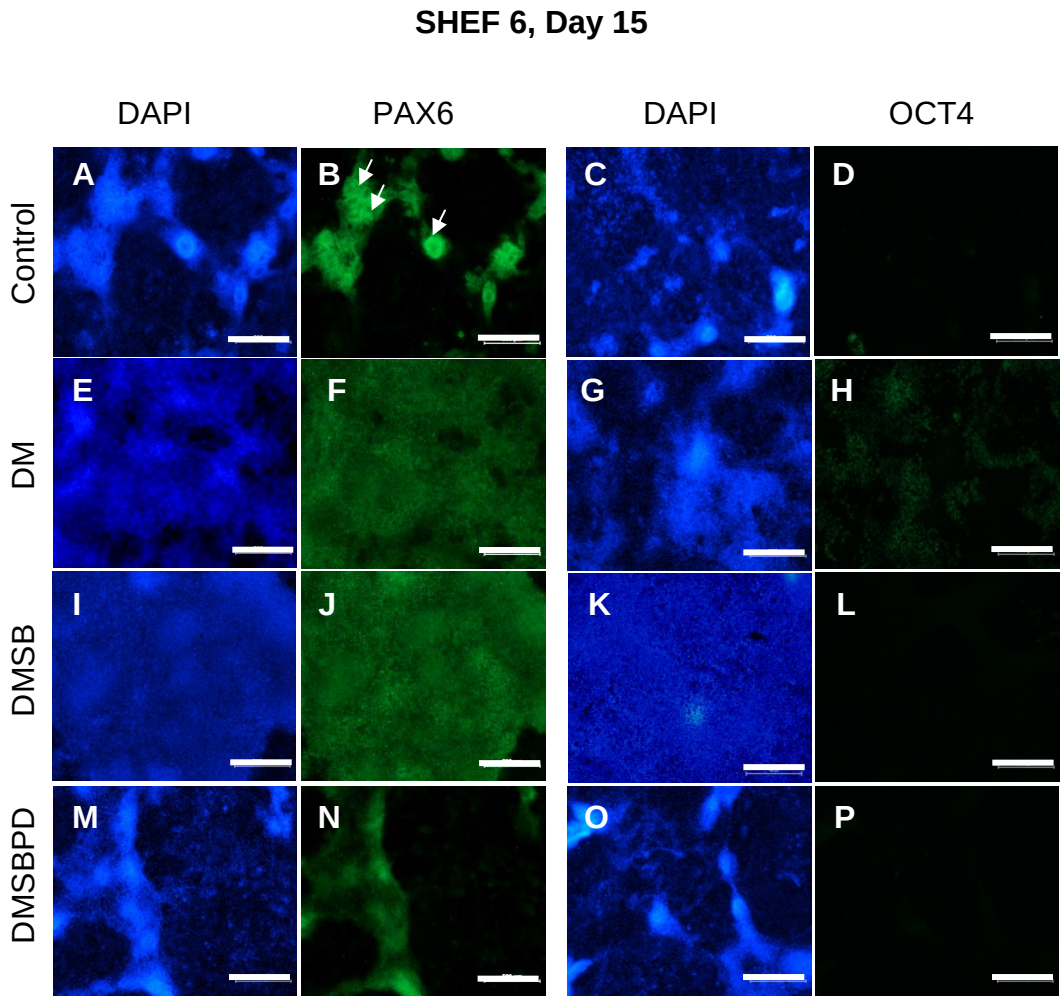

Figure 5.2 Small molecule inhibitors control neuroectoderm differentiation in Shef6. Immunocytochemistry for pax6 and Oct4 following ten days of differentiation in the presence of small molecules. (A-D) Control samples (DMSO only). Pax6 positive neural rosettes were abundant on thick ridges in day 15 control samples (B, arrows), Oct4 was not detected (C,D). (E-H) BMP/activin inhibitor dorsomorphin 1µm only. Neural rosettes were no longer visible but contiguous sheets of Pax6 positive cells had formed (F), a faint Oct4 signal was also detected (H). (I-L) 1µm dorsomorphin + activin/nodal inhibitor SB431542 10 µm. A highly compacted contiguous sheet of Pax6 positive cells similar to the Dorsomorphin only condition had formed (J), Oct4 was not detected (L). (M-P) 1µm Dorsomorphin + 10 µm SB431542 + FGF/ERK inhibitor PD0325901 1µm. Pax6 positive cells appeared only on thickened islands, similar to the control condition (N), Oct4 was not detected.

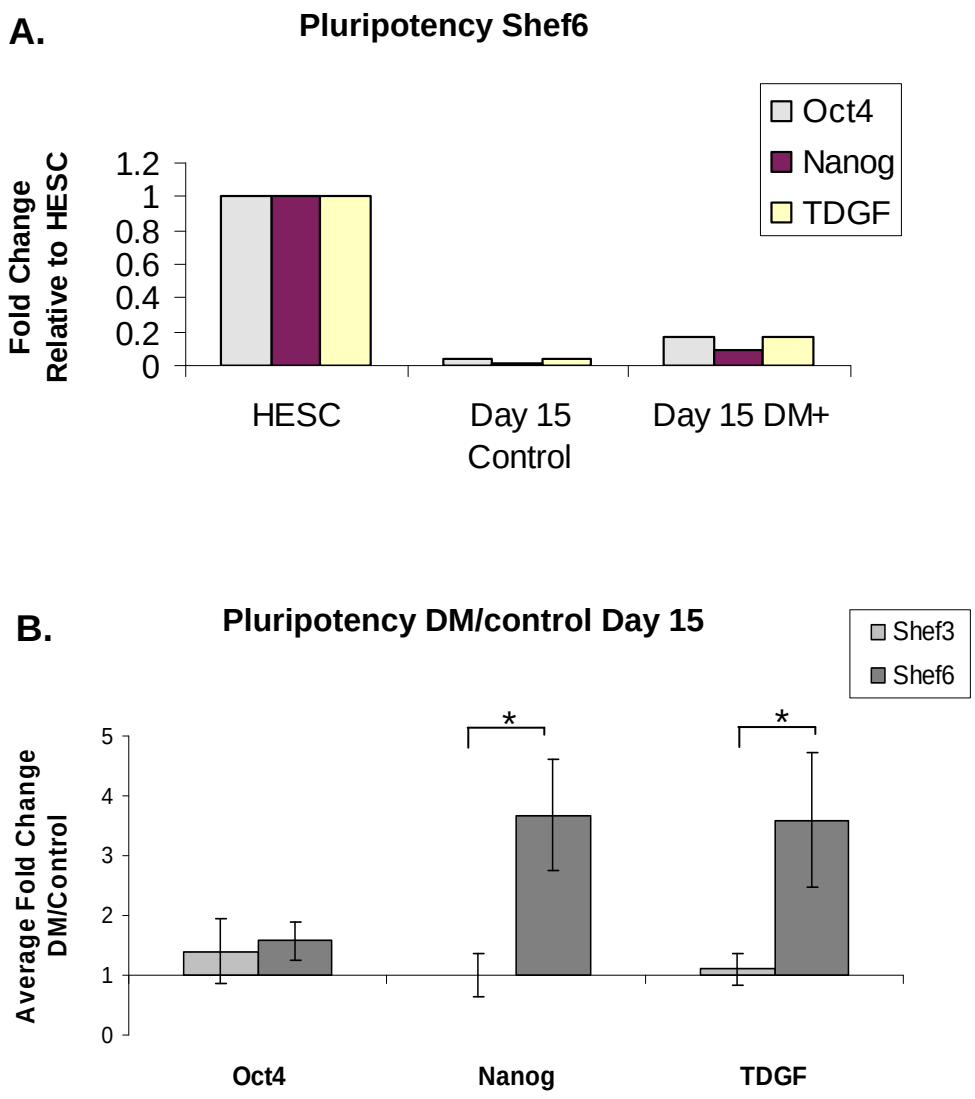

Figure 5.3 Dorsomorphin (DM) suppresses the down regulation of pluripotency gene expression. .(A) QPCR showing the expression of pluripotency genes Oct4, Nanog and TDGF in Shef6 at day 15 relative to HESC. All pluripotency genes are down regulated at day 15 of differentiation relative to HESC in both dorsomorphin and control wells. (B) QPCR showing the expression of pluripotency genes at day 15 in dorsomorphin treated relative to control wells in Shef6 and Shef3. In the presence of dorsomorphin the expression of Nanog and TDGF is higher in Shef6 than in control Shef3. There were no significant differences between Dorsomorphin and control samples in Shef3 however. There was a significant difference in the day 15 TDGF and Nanog expression relative to controls between the two cell lines ($p<0.05$, N=3, student's unpaired t-test).

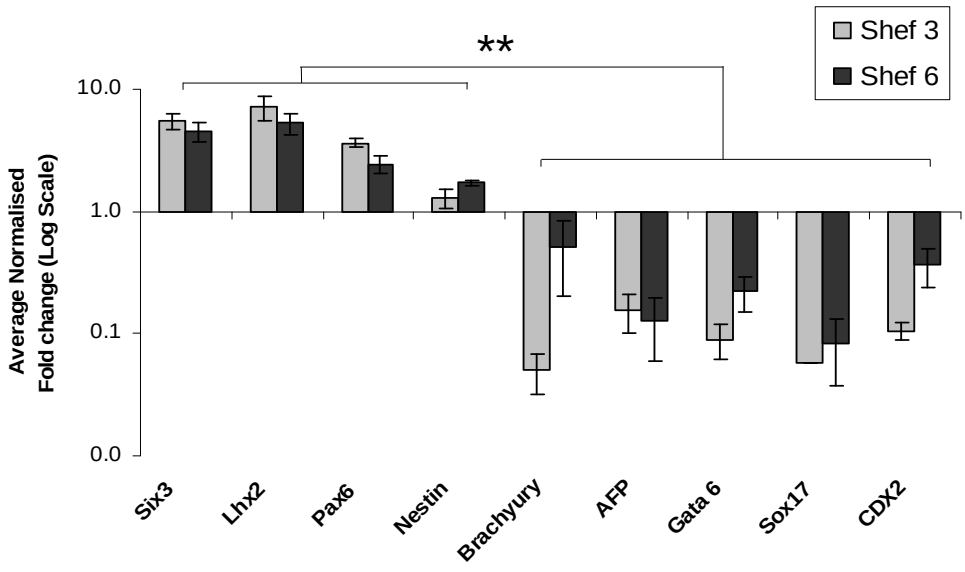

Figure 5.4 Dorsomorphin enhances neuroectoderm and suppresses mesoderm, endoderm and trophectoderm gene expression relative to untreated controls. Normalised relative expression of markers of mesoderm (Brachyury, AFP), endoderm (Sox17, Gata6) and trophectoderm (CDX2) following 10 days of differentiation in the presence of dorsomorphin relative to DMSO control wells (shef3-light bars, Shef6-dark bars). One way ANOVA demonstrated a significant difference between the expression of markers of the different germ layers (neuroectoderm, mesoderm, endoderm and trophectoderm) in both cell lines Shef6 ($F(3,26)=13.3$, $p<0.001$) and Shef3 ($F(23,3) = 10.5$, $p< 0.001$). Post hoc analysis (unpaired student's t-test) revealed a significant up regulation in neuroectoderm marker expression (Six3, Lhx2, Pax6, Nestin) relative to dorsomorphin induced changes in the other germ layers in both cell lines (**$p<0.001$), suggesting that dorsomorphin had a specific affect of up regulating neuroectoderm gene expression.. There was a significantly greater down regulation of mesoderm/endoderm/trophectoderm markers in Shef3 relative to Shef6 (one way ANOVA $F(1,28) = 3.8$ $p<0.05$, but no overall difference between the cell lines in the upregulation of neuroectoderm markers.

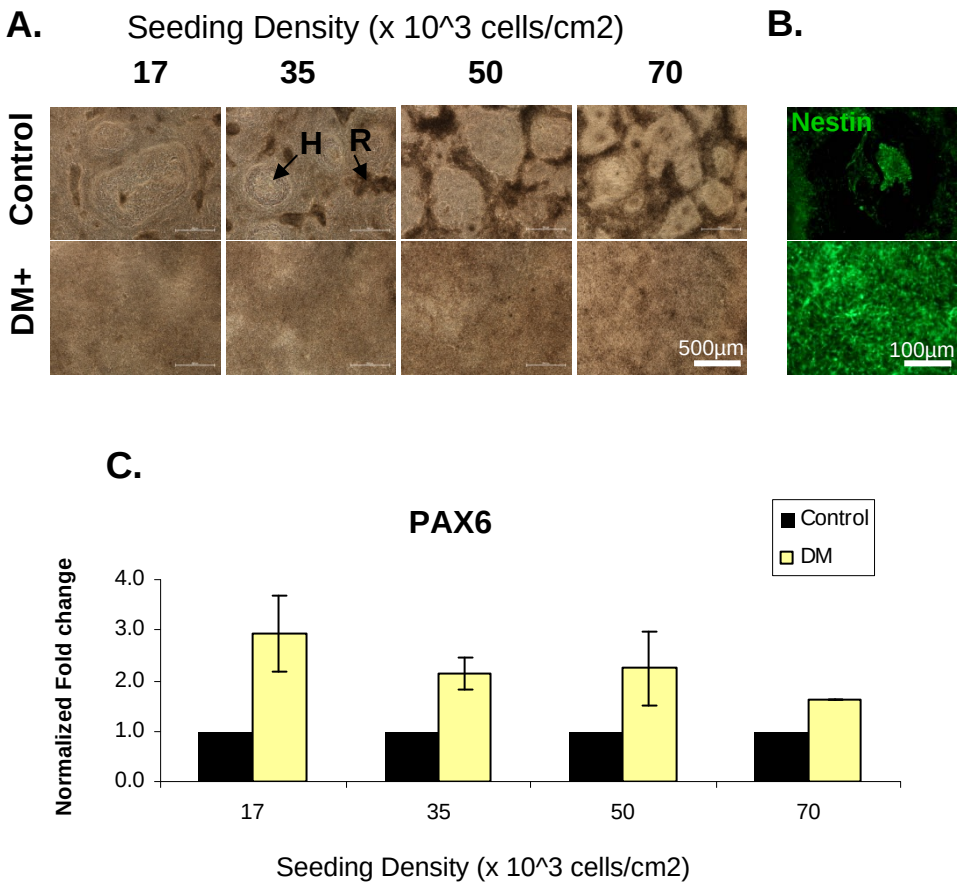

Fig 5.5 Dorsomorphin (DM) enhances neuroectoderm differentiation at a range of seeding densities. (A) Bright field images of cells seeded over a range of densities and differentiated in 1µm dorsomorphin or control media, control wells contain distinctive circular holes of flattened, non-compacted cells (labelled H) surrounded by thickened ridges (labelled R). (B) The non-compacted holes found in control wells are immunonegative for Nestin, compacted cells in DM+ cultures are Nestin positive. (C) QPCR showing relative expression of Pax6 at day 15 (DM/Control) over a range of densities. The relative fold increase in Pax6 expression declined slightly with increasing seeding density but not significantly. Bars represent average normalised fold increase in dorsomorphin treated over control wells at the same density in two separate passages (N=2).

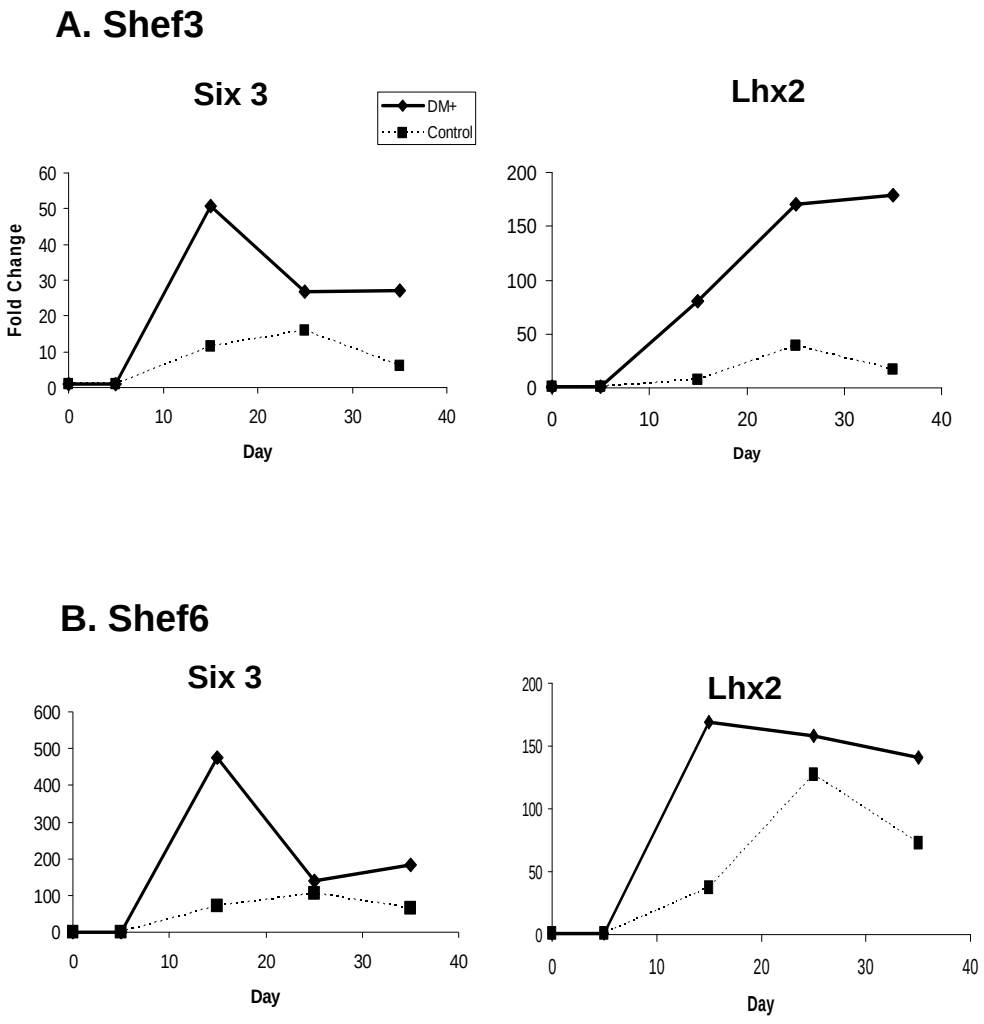

Figure 5.6 Time course analysis of neuroectoderm and eye field transcription factor gene expression. QPCR analysis shows the change in mRNA levels of eye field transcription factors Six3 and Lhx2, expressed relative to undifferentiated HESC in cells induced with dorsomorphin (thick black line), and cells from the same starter culture treated with DMSO only (thin line). Experiments were carried out in shef6 (A) and Shef3 (B).

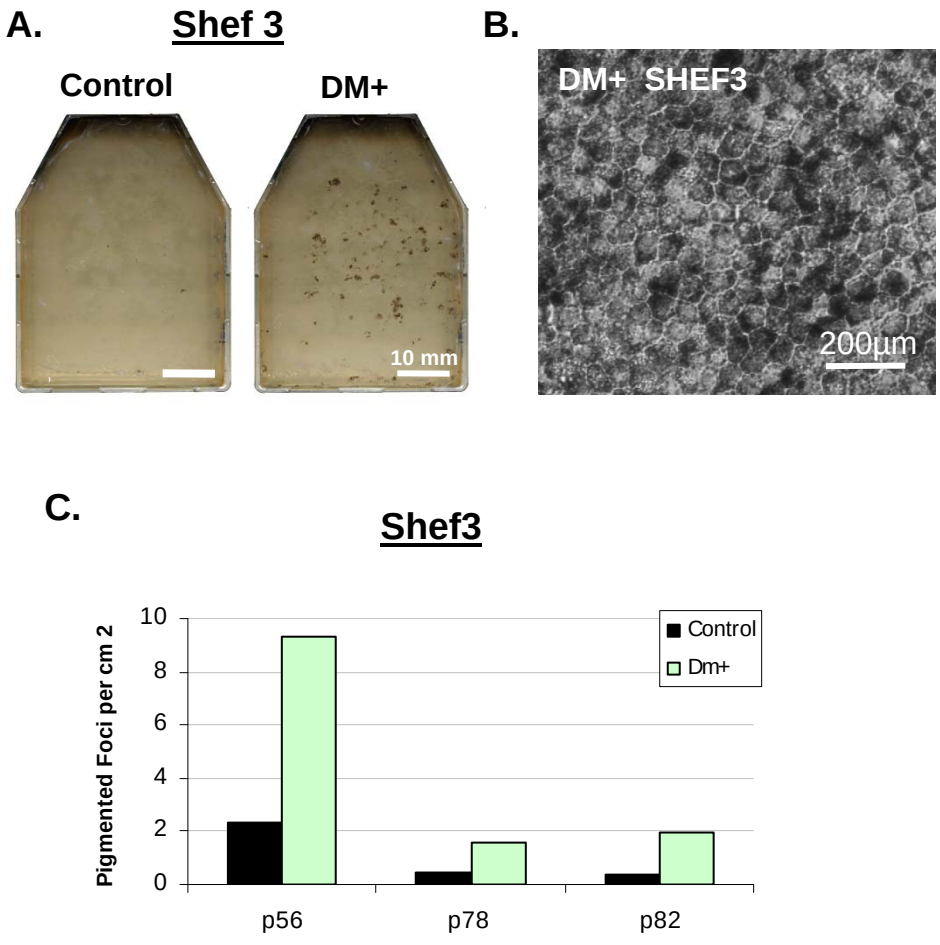

Figure 5.7 Dorsomorphin enhances RPE yield in Shef3 MEFs co-culture. (A) Scanned images of Shef3 flasks at passage 56 following 50 days of differentiation with (DM+) or without (control) a ten day dorsomorphin induction step. (B) Phase contrast image of expanding pigmented cells, derived from dorsomorphin induced flasks. Dorsomorphin derived pigmented cells have typical RPE morphology. (C) Pigmented foci yields per cm2, assessed using the auto-count method at day 50 in dorsomorphin treated (DM+) and control flasks over a range of passage numbers. The average fold increase dorsomorphin/control was 4.1±0.4 (N=3).

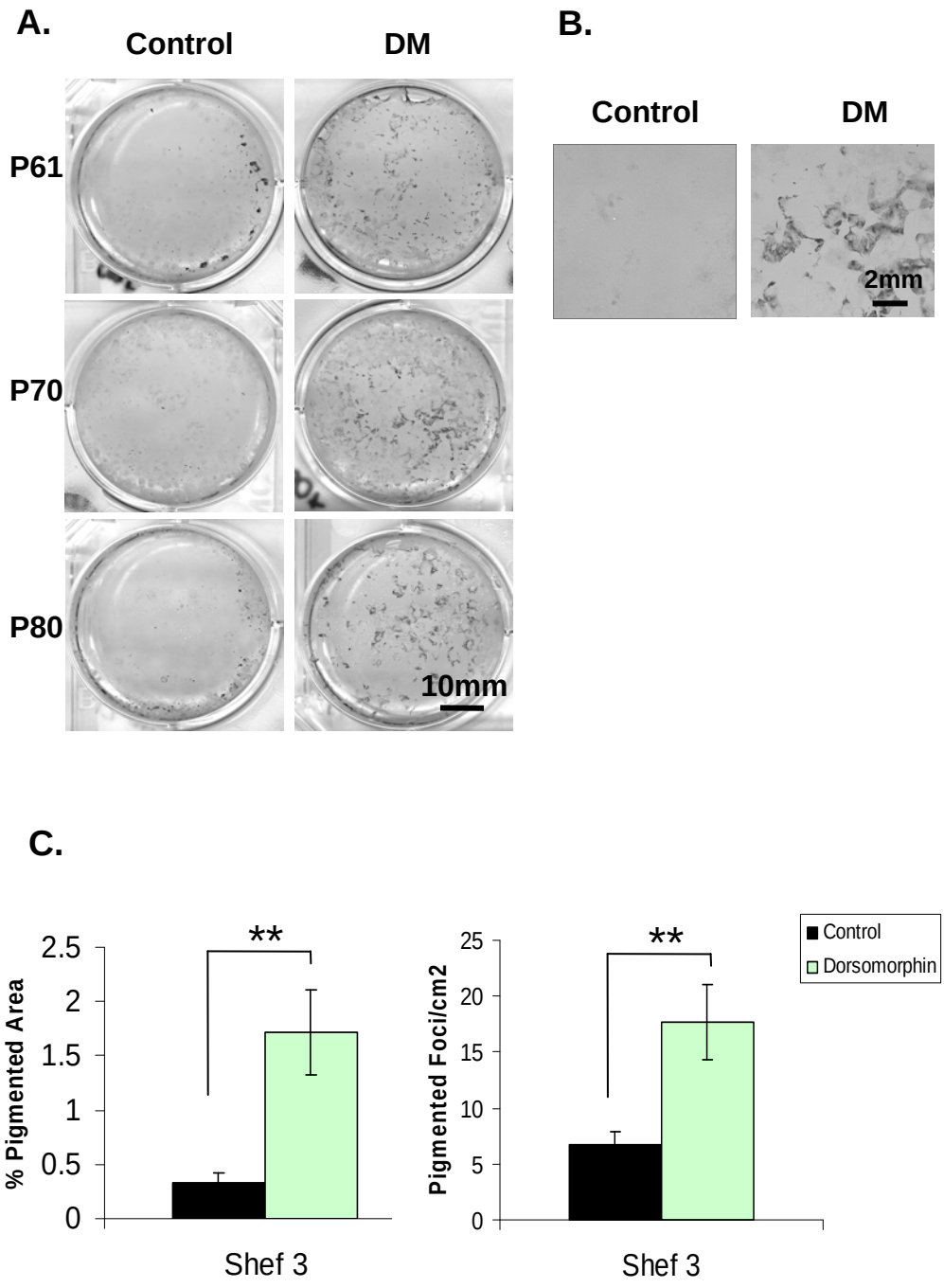
A.
Control
DM
P61
P70
P80
10mm
B.
Control
DM
2mm
C.
**
% Pigmented Area
2.5
2
1.5
1
0.5
0
Shef 3
**
Pigmented Foci/cm2
25
20
15
10
5
0
Shef 3
Control
Dorsomorphin

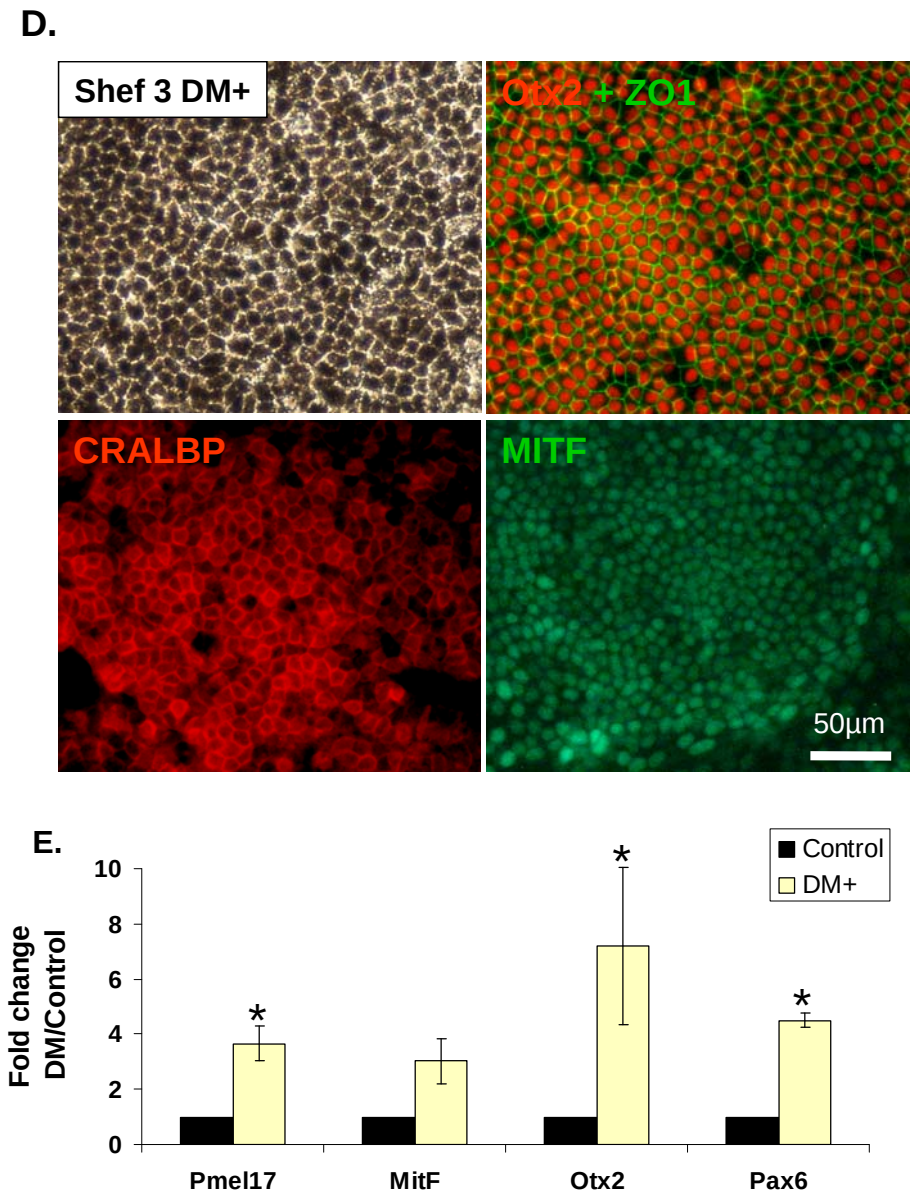

Figure 5.8 Dorsomorphin robustly enhances RPE differentiation efficiency in shef3. (A) Representative scanned images of 6 well plates at day 50 in control and dorsomorphin treated wells from passage numbers (P) 61, 70 and 80. (B) Enlarged areas from of dorsmorphin and DMSO control wells demonstrating a significant increase in pigmented cell yield. (C) Average % pigmented area and number of foci per cm2 in control and dorsomorphin wells (error bars = SEM, N=6). Dorsomrophin induced a statistically significant increase in % pigmentation the (ANOVA $F(1,10) = 8.0$) and in the number of foci/cm2 ($F(1,10)=9.6$), $^{**}p<0.01$, N=6. The average fold increase pigmented area dorsomorphin/controls = 5.0 ± 0.7. (D) Bright field and immunofluorescence images of expanding RPE taken from dorsomorphin treated wells at day 50. Pigmented cells have typical RPE morphology and express RPE markers Otx2, ZO1, MitF and Pax6. (E) QPCR at day 50 in 4 separate experiments shows the up regulation in RPE associated genes Pmel17, MitF, Otx2 and Pax6 relative to controls (N=4, * $p<0.05$, student's paired t-test).

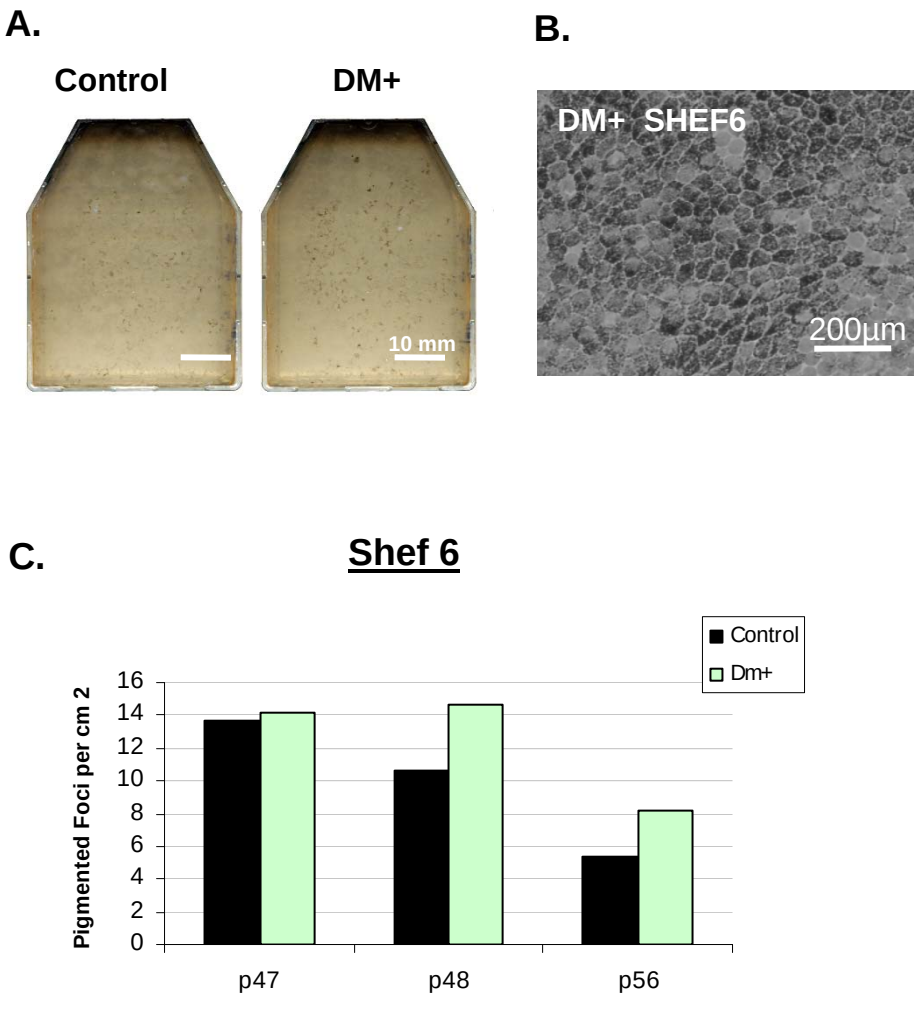

Figure 5.9 Dorsomorphin and RPE yield in Shef6 MEFs co-culture. (A) Scanned images of Shef6 flasks at passage 56 following 50 days of differentiation with (DM+) or without (control) a ten day dorsomorphin induction step. (B) Phase contrast image of expanding pigmented cells, derived from dorsomorphin induced flasks. Dorsomorphin derived pigmented cells have typical RPE morphology. (C) Pigmented foci yields per cm2 in Shef6, assessed using auto-count method (chapter 2, methods) at day 50 in dorsomorphin treated (DM+) and control flasks over a range of passage numbers (p47-56). The difference between control and DM+ flasks was not significant. The average fold increase was 1.3 ± 0.1 (N=3).

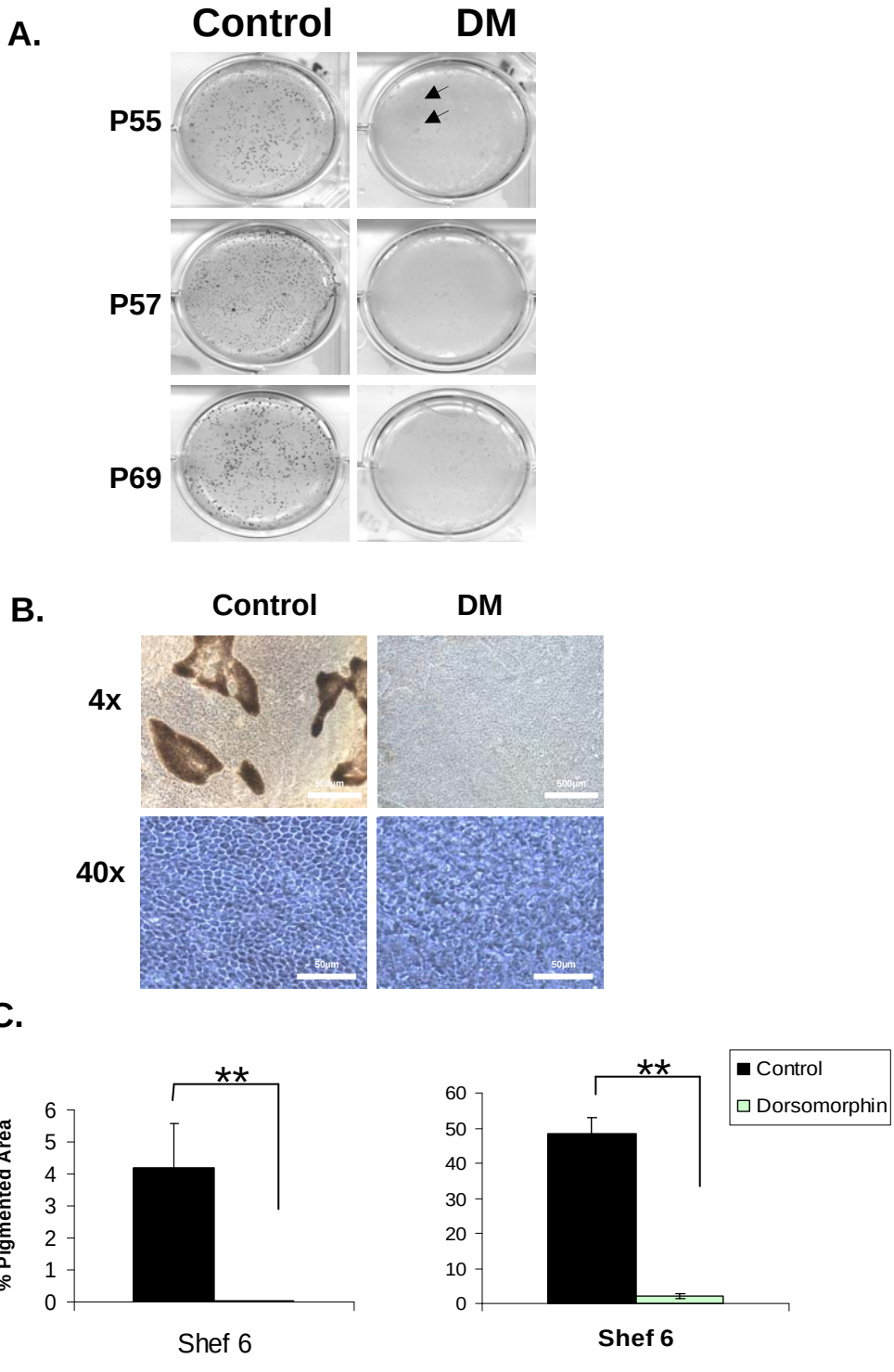
A.
Control
DM
P55
P57
P69
B.
Control
DM
4x
40x
C.
**
% Pigmented Area
6
5
4
3
2
1
0
Shef 6
**
60
50
40
30
20
10
0
Shef 6
Control
Dorsomorphin

D.

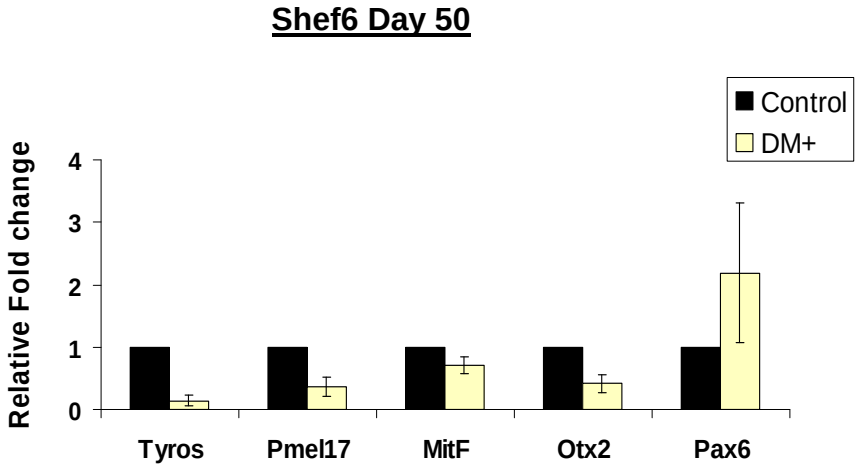

Figure 5.10 Dorsomorphin and RPE differentiation efficiency in Shef6. (A) Scanned images of 6 well plates at day 50 showing typical DMSO control and dorsomorphin treated wells from passage numbers (P) 55, 57 and 69. (B) Microscope images day 50 taken at 4x and 40x magnification. Control wells contain pigmented foci with cobblestone RPE morphology whereas dorsomorphin treated wells contain non pigmented cells with a disordered morphology, scale bars = 500µm (upper) and 50µm (lower). (C) Average % pigmented area and number of foci per cm2 in control and dorsomorphin treated wells at day 50. Error bars = SEM, N=6, (ANOVA $F(1,10)= 8.2$, ** $p<0.01$). (D) QPCR analysis on day 50 samples from 3 separate experiments showing the relative down regulation in expression of RPE associated genes Tyrosinase, Pmel17, MitF, Otx2, but a relative increase in RPE/neural retina gene Pax6 (Error bars = SEM, N=3). One way ANOVA revealed a statistically significant difference in the dorsomorphin induced expression of RPE genes (MitF, Pmel17, Otx2) in Shef6 vs. Shef3 ($F(1,19) = 5.5$ $p<0.01$).

A.

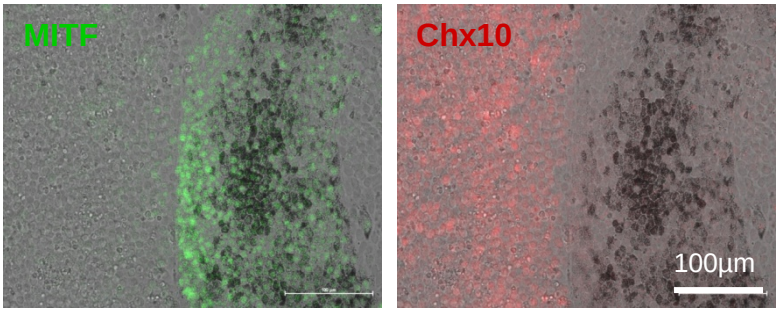
MITF
Chx10
100µm

B.

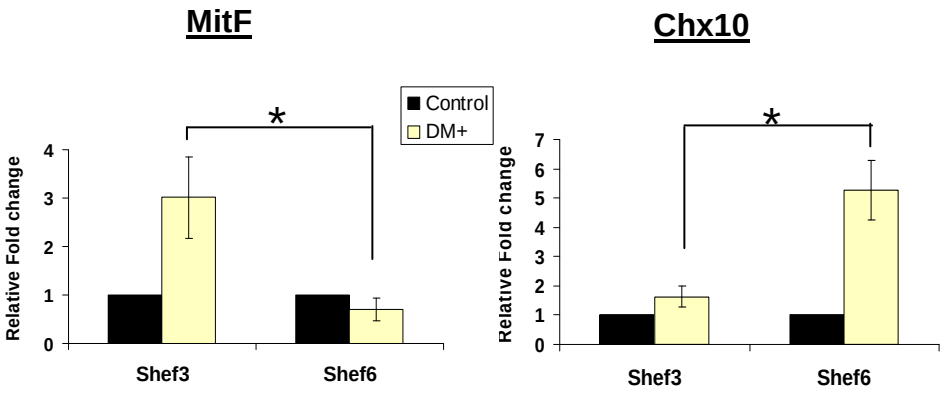
MitF
Chx10
Control
DM+
Relative Fold change
0
1
2
3
4
5
6
7
*
*
Shef3
Shef6
Shef3
Shef6

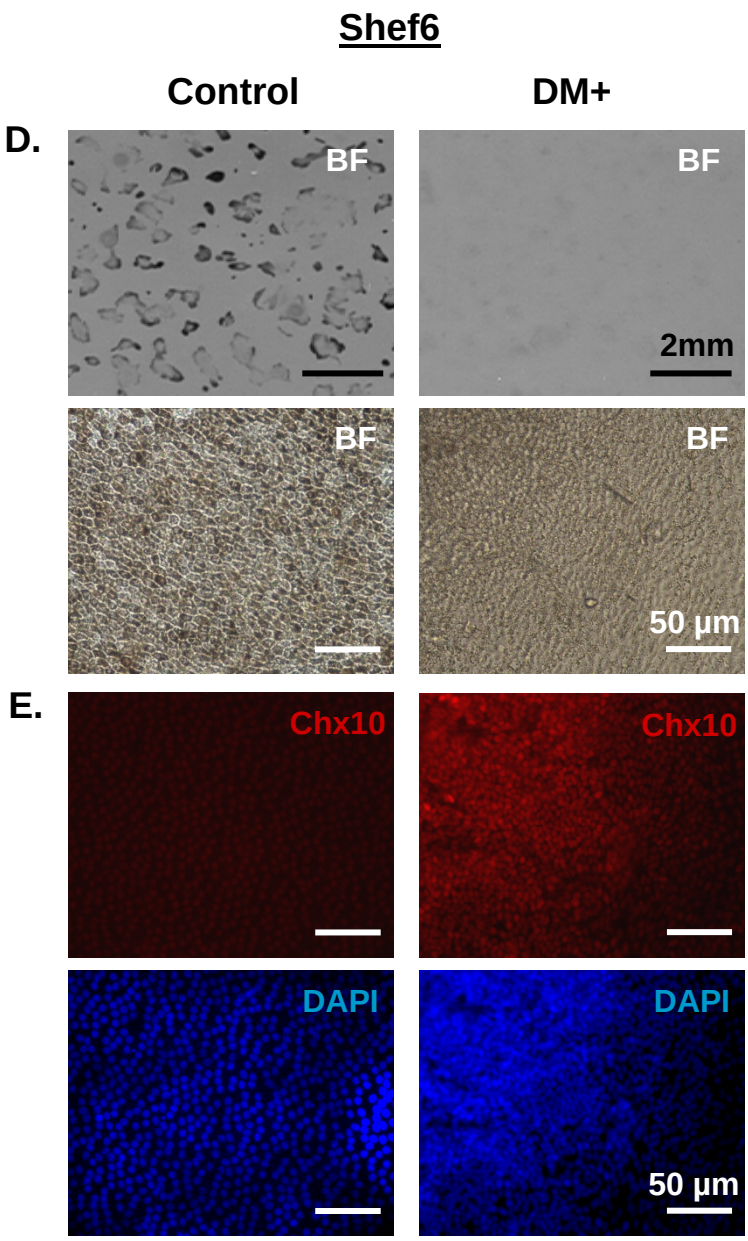

Figure 5.11 Chx10 and MitF expression at day 50 in Shef6 and Shef3. (A) Immunocytochemistry in Shef6–RPE shows the mutually exclusive expression of MitF and Chx10. (B-C) QPCR showing the relative expression of Chx10 and MitF in day 50 samples of dorsomorphin treated and control shef6 (N=3) and shef3 (N=4). The difference between dorsomorphin induced Chx10 augmentation in Shef6 and Shef3 was significant (ANOVA $F(1,5) = 15.0$, $p<0.05$). MitF expression was up regulated in dorsomorphin treated Shef3 and down regulated in dorsomorphin-treated Shef6 relative to control wells. The difference in dorsomorphin induced expression was significant ANOVA $F(1,5) = 2.4$, $p<0.05$). (D) Bright field images at low and high magnification show the presence of pigmented RPE cells in control wells, and their absence in dorsomorphin treated wells. (E) The non pigmented cells found in dorsomorphin treated wells stained positively for neural retinal marker Chx10.

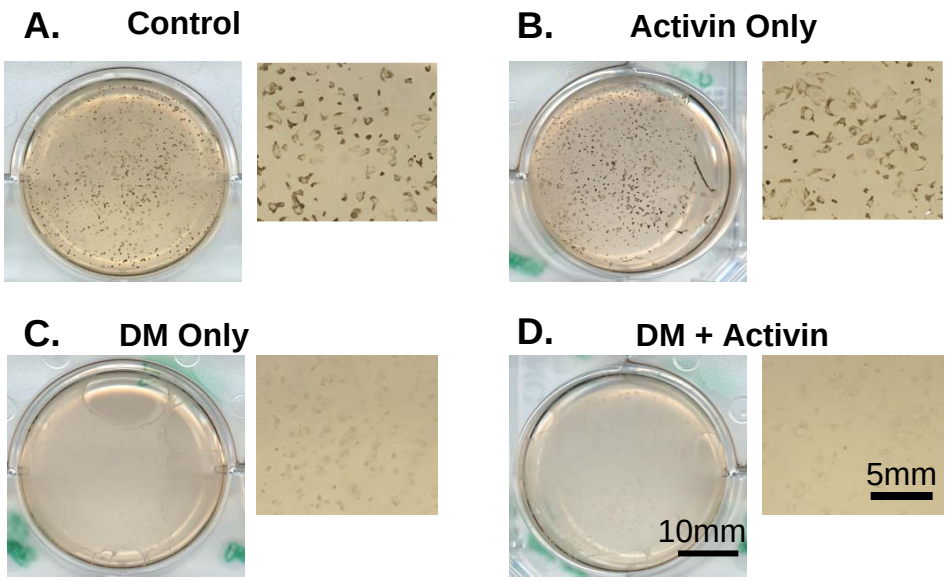

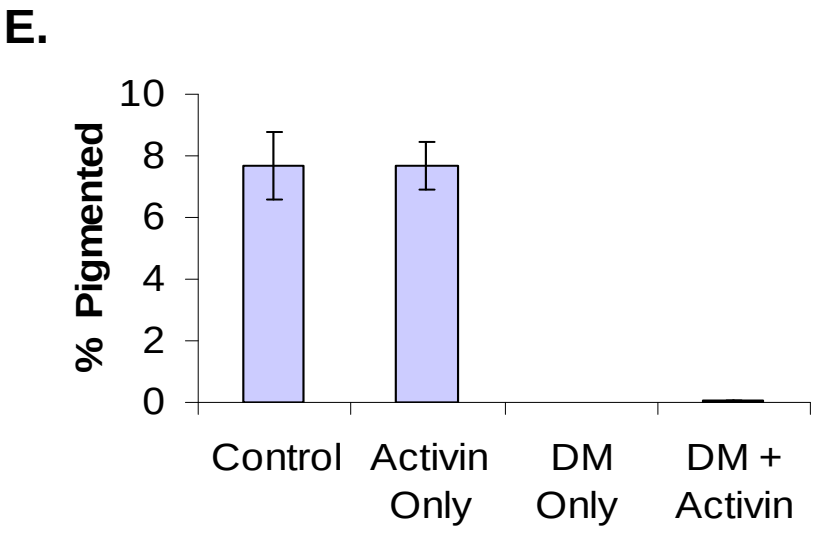

Figure 5.12 100ng/ml activin A supplemented from days 20-40 has no impact on pigmented cell yield in DM or control wells. (A-D) Scanned and enlarged images of typical wells depicting pigmentation at day 50 in control (A), activin only (B), dorsomorphin only (C) and dorsomorphin + activin A (D) treated wells at day 50. (E) Graph shows the average % pigmentation at day 50 in the four conditions (N=3). Activin A had no significant impact on pigmentation in dorsomorphin induced or control wells.